Docking, synthesis, and characterization of novel heterocyclic ring system and their evaluation for mGlu8 receptor agonist as anticonvulsant agents

Sindiya D Naik[a], Sachin K Chandavarkar*[b], Shilpa S Tawade[a], Sunil G Shingade[c],
Mahesh B Palkar[d] & Shivalingrao N Mamle Desai[a]

[a] Department of Pharmaceutical Chemistry, PES's Rajaram and Tarabai Bandekar College of Pharmacy, Farmagudi, Goa 403 401, India

[b] Department of Pharmacognosy, ASPM College of Pharmacy, Sangulwadi, Dist. Sindhudurg 416 810, India

[c] Department of Pharmaceutical Chemistry, SSP's V P College of Pharmacy, Madkhol, Dist. Sindhudurg 416 510, India

[d] Department of Pharmaceutical Chemistry, KLEU's College of Pharmacy, Hubli 580 031, India

E-mail: chandsachin@gmail.com; smamledesai@rediffmail.com

This research work involves the synthesis of a series of substituted 1-(4-methoxy-1-phenyl/methyl-2-thioxo-1,2-dihydroquinolin-3-yl)ethanone [IVa/b(1-5)] derivatives by dimerization at third position and evaluation of their anticonvulsant activity. The starting material 3-acetyl-4-hydroxy-1-phenyl/methylquinolin-2(1*H*)-one **Ia/b** has been treated with P_4S_{10}:Al_2O_3 to yield compound 1-(4-hydroxy-1-phenyl/methyl-2-thioxo-1,2-dihydroquinolin-3-yl)ethanone (**IIa/b**). Compound **IIa/b** has been methylated to yield compound 1-(4-methoxy-1-phenyl/methyl-2-thioxo-1,2-dihydroquinolin-3-yl)ethanone (**III**a/b) which, on condensation with ketones forms dimers giving the title compounds **IVa-b** (**1-5**). All the synthesized compounds are satisfactorily characterized by spectral data. The *in silico* pharmacophore modeling of the title compounds has been performed using Molegro Virtual Docker (MVD-2007 software and mGlu8 is the target and *in vivo* anticonvulsant activity by phenylenetetrazole (PTZ) induced convulsion method. The results of docking have revealed that the synthesized compounds exhibit well-conserved hydrogen bonds with one or more amino acid residues in the active pocket of metabotropic glutamate receptor mGluR8 complexed with (S)-3,4-dicarboxyphenylglycine (DCPG) (PDB ID:6E5V)LY341495 antagonist (PDB ID: 3MQ4). The MolDock Score of compound 2,6-bis(4-methoxy-1-phenyl-2-thioxo-1,2-dihydroquinolin-3-yl)hepato-2,5-dien-4-one (**IVa-1**) has been found to be −141.617. The *in vivo* anticonvulsant activity results show that compound 2,6-bis(4-methoxy-1-phenyl-2-thioxo-1,2-dihydroquinolin-3-yl)hepato-2,5-dien-4-one (**IVa-1**), 2,7-bis(4-methoxy-1-phenyl-2-thioxo-1,2-dihydroquinolin-3-yl)octa-2,6-dien-4,5-dione (**IVa-2**), 2,6-bis(4-methoxy-1-methyl-2-thioxo-1,2-dihydroquinolin-3-yl)hepato-2,5-dien-4-one (**IVb-2**) and (2E,6E)-2,6-bis(4-methoxy-1-phenyl-2-thioxo-1,2-dihydroquinolin-3-yl) cyclohexanone (**IVb-4**) have been found to be most potent against pentylenetetrazole induced convulsion.

Keywords: Quinolin-2(1*H*)-one, anticonvulsant, mGlu8 receptor, phenylenetetrazole

Epilepsy is the most prevalent neurological disorder affecting more than 0.5% of world population[1]. Epilepsy is highest among children younger than 5 years and elderly older than 65 years of age[2]. Most of the drugs ex. valproic acid, phenytoin, carbamazepine, are effective against newly diagnosed seizure disorders and effectiveness hampers after prolonged exposure. These drugs are also been associated with toxic effects like sedation, ataxia, weight loss (Topiramate), weight gain (Sodium veloproate), hepatotoxicity, tertogenesis, life threatening skin rashes and aplastic anemia[3-7].

Present clinically used antiepileptic drugs act by inducing prolonged inactivation of the Na^+ channels by blocking Ca^{+2} channel currents or by increasing Cl^- conductance at $GABA_A$ receptors Ex. benzodiazepines, barbiturates[8].

Glutamate Receptors

The neurotransmitter glutamate(Glu) mediate most of the fast excitatory transmission that control all brain functions especially learning and memory processes[9]. Excessive glutamergic neurotransmission is understood to be one of the primary metabolic or pathological reason behind the etiology of numerous types of epilepsy[10]. Glu can also activate G-Protein coupled metabotropic receptors(mGluRs) leading to inhibiting and excitatory effects. G-Protein Coupled Receptors (GPCRs) are the largest family of receptors having an extracellular N-terminal domain, an intracellular C-Terminal domain, seven α- helical transmembrane segments and an intracellular loop that binds to G-proteins to produce second messanger signals. Metabotopic glutamate receptors (mGluR) are

coupled receptors (GPCRs) controlling excitatory synapses. mGluRs are classified into three groups differentiated by their sequence homology, second messenger effects and pharmacology. The postsynaptic Group I (mGluR1 and mGluR5) receptors control excitatory neurotransmission, instead Group II (mGluR2 and mGluR3) and Group III metabotopic glutamate receptors (mGluR4 and mGluR7 and mGluR8) are located presynaptically and their activation reduces glutamate release. Many reporters identified mGlu group II and III agonists are the targets for novel antiepileptic agents[11-14]. Literature also reveals the novel group III mGlu receptor agonist (1S,3R,4S)-1-aminocyclopentane-1,2,4-tricarboxylic acid (ACPT-1) has a high affinity for mGlu8 receptor and shows potent anticonvulsant activity[15].

Quinolin-2-one is an important ring system present in alkaloids of Rutaceae family Ex. flindersine, dictamine, walerthione A, B,C, *etc*. Also synthetic derivatives of quinolin-2-one are of wide clinical impotance *viz*. aripiperazole, brespriprazole as antischizoprenic, careolol as an β-blocker in ophthalmic preparation, rebapimide as an antiulcer drug[16,17].

In the present investigation a dimer of substituted 1-(4-methoxy-1-phenyl/methyl-2-thioxo-1,2-dihydroquinolin-3-yl)ethanone were synthesised and mGluR8 agonist activity was performed to know antiepileptic activity of the derivatives.

Result and Discussion

The starting material for the synthesis of title compounds was prepared following the literature[18-20]. The starting material 4-hydroxy-1-methyl/phenyl-3-acetylquinolin-2(1*H*)-one was subjected to thionation using phosphorous pentasulfide in presence of aluminium oxide as a catalyst. Thionated compound was subjected to *O*-methylation of hydroxyl group to avoid keto-enoltautomerism at 3rd and 4th position, might have been interfered with crossed aldol condensation reaction. Compound IIIa/IIIb further reacted with different ketones by crossed aldol condensation to yield title compounds in a manner as shown in Scheme I. The physical data the title compounds are shown in Table I. The spectral characterization of selective representative structure was satisfactorily performed by UV, IR, ^{1}H NMR and ^{13}C NMR spectroscopy and by Mass spectral data. The molecular docking study was performed using Molegro Virtual Docker 2007 (version 6.0). Many have shown good binding to mGluR8 receptor in comparison to ligand and standard drug. The Mol Dock score of the title compounds are shown in
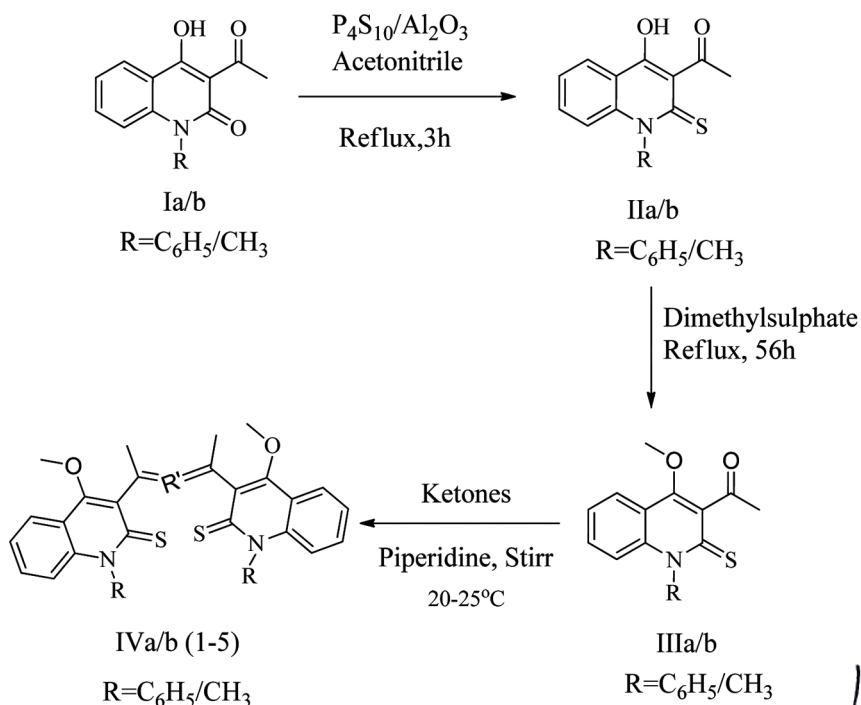
Scheme I

Table I — List of the synthesized derivatives and their physical data

Compd	R	R₁	Mol. Formula	Mol. Wt.	m.p. (ºC)	Yield (%)	λ_max	R_f Value
IVa-1	C_6H_5-	CH-CO-CH	$C_{39}H_{32}N_2O3S_2$	640.81	>300	65.22	232.7	0.67
IVa-2	C_6H_5-	CH-CO-CO-CH	$C_{40}H_{32}N_2O_4S_2$	668.82	>300	68.25	231.6	0.67
IVa-3	C_6H_5-	CHCH₂(CO)CH₂CH	$C_{41}H_{34}N_2O_3S_2$	666.85	>300	60.16	235.8	0.73
IVa-4	C_6H_5-	CH(CH₂)₃COCH	$C_{42}H_{36}N_2O_3S_2$	680.88	>300	58.84	233.1	0.72
IVa-5	C_6H_5-	CHCH₂(CO)₂ CH₂CH	$C_{42}H_{36}N_2O_4S_2$	696.88	>300	62.01	229.4	0.75
IVb-1	CH_3-	CH-CO-CH	$C_{29}H_{28}N_2O_3S_2$	516.67	>300	51.75	236.7	0.76
IVb-2	CH_3-	CH₂-CO-CO-CH	$C_{30}H_{28}N_2O_4S_2$	544.68	>300	53.54	234.09	0.77
IVb-3	CH_3-	CHCH₂(CO)CH₂CH	$C_{31}H_{30}N_2O_3S_2$	542.71	>300	45.21	236.09	0.88
IVb-4	CH_3-	CH(CH₂)₃COCH	$C_{32}H_{32}N_2O_3S_2$	556.74	>300	61.65	230.44	0.89
IVb-5	CH_3-	CHCH₂(CO)₂ CH₂CH	$C_{32}H_{30}N_2O_4S_2$	570.72	>300	66.04	236.90	0.93

Table II — Results of the molecular docking study showing MolDock Scores of target compounds

Name	MolDock score	Rerank score	H Bond
IVa-1	−141.617	−102.141	−7.5
IVa-2	−120.241	−15.833	−2.5
IVa-3	−107.622	−60.5549	−0.06391
IVa-4	−111.881	−51.4096	−6.76057
IVa-5	−94.4933	−70.1609	−7.86196
IVb-1	−115.194	−49.785	−1.05641
IVb-2	−97.1308	−55.7571	−1.77508
IVb-3	−126.335	−34.8722	−4.78532
IVb-4	−134.099	−16.5003	−2.5
IVb-5	−112.230	−102.015	−22.3947
Active Ligand (DCPG)	−133.79	−103.287	−26.1403
Diazepam	−84.3509	−68.1236	−7.01865

Table II and graphical pictures in Figure 1 and Figure 2 A-G. The anticonvulsant activity was performed using pentylenetetrazole (PTZ) induced convulsions and many compounds IVa-1, Iva-2, IVb-1 and IVb-4 have shown protection for convulsions compared to that of standard drug diazepam. Mol dock score of the active compounds are matching with biological active compounds and indicating mGluR8 agonstic activity.

Experimental Section

Chemicals used for the synthesis were purchased from Molychem (Mumbai) and SD-Fine Chem Ltd. (Mumbai). All the reagents and solvents were of laboratory grade. The reactions were monitored by Thin Layer Chromatography (TLC) using precoated plates. Melting Points of the synthesized compounds were determined by Thiele's melting point apparatus and are uncorrected. The UV-Visible absorbance was recorded on Shimadzu UV-Visible Spectrophotometer 1800. Fourier Transform Infrared (FTIR) spectra were recorded on SHIMADZU IR AFFINITY-1 spectrophotometer by KBr disc method. The ¹H NMR and ¹³C NMR were recorded on Bruker Avance II 400
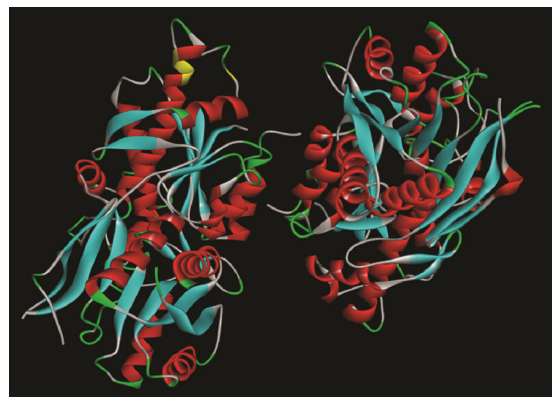

Figure 1 — Structure of human mGlu8 receptor amino terminal domain in complex with (S)-3,4-Dicarboxyphenylglycine (DCPG) obtained from protein data bank with the PDB ID:6E5V

NMR spectrometer using deuterated dimethylsulfoxide (DMSO-d_6) as the solvent and tetramethylsilane (TMS) as an internal standard. Chemical shifts are expressed as delta (δ) values in parts per million (ppm). The Mass spectra (MS) were recorded on Waters, Q-TOF Micromass. *In-silico* molecular docking study was carried out on the synthesized derivatives using Molegro Virtual Docker2007 (version6.0).
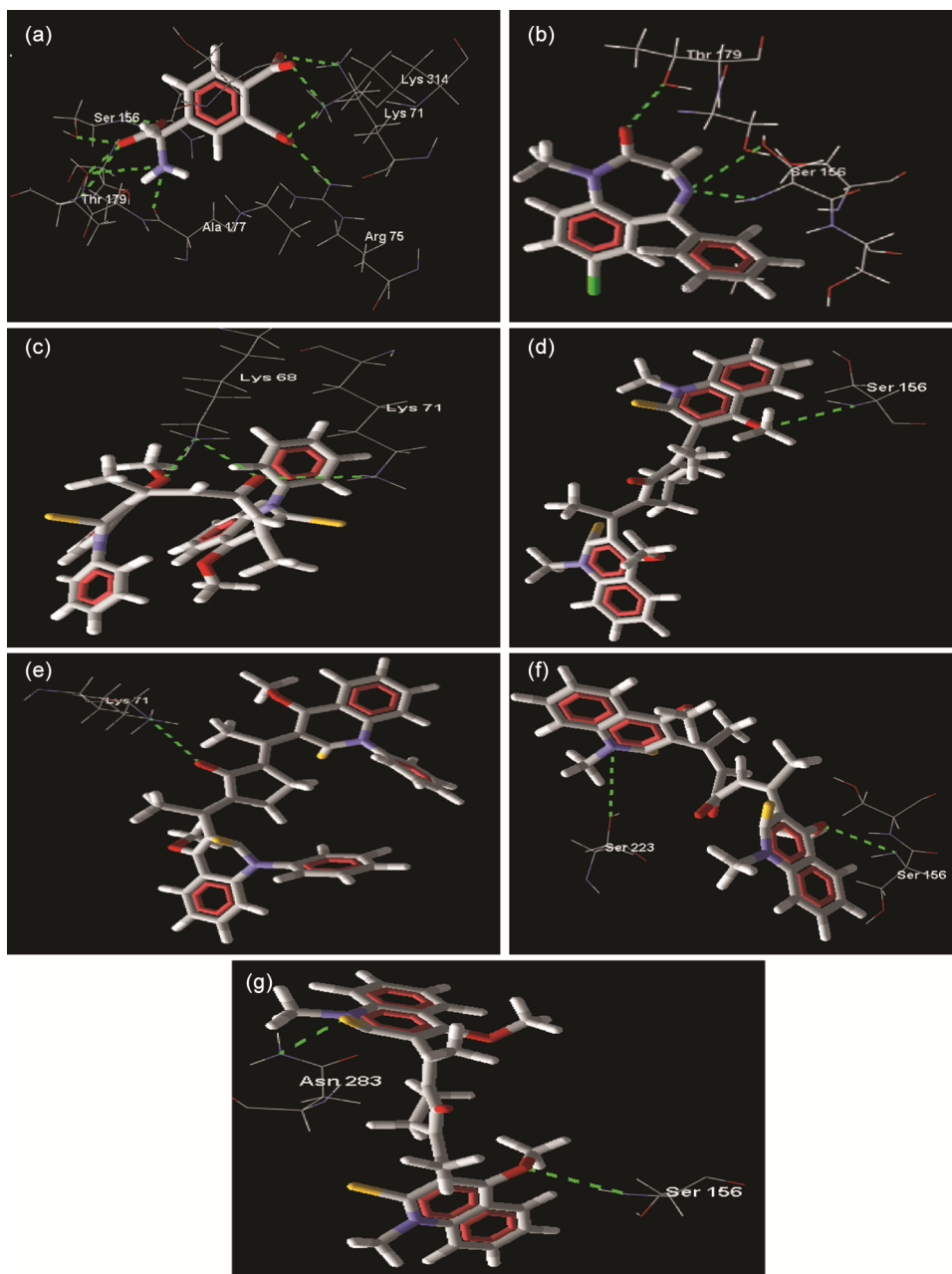
Figure 2 — Hydrogen bonding interactions of best poses of representative compounds with amino acid residues at the active site of protein human mGlu8 receptor amino terminal domain in complex with (S)-3,4-Dicarboxyphenylglycine (DCPG) (**A**) DCPG (active ligand) (**B**) Diazepam; (**C**) IVa-1; (**D**) IVb-4; (**E**)IVa-3; (**F**) IVb-2, (**G**) IVb-3.

Synthesis

Synthesis of 1-(4-hydroxy-1-phenyl/methyl-2-thioxo-1,2-dihydroquinolin-3-yl)ethanone (IIa/b)

Compound4-hydroxy-1-methyl/phenyl-3-acetylquinolin-2(1*H*)-one (Ia/Ib) was subjected to thionation by stirring with phosphourspentasulfide in presence of aluminium oxide as a catalyst using acetonitrile as a solvent. The resultant viscous liquid was then extracted with hexane or diethylether, crude solid was obtained after removal of solvent using IKA make rotaevoporator, recryalllised using toluene as solvent.

Synthesis of 1-(4-methoxy-1-phenyl/methyl-2-thioxo-1,2-dihydroquinolin-3-yl)ethanone (IIIa/b)

O-Methylation of compound **IIa/b** was performed by refluxing with dimethylsulphate and potassium carbonate in acetone for 48-56 hours, solvent was removed by evaporation, reddish brown solid

obtained was washed with water, filtered and recrystallized using ethanol.

Synthesis of substituted 1-(4-methoxy-1-phenyl/methyl-2-thioxo-1,2-dihydroquinolin-3-yl) ethanone [IVa/b (1-5)]

Compound IIIa and IIIb were divided into two portions, the first portion was vigorously stirred mechanically using piperdine base and aqueous ethanol as solvent at temperature of 20-25°C for 20 minutes. And the second half was added slowly and further stirred for 30 minutes. Filtered and washed with water to remove alkali and recrystallized with ethanol.

Molecular Docking Study

A pharmacophore model of the title compounds were built for rational design of novel anticonvulsant agents and mGluR8 receptor was the target. *In silico* molecular docking study of the title compounds were carried out using Molegro Virtual Docker (MVD) 2007 (version 6.0). The selected molecules were built using Chemdraw 12.0.2. The 2D structures were then converted into energy minimized 3D structures, which were saved as MDL MolFile (.mol2). The coordinate file and crystal structure of human mGlu8 receptor amino terminal domain in complex with (S)-3,4-dicarboxyphenylglycine (DCPG) (PDB ID:6E5V) were obtained from the RCSB-PDB website. The protein file was prepared by the removal of water molecules, addition of polar hydrogens, and removal of other bound ligands. The site at which binding of the complexes of agonist occurs was selected as the active site for docking of the test derivatives. The docking protocol was carried out for synthesized compounds with MVD-2007 (version 6.0) software using the standard operating procedure. The MolDock scores and the hydrogen bonding of the test compounds were compared with those of (S)-3,4-dicarboxyphenylglycine (DCPG) (active ligand) and diazepam; taken as reference standard for the study.

The site at which the known DCPG agonist binds with the target protein was selected as the active site domain. It is lined with amino acid residues such as Lys 68, Lys71, Lys314, Ser156, Thr179, Arg75 and Ala177, *etc*. Hence to identify other residual interactions of the tested compounds, a grid box (include residues within a 15.0 A radius) large enough to accommodate the active site was constructed. Since DCPG is a known agonist, the centre of this site was considered as the centre of search space for docking.

Docking of the synthesized compounds with human mGlu8 receptor amino terminal domain in complex with (S)-3,4-Dicarboxyphenylglycine (DCPG) domain exhibited well conserved hydrogen bonding with the amino acid residues at the active site. The MolDock scores of the test compounds ranged from -94.4933 to -141.617 while that of DCPG agonist was -133.79. Diazepam was used as the reference standard for comparison of efficiency and exhibited MolDock score of -84.3509. Most of the designed molecules exhibited MolDock score higher than that exhibited by diazepam; with compound 2,6-bis(4-methoxy-1-phenyl-2-thioxo-1,2-dihydroquinolin-3-yl)hepato-2,5-dien-4-one(IVa-1) having a highest MolDock score of -141.617. The best poses of test derivatives exhibiting the most promising hydrogen bonding are shown in Figure 2. Hydrogen bonding was observed between –O of C=O of IVa-1 derivative with -NH of Lys71 and Lys68, -O of methoxy group showed interaction with –NH of Lys68. Compound IVb-4 with MolDock score -134.099 showed hydrogen bonding with methoxy oxygen forming bond with –NH of Ser156. Compound IVa-3 with MolDock score -107.622 showed hydrogen bond with oxygen of cyclopentanone ring with –NH of Lys71. Compound IVb-3 and IVb-2 with MolDock score -126.335 and -97.1308 respectively also exhibited hydrogen bonding interaction of methoxy oxygen with –NH of Ser156. These results show that the novel quinol-2(1*H*)-one derivatives IVa-1 and IVb-4 possess higher affinity than active ligand and standard drug diazepam towards the active site of the target protein while test derivatives IVa-3, IVb-2 and IVb-3 possess higher affinity towards active site than standard drug diazepam.

Anticonvulsant Activity

The animal experiment was conducted by the approval of Institutional Animal Ethics Committee vide letter No. 1659/PO/Re/S/12CPCSEA dtd. 14.11.2018. Acute oral toxicity study was carried out as per OECD Guidelines 423 Acute Toxic Class Method for 14 days. Male albino mice of either sex weighing 25-30g were used as experimental animals. Test compounds were suspended in tween80 for PTZ

screening. The animals were maintained at an ambient temperature 22 ± 1°C, in groups of six per cage under standard laboratory conditions.

PTZ Method

The phenylenetetrazole (PTZ) test primarily identifies compounds that raise seizure threshold. The PTZ a dose of 85 mg/kg by intraperitoneal route (i.p) was administered. This produces clonic and tonic seizures lasting for a period of at least five seconds in 97 percent of animals tested. Animals were divided into twelve groups, six animals in each group. Mice of either sex weighing between 20-30g were fasted 12h prior to the experiment. Solutions of test derivatives were administered orally at dose level of 100 mg/kg to test groups (group3-group12) and standard group (group 2) received diazepam at dose level 5mg/kg by i.p route, 45 min later PTZ was administered intraperitoneally (i.p) at dose level of 85mg/kg and animals were observed over a 30 min period. Latency to clonic and tonic seizure and survival of mice in the observed time period indicated the compounds ability to abolish the effect of pentylenetetrazole on seizure threshold. Control group (group1) received PTZ at dose of 85mg/kg by i.p route, the results were compared with control group are given in Table III. It was observed that there were significant variations ($^{***}=p<0.001$) in latency time to clonic and tonic convulsions between the treated and control groups. Dunnett's method revealed that derivatives IVa-1, IVa-2, IVb-1 and IVb-4 at dose of 100 mg/kg antagonised seizure elicited by pentylenetetrazole in mice and there was significantly increased latency period to clonic and tonic convulsion and showed 83% protection as compared to control. The dimmers formed by the acetone, 2,3-butadione have exhibited

higher protection for tonic and clonic seizure. The rational of *in-silico* design matches with *in-vivo* biological activity.

Results of PTZ Method

The synthesized compounds were characterized by spectral analysis. Spectral data of representative compounds is presented herewith.

Spectral data 1-(4-hydroxy-1-phenyl-2-thioxo-1,2-dihydroquinolin-3-yl)ethanone (II-a):

IR (KBr, cm^{-1}): 3269.34 (broad band of -OH); 3005.10, 2945.30 (aromatic C-H stretch); 2883.58 (aliphatic C-H stretch); 1658.85(-C=O acetyl); 1213.23 (-C=S).

Spectral data of 1-(4-hydroxy-1-methyl-2-thioxo-1,2-dihydroquinolin-3-yl)ethanone (II-b):

IR (KBr, cm^{-1}): 3290.56 (broad band of -OH); 3005.10, 2945.30 (aromatic C-H stretch); 2887.44; (aliphatic C-H stretch); 1656.85 (C=O acetyl; 1242.16 (-C=S).

Spectral data of 1-(4-methoxy-1-phenyl-2-thioxo-1,2-dihydroquinolin-3-yl)ethanone (III-a):

IR (KBr, cm^{-1}): 3055.24, 3010.88 (aromatic C-H stetch); 2974.23, 2899.01 (aliphatic C-H stretch); 1654.92 (-C=O acetyl); 1213.23 (-C=S); 1265.30 (C-O). ^{1}H NMR (DMSO-d_6, δ ppm): 7.64-6.53 (m, 9H, Ar-H), 3.40 (s, 3H, -OCH$_3$); 2.51 (s, 3H, -COCH$_3$).

Spectral data of 1-(4-methoxy-1-methyl-2-thioxo-1,2-dihydroquinolin-3-yl)ethanone (III-b):

IR (KBr, cm^{-1}): 3080.32, 3045.60 (aromatic C-H stretch); 2943.37, 2885.51 (aliphatic C-H stretch); 1649.14 (-C=O acetyl); 1242.16 (-C=S); 1284.59 (C-O). ^{1}H NMR (DMSO-d_6, δ ppm): 8.10-7.30 (m, 4H, Ar-H), 3.55 (s, 3H, -OCH$_3$); 3.38 (s, 3H, -N-CH$_3$); 2.72 (s, 3H, -COCH$_3$).

Spectral data of 2,6-bis(4-methoxy-1-phenyl-2-thioxo-1,2-dihydroquinolin-3-yl)hepta-2,5-dien-4-one (IVa-1):

IR (KBr, cm^{-1}): 3074.53, 3053.32, 3010.88 (aromatic C-H stretch); 2918.30 (aliphatic C-H stretch); 1656.85 (-C=O acetyl); 1614.42 (-C=C stretch); 1265.30 (C-O stretch); 1215.15 (C=S). ^{1}H NMR (DMSO-d_6, δ ppm): 7.95-7.18 (m,

Table III — Result of anticonvulsant activity of title compounds

Compd	Latency to clonic (in min)	Latency to tonic (in min)	% Protection
Control	3.187± 0.3029	3.338±0.2909	00
Diazepam	9.440± 0.2291***	14.00±0.1647***	83
IVa-1	8.370± 0.4215***	11.60±1.028***	83
IVa-2	8.458± 0.5863***	11.09±1.011***	83
IVa-3	3.552± 0.4051^{ns}	4.345±0.4913^{ns}	33.33
IVa-4	3.575± 0.6964^{ns}	8.938±0.3507***	50
IVa-5	2.832± 0.4126^{ns}	2.872±0.4260^{ns}	16.66
IVb-1	7.580± 0.4353***	10.31±1.001***	83
IVb-2	7.120± 0.08046***	7.173±0.4413***	66.66
IVb-3	4.082± 0.2824^{ns}	4.212±0.3319^{ns}	16.66
IVb-4	9.485± 0.5081***	10.42±0.6304***	83
IVb-5	3.755± 0.5388^{ns}	6.620±0.2295**	33

18H, Ar-H), 6.50 (s, 2H, -C-CH) 3.55 (s, 6H, -OCH$_3$); 2.50 (s, 6H,=C-CH$_3$). MS: m/z = 642 (m+1 peak).

Spectral data of 2,7-bis(4-methoxy-1-phenyl-2-thioxo-1,2-dihydroquinolin-3-yl)octa-2,6-diene-4,5-dione (**IVa-2**):

IR (KBr, cm^{-1}): 3049.46, 3008.95 (aromatic C-H); 2879.72 (aliphatic C-H); 1654.92 (-C=O acetyl); 1614.42 (-C=C); 1265.30 (C-O); 1215.15 (C=S). ^{1}H NMR (DMSO-d_6, δ ppm): 7.95-7.18 (m, 18H, Ar-H), 6.50 (s, 2H, -C-CH) 3.55 (s, 6H, -OCH$_3$); 2.50 (s, 6H,=C-CH$_3$). MS: m/z = 670 (m + 1).

Spectral data of 2,6-bis(4-methoxy-1-methyl-2-thioxo-1,2-dihydroquinolin-3-yl)hepta-2,5-dien-4-one (IVb-1):

IR (KBr, cm^{-1}): 3091.89, 3028.24 (aromatic C-H stretch); 2976.16, 2941.44 (aliphatic C-H stretch); 1651.07(-C=O acetyl); 1620.21 (-C=C stretch); 1284.59 (C-O); 1242.16 (C=S). ^{1}H NMR (DMSO-d_6, δ ppm): 7.95-7.18 (m, 8H, Ar-H), 6.50 (s, 2H, -C=CH) 3.55 (s, 6H, -OCH$_3$); 3.40 (s, 6H,-N- CH$_3$) 2.50 (s, 6H,=C-CH$_3$).

Spectral data of 2,6-bis(1-(4-methoxy-1-methyl-2-thioxo-1,2-dihydroquinolin-3-yl)cyclohexanone (IVb-4):

IR (KBr, cm^{-1}): 3080.32, 3005.10 (aromatic C-H stretch); 2943.37, 2885.51 (aliphatic C-H stretch); 1649.14(-C=O acetyl); 1620.21 (-C=C stretch); 1282.66 (C-O); 1242.16 (C=S).

Spectral data of 2,5-bis(1-(4-methoxy-1-methyl-2-thioxo-1,2-dihydroquinolin-3-yl)cyclopentanone (IVb-3):

IR (KBr, cm^{-1}): 3091.89, 3028.24 (aromatic C-H stretch); 2976.16, 2941.44, 2889.37 (aliphatic C-H stretch); 1651.07 (-C=O acetyl); 1620.21 (-C=C stretch); 1284.59 (C-O); 1242.16 (C=S). ^{13}C NMR (DMSO-d_6, δ ppm): 197.93(1C, -C=O); 175.38 (2C, -C=S); 164.40 (2C, -C-O-CH$_3$); 155.98 (2C, -C-CH$_3$); 140.70 (2C, CH of cyclohexanone); 139.88-108.29 (14C, Ar-C); 62.41 (2C, -O-CH$_3$); 56.76 (2C, -N-CH$_3$); 33.39 (4C, -CH$_2$ of cyclohexanone); 27.98 (2C, -C-CH$_3$). MS: m/z = 544 (m+1).

References

1   McAfee A T, Chilcott K E & Johannes C B, *Epilepsia*, 48 (2007) 1075.
2   Theodore W H, Spencer S S & Wiebe S, *Epilepsia*, 47 (2006) 1700.
3   Celine T, Maryam Y N, Nicholas S A, Daniel J L, William G & Rui X, *Epilepsia*, 61 (2020) 822.
4   Lindhout D, *Neurology*, 42, Suppl-5 (1992) 43.
5   Patsalos P N & Perucca E, *Lancet Neurol*, 2 (2003) 347.
6   Mayer M L, *Curr Opin Neurobiol*, 15 (2005) 282.
7   Foster A C & Kemp J A, *Curr Opin Pharmacol*, 6 (2006) 7.
8   Ranadol X M, Astrid G C, Giovambattista D S & Brian S M, *Eur J Pharmacol*, 476 (2003) 3.
9   Bourgeois B F, *Arch Neurol*, 55 (1998) 1181.
10 Chapman A G, Elwes R D C, Millan M H, Polkey C E & Meldrum B S, *Prog Natl Epileptogenesis*, 12 (1996) 239.
11 Chapman A G, Nanan K, Yip K & Meldrum B S, *Eur J Pharmacol*, 383 (1996) 23.
12 Chapman A G, Smith S F & Meldrum B S, *Epilepsy Res*, 9 (1991) 92.
13 Doherty A J & Dingledine R, *Current Drug Targets*: *CNS Neurol Dis*, 1 (2002) 251.
14 Rouse S T, Marino M J , Bradley S R, Awad H, Wittmann M & Conn P J, *Pharmacol Therap*, 88 (2001) 427.
15 Sansiq G, Bishell T J, Clarke V R, Rozor A, Burnasher N & Portet C, *J Neurosci*, 21 (2001) 8734.
16 Soares A D, Mamle Desai S N, Tiwari P, Palkar M B & Shingade S G, *Indian J Chem*, 58B (2019) 1167.
17 Priolkar R N S, Shingade S G, Palkar M B & Mamle Desai S N, *Curr Drug Discov Technol*, 17 (2020) 203.
18 Maria G R, Mamle Desai S N, Soniya N, Jairus F & Prassad T, *Indian J Chem*, 55B (2016) 1254.
19 Peter R, Werner F & Woifgang S, *J Hetrocycl Chem*, 29 (1992) 225.
20 Shindikar A, Khan F & Viswanathan C, *Eur J Med Chem*, 41 (2006) 786.

Principal
V P College Of Pharmacy, Madkhol
Tal. Sawantwadi, Dist. Sindhudurg

**Advances
in
Bioresearch**

ORIGINAL ARTICLE

Heat Stability and Mosquito Larvicidal activity of *Brahmi* Phytoconstituents

[1]**Manali Vaidya**, [1]**Nikita Shet**, [2]***Mythili K. Jeedigunta**, [3]**Janani Jacob**, [4]**Raghuvir R. Pissurlenkar**,
[5]**Rahul Chodankar**, [6]**Ajit K. Mohanty**, [7]**Arun B. Joshi**

[1]M.Pharm, Department of Pharmacognosy, Goa College of Pharmacy, Panaji, Goa, 403001.
[2]Assistant Professor, Dept. of Pharmacognosy, Goa College of Pharmacy, Panaji, Goa - 403001
[3]Junior Research Officer, Department of Phytochemistry, Natural Remedies Private Ltd. Benguluru, Karnataka, 560100.
[4] Associate Professor, Department of Pharmaceutical Chemistry, Goa College of Pharmacy, Panaji, Goa, 403001.
[5] Assistant Professor, Department of Pharmaceutical Chemistry, Goa College of Pharmacy, Panaji, Goa, 403001.
[6]Scientist B, ICMR- National Institute of Malaria Research, Panaji, Goa, 403001.
[7]Professor, Department of Pharmacognsoy, Goa College of Pharmacy, Panaji, Goa, 403001
* Corresponding Email: jsnrkmyth@gmail.com

ABSTRACT
Vector borne diseases, illnesses that occur due to the transmission of the parasites/pathogens are one of the main illnesses of human population. The efforts made in research so far could not completely over power these pathogens. More toil and travail are required in every possible direction to search for a good combat agent. Medicinal plants have undoubtedly been a good source of panacea for many ailments. In the present study one such medicinal plant, Brahmi, is examined concerning its larvicidal activity. The methanolic extract has been subjected to heat treatment for understanding any modifications in the major phytoconstituents; followed by a molecular modeling analysis of them with one of the major receptors (ecdysone) involved in the anti-larval activity. With the encouraging results obtained from the computational study a detailed bioassay was carried out using the extract on the three larvae Anopheles stephensi, Aedes aegypti and Culex quinquefasciatus. From the study it can be concluded that Brahmi can be used as a potent anti-larval agent in a formulation.
KEY WORDS: *Brahmi, Larvicidal, Molecular Modeling, Bioassay*

How to cite this article:
M Vaidya , N Shet , M K. Jeedigunta, J Jacob, R R. Pissurlenkar, R Chodankar, A K. Mohanty, A B. Joshi. Heat Stability and Mosquito Larvicidal activity of *Brahmi* Phytoconstituents. Adv. Biores. Vol 13 [5] September 2022. 45-53

INTRODUCTION
The word *Brahmi* or *Brahman* represents the creative principle that lies realized in the whole world. It is the concept found in the *Vedas* and *Upanishads*. It is essentially related to all those properties which are related to the memory, learning and understanding of intellectual matter. *Brahmi* originates from *Brahma* which is the mind-born divine mother [1,2,3]. From this preamble, it can be easily perceived about the qualities of a plant which has been named *Brahmi*.
Two plants are frequently referred by this name *Brahmi* – *Bacopa monneiri* and *Centella asiatica*. However, the majority of the references correspond to the former and the latter is synonymously called *Mandukaparni* or *Gotu Kola*. Both the plants show significant differences morphologically and chemically which assists in easy identification but share an array of pharmacological activities. Morphological, majorly include the leaves of both the plants. Sessile and ovate-obovate leaves of *Brahmi* whereas petiolate and sub-reniform leaves of *Mandukaparni*, give a striking difference for identification. Chemically- though both contain the glycosides the aglycones differ. The glycosides of *Bacopa monneiri* are triterpenoid saponin with dammarane type (jujubogenin or pseudojujubogenin) and phenylethanoid

type of aglycones. The dammarane type of glycosides - Bacoside A {Bacoside A3, Bacopaside II, Bacopaside X and Bacopasaponin C} and Bacoside B {Bacopaside N1, Bacopaside N2, Bacopaside IV and Bacopaside V}[4-6]. These are considered as the major phyto-constituents responsible for the activity and are referred to as the biomarkers [7]. The phenylethanoid glycosides include the Monnieraside I-III and Plantainoside B. In addition to these *Bacopa* also contain Curcubitacins which are tetracyclic terpenes with steroidal structures which function as kairamones [8]. The phytoconstituents of *Centella asiatica* include glycosides with triterpene – Ursane-Oleanane type of aglycone, Madecassoside and Asiaticoside. In addition to these glycosides, it is also reported to contain polyacetylenes (Centellin, asiaticin and centelicin), flavonoids – quercetin, kaemferol and phytosterols – campsterol, sitosterol, stigmasterol[9].

Both plants have been reported to contain a wide range of pharmacological activities. However, the majority of the reports have been primarily about the cognitive enhancing effects with a specific mention about memory, concentration, and learning [10]. In addition to these, the other major activities reported are the cardiac and respiratory activity and in the treatment of certain neuropharmacological disorders like insomnia, insanity, depression, stress, epilepsy and psychosis [11]. They are also found to be possessing anti-inflammatory, antipyretic, analgesic, free radical scavenging, and lipid peroxidative activities [12]. However, *Bacopa* is considered to be more potent and safer than *Centella* and there is a degree of variation in the side effects as well.

In the present study *Brahmi (Bacopa monneiri)* has been considered. The methanolic extract is subjected to chromatography for the isolation of the biomarker Bacoside A, separated into its components and has been characterized with spectroscopic data in comparision with the standard literature. The extract has been subjected to heat treatment. The pattern observed after the heat treatment will assist in understanding the stability of Bacoside A especially during the process of soxhlet which is generally employed for extraction. Besides the established pharmacological activities, one of the effects which has not been analyzed in detail so far is the larvicidal activity of *Brahmi*. Based on the preliminary report about the larvicidal activity of the *aqueous* extract of *Brahmi*, detailed molecular docking studies were carried out using ecdysone receptor [13]. This is the key receptor involved in the hormonal regulation of various stages in the insect development (molting and metamorphosis of the epidermis and the nervous system)[14]. As the docking score indicated that the ligands of phenylethanoid glycosides and flavonoids of Brahmi have a greater docking score than the dammarane glycosides, the entire *methanolic* extract was subjected to bioassay against the 3rd instar larvae of *Anopheles stephensi*, *Culex quinquefasciatus* and *Aedes aegypti* mosquitoes.

MATERIAL AND METHODS
ISOLATION AND PURIFICATION:

The methanolic extract was subjected to column chromatography (Column:1) on silica gel (60-120 mesh) using a gradient elution of Pet. Ether: Ethyl acetate and ethyl acetate: Methanol with an increasing proportion of ethyl acetate and methanol respectively. A total of 41 fractions showing similar patterns were pooled. Fractions 15-18 eluted with ethyl acetate: Methanol (6:4) were further subjected to chromatography (Column:2) with reverse-phase silica (230-400 mesh) and gradient elution using chloroform: methanol: water (starting from chloroform 100% and changing it gradients and keeping methanol and water constant i.e., 7:1:0.1 to 1:1:0.1). 17 fractions were collected and concentrated on a rotary evaporator. Fractions 7-8 eluted using methanol: water (6:4) showed a similar pattern. This portion was subjected to reverse phase chromatography (Column:3) using silica (230-400 mesh). The column was subjected to gradient elution from 55% methanol: water to 100% methanol. From the 13 fractions obtained, fractions 2-5 showed similar peaks. These were pooled and further subjected to preparative HPLC using Kromasil C18 column and isocratic elution using 65% methanol:water. Two pure compounds BMM-01 (2g) and BMM-02 (3.2g) were obtained after rotary evaporation. The fraction 6 from the third column was further subjected to reverse phase chromatography (Column:4) using 55% methanol: water gradient till 100% methanol. From the fractions 9-10 a single compound BMM-03 (3.5g) was obtained. The fractions 7-9 from the third column were pooled and evaporated to give a pure compound of BMM-04 (2.4g). The individual isolated compounds have shown a positive reaction to qualitative tests like Libermann-Buchard test and Molisch test. The compounds were then determined for their melting point and other spectral characterization using IR, 1H and 13C NMR and Mass was performed and the data obtained were correlated with the standard.

HEAT TREATMENT:
About 50mg of *Bacopa monnieri* methanolic extract, Bacoside A, and the individual constituents were subjected to heat treatment at 110ºC in a hot air oven. The samples were collected after 2hrs. Subsequently, the samples were taken after 4hrs, 6hrs, 8hrs and 12hrs. The extract was targeted for Bacoside A and the individual constituents - Bacoside A3, Bacopaside II, Bacopaside X, and Bacopasaponin C.

MOLECULAR DOCKING STUDIES:
The docking studies were carried out by using Glide v7.8, Schrödinger Suite 2018 (Trial Edition) (Glide, Schrödinger, LLC, New York, NY, 2018.) on Intel hexacore processor-based linux workstation.[15-17]

PROTEIN AND LIGAND PREPARATION:
The X-ray crystal structure of ecdysone receptor (organism), PDB code 1R20 (was retrieved from Protein Data Bank[18,19]. The receptor crystal structure was prepared for docking using the Protein Preparation Wizard in the Schrodinger Suite 2018[20]. The bound crystal water was removed, hydrogen atoms were added and A chain was removed. The ionizable groups were optimized at a physiological pH of 7.0 followed by energy minimization using OPLS3 Force field to relax any crystal restrains on the structure till a convergence of 0.05 RMSD was met for the heavy atoms. The bacosides used in docking studies were prepared using Ligprep. (LigPrep, Schrödinger, LLC, New York, NY, 2018). The atom types and partial charges were assigned based on the OPLS3 force field. The molecules were ionized using Epik at pH 7.0 to generate possible tautomeric states; multiple conformations were identified while retaining the specific chirality.

DOCKING STUDIES:
A grid was generated in the active site to dock the bacosides based on the bound ligand. The extents of the inner and outer grid box were set to 15 Å and 20 Å along the x, y and z directions respectively, providing ample space for the generation of varied ligand confirmation at the ligand-binding pocket. The Vdw (Van der Waals) radius scaling was set to default 1.0 Å to soften the potential over the non-polar areas of the enzyme that lie within the grid extents and the partial atomic charges were set to 0.25 of the exact values. The receptor atoms outside the grid were not scaled. The hydroxyl group of the amino acid serine, threonine and tyrosine were set to rotate to increase the probability of hydrogen bond formation. Subsequent the bacosides were docked to the receptor to find the best poses which were scored by GlideScore SP.

DETERMINATION OF LARVICIDAL ACTIVITY:
The 3rd *instar* larvae of the mosquito species, *Anopheles stephensi, Aedes agyepti,* and *Culex quinquefasciatus* were used for the study. They were obtained from the insectary of National Institute of Malaria Research, Goa Theses immature were maintained at 27 ± 2°c, 70-80% relative humidity (RH).

SAMPLE PREPARATION:
A Hundred milligrams of methanolic extract of *Bacopa monnieri* was dissolved in Dimethyl Sulphoxide (DMSO) to obtain 100ppm, 200ppm, 300ppm, 500ppm, 800ppm and 1000ppm concentration.

Figure no 1: Experimental set up for Larvicidal activity

The bowls used for the experiment were washed with sterile water and later on with spirit. The bowls were dried and then kept in the autoclave for 20 minutes. Different concentrations of the suspensions were fed to 25 healthy 3rd *instar* test larvae species in 500 ml plastic bowls containing 250ml of sterile distilled water. The percent mortality of the larvae was recorded after 24 and 48 hours of exposure by counting the living and dead larvae. All the tests were conducted under controlled temperature (28ºC± 2ºC) and each test was replicated at least thrice.[21] Activity of the extract against test mosquito larvae in terms of LC_{50} and LC_{90} was studied by analyzing dose mortality responses of individual strains by probit analysis using SPSS software.

If the mortality in control was more than 5%, Abbott's corrective formula was applied.

% Mortality = Number of dead larvae/total number of larvae*100

Corrected Mortality (%) = (% test mortality - % control mortality) /(100 - % control mortality)*100[21]

RESULTS AND DISCUSSION
CHARACTERIZATION:

Compound 1

Melting point: 247°C; IR (KBr) : 3445.01, 2943.50, 2870.20, 1678.14, 1454.39, 1375.30, 1289.47, 1079.22 cm^{-1}; LC-MS (negative) *m/z* 927.50 (M-H)$^-$; ^{1}H NMR (DMSO) and ^{13}C NMR data was compared with the standard. The compound was identified to be Bacoside A$_3$[22].

Compound 2

Melting point: 253°C; IR (KBr) : 3445.60, 2942.63, 1454.39, 1372.41, 1285.58, 1214.24, 1289.47, 1081.51 cm^{-1}; LC-MS (negative) *m/z* 927.33 (M-H)$^-$; ^{1}H NMR (DMSO) and ^{13}C NMR data was compared with the standard. The compound was identified as Bacopaside II[23].

Compound 3

Melting point: 230°C; IR (KBr): 3419.94, 2943.50, 2865.38, 1653.07, 1453.43, 1381.09, 1288.50, 1216.17, 1077.29 cm^{-1}; LC-MS (negative) *m/z* 897.25 (M-H)$^-$; ^{1}H NMR (DMSO) and ^{13}C NMR data was compared with the standard. The compound was identified as Jujubogenin isomer of Bacopasaponin C (Bacopaside X)[5].

Compound 4

Melting point: 291°C; IR (KBr): 3429.43, 2939.52, 1456.26, 1381.03, 1078.21 cm^{-1}; LC-MS (negative) *m/z* 897.67 (M-H)$^-$; ^{1}H NMR (DMSO) and ^{13}C NMR data was compared with the standard. The compound was identified as Bacopasaponin C[5].
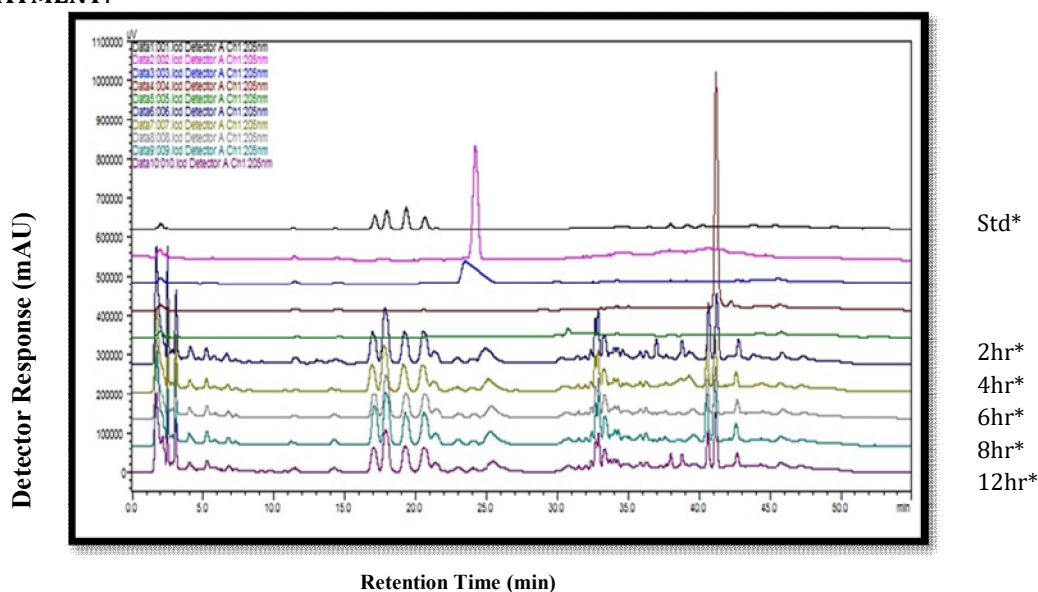
HEAT TREATMENT:

Figure No 2: HPLC of heat treated extract sample at 110 °C
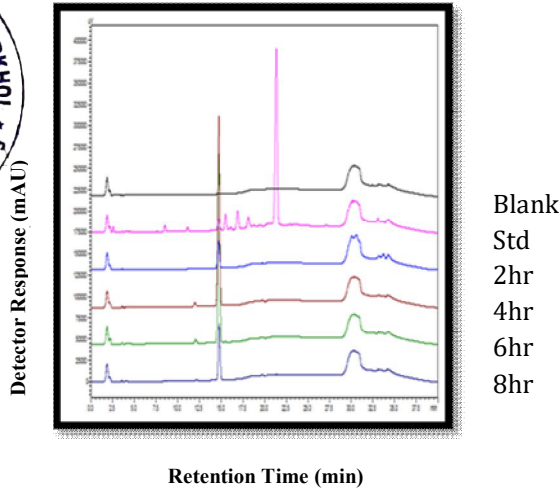*-Detector response of the standard and the samples collected after respective time intervals

Figure No 3: (a) HPLC of heat treated Bacoside A₃
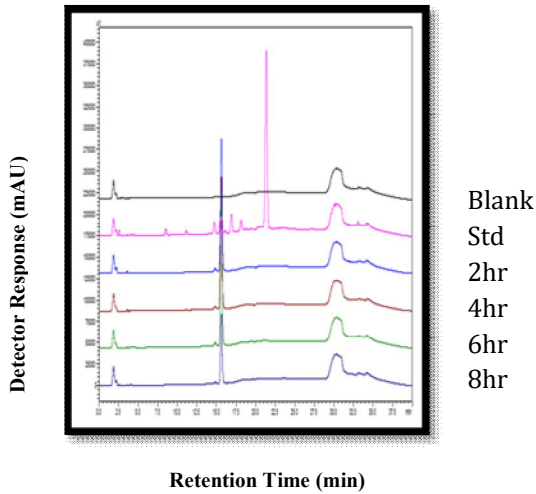*-Detector response of the standard and the samples collected after respective time intervals

Figure No 3: (b) HPLC of heat treated Bacopaside II
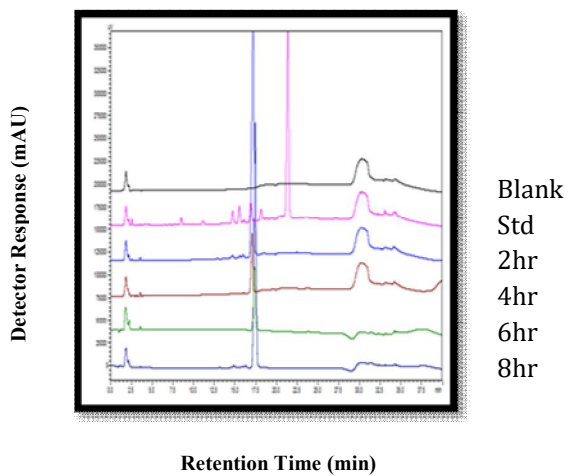*-Detector response of the standard and the samples collected after respective time intervals

Figure No4:(a) HPLC of heat treated Bacopaside X
*-Detector response of the standard and the samples collected after respective time intervals
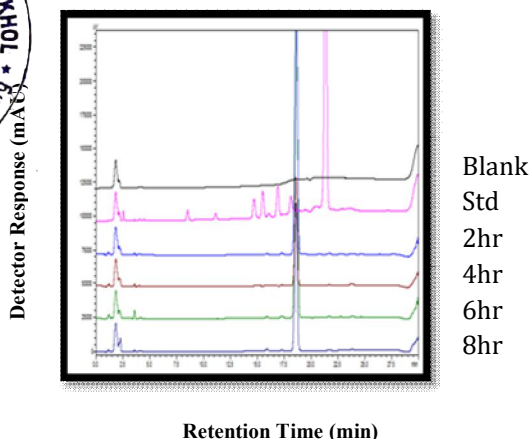
Retention Time (min)

Figure No 4 (b) HPLC of heat treated Bacopasaponin C

*-Detector response of the standard and the samples collected after respective time intervals

The Figure No. 2 indicates the comparison of the standard of Bacoside A with that of the extract subjected to heat treatment at 110°C at an interval of 2hrs. The results showed no significant change in the pattern. Figure No. 3(a) and (b) as well as Figure No. 4(a) and (b), suggest no significant change in the individual components of the glycosides subjected to the heat treatment as well.

MOLECULAR DOCKING:

Ligands   Docking score

1. Monnieraside C – GlideScore SP of -9.70
2. Plantainoside - Glide Score SP of -9.41
3. Monnieraside B - Glide Score SP of -9.00
4. Apigenin-7-glucoside - Glide Score SP of -8.36
5. Luteolin-7-glucoside - Glide Score SP of -7.96
6. Monnieraside A - Glide Score SP of -7.68
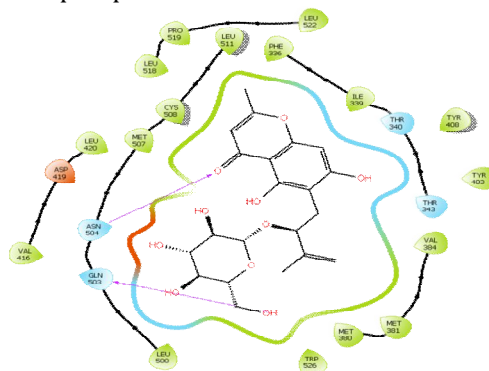7. Jujubogenin isomer of Bacopasaponin C - Glide Score SP of -5.78

Figure No 5: Interaction of the ligand Monnieraside C with *Heliothis virescens* ecdysone
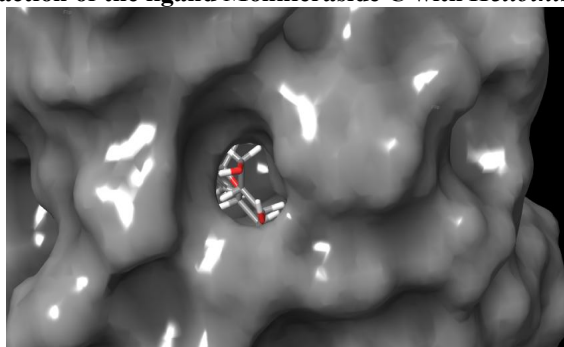

Figure No 6: Monnieraside C docked into the binding site of *Heliothis virescens* ecdysone receptor.

The comparison of docking score of various glycosides of the *Brahmi* with that of Ecdysone receptor suggested good docking of the constituents with Monnieraside C having the best Glide score. Fig No 5 and 6 show the three dimensional interaction between this ligand and the receptor. The binding interactions between all the ligands and the receptor has been shown in the Table No. 1**.**

Table No. 1: Binding interactions of the ligands to the *Heliothis virescens* ecdysone receptor

Serial no	Ligands	Interactions		
		Hydrogen bond	Hydrophobic	Polar
1	Monnieraside C (Fig no 5 and 6)	THR340, THR 343, GLN 503	ILE 339, LEU 522, PH 336, TRP 526, LEU 518, PRO 519, TYR 408, TYR 403, LEU 420, VAL 416, LEU 500, VAL 384, MET 381, MET 380, MET 507, CYC 508, LEU 511	THR 340, THR 343, ASN 504, GLN 503
2	Plantainoside	ASN 504, GLN 503,	LEU 522, PHE 336, LEU 511, PRO 519, LEU 518, CYS 508, MET 507, LEU 420, VAL 416, LEU 500, YRP 526, MET 380, MET 381, VAL 384, TYR 408, TYR 403, ILE 339	ASN 504, GLN 503, THR 340, THR 343
3	Monnieraside B	-	ILE 339, PHE 336, LEU 522, LEU 511, CYC 508, MET 507, LEU 518, TRP 526, TYR 408, TYR 403, VAL 384, MET 381, MET 380, LEU 420, ILE 417, VAL 416, TYR 415, MET 413, LEU 500	THR 340, ASN 596, THR 343, ASN 504, GLN503.
4	Apigenin-7-glucoside	GLN 503	TRP 526, TYR 408, ILE 339, TYR 403, MET 380, MET 381, LEU 420, LEU 500, VAL 416, TYR 415, MET 507	THR 343, THR 340, GLN 503, ASN 504, ASN 506, SER 510
5	Luteolin-7-glucoside	THR 343, TYR 408, TYR 415	TYR 403, ILE 339,LEU 511,PHE 336, LEU 518,LEU 522,TRP 526,TYR 408,MET 380,MET 381,LEU 420,VAL 416,TYR 415,MET 413,LEU 500, MET 507,CYC 508	THR 340,THR 343,ASN 506,ASN 504,GLN 503
6	Monnieraside A		TYR 403, MET 381, MET 380, LEU 522, ILE 339, PHE 336, TRP 526, LEU 511, TYR 408, CYC 508, MET 507, MET 413, TYR 415, VAL 416, LEU 500, LEU 420, MET 381, MET 380	THR 343, THR 340, ASN 504, GLN 503
7	Jujubogenin isomer of Bacopasaponin C	ASN506	ILE509, MET507, MET502, VAL 416, TYR 415	SER 510, ASN506, SER 506, ASN504, GLN 503, THR 499

LARVICIDAL ACTIVITY:
The larvicidal activity in terms of LC_{50} and LC_{90} values of the methanolic extract against laboratory reared 3rd instar larvae of *An. stephensi*, *Cx. quinquefasciatus* and *Aedes aegypti* are shown in table (2).
The methanolic extract was found more effective against *Culicine* followed by *Anopheline* and *Aedes* larvae after 24 and 48 hrs of exposure. Methanolic extract showed highest larval mortality against *Culex quinquefasciatus* with LC_{50} = 203ppm and LC_{90} = 682 ppm, followed by *An. stephensi* with LC_{50} = 406 ppm, LC_{90} = 795 ppm and *Aedes aegypti* with LC_{50} = 725 ppm, LC_{90} = 1194 ppm respectively at 24 hrs.
Plant based biocides have an advantage over synthetic pesticides because they are generally eco-friendly, readily biodegradable, target specific and less prone to the development of resistance in mosquitoes. The

Principal
V P College Of Pharmacy, Madkhol
Tal. Sawantwadi, Dist. Sindhudurg

present study has shown that the methanolic extracts of *Bacopa monnieri* cause extensive mortality in the 3rd *instar* larvae of all the three test mosquito species. This broad spectrum of activity is desirable in the integrated vector management (IVM) against many vector species simultaneously breeding in inter-specific associations.[24] This study suggests that methanolic extract of *Bacopa monnieri* could be developed as a potent herbal insecticide for the control of mosquito vectors.

Table No:2 Larvicidal activity of methanolic extract of *Bacopa monnieri* against third *instar* larvae of Mosquitoes

Mosquito species (n=25)	24 hours[a]		48 hours[a]	
	LC_{50}*	LC_{90}*	LC_{50}*	LC_{90}*
Anopheles stephensi	406.182 (323.831-509.476)	795.724 (634.395-998.079)	271.061 (211.616-347.205)	584.182 (456.068-748.285)
Aedes aegypti	725.798 (602.409-874.461)	1194.717 (991.609-1439.427)	300.027 (236.142-381.195)	617.589 (486.085-784.669)
Culex quinquefasciatus	203.546 (136.788-302.886)	682.915 (458.935-1016.207)	120.493 (86.676-167.503)	306.075 (220.175-425.490)

* - 95% Confidence limit (lower –upper)

[a] – time after which the readings were taken

n- the no.of third *instar* larvae of mosquitoes considered for the study

CONCLUSION

Brahmi (*Bacopa monnieri*) has been used in Ayurveda and other alternative systems of medicine for a wide array of pharmacological benefits. However, with the advent of modern technology and the scale of manufacture of the formulations, it is but imperative to understand the stability of the constituents during the processing. Also, one of the obligatory effects of the extract i.e larvicidal activity has been studied in detail taking the fulcrum of molecular docking studies for the confirmation. It can be concluded decisively that this significant herb is stable during various heat treatments it may be subjected to during extraction and has a perceivable larvicidal activity.

CONFLICT OF INTEREST: NIL

REFERENCES
1. Mukerjee DG, Dey CD. (1996) Clinical trial on Brahmi. J. Exp. Med. Sci. 10 Suppl 1: 5-11.
2. Kapoor LD. (2000). Hand Book of Ayurvedic Medicinal Plants. Boca Raton: CRC Press.
3. Garai S, Mahato SB, Ohtani K, Yamasaki K. (1996) Bacopasaponin D - a pseudojujubogenin glycoside from *Bacopa monnieri*. Phytochemistry. 43 Suppl 2:447-449.
4. Deepak M, Sangli GK, Arun PC, Amit A. (2005) Quantitative determination of the major saponin mixture bacoside A in *Bacopa monnieri* by HPLC. Phytochem. Anal. 16: 24-29.
5. Sivaramakrishna C, Rao CV, Trimurtulu G, Vanisree M, Subharaju GV. (2005) Triterpenoid glycosides from *Bacopa monnieri*. Phytochemistry. 66: 2719-2728.
6. Russo A, Borrelli F. (2005) *Bacopa monniera*, a reputed nootropic plant: an overview. Phytomedicine. 12 Suppl 4:305-317.
7. Deepak M, Amit A. (2004) The need for establishing identities of bacoside A and B, the putative major bioactive saponins of Indian medicinal plant *Bacopa monnieri*. Phytomedicine. 11: 264-268.
8. Pamita B, Neeraj K, Bikram S, Vijay KK. (2007) Cucurbitacins from *Bacopa monnieri*. Phytochemistry. 68:1248-1254.
9. Siddiqui BS, Aslam HS, Khan AS, Begum S. (2006) Chemical constituents of *Centella asiatica*. Journal of Asian Natural Product Research. 9 Suppl 4:407-414.
10. Nadkarni KM. (1988) The Indian Materia Medica. Bombay: Popular Prakashan.
11. Kishore K, Singh M. (2005) Effect of bacosides, an alcoholic extract of *Bacopa monniera* Linn. (brahmi), on experimental amnesia in mice. Indian J. Exp. Biol. 43 Suppl 7:640-645.
12. Anbarasi K, Vani G, Balakrishna K, Desai CS. (2005) Creatine kinase isoenzyme patterns upon exposure to cigaratte smoke: protective effect of Bacoside A. Vascul. Pharmacol. 42 Suppl 2:57-61.
13. Rathy MC, Sajith U, Harilal CC. (2015) Plant diversity for mosquito control: A preliminary study. International Journal of Mosquito Research. 2 Suppl 1: 29-33.
14. Riddiford LM, Cherbas P, Truman JW. (2000) Ecdysone receptor and their biological actions. Vitam. Horm. 60:1-73.

Principal
V P College Of Pharmacy, Madkhol
Tal. Sawantwadi, Dist. Sindhudurg

Friesner RA, Murphy RB, Repasky MP, Frye LL, Greenwood JR, Halgren T, et.al. (2006) Extra Precision Glide: Docking and Scoring Incorporating a Model of Hydrophobic Enclosure for Protein-Ligand Complexes. J. Med. Chem. 49 Suppl 21:6177–6196.

16. Halgren TA, Murphy RB, Friesner RA, Beard HS, Frye LL, Pollard WT, et.al. (2004) Glide: A New Approach for Rapid, Accurate Docking and Scoring. 2. Enrichment Factors in Database Screening. J. Med. Chem. 47 Suppl 7:1750–1759.

17. Friesner RA, Banks JL, Murphy RB, Halgren TA, Klicic JJ, Mainz DT, et.al. (2004) Glide: A New Approach for Rapid, Accurate Docking and Scoring. 1. Method and Assessment of Docking Accuracy. J. Med. Chem. 2004; 47 Suppl 7:1739–1749.

18. Billas IML, Iwema T, Garnier JM, Mitschler A, Rochel N, Moras D. (2003) Structural adaptability in the ligand binding pocket of the ecdysone receptor. Nature. 2003; 426:91-96.

19. Berman HM, Westbrook J, Feng Z, Gilliland G, Bhat TN, Weissig H, et.al. (2000) The Protein Data Bank. Nucleic Acids Research. 2000;28 Suppl 1:235-242.

20. Sastry GM, Adzhigirey M, Day T, Annabhimoju R, Sherman W. (2013) Protein and ligand preparation: Parameters, protocols, and influence on virtual screening enrichments. J. Comput. Aided. Mol. Des. 2013; 27 Suppl 3: 221-234.

21. Ajeet KM, Sandeep G, Kulvir D, Ashwani K. (2017) Variable Region of 16s rRNA is Essential for the Identification of Group 1 Mosquito- Pathogenic Strains of *Lysinibacillus*. Adv Biotech & Micro. 2017. 2 Suppl 2:555583.

22. Rastogi S, Pal R, Kulshreshtha DK. (1994) Bacoside A3-A triterpenoid saponin from *Bacopa monniera*. Phytochemistry. 1994; 36 Suppl 1:133-137.

23. Chakravarty AK, Sarkar T, Masuda K, Shiojima K, Nakane T, Kawahara N. (2001) Bacopaside I and II: two pseudojujubogenin glycosides from *Bacopa monniera*. Phytochemistry. 2001; 58 Suppl 4:553-556.

24. World Health Organization (WHO). Planning and Implementation. Handbook for Integrated Vector Management. Geneva, 2012. (WHO/HTM/NTD/VEM/2012.3): 32.

Principal
V P College Of Pharmacy, Madkhol
Tal. Sawantwadi, Dist. Sindhudurg

Assessment of elementary derivatives of 1,5-benzodiazepine as anticancer agents with synergy potential

Sinthiya J. Gawandi [a], Vidya G. Desai [a,*], Shrinivas Joshi [b], Sunil Shingade [c], Raghuvir R. Pissurlenkar [d]

[a] Department of Chemistry, Dnyanprassarak Mandal's College & Research Centre, Assagao, Bardez, 403507, India
[b] Novel Drug Design and Discovery Laboratory, Department of Pharmaceutical Chemistry, S.E.T.'s College of Pharmacy, Sangolli Rayanna Nagar, Dharwad 580 002, Karnataka, India
[c] SSPM's V P College of Pharmacy, Madkhol, Sawantwadi, Sindhudurg, Maharashtra
[d] (Bio) Molecular Simulations Group, Department of Pharmaceutical Chemistry, Goa College of Pharmacy, Panaji, Goa, India

ARTICLE INFO

ABSTRACT

Herein, we designed and synthesized 1,5-benzodiazepines as a lead molecule for anticancer activity and as potent synergistic activity with drug Methotrexate. Working under the framework of green chemistry principles, series of 1,5-benzodiazepine derivatives **(3a-3a^1)** were synthesized using biocatalyst i.e. thiamine hydrochloride under solvent free neat heat conditions. These compounds were screened for _in vitro_ anti cancer activity against couple of cancer cell lines (HeLa and HEPG2) and normal human cell line HEK-293 via MTT assay. The IC$_{50}$ values for the compounds were in the range 0.067 to 0.35 μM, better than Paclitaxel and compatible with the drug Methotrexate. Compound **3x** was found to be influential against both the cell lines with IC$_{50}$ values of 0.067 ± 0.002 μM against HeLa and 0.087 ± 0.003 μM against HEPG2 cell line, having activity as compatible to the standard drug Methotrexate. Bioinformatic analysis showed that these compounds are good tyrosine kinase inhibitors which was then proved using enzyme inhibition assay. The studies of apoptosis revealed late apoptotic mode of cell death for the compounds against HEPG2 cancer cell line using flow cytometry method. Synergistic studies of compound **3x** and drug Methotrexate showed that the combination was highly active against cancer HeLa and HEPG2 cell line with IC50 value 0.046 ± 0.002 μM and 0.057 ± 0.002 μM respectively, which was well supported by apoptosis pathway. Further the compounds proved its scope as DNA intercalating agents, as its molecular docking and DNA binding studies revealed that the compounds would fit well into the DNA strands.

1. Introduction

Cancer is one of the topmost malignant diseases responsible for millions of demise of people per year worldwide. Principally, numbers of deaths arise from leukemia, breast, cervical and liver cancer. There is a continuous struggle for the advancement of new drug therapies for safe and effective treatment of cancer disease [1,2,3]. One of the therapies that have proven it has been the drug combination therapy [4,5,6]. Combinations of two or more drugs can conquer over toxicity and other side effects linked with steep shot of single drugs by resisting biological compensation, thereby treating multifactorial disease. Synergistic drug combination studies have gained a promising research strategy with the motif of enhancing drug effect; improve drug selectivity by overcoming unwanted side effects, host immunity and lowering normal cell toxicity

current drug therapeutics by development of novel drug treatment strategies. Administering more than one drug can provide several benefits that include better efficacy, lower toxicity, and much delay in onset of acquired drug resistance [7,8,9]

In cancer drug discovery, Tyrosine kinase is the key enzyme in the sub group of protein kinases, responsible for phosphate group transfer from ATP to a protein in a cell which is a vital mechanism in signal transduction and cell regulation [10,11,12]. Epidermal growth factor receptor (EGFR)-TK is found to be over expressed in most of the solid tumors. It leads to autophosphorylation of protein, thus triggering the tumor growth and expansion leading to malignant progression [13,14]. The most common drugs known for inhibition of these enzymes are Gefitinib [15], Imatinib [16], Erlotinib [17], etc. (Fig. 1)

Kinase inhibitors as monotherapy have not been so effective for

---

treating large cases of malignances and hence synergistic combination is an alternative to look forward to [18]. Simple compounds have been synergised with EGFR tyrosine inhibitors in an anticancer synergy [19,20]. A potential combination therapy for the treatment of advanced ovarian cancer has been reported involving FDA-approved targeted drugs—sunitinib, dasatinib, and everolimus [21]. *In silico* modelling methods have been used to predict synergism of cancer drug combinations [22].

The mechanism of action of main anticancer drugs like Cis-platin, Paclitaxel and Methotrexate takes place by inhibiting DNA synthesis and suppressing RNA transcription [23], stabilization of microtubule [24] and by inhibition of dihydrofolate reductase [25] respectively, can hold a great scope in combination therapy. (Fig. 2)

Amongst these, Methotrexate is one such drug which acts by reducing the amount of tetrahydrofolate required for the synthesis of purine bases. This action results in death of cancer cells [26]. Being also a powerful medication for variety of autoimmue disorders such as psoriasis [27] and rheumatoid arthritis [28], it has been commonly used in synergy with variety of drugs that include 5-Fluorouracil [29], Infliximab [30], Cytarabine [31] etc. Despite efforts, developing an attractive experimentation on synergism for cancer drug development is indeed a challenging task.

Benzodiazepine a pharmacophoric scaffold containing a ring complex made up of a benzene ring and a diazepam ring represents a class of psychoactive drugs. Besides, enhancing the effect of gamma-aminobutyric acid at the GABA receptor resulting in the sedative, hypnotic and anti-depressant activity, benzodiazepines exhibit wide range other significant biological applications [32–38]. Moreover, benzodiazepines have attracted attention of chemist in the field of drugs and pharmaceuticals [39].

The most commonly employed synthetic protocol for 1,5-benzodiazepines includes coupling diamines with α,β-unsaturated ketone [40,41], aliphatic ketones [42], β- diketones [43], β-ketoesters [44] in presence of acid or base. Distinct range of catalysts have been employed in the synthesis of 1,5-benzodiazepines [45–56]. Solvent free organic synthesis and transformations are said to be industrially constructive and green [57]. In our synthetic strategy towards 1,5-benzodiazepines, we choose Thiamine hydrochloride also called as vitamin B1, a water soluble vitamin employed as organocatalyst by virtue of its properties such as non– toxic, metal free, inexpensive, ease of isolation procedures etc. As a result of its structural appearance it has been considered as a powerful biocatalyst for various organic transformations by many synthetic organic chemists.[58–61] (Fig. 3)

As an extension to our work towards the development of methodologies for the synthesis of heterocyclic compounds, we hereby report an efficient and ecofriendly method for the synthesis of 1,5-benzodiazepines from substituted o-phenylenediamine and ketones. A simple model substrate was examined to establish the viability of the approach and to optimize the reaction conditions in presence of a biocatalyst under solvent free conditions. In view of the recent developments towards metal free synthesis, we decided to explore thiamine hydrochloride as catalyst.

2. Results and discussion

2.1. Chemistry

Derivatives of 2-Methyl-2,4-diphenyl-2,3-dihydro-1H-benzo [1,5] diazepine have been synthesized by condensation of substituted 2,3-diamino benzenes with different ketone substrates in presence of thiamine hydrochloride as a catalyst under solvent free neat heat conditions at 70–80 °C. The synthesis of compounds **3a-3a**[1] has been carried out as outlined in (scheme 1). To synthesize compounds **3a-3e** the condensation was carried out between o-phenylene diamine and substituted ketones. Similarly, to obtain compound **3f − 3 l** and **3 m − 3 s** 4-methyl-2-nitro-aniline and 4-chloro-2-nitro-aniline were initially reduced to 4-methyl-1,2-diamino benzene and 4-chloro-1,2 diamino benzene respectively using Sn/ HCl and were then condensed with ketone substrates using the same model methodology. The benzodiazepine derivatives **3 t-3w** were synthesized by condensation of ketones with 4-bromo-1,2 diamino benzene.

In the initial experiment, optimization was carried out wherein; acetophenone substrate was used as a representative substrate. The efficiency of the reaction depends on the physical factors such as amount of catalyst, temperature of the reaction and the type of solvent used. The optimal reaction conditions were investigated by varying the temperature, catalyst and solvent of the reaction system. Ultimately, 5 mol% of catalyst under solvent free neat heat reaction condition was witnessed as the most efficient method to carry out the synthesis. To study the synthetic utility of the employed catalyst and optimized reaction conditions, the methodology was applied on differently substituted o-phenylenediamine and ketone substrates. All the substituted aromatic and heterocyclic ketone substrates as well as substituted diamines reacted well to afford respective derivatives in good yields.

In all the cases, the reaction was monitored using thin layer chromatography. After completion, the reaction was quenched in water, followed by extraction in ethyl acetate. The crude product obtained was further isolated using column chromatography. The scope and generality of this method was extended by scrutinizing electronically divergent substituted ketones bearing various electron withdrawing or electron donating groups at ortho, meta, or para positions of the aromatic ring. Substitution pattern in target synthesis plays an important role in drug development. Presence of specific substituents such as halogens, alkyl and nitro, methoxy can be of great utility towards structure activity relationship studies. The results are encapsulated in Table 1. Para substituted nitro acetophenone was found to be most reactive for the condensation to take place with all the different substituted o-phenylenediamines. It was also inferred from the results that the yields of the product with respect to electron withdrawing substrates were higher in comparison to that of the electron donating substrates. Likewise, parent o-phenylene diamine showed better reactivity in terms of yields as compared to those of the substituted diamines

In order to investigate the feasibility of this synthetic methodology, towards differently substituted substrates and with a perspective of developing a better biologically active molecule, we synthesized scaffolds containing benzodiazepine. Pyridine being part of many natural products such as vitamins coenzymes is an interesting molecule with its
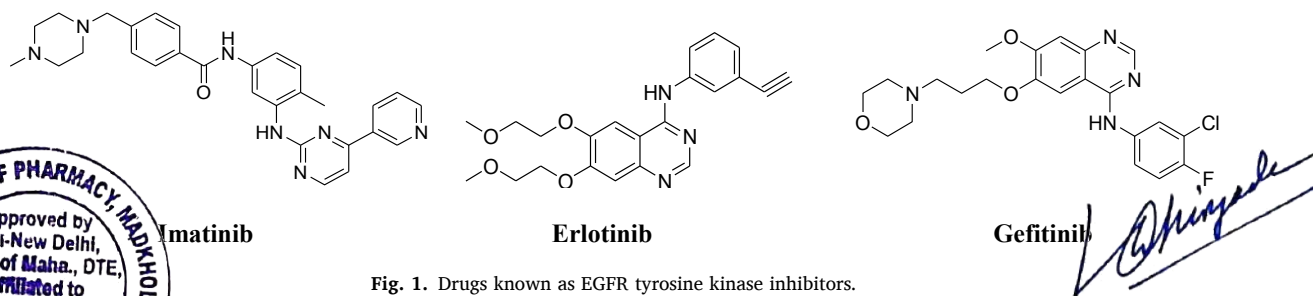

Imatinib　　　　　　**Erlotinib**　　　　　　**Gefitinib**

Fig. 1. Drugs known as EGFR tyrosine kinase inhibitors.
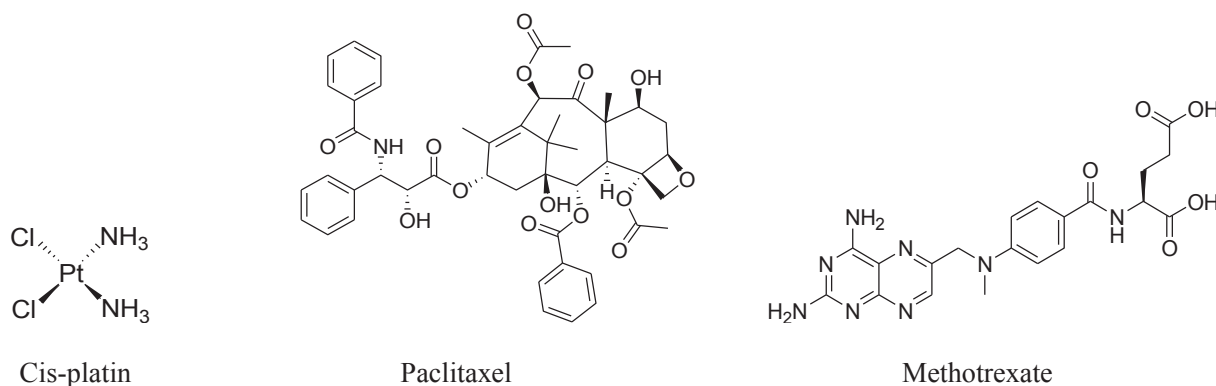
Fig. 2. Standard drugs used as anticancer agents.

Cis-platin   Paclitaxel   Methotrexate
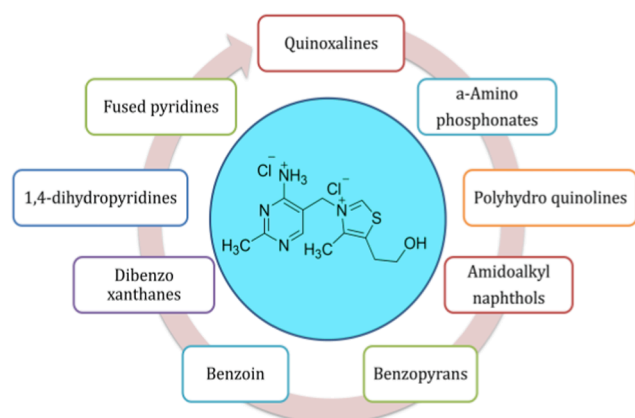

Fig. 3. Thiamine Hydrochloride (Vitamin B1).

beneficial drug favoring characteristics which includes its smaller size, basicity, water solubility, hydrogen bonding capability [62]. Naphthalene has also been seen as one of the most privileged molecule in the drug discovery field and has also been reported to possess anticancer properties [63,64]. Thus, to study the effect of these moieties in combination with benzodiazepine molecule we designed few molecules and examined the alterations in the biological properties. The synthesis was accomplished through a condensation reaction between substituted 1,2-diaminobenzenes with 2-acetyl pyridine, 4-acetyl pyridine and 2- acetyl naphthalene compounds (scheme 2).

The newly synthesized compounds have been characterized by ^{1}H NMR, ^{13}C NMR and mass spectroscopy. 1H NMR analysis confirms the formation of 1,5 -benzodiazepine structure. The main distinctive peaks in the spectra of all the target compounds is the appearance of two doublets in the range of δH at 2.5 to 3.5 ppm signifying the CH$_2$ protons at C3 of the seven membered benzodiazepine ring. The most deshielded proton was observed in case of the aromatic hydrogen present on the

phenyl ring substituted on C4 of the benzodiazepine ring. All the aromatic protons appeared as multiplets in the region δH 8.00 to 6.5 ppm, thereby marking the formation of 1,5-benzodiazepine derivatives. Along with this, ^{13}C NMR spectroscopic study also signifies the benzodiazepine formation. In C13 NMR spectra of all the compounds the characteristic peak of C4 (C=N) of the benzodiazepine ring appeared in the range of 164.7–167.2 ppm. Signal due to *C*2 was observed in the range of 72.7–73.4 ppm. Characteristic peak of formation of benzodiazepine ring signifying C3 (methylene-CH$_2$) carbon appeared at 42.9–43.4 ppm which was also confirmed in DEPT analysis. The exact molecular weight was also characterized and confirmed by HRMS studies. Purity of the compounds was checked using HPLC studies.

2.2. Biological activity

2.2.1. In-vitro screening

2.2.1.1. Cytotoxicity assay. In vitro cytotoxicity of the selected compounds **3a**, **3 k**, **3q**, **3w**, **3y** and **3x** was determined by the MTT [(3-(4,5-dimethyl-2- thiazolyl) 2,5-diphenyl-2H-tetrazolium bromide)] assay against a panel of three different human cancer cell lines namely; HEPG2 (human liver carcinoma), HeLa (human cervical) and HEK-293 T (Human embryonic kidney cells) normal cell line. The concentration required to suppress 50% of the tumor cells i.e. IC$_{50}$ values of the screened compounds and the reference drugs, Paclitaxel and Methotrexate are outlined in Table 2. As noticed, all compounds showed significant antitumor activities with IC$_{50}$ values in the range of 0.067–1.65 μM, this indicated that the 1,5-benzodiazepine group can intensify the antitumor effects. Compound **3x** bearing the 2,4-dipyridinyl group, on the benzodiazepine nucleus was found to be the most potent among all the screened compounds and showed enhanced activity (IC$_{50}$ values 0.067 μM against HeLa cell line and 0.087 μM against HepG2 cell line) against both the cancer cell lines . This was followed by compound **3q** with 3′-nitro substituted phenyl group on benzodiazepine ring, which displayed 0.10 ± 0.004 μM against HeLa cell line and 0.16 ± 0.01 μM
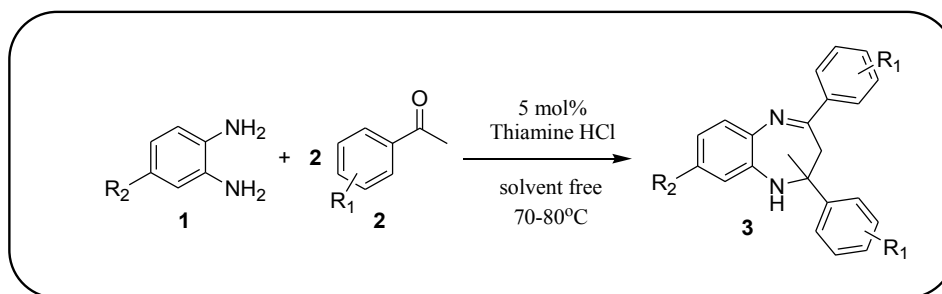

Scheme 1. Methodology for the synthesis of 1,5-benzodiazepines derivatives.

3

Table 1

List of synthesized 1,5-benzodiazepine derivatives detailing substrate scope for the reaction.

Compound	R_1	R_2	Time in h	% yield	Expt. M. Pt. °C	Lit M. Pt. °C
3a	H	H	1	66	140–142	143–145
3b	4-Br	H	3	66	140–144	145–146
3c	4-Cl	H	4	72	138–144	140–142
3d	4-NO$_2$	H	3	75	146–148	148–150
3e	3-NO$_2$	H	3.5	68	156–160	158–160
3f	H	CH$_3$	4.5	27	148–150	148–150
3g	4-NO$_2$	CH$_3$	3.5	55	146–150	N.R
3h	4-Br	CH$_3$	4	55	156–160	N.R
3i	4-Cl	CH$_3$	2.5	49	138–142	N.R
3j	3-Br	CH$_3$	4	50	150–154	N.R
3k	3-NO$_2$	CH$_3$	3	52	134–136	N.R
3l	4-OMe	CH$_3$	3	52	78–80	N.R
3m	H	Cl	3.5	62	138–140	138–142
3n	4-NO$_2$	Cl	3	66	162–164	N.R
3o	4-Br	Cl	3	58	154–156	N.R
3p	4-Cl	Cl	3.5	54	146–148	N.R
3q	3-NO$_2$	Cl	3.5	57	138–140	N.R
3r	3-Br	Cl	3	57	124–126	N.R
3s	4-F	Cl	3.5	35	138–140	N.R
3t	4-NO$_2$	Br	2.5	62	162–164	N.R
3u	4-Cl	Br	3.5	56	172–174	N.R
3v	3,4-OMe	Br	3.5	45	122–124	N.R
3w	3- NO$_2$	Br	4	57	136–138	N. R
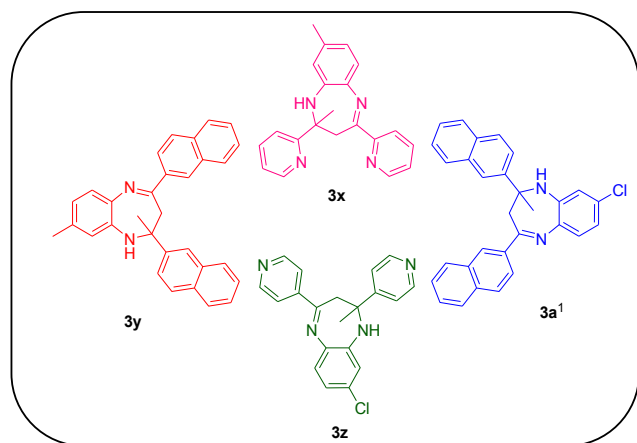
Scheme 2. Synthesis of scaffold containing 1,5-benzodiazepines.

against HepG2 cancer cell line. All the screened compounds **3a**, **3 k**, **3q**, **3w**, **3x** and **3y** were found to show better activity (0.067–0.21 μM) against HeLa cell lines compared to one of the reference compound

Paclitaxel (IC$_{50}$ values 0.23 μM). Compound **3x** showed analogous activity with respect to the other reference compound Methotrexate (IC$_{50}$ values 0.057 and 0.083 μM). Other screened compounds also showed good activity against both the cell lines. It is clear from the results that almost all the targets exhibit moderate to good cytotoxicity against human liver carcinoma and cervical cancer cell lines although very weakly toxic against normal human embryonic kidney cells. The cell viability action was observed in a dose-dependent manner. Impressively, the cell viability decreased with the increase in concentration of the compounds against the tabbed cancer cell lines. In case of compound **3x** the cell viability dropped off significantly to 65.7%, 48.3%, 38.4%, 34.7%, 29.2%, 24.9% with the concentrations of 12.5, 25, 50, 100, 200 and 400 μg/mL respectively. Fig. 4.

On the basis of these results structure activity relationship studies were executed by understanding the effect of substituents on cytotoxicity of the compounds. Compound **3a** with no substitution on either of the rings displayed moderate activity. Replacement of phenyl ring with heterocyclic ring i.e. 2-pyridinyl moiety resulted in highest activity whereas substitution with a non-heterocyclic moiety like naphthalene showed lowest activity among all the compounds. Considering the substitution on 2 and 3 position on benzodiazepine ring the order of cytotoxicity can be drawn as follows 2-pyridinyl > 4-NO$_2$-phenyl > H > 2-Naphthyl. Substitution variation on the phenyl ring of the benzodiazepine ring was also studied. Presence of electron withdrawing group such as Cl and Br showed good activity compared to the electron donating methyl group. Among the two halogens, the most electronegative Chlorine group showed better activity as compared to bromine group. With respect to phenyl ring substitution, the cytotoxicity order is Cl > Br > H > CH$_3$. The selectivity index (SI) value > 2 proved better selectivity and lower cytotoxicity of the synthesized compounds.

2.2.1.2. EGFR-Tyrosine kinase inhibition assay. These potent molecules were aimed as EGFR- tyrosine kinase inhibitors. To study the strength of inhibitory activity and inhibition pathway, the inhibitory concentration IC$_{50}$ values were determined against EGFR- tyrosine kinase enzyme using ELISA method. The IC$_{50}$ values of the synthesized compounds against ranged from 0.156 to 0.514 μM (Table 3). Interestingly, among all the studied derivatives, compound **3x** displayed prominent inhibition with IC$_{50}$ value 0.156 ± 0.003 μM. Structural divergences appeared to affect the potency of these compounds against the screened enzyme (Fig. 5).

2.2.1.3. Annexin V- FITC/ propidium iodide dual staining assay. To investigate the mechanism underlying the antiproliferative effect of these potent compounds, the mode of tumor cell death was analyzed by fluorescence activated cell sortor (FACS) caliber on HepG2 liver cancer cells treated with 20 μM of selected compounds for 24 h. The most prevailing technique used to study cell apoptosis/ necrosis is flow cytometry using propidium iodide (PI) and annexin V-FITC as dyes to

Table 2

Evaluation of cytotoxicity against carcinoma cells (IC$_{50}$ values in μM) of the selected synthesized compounds.

Compound	R	R_1	HeLa[a]	HepG2[b]	HEK293[c]	SI[d]-HeLa	SI-HEPG2
3a	H	H	0.13 ± 0.008	0.34 ± 0.02	0.72 ± 0.03	5.53	2.11
3k	3-NO$_2$	CH$_3$	0.15 ± 0.006	0.35 ± 0.04	0.39 ± 0.02	2.60	1.11
3q	3-NO$_2$	Cl	0.10 ± 0.004	0.16 ± 0.01	1.65 ± 0.03	16.50	16.5
3w	3-NO$_2$	Br	0.13 ± 0.007	0.16 ± 0.02	0.53 ± 0.01	4.07	10.31
3y	2-Naphthyl	CH$_3$	0.21 ± 0.01	0.22 ± 0.03	0.61 ± 0.04	2.90	2.90
3x	2-pyridinyl	CH$_3$	0.067 ± 0.002	0.087 ± 0.003	0.31 ± 0.02	4.62	3.56
Paclitaxel			0.23 ± 0.02	0.28 ± 0.03	–	–	–
Methotrexate			0.057 ± 0.001	0.083 ± 0.002	0.44 ± 0.01	–	–

[a] : human cervical cancer cell line
[b] : human liver carcinoma cell line
[c] : human embryonic kidney cell line
[d] : selectivity index was calculated as ratio of IC$_{50}$ value of normal human cell line to that of the cancerous cell line. IC$_{50}$ values are obtained as the mean ± SD (μM) from three different experiments.
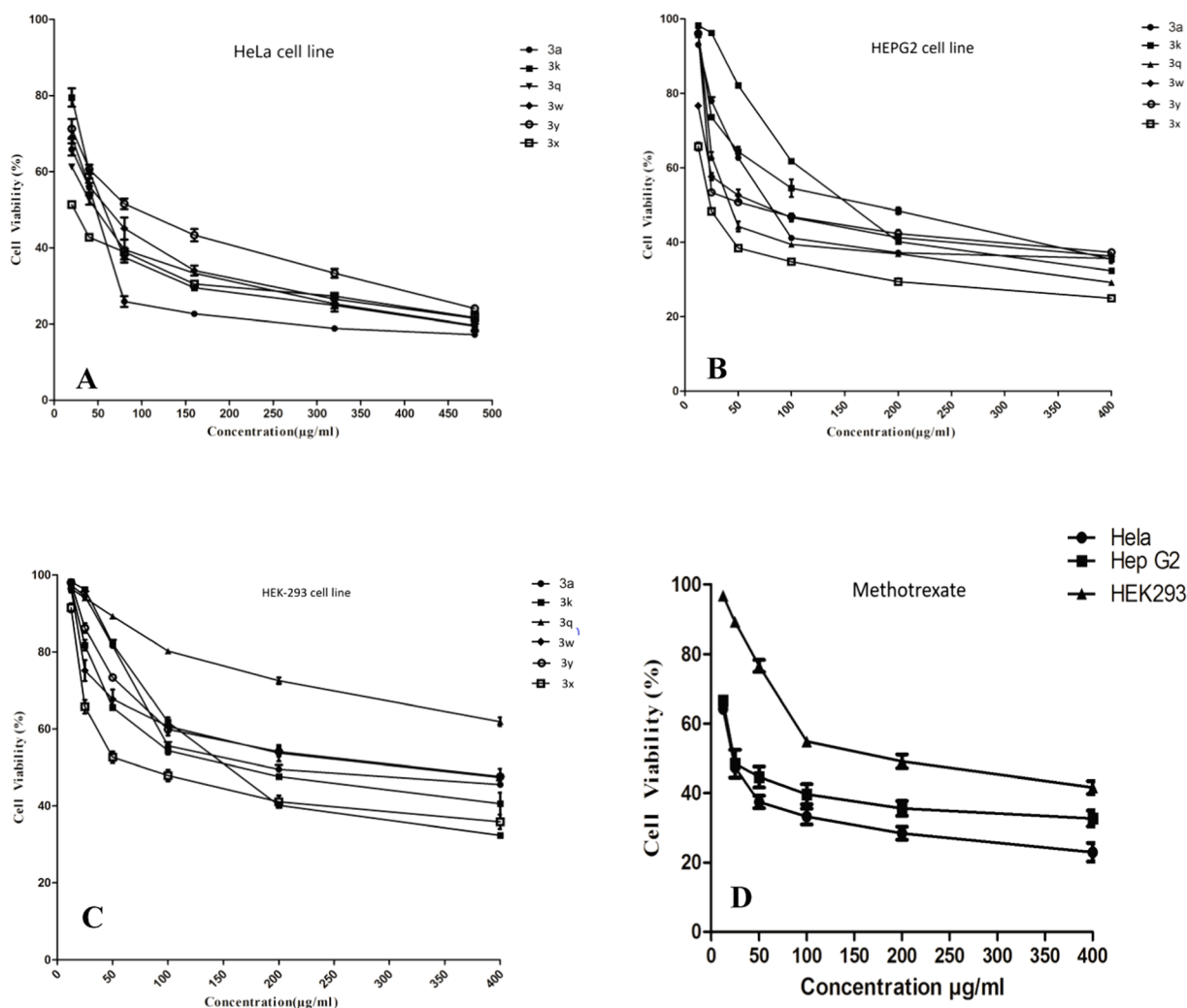
Fig. 4. Dose- dependent effect on cell viability of selected compounds for three different cell lines a: for HeLa cell line, b: for HepG2 cell line c: for HEK-293 cell line, d: cell viability exhibited by methotrexate for all the three cell lines.

Table 3

IC_{50} values of *in vitro* tyrosine kinase inhibition assay.

Compound	Tyrosine Kinase Inhibition($IC_{50 \text{ in }}$ μM)[a]
3d	0.514 ± 0.003
3 k	0.404 ± 0.002
3y	0.191 ± 0.005
3x	**0.156 ± 0.003**
Erlotinib	**0.08 ± 0.04**

[a] : Data are average of two independent runs

spot viable and dead cells. A negative control was used for the analysis. This assay facilitate the detection of live cells (Q1-LL; AV-/PI-), early apoptotic cells (Q1-LR; AV+/PI-), late apoptotic cells (Q1-UR; AV+/PI +) and necrotic cells (Q1-UL; AV-/PI +). As shown in Fig. 6, flow cytometry analysis revealed that HepG2 cells treated with compounds **3q**, **3w**, **3y** and **3x** showed apoptosis. The percentage of late apoptotic cells induced by compound **3q**, **3w**, **3y** and **3x** was 10.2%, 13.0%, 5.54% and 64.6% respectively.

2.2.1.4. Synergistic activity of compound 3x with drug Methotrexate. Synergistic drug combination studies have gained a promising research strategy with the motif of enhancing drug effect; improve drug selectivity by overcoming unwanted side effects, host immunity and normal cell toxicity current drug therapeutics by development of new
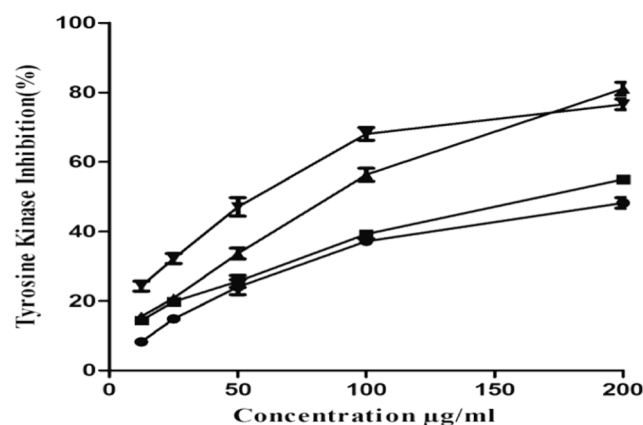

Fig. 5. Graphical representation of tyrosine kinase inhibition activity.

drug treatment strategies. Synergistic combinations of two or more drugs can conquer over toxicity and other side effects linked with steep shot of single drugs by resisting biological compensation, thereby treating multifactorial diseases. Striving to implement this strategy using our synthesized compound, we combined it with the methotrexate drug which is widely known as anti cancer agent. Synergistic studies
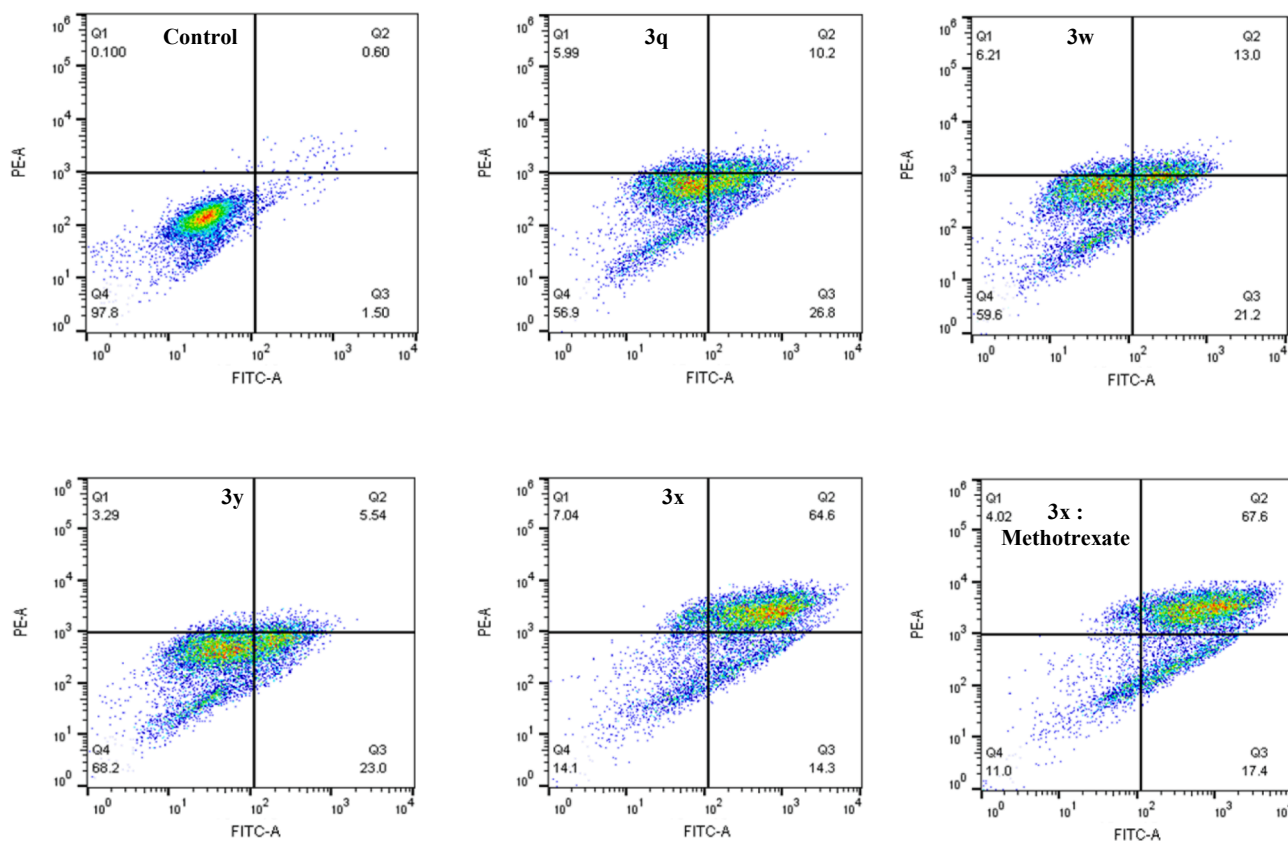
Fig. 6. The apoptosis of HepG-2 cells was detected by flow cytometry. HepG-2 cells were pre-treated without the addition of any samples, the control (C) (I); with a dose of 20 µM of compounds for 24 h. Cells were stained with Annexin-V and PI. The evaluation of apoptosis is via Annexin V: FITC Apoptosis Detection Kit per manufacture's protocol. And the quantitative results were shown in (V). In each scatter diagrams, the abscissa represents the fluorescence intensity of the cells dyed by Annexin V; and the ordinate represents the fluorescence intensity of the cells dyed by PI. The percentage of cells positive for Annexin V-FITC and/or Propidium iodide is represented inside the quadrants. Cells in the upper left quadrant (Q1-UL; AV-/PI +): necrotic cells; lower left quadrant (Q1-LL; AV-/PI-): live cells; lower right quadrant (Q1-LR; AV+/PI-): early apoptotic cells and upper right quadrant (Q1-UR; AV+/PI +): late apoptotic cells.

were carried out against HeLa and HEPG2 cancer cell lines using combination of compound **3x** and drug Methotrexate. As can be seen in Table 4, the results showed very good activity higher than the individual IC_{50} values against both the tested cancer cell lines. The combination resulted in improved activity with IC_{50} values of 0.046 ± 0.002 against HeLa cell line and 0.057 ± 0.002 against HEPG2 cell line. Enhancement in activity was also observed in case of flow cytometric analysis for cell death mode studies. The percentage of late apoptotic cells induced by the combination was 67.6% as shown in Fig. 6.

2.2.2. Molecular docking studies

2.2.2.1. As dihydrofolate reductase inhibitors (anticancer agents). To investigate the mechanism of antitumor activity and detailed intermolecular interactions between the synthesized compounds, molecular docking studies were performed on the crystal structure of dihydrofolate

reductase complexed with NADPH and Methotrexate using the surflex-dock programme of sybyl-X 2.0 software. All the inhibitors were docked into the active site of enzyme as shown in Fig. 7 (A and B). The docking study revealed that all the compounds have showed very good docking score as dihydrofolate reductase inhibitors.

As depicted in the Fig. 8(A and B), compound **3q** makes five hydrogen bonding interactions at the active site of the enzyme (PDB ID: 1DF7), among those three interactions were of oxygen atom of nitro group present at 3rd position of phenyl ring with hydrogen atoms of ARG60 and ARG32 (O——H-ARG60, 2.20 Å, 2.57 Å; O——H-ARG32, 2.14 Å), another oxygen atom of nitro group present at 3rd position of phenyl ring makes hydrogen bonding interaction with hydrogen atom of ARG32 (O——H-ARG60, 2.14 Å) and nitrogen atom of nitro group present at 3rd position of phenyl ring makes hydrogen bonding interaction with hydrogen atom of ARG60 (N——H-ARG60, 2.49 Å).

As depicted in the Fig. 9(A and B), compound **3w** makes six hydrogen

Table 4
Synergistic activity of compound **3x** with Methotrexate for cytotoxicity studies.

Compound	R	R_1	HeLa[a]	HEPG2[b]	HEK293[c]	SI[d]-HeLa	SI-HEPG2
3x	2-pyridinyl	CH_3	0.067 ± 0.002	0.087 ± 0.003	0.31 ± 0.02	4.62	3.56
3x :Methotrexate	–	–	0.046 ± 0.002	0.057 ± 0.002	–	–	–
Methotrexate			0.057 ± 0.001	0.083 ± 0.002	0.44 ± 0.01	–	–

[a] : human cervical cancer cell line.
[b] : human liver carcinoma cell line.
[c] : human embryonic kidney cell line.
[d] : selectivity index was calculated as ratio of IC_{50} value of normal human cell line to that of the cancerous cell line. IC_{50} values are obtained as the mean ± SD (µM) from three different experiments.
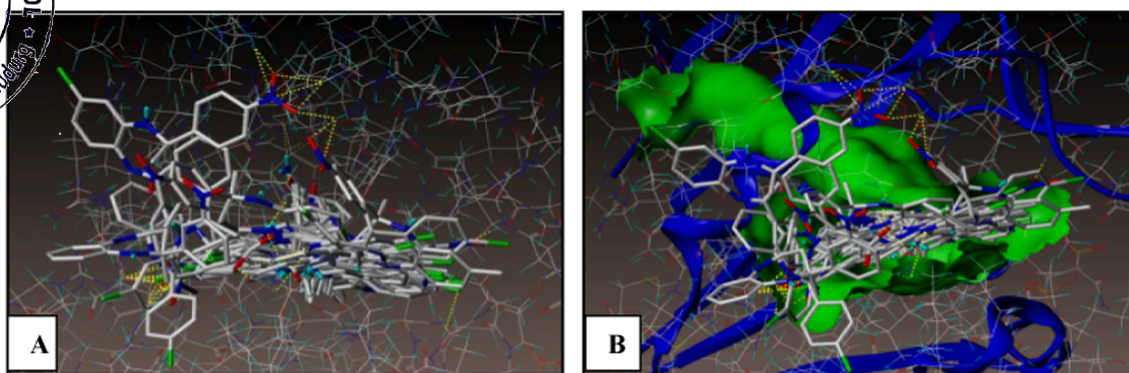
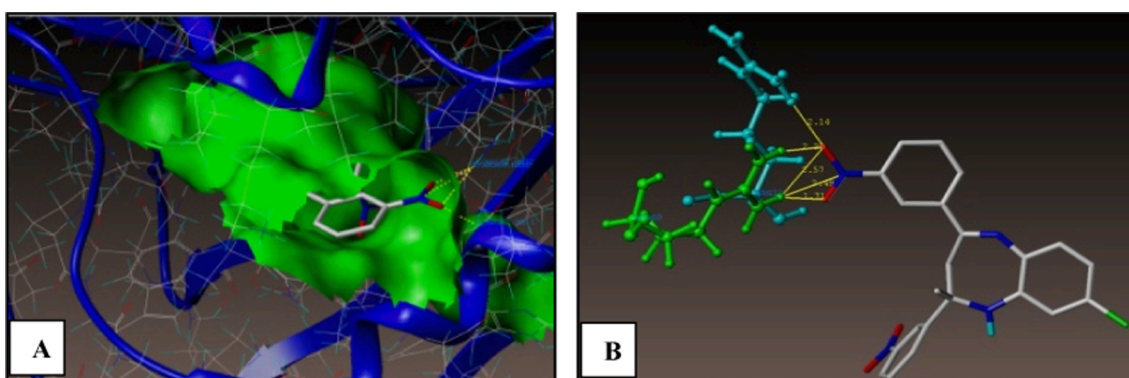**Fig. 7.** Docked view of all the compounds at the active site of the enzyme PDB ID: 1DF7.

Fig. 8. Docked view of compound **3q** at the active site of the enzyme PDB: 1DF7.

bonding interactions at the active site of the enzyme (PDB ID: 1DF7), among those three interactions were of oxygen atom of nitro group present at 3rd position of phenyl ring with hydrogen atoms of ARG60 and ARG32 (O——H-ARG60, 2.60 Å, 2.25 Å; O——H-ARG32, 2.18 Å), another oxygen atom of nitro group present at 3rd position of phenyl ring makes hydrogen bonding interactions with hydrogen atoms of ARG32 and TYR100 (O——H-ARG60, 1.71 Å; O——H-TYR100, 2.55 Å) and nitrogen atom of nitro group present at 3rd position of phenyl ring makes hydrogen bonding interaction with hydrogen atom of ARG60 (N——H-ARG60, 2.50 Å).

The binding interaction of 1DF7 ligand with dihydrofolate reductase active sites shows thirteen bonding interactions. The synthesized compounds bind to the enzyme in similar manner as that of 1DF7 ligand. The compounds have same H-bonding interactions with same amino acids ARG60, ARG32 and TYR100 as that of 1DF7 ligand. Fig. 10 (A and B)

represents the hydrophobic and hydrophilic amino acids surrounded to the studied compound **3q** and **3w**. All the compounds showed consensus score in the range 8.73–1.57, indicating the summary of all forces of interaction between ligands and the enzyme. These scores and interactions indicate that molecules preferentially bind to the enzyme in comparison to the reference 1DF7 ligand.

2.2.2.1.1. As tyrosine kinase inhibitors. In silico molecular docking study was performed on the compounds with Molegro Virtual Docker (MVD-2007, 6.0). Fig. 11 shows the structure of EGFR-tyrosine kinase complexed with a 4-anilinoquinazoline inhibitor obtained from Protein Data Bank with the PDB ID: 1 m17.

The crystal structure of the target enzyme including forty amino acids from the carboxyl-terminal tail has been determined to 2.6 A resolution. Unlike any other kinase enzymes, the EGFR family members possess constitutive kinase activity without a phosphorylation event
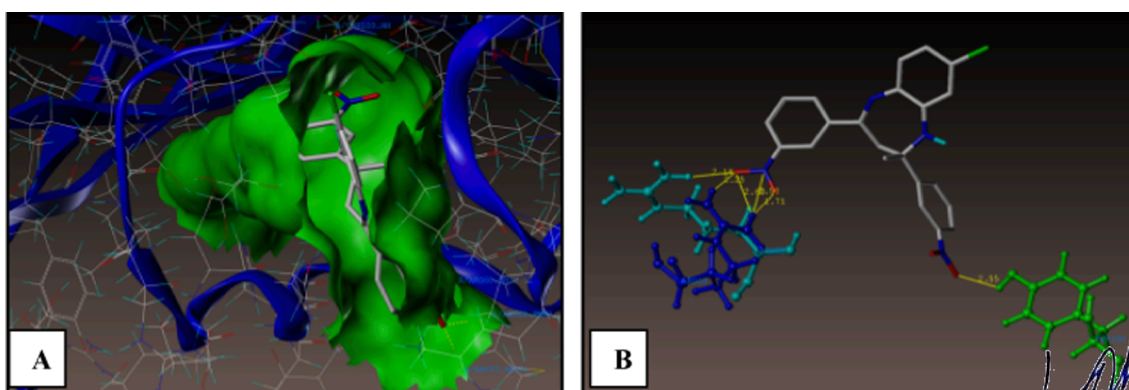

Fig. 9. Docked view of compound **3w** at the active site of the enzyme PDB: 1DF7.
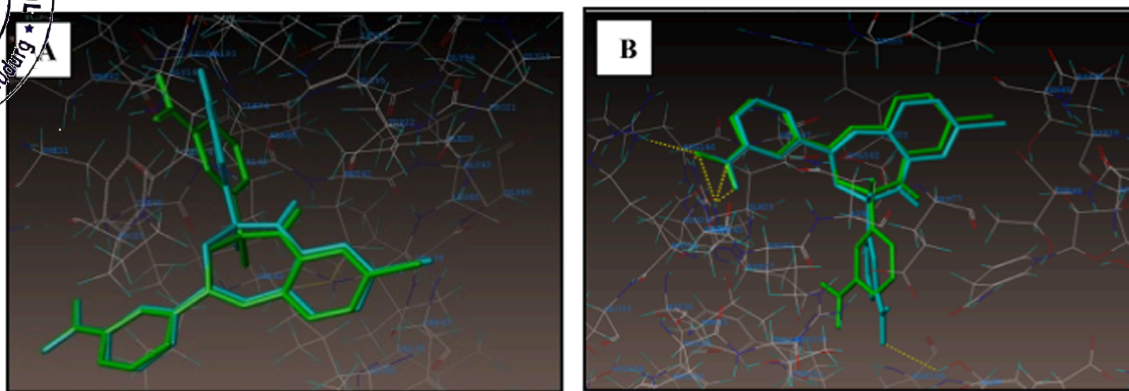
Fig. 10. A) Hydrophobic amino acids surrounded to compounds **3q** (green colour) and **3w** (cyan colour) B) Hydrophilic amino acids surrounded to compounds **3q** and **3w**.
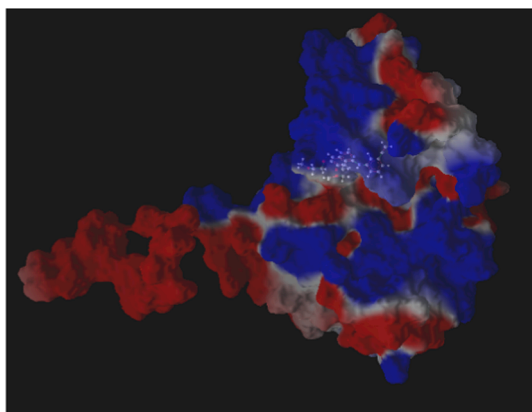

Fig. 11. Structure of EGFR-tyrosine kinase domain complexed with 4-anilino-quinazoline inhibitor. (PDB ID: 1m17)

within their kinase domains. Despite its lack of phosphorylation, the EGFRK activation loop adopts a conformation similar to that of the phosphorylated active form of the kinase domain from the insulin receptor. It is observed that the key residues of a dimerized structure lying between the EGFRK domain and carboxyl terminal substrate docking sites are found in close contact with the kinase domain. The site at which the known 4-anilinoquinazoline inhibitor binds with the target protein was selected as the active site. It is lined with amino acid residues such as Leu694, Met769, Thr830, Asp831, Glu738, Lys721, Cys773; *etc*.

Hence to identify other residual interactions of the tested compounds, a grid box (include residues within a 15.0 A radius) large enough to accommodate the active site was constructed. Since 4-Anilinoquinazoline is a known inhibitor, the centre of this site was considered as the centre of search space for docking. Docking of the synthesized compounds with EGFR tyrosine kinase domain exhibited well conserved hydrogen bonding with the amino acid residues at the active site. The MolDock scores of the test compounds ranged from −86.2649 to −116.861 while that of 4-anilinoquinazoline was −127.098.

The molecular docking study revealed that compounds **3n**, **3 s**, **3y** and **3x** acts as good inhibitors of tyrosine kinase due to characteristic features. However, compounds **3a-3a'** were found to be active with the target PDB ID: 1 M17. The best docked poses of the compounds are depicted in Fig. 12. Compound **3n** makes two hydrogen bond interactions at the active site of the enzyme. The interactions are raised by nitro group present on phenyl rings with Thr766 and Thr830. Compound **3z** and **3x** exhibited three hydrogen interactions of which two are of nitrogen of pyridine rings with Thr766 and Thr830 and the third

interaction is of nitrogen of benzodiazepine ring with Thr766.(See Figs. 13 and 14)

2.2.2.2. Docking studies on DNA intercalation:. A drug is known to act by interaction with macromolecules like DNA and proteins as a target. The studies of interaction of drug molecule with DNA have been an interesting path towards design and development of novel highly effective drug molecules. Interaction of drug molecule with DNA leads to a sequence of operations such as structural modifications, thereby killing the unwanted cells via disrupting its replication, transcription and repair. To study the interactions of the most active benzodiazepine **3x** among the synthesized derivative and to indicate the site of interaction, primary molecular docking studies were performed.

The molecule **3x** had high docking score of —8.3 kcal/mol. Visual inspection revealed that the ligands get intercalated in the minor grove of the DNA fragment. N^1 atom of benzodiazepine forms hydrogen bond with Thiamine while N atom of 4-pyridine ring forms hydrogen bond with adenine of the chain B of the DNA fragment. The 2-pyridine ring exhibits pi-stacked in-between two adenine rings of the DNA chain A.

2.2.2.2.1. Analysis of drug scan. For a molecule to be 'druglike', its molecular structure and biological effectiveness must be in a perfect harmony. There are various methods wherein the druglikeness can be analysed virtually considering the lipinski's RO5. In view of this, the toxicity and its feasibility to act like a drug were predicted for the synthesized compounds using Data Warrior 5.2.1. The toxicity results are presented in the following Tables 5 and 6. Based on the property calculation have favorable cLogP which should be ideally between 2.0 and 5.0 with some outliers (**3b**, **3c**, **3 h**, **3i**, **3j**, **3 m**, **3o**, **3p**, **3r**, **3 s**, **3u**, **3y**, **3a'**). Compounds that exhibit drug likeliness based on the prediction are **3a**, **3c**, **3f**, **3 l**, **3 m**, **3p**, **3v**, **3x**, **3y**, **3z**, **3a'**. Most of the compounds are devoid of toxicities except **3 l** and **3u** which are possibly mutagenic while **3a** and **3f** are probably teratogenic.

3. Conclusion

In conclusion, we have developed an efficient and convenient catalytic method for the synthesis of new derivatives of 2-Methyl-2,4-diphenyl-2,3-dihydro-1H-benzo[1,5]diazepine under solvent free reaction conditions. The current method is advantageous due to low environmental impact, clean reaction conditions, wide substrate scope of the reaction, use of non-toxic, metal free and inexpensive catalyst which makes this procedure a green alternative to the reported tedious methods for the synthesis of 1,5-benzodiazepines. The synthesized derivatives were characterized using NMR and Mass spectroscopy. Based on the molecular docking study, the best docked compounds **3g**, **3 k**, **3q**, **3w**, **3x** and **3y** were screened biologically for their anti tumor activity studies. Significant anti-proliferative activity was demonstrated by all the assessed compounds against the HeLa (human cervical cancer),
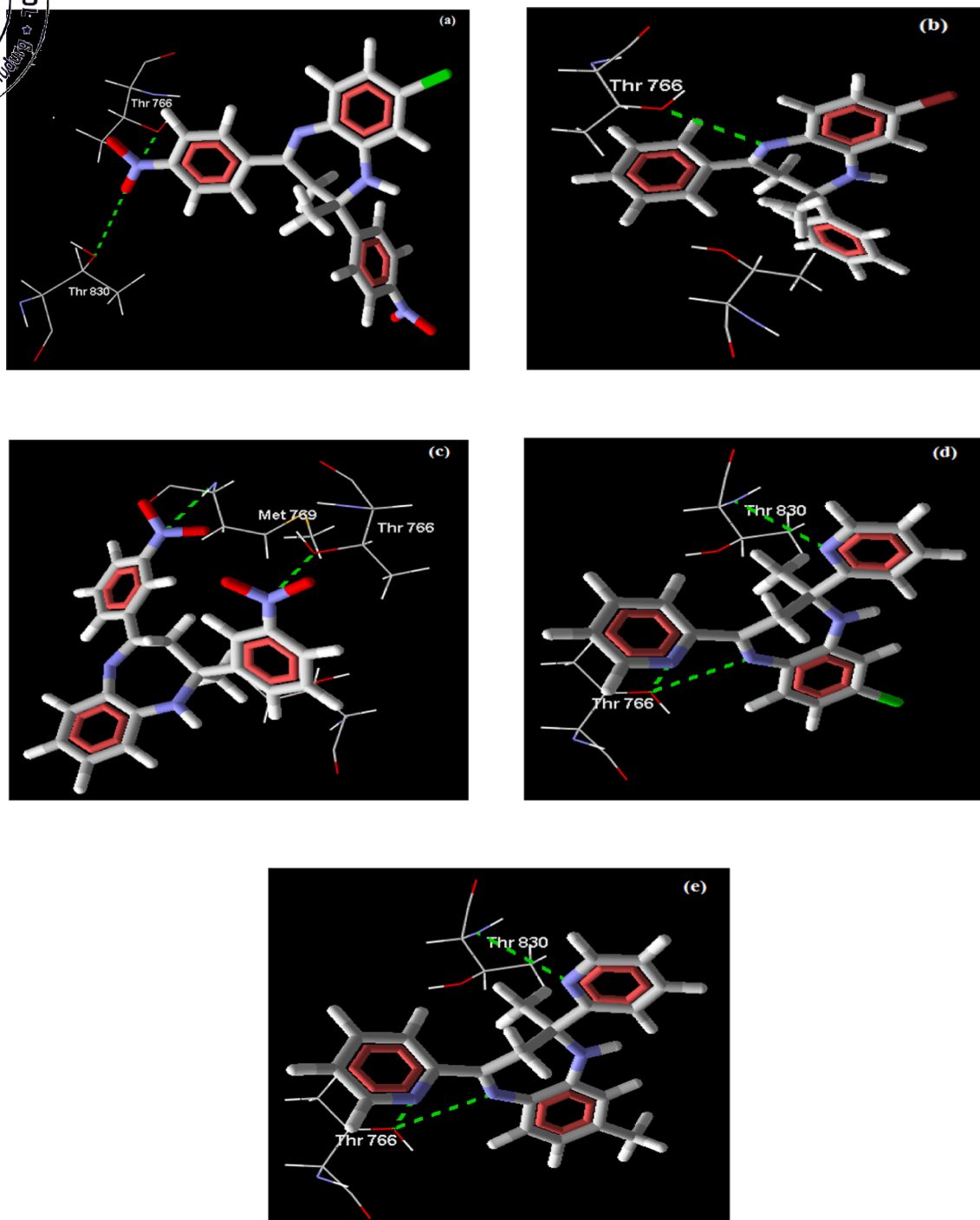
Fig. 12. Molecular docking data: The compounds docked in best of its conformation into the binding site of 1 M17. **a** Binding mode of compound 3 l forming two H bonds with Thr766 and Thr830;**b** binding mode of compound 3n forming one H bonds with Thr766; **c** binding mode of compound 3 s forming two H bonds with Met769 and Thr766; **d** & **e** binding modes of compound 4 g and 4 h forming two H bonds with Thr766 and Thr830, one H bond with Thr766.

HEPG2 (human liver carcinoma) cancer cell line and HEK-293 (normal human embryonic kidney) cell line. Compound **3x** was found to be the most versatile amongst all the compounds exhibiting both anti-tumor with the IC_{50} value of 0.067 ± 0.002 against HeLa cell line supported by apoptosis inducing mode of cell death. Drug synergism plays a key role in improving efficacy of drug. In order to exploit the synergistic behavior of the most potent compound **3x**, we performed synergistic activity in cytotoxicity studies of the same with drug Methotrexate. These studies were performed against HepG2 and HeLa cell lines with IC_{50} values of 0.046 ± 0.002 and 0.057 ± 0.002 which were better than the values of drug alone. Further this combination also showed promising results in apoptosis studies. The anticancer mechanistic studies indicated the compound **3x** to be good DNA intercalating agent. This proved that compound **3x** has a potency to be good lead to develop into drug molecule. DNA toxicity assessment prediction studies revealed the drug likeness of such compounds. Moreover, the present study endeavors an initiative approach for development of such targets, as good leads for enhancing the research scope for further exploitation of these molecules by broadening the efficacy of such novel molecules as potential anticancer agents.

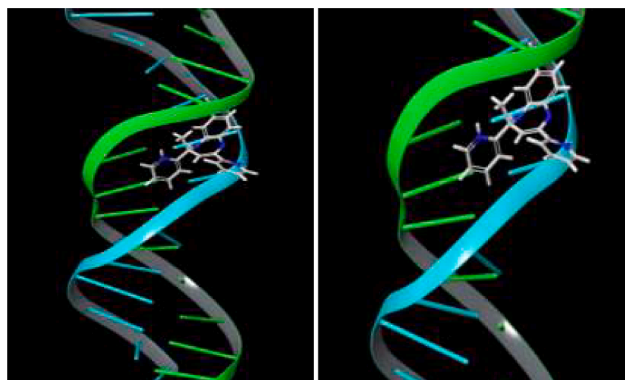| Ligand	2K4L	
	Docking Score	MMGBSA bind
3x	-8.318	-60.49

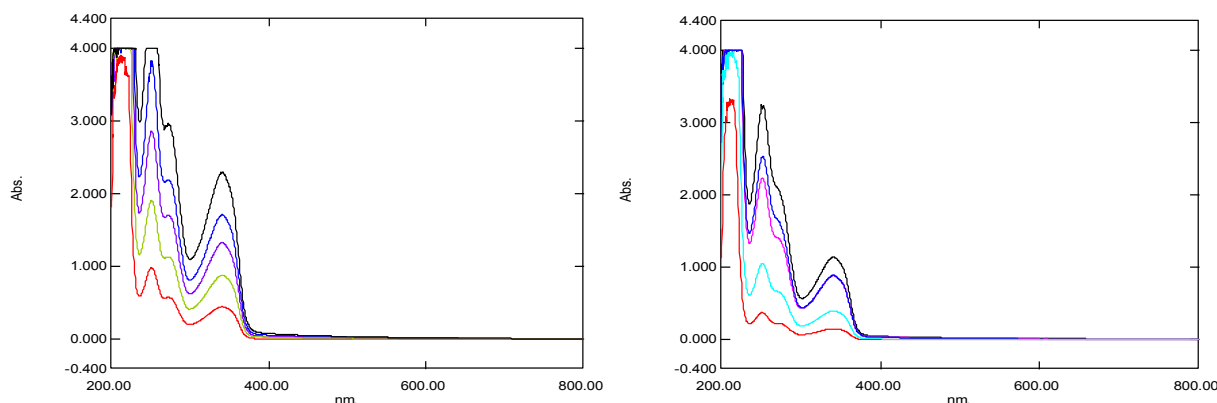**Fig. 13.** Docked view of compound **3x** intercalated into the DNA fragment.

Fig. 14. DNA binding studies using UV spectroscopy.

4. Experimental

4.1. Material methods

All commercially available solvents and reagents were purchased from SD-fine, Loba Chemie and Avra synthesis. o-phenylenediamines were used after recrystallization. Melting points were measured using open capillary tube method. The reactions were monitored by TLC carried out on Macherey – Nagel pre-coated TLC sheets SIL G/UV254 and visualized under UV light. SDFCL silica gel (200–400 mesh) was used for flash chromatography (Combi Flash Companion by Teledyne Isco). 1H and 13C NMR spectra were recorded on Bruker model 400 MHz instrument using CDCl3 solution. Chemical shifts (δ) are expressed in ppm (parts per million) relative to the residual solvent peaks as an internal standard (1H NMR: CDCl3 at 7.24 ppm, 13C NMR at 77.00 ppm) and coupling constant (J) are given in hertz. IR spectra were recorded on a Schimadzu Fourier Transform Infrared Spectrometer using KBr pallets. High resolution mass spectroscopy data were obtained in electron impact (EI) mode. Intensities are reported as percentages relative to the base peak (I = 100%).

4.2. General procedure for synthesis

o-phenylene diamine substrate (1 mmol) and substituted ketone derivative (2 mmol) were taken in a round bottom flask. To that 5 mol% of thiamine hydrochloride was added and heated on water bath at 70–80 °C for the time indicated in scheme 2. The reaction was monitored periodically till its completion. The reaction mixture was then quenched in cold water (15 mL), which was further extracted using ethyl acetate (3 × 10 mL) and dried over anhydrous Na$_2$SO$_4$. The crude product obtained was further purified using column chromatography pet ether-EtOAc (9:1). The isolated pure product was then characterized using IR, NMR and Mass spectropscopy.

4.3. Spectral data

4.3.1. 2,8-Dimethyl-2,4-bis-(4-nitro-phenyl)-2,3-dihydro 1H-benzo[b][1,4]diazepine (3g)

Orange solid, mp: 168–170 °C; IR (KBr) (ν_{max}, cm^{-1}): 3315, 1597, 1517, 1350. ^{1}HNMR(400 MHz, CDCl$_3$) (δ, ppm): 2.72 (s, 3H, CH$_3$–

Table 5
Toxicity prediction using data warrior 5.2.1.

Ligands	Mutagenic	Tumorigenic	Teratogenic	Irritant
3a	none	none	**high**	none
3f	none	none	**high**	none
3 l	**high**	none	none	none
3u	**high**	none	none	none

10

predicted with druglike properties obeying lipinski's RO5 with no toxicity parameters.

Ligands	Total Mol Weight	cLogP	H-bond Acceptors	H-bond Donors	Total Surface Area	Druglikeness
3b	402.41	2.66	8	1	297.48	−3.80
3e	402.41	2.66	8	1	297.48	−3.80
3g	416.44	3.00	8	1	309.74	−3.80
3k	416.44	3.00	8	1	309.74	−3.80
3n	452.90	3.26	8	1	312.90	−3.72
3q	436.85	3.26	8	1	312.90	−3.72
3t	481.31	3.38	8	1	316.11	−5.59
3w	402.41	2.66	8	1	297.48	−3.80
3x	328.42	2.95	4	1	259.92	1.37
3z	348.84	3.11	4	1	263.08	1.43

cyclic), 2.33 (s, 3H, CH$_3$– Ar) 2.88 (d, 1H, J = 13.2 Hz, CH$_2$[a]), 3.08 (d, 1H, J = 13.2 Hz, CH$_2$[b]), 3.4 (s, 1H, –NH), 6.64 (d, 1H, Ar-H, J = 0.8 Hz), 6.74 (d, 1H, Ar-H, J = 8 Hz), 6.86–6.89 (dd, 1H, Ar-H, J = 1.8 Hz, J = 8 Hz), 7.55–7.11 (m, 8H, Ar-H) ^{13}C NMR (75 MHz, CDCl$_3$) (δ, ppm): 165.6, 155.3, 150.7, 145.6, 136.0, 135.6, 134.6, 133.2, 131.2, 131.0, 129.2, 128.0, 123.3, 118.9, 113.4, 73.2, 43.2 (CH$_2$), 29.2, 21.2; HRMS (ESI-TOF, [M]$^+$) : calcd for C$_{23}$H$_{20}$N$_4$O$_4$, 416.15; found 416.1527.

4.3.2. 2,4-Bis-(4-bromo-phenyl)-2,8-dimethyl-2,3-dihydro-1H-benzo[b][1,5]diazepine (3h)

Yellow solid, mp: 142–144 °C; IR (KBr) (ν_{max}, cm^{-1}): 3323, 1601, 1510, 784. ^{1}HNMR(400 MHz, CDCl$_3$) (δ, ppm): 1.76 (s, 3H, CH$_3$– cyclic), 2.36 (s, 3H, CH$_3$– Ar) 2.90 (d, 1H, J = 13.2 Hz, CH$_2$[a]), 3.08 (d, 1H, J = 13.2 Hz, CH$_2$[b]), 3.4 (s, 1H, Ar-H, J = 0.8 Hz), 6.74–7.76 (m, 10H, Ar-H) ^{13}C NMR (75 MHz, CDCl$_3$) (δ, ppm): 165.0, 149.5, 141.5, 137.4, 136.9, 136.8, 132.4, 130.2, 130.0, 129.5, 129.0, 128.9, 125.3, 124.3, 73.1, 43.2(CH$_2$), 29.8, 21.1; Mol. formula : calcd for C$_{23}$H$_{20}$N$_2$Br$_2$, 481.99.

4.3.3. 2,4-Bis-(4-chloro-phenyl)-2,8-dimethyl-2,3-dihydro-1H-benzo[b][1,5]diazepine (3i)

Yellow solid, mp: 156–158 °C; IR (KBr) (ν_{max}, cm^{-1}): 3061, 1604, 1487, 1328, 831. ^{1}HNMR(400 MHz, CDCl$_3$) (δ, ppm): 1.56 (s, 3H, CH$_3$– cyclic), 1.85 (s, 3H, CH$_3$– Ar) 3.0 (d, 1H, J = 13.2 Hz, CH$_2$[a]), 3.72 (d, 1H, J = 13.2 Hz, CH$_2$[b]), 3.75 (s, 1H, –NH), 6.90–8.08 (m, 11H, Ar-H) ^{13}C NMR (75 MHz, CDCl$_3$) (δ, ppm): 165.1, 145.9, 140.1, 137.9, 137.0, 136.1, 135.0, 133.2, 131.7, 129.7, 129.5, 129.3, 129.1, 128.8, 128.2, 127.3, 126,9, 121.6, 72.7, 42.9 (CH$_2$), 29.5, 20.5; Mol. formula: Calcd for C$_{23}$H$_{20}$N$_2$Cl$_2$, 394.10

4.3.4. 2,4-Bis-(3-bromo-phenyl)-2,8-dimethyl-2,3-dihydro-1H-benzo[b][1,5]diazepine (3j)

Orange solid, mp: 138–140 °C; IR (KBr) (ν_{max}, cm^{-1}): 3315, 1597, 1517, 1350, 752. ^{1}HNMR(400 MHz, CDCl$_3$) (δ, ppm): 1.74 (s, 3H, CH$_3$– cyclic), 2.34 (s, 3H, CH$_3$– Ar) 2.88 (d, 1H, J = 13.2 Hz, CH$_2$[a]), 3.07 (d, 1H, J = 13.2 Hz, CH$_2$[b]), 3.43 (s, 1H, –NH), 6.75–7.73 (m, 11H, Ar-H) ^{13}C NMR (75 MHz, CDCl$_3$) (δ, ppm): 164.9, 149.5, 141.5, 137.3, 136.9, 132.4, 130.2, 129.9, 129.4, 128.9, 125.4, 124.32, 122.72, 122.41, 73.3, 43.3 (CH$_2$), 29.8, 21.0; HRMS (ESI-TOF, [M]$^+$) : calcd for C$_{23}$H$_{20}$N$_2$Br$_2$, 482.00; found 482.0059.

4.3.5. 2,8-Dimethyl-2,4-bis-(3-nitro-phenyl)-2,3-dihydro-1H-benzo[b][1,5]diazepine (3k)

Orange solid, mp: 134–136 °C; IR (KBr) (ν_{max}, cm^{-1}): 3313, 1598, 1516, 1349. ^{1}HNMR(400 MHz, CDCl$_3$) (δ, ppm): 1.72 (s, 3H, CH$_3$– cyclic), 2.33 (s, 3H, CH$_3$– Ar), 2.87 (d, 1H, CH$_2$[a]), 3.08 (d, 1H, J = 13.2 Hz, CH$_2$[b]), 3.43 (s, 1H, –NH), 6.64 (d, 1H, Ar-H, J = 1.2 Hz), 6.73–7.49(m, 10H, Ar-H) ^{13}C NMR (75 MHz, CDCl$_3$) (δ, ppm): 164.9, 149.5, 141.5, 137.3, 136.9, 136.8, 132.4, 130.2, 130.0, 129.8, 129.0, 129.4, 129.0, 128.9, 125.4, 124.3, 122.7, 122.41, 121.62,73.1, 43.2 (CH$_2$), 29.8, 21.8; HRMS (ESI-TOF, [M]$^+$) : Calcd for C$_{23}$H$_{20}$N$_4$O$_4$, 416.15; found 416.1659.

4.3.6. 2,4-Bis-(4-methoxy-phenyl)-2,8-dimethyl-2,3-dihydro-1H-benzo[b][1,5]diazepine (3l)

Yellow solid, mp: 102–104 °C; IR (KBr) (ν_{max}, cm^{-1}): 3331, 1589, 1508, 1247. ^{1}HNMR(400 MHz, CDCl$_3$) (δ, ppm): 1.65 (s, 3H, CH$_3$– cyclic), 2.26 (s, 3H, CH$_3$– Ar), 2.84 (d, 1H, J = 13.2 Hz, CH$_2$[a]), 2.98 (d, 1H, J = 13.2 Hz, CH$_2$[b]), 3.42 (s, 1H, –NH), 3.67 (s, 3H, OMe), 3.72 (s, 3H, OMe) 6.59–7.60 (m, 11H, Ar-H) ^{13}C NMR (75 MHz, Mol. formula : Calcd for C$_{25}$H$_{26}$O$_2$N$_2$, 386.20.

4.3.7. 8-Chloro-2-methyl-2,4-bis-(4-nitro-phenyl)-2,3-dihydro-1H-benzo[b][1,5]diazepine (3n)

Orange solid, mp: 162–164 °C; IR (KBr) (ν_{max}, cm^{-1}): 3383, 1597, 1517, 1348, 856. ^{1}HNMR(400 MHz, CDCl$_3$) (δ, ppm): 1.77 (s, 3H, CH$_3$– cyclic), 2.84 (d, 1H, J = 13.76 Hz, CH$_2$[a]), 3.02 (d, 1H, J = 13.76 Hz, CH$_2$[b]), 3.37 (s, 1H, –NH), 6.87–7.58 (m, 11H, Ar-H) ^{13}C NMR (75 MHz, CDCl$_3$) (δ, ppm): 163.8, 153.5, 148.4, 147.0, 138.3, 136.7, 132.7, 131.3, 127.6, 126.7, 123.7, 123.5, 122.0, 120.4, 72.5, 43.2 (CH$_2$), 30.6; HRMS (ESI-TOF, [M]$^+$) : calcd for C$_{22}$H$_{17}$N$_4$O$_4$Cl, 436.098; found 436.1004.

4.3.8. 2,4-Bis-(4-bromo-phenyl)-8-chloro-2-methyl-2,3-dihydro-1H-benzo[b][1,5]diazepine (3o)

Brownish yellow solid, mp: 154–156 °C; IR (KBr) (ν_{max}, cm^{-1}): 3279, 1604, 1589, 1517, 831, 720. ^{1}HNMR(400 MHz, CDCl$_3$) (δ, ppm): 1.73 (s, 3H, CH$_3$– cyclic), 2.85 (d, 1H, J = 18 Hz, CH$_2$[a]), 3.11 (d, 1H, J = 18 Hz, CH$_2$[b]), 3.52 (s, 1H, –NH), 6.75–7.72 (m, 11H, Ar-H) ^{13}C NMR (75 MHz, CDCl$_3$) (δ, ppm): 166.1, 145.9, 140.8, 138.7, 137.7, 136.1, 131.4, 131.3, 130.1, 129.8, 128.6, 128.5, 128.0, 127.3, 126.8, 125.0, 124.8, 122.4, 121.4, 120.61, 72.7, 43.0 (CH$_2$), 29.6; HRMS (ESI-TOF, [M]$^+$) : Calcd for C$_{22}$H$_{17}$N$_2$Br$_2$Cl, 501.95; found 501.9589.

4.3.9. 8-Chloro-2,4-bis-(4-chloro-phenyl)-2-methyl-2,3-dihydro-1H-benzo[b][1,5]diazepine (3p)

Yellow solid, mp: 146–148 °C; IR (KBr) (ν_{max}, cm^{-1}): 3269, 1604, 1591, 1469, 810. ^{1}HNMR(400 MHz, CDCl$_3$) (δ, ppm): 1.74 (s, 3H, CH$_3$– cyclic), 2.87 (d, 1H, J = 13.5 Hz, CH$_2$[a]), 3.08 (d, 1H, J = 13.5 Hz, CH$_2$[b]), 3.51 (s, 1H, –NH), 6.73–7.50 (m, 11H, Ar-H) ^{13}C NMR (75 MHz, CDCl$_3$) (δ, ppm): 166.2, 145.4, 141.0, 138.7, 137.6, 136.3, 133.3, 131.5, 130.5, 130.1, 128.5, 128.4, 128.3, 128.0, 127.0, 126.3, 122.5, 121.8, 120.7, 73.7, 43.1 (CH$_2$), 29.7; HRMS (ESI-TOF, [M]$^+$) : Calcd for C$_{22}$H$_{17}$Cl$_3$N$_2$, 414.05; found 414.0513.

4.3.10. 8-Chloro-2-methyl-2,4-bis-(3-nitro-phenyl)-2,3-dihydro-1H-benzo[b][1,5]diazepine (3q)

Orange solid, mp: 138–140 °C; IR (KBr) (ν_{max}, cm^{-1}): 3317, 1605, 1518, 1350. ^{1}HNMR(400 MHz, CDCl$_3$) (δ, ppm): 1.97 (s, 3H, CH$_3$– cyclic), 2.95 (d, 1H, J = 13.5 Hz, CH$_2$[a]), 3.30 (d, 1H, J = 13.5 Hz, CH$_2$[b]), 3.90 (s, 1H, –NH), 6.92–8.38 (m, 11H, Ar-H) ^{13}C NMR (75 MHz, CDCl$_3$) (δ, ppm): 164.1, 148.7, 148.2, 148.0, 140.4, 138.4, 137.2, 132.5, 132.2, 131.9, 130.5, 129.6, 129.3, 124.6, 122.4, 122.0, 121.6, 120.8, 120.7, 73.3, 43.1 (CH$_2$), 30.3; HRMS (ESI-TOF, [M]$^+$) : Calcd for C$_{23}$H$_{17}$N$_4$O$_4$Cl, 436.09; found 436.1004.

4,2-Bis-(5-bromo-phenyl)-8-chloro-2-methyl-2,3-dihydro-1H-benzo[b][1,5]diazepine (3r)

solid, mp: 124–126 °C; IR (KBr) (ν_{max}, cm^{-1}): 3277, 1605, 1581, 1485, 821, 715. ^{1}HNMR(400 MHz, CDCl$_3$) (δ, ppm): 1.71 (s, 3H, CH$_3$– cyclic), 2.85 (d, 1H, $J = 18$ Hz, CH$_2^a$), 3.05 (d, 1H, $J = 18$ Hz, CH$_2^b$), 3.62 (s, 1H, –NH), 6.83–7.65 (m, 11H, Ar-H) ^{13}C NMR (75 MHz, CDCl$_3$) (δ, ppm): 166.1, 149.0, 141.1, 138.7, 137.7, 132.8 131.6, 130.1, 129.0, 128.0, 126.8, 126.5, 125.5, 124.3, 122.8, 122.5, 121.7, 120.7, 73.2, 43.3 (CH$_2$), 30.1; HRMS (ESI-TOF, [M]$^+$) : Calcd for C$_{22}$H$_{17}$N$_2$Br$_2$Cl, 501.95; found 501.9589.

4.3.12. 8-Chloro-2-methyl-2,4-bis-(4-fluoro-phenyl)-2,3-dihydro-1H-benzo[b][1,5]diazepine (3q)

Orange solid, mp: 138–140 °C; IR (KBr) (ν_{max}, cm^{-1}): 3317, 1605, 1518, 1350. ^{1}HNMR(400 MHz, CDCl$_3$) (δ, ppm): 1.73 (s, 3H, CH$_3$– cyclic), 2.87 (d, 1H, $J = 13.5$ Hz, CH$_2^a$), 3.09 (d, 1H, $J = 13.5$ Hz, CH$_2^b$), 3.48 (s, 1H, –NH), 6.82–7.52 (m, 11H, Ar-H) ^{13}C NMR (75 MHz, CDCl$_3$) (δ, ppm): 166.5, 142.6, 138.7, 138.2, 136.3, 135.4, 131.2, 129.9, 129.0, 127.4, 127.3, 126.1, 122.6, 121.8, 120.8, 115.2, 115.0, 114.8, 73.1, 43.4 (CH$_2$), 30.2; HRMS (ESI-TOF, [M]$^+$) : Calcd for C$_{23}$H$_{17}$N$_2$F$_2$Cl, 382.10; found 382.1169.

4.3.13. 8-Bromo-2-methyl-2,4-bis-(4-nitro-phenyl)-2,3-dihydro-1H-benzo[b][1,5]diazepine (3t)

Orange solid, mp: 162–164 °C; IR (KBr) (ν_{max}, cm^{-1}): 3390, 1597, 1517, 1347. ^{1}HNMR(400 MHz, CDCl$_3$) (δ, ppm): 1.83 (s, 3H, CH$_3$– cyclic), 2.97 (d, 1H, $J = 13.32$ Hz, CH$_2^a$), 3.35 (d, 1H, $J = 13.32$ Hz, CH$_2^b$), 3.72 (s, 1H, –NH), 7.04–8.06 (m, 11H, Ar-H) ^{13}C NMR (75 MHz, CDCl$_3$) (δ, ppm): 166.6, 142.6, 138.8, 138.2, 136.3, 135.4, 131.2, 129.9, 129.2, 129.1, 127.4, 127.3, 126.1, 122.6, 121.8, 120.8, 115.2, 115.1, 115.0, 73.1, 43.4(CH$_2$), 30.1; HRMS (ESI-TOF, [M]$^+$) : calcd for C$_{22}$H$_{17}$N$_4$O$_4$Br, 480.042; found 480.0500.

4.3.14. 8-Bromo-2,4-bis-(4-chloro-phenyl)-2-methyl-2,3-dihydro-1H-benzo[b][1,5]diazepine (3u)

Orange solid, mp: 172–174 °C; IR (KBr) (ν_{max}, cm^{-1}): 3269, 1604, 1469, 831. ^{1}HNMR(400 MHz, CDCl$_3$) (δ, ppm): 1.77 (s, 3H, CH$_3$– cyclic), 2.84 (d, 1H, $J = 13.76$ Hz, CH$_2^a$), 3.03 (d, 1H, $J = 13.76$ Hz, CH$_2^b$), 3.37 (s, 1H, –NH), 6.93–7.58 (m, 11H, Ar-H) ^{13}C NMR (75 MHz, CDCl$_3$) (δ, ppm): 166.1, 145.3, 140.9, 138.7, 137.9, 137.5, 136.5, 136.2, 133.2, 131.4, 130.1, 128.5, 128.3, 128.0, 127.0, 126.3, 122.5, 121.8, 120.6, 73.6, 43.1(CH$_2$), 30.0; HRMS (ESI-TOF, [M]$^+$) : calcd for C$_{22}$H$_{17}$BrCl$_2$N$_2$, 458.00; found 458.0038.

4.3.15. 8-Bromo-2,4-bis-(3,4-dimethoxy-phenyl)-2-methyl-2,3-dihydro-1H-benzo[b][1,5]diazepine (3v)

Yellow solid, mp: 122–124 °C; IR (KBr) (ν_{max}, cm^{-1}): 3299, 1589, 1566, 1446, 1252. ^{1}HNMR(400 MHz, CDCl$_3$) (δ, ppm): 1.76 (s, 3H, CH$_3$– cyclic), 2.82 (d, 1H, $J = 13.32$ Hz, CH$_2^a$), 3.02 (d, 1H, $J = 13.32$ Hz, CH$_2^b$), 3.37 (s, 1H, –NH), 3.65 (s, 3H, OCH$_3$), 3.66 (s, 3H, OCH$_3$), 3.79 (s, 3H, OCH$_3$), 3.84 (s, 3H, OCH$_3$), 7.48–6.62 (m, 9H, Ar-H) ^{13}C NMR (75 MHz, CDCl$_3$) (δ, ppm): 167.2, 153.3, 149.0, 147.6, 147.3, 140.5, 137.3, 130.5, 127.2, 123.0, 121.2, 119.15, 114.6, 114.2, 112.5, 110.0, 109.9, 73.3, 56.1, 43.3(CH$_2$), 26.3; HRMS (ESI-TOF, [M]$^+$) : Calcd for C$_{26}$H$_{27}$Br$_3$N$_2$O$_4$, 510.37; found 510.3710.

4.3.16. 8-Chloro-2-methyl-2,4-bis-(3-nitro-phenyl)-2,3-dihydro-1H-benzo[b][1,5]diazepine (3w)

Orange solid, mp: 138–140 °C; IR (KBr) (ν_{max}, cm^{-1}): 3319, 1604, 1519, 1348. ^{1}HNMR(400 MHz, CDCl$_3$) (δ, ppm): 1.84 (s, 3H, CH$_3$– cyclic), 2.94 (d, 1H, $J = 13.2$ Hz, CH$_2^a$), 3.27 (d, 1H, $J = 13.2$ Hz, CH$_2^b$), 3.91 (s, 1H, –NH), 6.77–8.40 (m, 11H, Ar-H) ^{13}C NMR (75 MHz, CDCl$_3$) (δ, ppm): 164.3, 148.7, 148.0, 140.4, 138.7, 136.5, 132.6, 131.9, 131.3, 130.7, 130.0, 129.6, 129.3, 124.8, 123.0, 122.4, 120.9, 73.9, 43.0(CH$_2$), 30.3; HRMS (ESI-TOF, [M]$^+$) : Calcd for C$_{23}$H$_{17}$N$_4$O$_4$Br, 480.04; found 480.0500.

4.3.17. 2,8-Dimethyl-2,4-di-pyridin-2-yl-2,3-dihydro-1H-benzo[b][1,5]diazepine (3x)

Orange solid, mp: 112–114 °C; IR (KBr) (ν_{max}, cm^{-1}): 3321, 1620, 1588, 1566, 1471. ^{1}HNMR(400 MHz, CDCl$_3$) (δ, ppm): 1.73 (s, 3H, CH$_3$–cyclic), 2.33 (s, 3H, CH$_3$– Ar) 2.87 (d, 1H, $J = 12.4$ Hz, CH$_2^a$), 3.05 (d, 1H, $J = 12.4$ Hz, CH$_2^b$), 3.42 (s, 1H, –NH), 6.64–7.55 (m, 11H, Ar-H) ^{13}C NMR (75 MHz, CDCl$_3$) (δ, ppm): 167.2, 163.4, 163.1, 160.9, 139.4, 129.7, 129.6, 128.6, 127.5, 127.4, 123.5, 115.4, 115.3, 115.2, 115.1, 73.4, 43.0(CH$_2$), 29.7, HRMS (ESI-TOF, [M]$^+$) : calcd for C$_{21}$H$_{20}$N$_4$, 328.18; found 328.1821.

4.3.18. 2,8-Dimethyl-2,4-di-naphthalen-2-yl-2,3-dihydro-1H-benzo[b][1,5]diazepine (3y)

Yellow solid, mp: 138–140 °C; IR (KBr) (ν_{max}, cm^{-1}): 3282, 1612, 1469,1321. ^{1}HNMR(400 MHz, CDCl$_3$) (δ, ppm): 1.87 (s, 3H, CH$_3$– cyclic), 2.37 (s, 3H, CH$_3$– Ar) 3.15 (d, 1H, $J = 13.2$ Hz, CH$_2^a$), 3.35 (d, 1H, $J = 13.2$ Hz, CH$_2^b$), 3.61 (s, 1H, –NH), 6.71 (d, 1H, Ar-H, $J = 0.8$ Hz), 6.80 – 8.10 (m, 17H, Ar-H) ^{13}C NMR (75 MHz, CDCl$_3$) (δ, ppm): 166.7, 145.0, 138.0, 137.7, 137.2, 136.9, 136.4, 135.5, 133.9, 133.8, 133.1, 132.7, 131.6, 128.7, 128.2, 127.6, 127.3, 126.8, 126.7, 126.1, 125.9, 124.3, 124.1, 124.0, 122.6, 73.3, 42.9(CH$_2$), 29.7, 20.6; HRMS (ESI-TOF, [M]$^+$) : calcd for C$_{31}$H$_{26}$N$_2$, 426.21; found 426.2162.

4.3.19. 8-Chloro-2-methyl-2,4-di-pyridin-4-yl-2,3-dihydro-1H-benzo[b][1,5]diazepine (3z)

Yellow solid, mp: 132–134 °C; IR (KBr) (ν_{max}, cm^{-1}): 3332, 1618, 1589, 1568, 1476. ^{1}HNMR(400 MHz, CDCl$_3$) (δ, ppm): 1.87 (s, 3H, CH$_3$–cyclic), 3.04 (d, 1H, $J = 12.4$ Hz, CH$_2^a$), 3.30(d, 1H, $J = 12.4$ Hz, CH$_2^b$), 3.68 (s, 1H, –NH), 6.84–8.45 (m, 11H, Ar-H) ^{13}C NMR (75 MHz, CDCl$_3$) (δ, ppm): 166.3, 155.5, 149.0, 147.3, 145.9, 138.0, 136.0, 133.3, 126.2, 124.8, 123.4, 121.9, 121.0, 118.5, 115.5, 73.4, 43.5(CH$_2$), 26.3; HRMS (ESI-TOF, [M]$^+$) : Calcd for C$_{20}$H$_{17}$N$_4$Cl, 348.11; found 348.1715.

4.3.20. 8-Chloro-2-methyl-2,4-di-naphthalen-2-yl-2,3-dihydro-1H-benzo[b][1,5]diazepine: (3a^1)

Yellow solid, mp: 168–170 °C; IR (KBr) (ν_{max}, cm^{-1}): 3327, 1597, 1574, 1450, 828. ^{1}HNMR(400 MHz, CDCl$_3$) (δ, ppm): 1.87 (s, 3H, CH$_3$–cyclic), 3.13 (d, 1H, $J = 13.2$ Hz, CH$_2^a$), 3.44 (d, 1H, $J = 13.2$ Hz, CH$_2^b$), 3.69 (s, 1H, –NH), 6.79 – 8.05 (m, 17H, Ar-H) ^{13}C NMR (75 MHz, CDCl$_3$) (δ, ppm): 167.8, 144.5, 130.1, 128.4, 128.3, 127.8, 127.7, 127.5, 127.4, 127.0, 126.4, 126.2, 124.2, 124.1, 123.9, 121.8, 73.5, 43.0(CH$_2$), 29.9; HRMS (ESI-TOF, [M]$^+$) : calcd for C$_{30}$H$_{23}$ClN$_2$, 446.15; found 446.1523.

4.4. Tyrosine kinase enzyme inhibition studies

4.4.1. Materials

FBS (Gibco, Invitrogen) Cat No −10270106, Antibiotic – Anti-mycotic 100X solution (Thermofisher Scientific)-Cat No-15240062, 96-well plates, Universal Tyrosine Kinase Assay Kit- Cat No –MK410

4.4.2. Methodology

4.4.2.1. Cell treatment. In a 96-well flat-bottom micro plate, maintained at 37 °C in 95% humidity and 5% CO2 for overnight, the cells were seeded at a density of approximately 1×105cells/well followed by treatment with different concentration of test samples. The cells were then incubated for another 24 h. The phosphate buffer solution, and 1 mL of extraction buffer was used to wash the cells in well for twice. The cells were then recovered carefully using cell scraper and were centri-fuged at 4 °C for 10 min at 10,000 rpm. The supernatant was collected and stored for further analysis.

4.4.2.2. Tyrosine kinase Assay. For carrying out the assay, collected supernatant was diluted by 25 times with kinase reacting solution. The diluted control and the treated sample were added in each well in

solution. This was followed by addition of 10 μL of 40 mM ATP-2Na into each well and was mixed thoroughly. Treated wells were incubated for 30 min at 37 °C. after removing the samples, wells were washed once with wash buffer. Next, 100 μL of blocking solution was added into each well and incubated for 30 min at 37 °C. The blocking solution was then discarded and 50 μL of Anti-phosphotyrosine - HRP solution was added into each well and incubated for 30 min at 37 °C. Once the antibody solution was discared each well was washed 4 times with washing buffer followed by addition of 100 μL of HRP substrate solution (TMBZ) into each well and incubation for 30 min at 37 °C . Then 100 μL of stop solution was added into each well in the same order as HRP substrate solution and finally absorbance was measured at 450 nm with a plate reader. The percent inhibition was calculated using the below formula

$$\%\text{Inhibition} = 1 - (\text{Abs of sample}/\text{Abs of control}) \times 100$$

The IC$_{50}$ of compounds was calculated using graph Pad Prism Version5.1 by taking a percentage of Inhibition Tyrosine Kinase Enzyme at six different concentrations of treatment.

4.5. Cytotoxicity assay

The in-vitro cytotoxicity studies of selective compounds **3a**, **3 k**, **3q**, **3w**, **3y** and **3x** was assessed by MTT assay [65] using three different cell lines namely HeLa, HEPG2 and HEK-293. Cytotoxicity studies were also evaluated against Paclitaxel and Methotrexate as standard drugs. Firstly, the cell lines were seeded in 96 well flat-bottom micro plate containing Dulbecco's Modified Eagle Media (DMEM) supplemented with 10% heat inactivated fetal bovine serum and 1% antibiotic- antimycotic 100X solution. The cells were maintained overnight at 37 °C in 95% humidity & 5% CO2 and were seeded in separate 96 well plates. The compound concentration of 400, 200, 100, 50, 25, 12.5 μg/mL was treated and cells were incubated for 48 hrs before addition of MTT solution. The wells were washed with phosphate buffer solution two times followed by addition of 20 μL of MTT solution and then incubated at 37 °C. After 4 h, formazan crystals were dissolved using 100 μL DMSO and absorbance was recorded at 570 nm using microplate reader. The IC$_{50}$ calculation was carried out using graph pad prism version 5.1.

4.6. Apoptosis studies using flowcytometry

4.6.1. Materials

Cell lines – Hep G2 (Liver cancer), DMEM with low glucose (Cat No-11875–093), FBS (Gibco, Invitrogen) Cat No −10270106, Antibiotic – Antimycotic 100X solution (Thermofisher Scientific)-Cat No-15240062, AnnexinV-FITC Kit (Beckman Coulter) Cat No –PN IM 3546–200 Tests, Propedium Idiode (Sigma-Aldrich) Cat No –P 4170

4.6.2. Methodology

A 24-well flat bottom micro plate containing cover slips, maintained at 37 °C in CO$_2$ incubator for overnight was used for seeding the cells. The cells were treated with 20 μg/ml of each sample compound at 24 hrs. After incubation, cells were then washed with PBS and Centrifuged for 5 min at 500 × g at 4 °C. Supernatant was discarded, and the cell pellets were resuspended in ice-cold 1X Binding Buffer to 1 x105 per mL. The tubes were kept on ice and 1 μL of annexin V-FITC solution and 5 μL PI was added. It was mixed gently and incubated for 15 min in the dark. Followed by this, 400 μL of ice-cold 1X binding buffer was added and mixed gently. The cell preparations were then analyzed by flowcytometry within 30 min.

4.7. Molecular docking:

4.7.1. As DHFR target

Molecular docking was used to clarify the binding mode of the compounds to provide straightforward information for further structural optimization. The crystal structure of dihydrofolate reductase complexed with NADPH and Methotrexate (PDB ID 1DF7, 1.7 Å X-ray resolutions) was extracted from the Brookhaven Protein Database (PDB http://www.rcsb.org/pdb). The proteins were prepared for docking by adding polar hydrogen atom with Gasteiger-Huckel charges and water molecules were removed. The 3D structure of the ligands was generated by the SKETCH module implemented in the SYBYL program (Tripos Inc., St. Louis, USA) and its energy-minimized conformation was obtained with the help of the Tripos force field using Gasteiger-Huckel charges and molecular docking was performed with Surflex-Dock program that is interfaced with Sybyl-X 2.0. and other miscellaneous parameters were assigned with the default values given by the software

4.7.2. As anticancer target

4.7.2.0.1. Ligand preparation.
The molecules **3b**, **3w** and **3x** were prepared using *LigPrep* module in the *Schrodinger Suite 2018–4* (Trial Version). The stereoisomerism of the chiral centers in the molecules synthesized was racemic, hence all the stereoisomers were generated for the purpose of docking. The molecules were neutral as a results ionization was not considered. Diverse conformations were generated for all the molecules which were subsequently used for docking studies.

4.7.2.0.2. Docking.
The active ligands were docked into the receptor grid generated around the inhibitor bound to the protein crystal structure. The outer grid 15 Å in x, y, and z extents while the inner grid was 10 Å in extents. To maximize the probability of forming hydrogen bonds between the residues in the enzyme active site and the ligand, the side chain hydroxyl groups of the amino acids serine, threonine, and tyrosine were allowed to rotate. All the calculations were carried with Schrödinger Suite 2018–4 (Trial Edition) running on Linux Workstation.

4.7.2.0.3. DNA binding studies. Methodology:
UV Absorption experiments were performed by maintaining a constant nucleotide concentration and varying samples concentration (10–2 μg/ml) in buffer. Solutions of calf thymus DNA in phosphate buffer gave a ratio of UV absorbance at 260 and 280 nm (A260/A280) 1.8–1.9, indicating that the DNA was pure and sufficiently free of contaminants like the proteins and RNA. The solution of DNA and desired compounds were kept to equilibrate at 25 °C for 20 min, after which absorption readings were noted. The data were then fit to following Eq. (1) to obtain intrinsic binding constant Kb.

$$[\text{DNA}]/[\in_a - \in_f] = [\text{DNA}]/[\in_b - \in_f] + 1/\text{Kb}[\in_b - \in_f] \tag{1}$$

Where, [DNA] = concentration of DNA in base pairs,

$\in_a$ is the extinction coefficient observed for the MLCT absorption band at the given DNA concentration,

$\in_f$ is the extinction coefficient of the complex without DNA

$\in_b$ is the extinction coefficient of the complex when fully bound to DNA.

Declaration of Competing Interest

The authors declare that they have no known competing financial interests or personal relationships that could have appeared to influence the work reported in this paper.

Appendix A. Supplementary material

Supplementary data to this article can be found online at https://doi.org/10.1016/j.bioorg.2021.105331.

References

[1] A. Rauf, M. Imran, M. Butt, M. Nadeem, D. Peters, M. Mubarak, Synthesis, Characterization and Evaluation of Anticancer Activity of Nanoresveratrol in B16 Melanoma Cell Line, Crit. Rev. Food Sci. Nutr. 58 (9) (2017) 1428.

[2] S. Cook, P. Salmon, G. Hayes, A. Byrne, P. Fisher, Predictors of emotional distress a year or more after diagnosis of cancer: A systematic review of the literature, Psycho-Oncology 27 (3) (2018) 791.

[3] Y. Youn, Y. Bae, Perspectives on the past, present, and future of cancer nanomedicine, Adv. Drug Deliv. Rev. 130 (2018) 3.

[4] R. Bayat, T. Homayouni, N. Baluch, E. Morgatskaya, S. Kumar, B. Das, Combination therapy in combating cancer, Oncotarget 8 (2017) 38022.

[5] A. Palmer, P. Sorger, Combination cancer therapy can confer benefit via patient-to-patient variability without drug additivity or synergy, Cell 171 (2017) 1678.

[6] R. Narayan, P. Molenaar, J. Teng, F. Cornelissen, I. Roelofs, R. Menezes, R. Dik, T. Lagerweij, A. Broersma, N. Petersen, J. Soto, E. Brands, P. Kuiken, M. Lecca, K. Lenos, S. Veld, W. Wieringen, F. Lang, E. Sulman, R. Verhaak, B. Baumert, L. Stalpers, L. Vermeulen, C. Watts, D. Bailey, B. Slotman, R. Versteeg, D. Noske, P. Sminia, B. Tannous, T. Wurdinger, J. Koster, B. Westerma, A cancer drug atlas enables synergistic targeting of independent drug vulnerabilities, Nat. Commun. 11 (2020) 2935.

[7] K. Sugahara, T. Teesalu, P. Karmali, V. Kotamraju, L. Agemy, D. Greenwald, Coadministration of a tumor-penetrating peptide enhances the efficacy of cancer drugs, Science 328 (2020) 1031.

[8] C. Holohan, S. Van Schaeybroeck, D. Longley, P. Johnston, Cancer drug resistance: an evolving paradigm, Nat. Rev. Cancer 13 (2013) 714.

[9] A.S. Crystal, A.T. Shaw, L.V. Sequist, L. Friboulet, M.J. Niederst, E.L. Lockerman, et al., Patient-derived models of acquired resistance can identify effective drug combinations for cancer, Science 346 (2014) 1480–1486, https://doi.org/10.1126/science.1254721.

[10] M. Paul, A. Mukhopadhyay, Tyrosine kinase – Role and significance in Cancer, Int. J. Med. Sci. 1 (2004) 101.

[11] T. Yamaoka, S. Kusumoto, K. Ando, A. Ohba, T. Ohmori, Receptor Tyrosine Kinase-Targeted Cancer Therapy, Int. J. Med. Sci. 19 (2018) 3491.

[12] Charles Pottier, Margaux Fresnais, Marie Gilon, Guy Jérusalem, Rémi Longuespée, Nor Eddine Sounni, Review: Tyrosine Kinase Inhibitors in Cancer: Breakthrough and Challenges of Targeted Therapy. Cancers 12 (2020) 1-17. 731.

[13] X. Yuan, Q. Yang, T. Liu, K. Li, Y. Liu, C. Zhu, Z. Zhang, L. Li, C. Zhang, M. Xie, J. Lin, J. Zhang, Yi Jin, Design, synthesis and in vitro evaluation of 6-amide-2-aryl benzoxazole/benzimidazole derivatives against tumor cells by inhibiting VEGFR-2 kinase, Eur. J. Med. Chem. 179 (2019) 147.

[14] M. Hossam, D. Lasheen, N. Ismail, A. Esmat, A. Mansour, A. Singab, K. Abouzida, Discovery of anilinofuro[2,3-d]pyrimidine derivatives as dual inhibitors of EGFR/HER2 tyrosine kinase and their anticancer activity, Eur. J. Med. Chem. 144 (2018) 330.

[15] J. Rawluk, Waller C, Small Molecules in Oncology, Gefitinib, 2018, p. 235.

[16] A. Tanaka, H. Nishikawa, S. Noguchi, D. Sugiyama, H. Morikawa, Y. Takeuchi, D. Ha, T. Kitawaki, Y. Maeda, T. Saito, Y. Shinohara, Y. Kameoka, K. Iwaisako, F. Monma, K. Ohishi, J. Karbach, E. Jager, K. Sawada, N. Katayama, N. Takahashi, S. Sakaguchi, Tyrosine kinase inhibitor imatinib augments tumor immunity by depleting effector regulatory T cells, J. Exp. Med. 217 (2019) 1.

[17] K. Gold, M. Kies, W. William, F. Johnson, J. Lee, Glisson, Erlotinib in the treatment of recurrent or metastatic cutaneous squamous cell carcinoma: A single-arm phase 2 clinical trial, Cancer 124 (2018) 2169.

[18] C. D'Amore, C. Borgo, S. Sarno, M. Salvi, Role of CK2 inhibitor CX-4945 in anti-cancer combination therapy – potential clinical relevance, Cellular Oncol. 43 (2020) 1003.

[19] Z. Yang, K. Tam, Anti-cancer synergy of dichloroacetate and EGFR tyrosine kinase inhibitors in NSCLC cell lines, Eur. J. Pharmacol. 789 (2016) 458.

[20] Z. Yang, X. Hu, S. Zhang, W. Zhang, K. Tam, Pharmacological synergism of 2,2-dichloroacetophenone and EGFR-TKi to overcome TKi-induced resistance in NSCLC cells, Eur. J. Pharmacol. 815 (2017) 80.

[21] W. Wen, E. Han, T. Dellinger, L. Lu, J. Wu, R. Jove, J. Yim, Synergistic Anti-Tumor Activity by Targeting Multiple Signaling Pathways in Ovarian Cancer, Cancers 12 (2020) 2586.

[22] P. Sidorov, S. Naulaerts, J. Ariey-Bonnet, E. Pasquier, P. Ballester, Predicting Synergism of Cancer Drug Combinations Using NCI-ALMANAC Data, Front. Chem. 7 (2019) 509.

[23] S. Manohar, N. Leung, Cis-platin nephrotoxicity: A review of the literature, Journal of Nephrology 31 (2018) 15.

[24] C. Yang, S. Horwitz, Taxol: The first microtubule stabilizing agent, Int. J. Mol. Sci. 18 (2017) 1733.

[25] M. Fawal, T. Jungas, A. Davy, Inhibition of DHFR targets the self-renewing potential of brain tumor initiating cells, Cancer Lett. 503 (2021) 129.

[26] M. Raimondi, O. Randazzo, M. Franca, G. Barone, E. Vignoni, D. Rossi, S. Collina, DHFR Inhibitors: Reading the Past for Discovering Novel Anticancer Agents 24(6) (2019) 1140.

[27] F. Saporito, M. Menter, Methotrexate and psoriasis in the era of new biologic agents, J. Am. Acad. Dermatol. 50 (2004) 301.

[28] D. Furst, The rational use of methotrexate in rheumatoid arthritis and other rheumatic diseases, British J. Rheumatol. 36 (1997) 1196.

[29] D. Fernandes, J. Bertino, 5-fluorouracil-methotrexate synergy: enhancement of 5-fluorodeoxyridylate binding to thymidylate synthase by dihydropteroylpolyglutamates, Proc. Natl. Acad. Sci. 77 (1980) 5663.

[30] J. Brande, M. Peppelenbosch, D. Hommes, Synergistic effect of methotrexate and infliximab on activated lymphocyte apoptosis, Inflamm. Bowel Dis. 13 (2007) 118.

[31] M. Akutsu, Y. Furukawa, S. Tsunoda, T. Izumi, K. Ohmine, Y. Kano, Schedule-dependent synergism and antagonism between methotrexate and cytarabine against human leukemia cell lines *in vitro*, Leukemia 2002 (1808) 16.

[32] E. Tietz, H. Rosenberg, T. Chiu, A comparison of the anticonvulsant effects of 1, 4-and 1, 5-benzodiazepines in the amygdala-kindled rat and their effects on motor function, Epilepsy Res. 3 (1989) 31.

[33] F. Guo, S. Wu, J. Julander, J. Ma, X. Zhang, J. Kulp, A. Cuconati, T. Block, Y. Du, J. Guo, J. Changa, A Novel Benzodiazepine Compound Inhibits Yellow Fever Virus Infection by Specifically Targeting NS4B Protein, J. Virol. 90 (2016) 10774.

[34] Y. An, Z. Hao, X. Zhang, L. Wang, Efficient Synthesis and Biological Evaluation of a Novel Series of 1,5-Benzodiazepine Derivatives as Potential Antimicrobial Agents, Chem. Biol. Drug Des. 88 (2016) 110.

[35] L. Wang, X. Li, Y. An, 1, 5-Benzodiazepine derivatives as potential antimicrobial agents: design, synthesis, biological evaluation, and structure–activity relationships, Org. Biomol. Chem. 13 (2015) 5497.

[36] M. Braccio, G. Grossi, G. Roma, L. Vargiu, M. Mura, M. Marongiu, 1,5-Benzodiazepines. Part XII. Synthesis and biological evaluation of tricyclic and tetracyclic 1,5-benzodiazepine derivatives as nevirapine analogues, Eur. J. Med. Chem. 36 (2001) 935.

[37] R. Gill, S. Kaushika, J. Chugh, S. Bansal, A. Shah, J. Bariwal, Recent Development in [1,4]Benzodiazepines as Potent Anticancer Agents: A Review *Mini-Reviews*, Med. Chem. 14 (2014) 229.

[38] R. Singh, D. Prasad, T. Bhardwaj, Design, synthesis and in vitro cytotoxicity study of benzodiazepine-mustard conjugates as potential brain anticancer agents, J. Saudi Chem. Soc. 21 (2017) S86.

[39] P. Salve, D. Mali, 1, 5-Benzodiazepine: A versatile pharmacophore, Int. J. Pharm. Bio. Sci. 4 (2013) 345.

[40] C. Escobar, Tauda; Maturana R; Sicker D, Synthesis of 1, 5-benzodiazepines with unusual substitution pattern from chalcones under solvent-free microwave irradiation conditions, Syn. Comm. 39 (2008) 166.

[41] S. Feng, X. Fan, Q. Shen, An Efficient Synthesis of 1,5-Benzodiazepine Derivatives by Lanthanide Trichloride-catalyzed Condensation of o-Phenylenediamine with α, β-Unsaturated Ketone under Mild Conditions, Chin. J. Chem. 26 (2008) 1163.

[42] J. Wu, F. Xu, Z. Zhou, Q. Shen, Efficient Synthesis of 1,5-Benzodiazepine Derivatives by Ytterbium Trichloride-Catalyzed Condensation of o-Phenylenediamine and Ketones, Syn. Comm. 36 (2006) 457.

[43] K. Okuma, Y. Tanabe, R. Itoyama, N. Nagahora, K. Shioji, One-pot Synthesis of 2, 3-Benzodiazepines from Arynes and β-Diketones, Chem. Lett. 42 (2013) 1260.

[44] P. Palanisamy, S. Jenniefer, P. Muthiah, S. Kumaresan, Synthesis, characterization, antimicrobial, anticancer, and antituberculosis activity of some new pyrazole, isoxazole, pyrimidine and benzodiazepine derivatives containing thiochromeno and benzothiepino moieties, RSC Adv. 3 (2013) 19300.

[45] Z. Yang, Z. Ding, F. Chen, Y. He, N. Yang, Q. Fan, Asymmetric Hydrogenation of Cyclic Imines of Benzoazepines and Benzodiazepines with Chiral, Cationic Ruthenium-Diamine Catalysts, Eur. J. Org. Chem. 2017 (1973) 2017.

[46] M. Weers, L. Lühning, V. Lührs, C. Brahms, S. Doye, One-Pot Procedure for the Synthesis of 1,5-Benzodiazepines from N-Allyl-2-bromoanilines, Chem. Eur. J. 23 (2017) 1237.

[47] S. Cacchi, G. Fabrizi, A. Goggiamani, A. Iazzetti, Construction of the 1,5-Benzodi-azepine Skeleton from o-Phenylendiamine and Propargylic Alcohols via a Domino Gold-Catalyzed Hydroamination/Cyclization Process, Org. Lett. 18 (2016) 3511.

[48] M. Chari, K. Syamasundar, Titanium-Catalyzed Hydroaminoalkylation of Vinylsilanes and a One-Pot Procedure for the Synthesis of 1,4-Benzoazasilines, Cat. Comm. 6 (2005) 67.

[49] Y. An, X. Li, X. An, L. Wang, FeCl3-SiO2 promoted one-pot, three-component synthesis of novel 1,5-benzodiazepine derivatives, Monatsh Chem. 146 (2015) 165.

[50] M. GodinoL, M. Diez, I. Matos, C. Valle, M. Bernardo, I. Fonseca, E. Mayoral, Enhanced Catalytic Properties of Carbon supported Zirconia and Sulfated Zirconia for the Green Synthesis of Benzodiazepines, Chem. Cat. Chem. 10 (2018) 5215.

[51] H. Alinezhad, M. Tajbakhsh, M. Norouzi, S. Bagher, An Efficient and Green Protocol for the Synthesis of 1,5-benzodiazepine and Quinoxaline Derivatives Using Protic Pyridinium Ionic Liquid as a Catalyst, World Appl. Sci. J. 22 (2013) 1711.

[52] M. Korbekandi, M. Esfahani, I. Baltork, M. Moghadam, S. Tangestaninejad, V. Mirkhani, Preparation and Application of a New Supported Nicotine-Based Organocatalyst for Synthesis of Various 1, 5-Benzodiazepines, Cat. Lett. 149 (2019) 1057.

[53] M. Pasha, V. Jayashankara, An expeditious synthesis of 1, 5-benzodiazepine derivatives catalysed by p-toluenesulfonic acid, J. Pharmacol. Toxicol. 1 (2006) 576.

[54] M. Baseer, khan A, Citric Acid-catalyzed Solvent Free an Efficient one-pot Synthesis of 2, 3-Dihydro-1H-1, 5-Benzodiazepine Derivatives, Recent Res. Sci. Technol. 3 (2011) 101.

[55] V. Sivamurugan, K. Deepa, M. Palanichamy, V. Murugesan, [(L)Proline]2Zn Catalysed Synthesis of 1,5-Benzodiazepine Derivatives Under Solvent-Free Condition, Syn. Comm. 34 (2004) 3833.

[56] L. Yin, L. Wang, Chemo-/regio-selective synthesis of 2-aryl-3-acetyl-2, 4-dihydro-1H-5H-1, 5-benzodiazepines using Lewis acid, CeCl3· 7H$_2$O, Tet. Lett. 57 (2016) 5935.

[57] A. Majee, A. Sarkar, S. Santra, S. Kundu, A. Hajra, G. Zyryanov, O. Chupakhin, V. Charushin, A decade update on solvent and catalyst-free neat organic reactions: a step forward towards sustainability, Green Chem. 18 (2016) 4475.

[58] O. Pawar, F. Chavan, V. Suryawanshi, V. Shinde, N. Shinde, Thiamine hydrochloride: An efficient catalyst for one-pot synthesis of quinoxaline derivatives at ambient temperature, J. Chem. Sci. 125 (2013) 159.

[59] L. Chen, S. Bao, L. Yang, X. Zhang, B. Li, Y. Li, Cheap thiamine hydrochloride as efficient catalyst for synthesis of 4H-benzo[b]pyrans in aqueous ethanol, Res. Chem. Intermed. 43 (2017) 3883.

[60] M. Lei, L. Ma, L. Hu, Thiamine hydrochloride as a efficient catalyst for the synthesis of amidoalkyl naphthols, Tet. Lett. 50 (2009) 6393.

[61] M. Lei, L. Ma, L. Hu, Thiamine Hydrochloride-Catalyzed One-Pot Synthesis of 1, 4-Dihydropyridine Derivatives Under Solvent-Free Conditions, Syn. Comm. 2011 (1969) 41.

[62] A. Altaf, A. Shahzad, Z. Gul, N. Rasool, A. Badshah, B. Lal, E. Khan, A Review on the medicinal importance of pyridine derivatives, J. Drug Des. Medicinal Chem. 1 (2015) 1.

[63] M. Abozeid, A. El-Sawi, M. Abdelmoteleb, H. Awad, M. Abdel-Aziz, A. Hassan Abdel-Rahman, E. Ibrahim El-Desoky, Synthesis of novel naphthalene-heterocycle hybrids with potent antitumor, anti-inflammatory and antituberculosis activities, RSC Adv. 10 (2020) 42998.

[64] G. Wang, W. Liu, Z. Peng, Y. Huang, Z. Gong, Y. Li, Design, synthesis, molecular modeling, and biological evaluation of pyrazole-naphthalene derivatives as potential anticancer agents on MCF-7 breast cancer cells by inhibiting tubulin polymerization, Bioorg. Chem. 103 (2020), 104141.

[65] S. Bhat, V. Revankar, V. Kumbar, K. Bhat, V. Kawade, Synthesis, crystal, structure and biological properties of a cis-dichloridobis(diimine)copper(II) complex, Acta Cryst. (2018) C74.

Available online at
www.anvpublication.org

Asian Journal of
Research in Pharmaceutical Sciences
Home page *www. ajpsonline.com*

RESEARCH ARTICLE

Formulation and Evaluation of Celecoxib loaded colon Targeted Microsponges

Pratik Terse*, Rashmi Mallya
V P College of Pharmacy, Madkhol, Tal- Sawantwadi, Maharashtra, India.
*Corresponding Author E-mail: **pratikterse@gmail.com**

ABSTRACT:

The present research work support preformulation, formulation, development and optimization of colon targeted microsponges containing Celecoxib as a nonsteroidal anti-inflammatory drug. The different batches of formulation were evaluated using celecoxib as active pharmaceutical ingredient, Eudragit as the pH sensitive polymer, polyvinyl alcohol and triethyl Citrate. Colon targeted microsponges of Celecoxib were prepared by Quasi-emulsion solvent diffusion method. The prepared formulations were evaluated for various parameters like Particle size, Percentage entrapment efficiency, Measurement of Zeta Potential, FTIR, in-vitro release study. The result were found to be within standard limits. FTIR study reports indicated that there was no interaction between Celecoxib and other excipients. Zeta Sizer shown that the microsponge size ranges from 61.12 μm to 67.59μm. Percent drug content was between 65.18%– 95.19%. Based on the resultants of the entrapment and particle size of microsponges, formulation M4 was observed to be optimized formulation. The optimized formulation exhibited 71.52% cumulative drug release after 10 h. The optimized batch shows 77.40% yield.

KEYWORDS: Celecoxib, Microsponges, Eudragit S100, Colon targeted, Novel drug delivery.

INTRODUCTION:

The present study was aimed at developing colon specific drug delivery system using eudragit S100 as a polymer in the formulation of microsponges. It was earlier reported that eudragit S100 can be used as a colon targeting polymer hence exploring his properties in the microsponge formulation.[1]

Microsponges are solid phase, porous, polymeric microspheres that have large porous surface for effective drug loading. Microsponges deliver a drug efficiently at minimum dose and also enhance the stability of drug, reduce side effects, and modify drug release profiles

Microsponges comprises of highly cross-linked, polymeric porous microspheres consisting numerous interconnected voids in the particle, loaded with active pharmaceutical agent within a collapsible structure. Microsponges have large porous surface to entrap wide range of active pharmaceutical agents in different doses that can be released at desired site of absorption. The pores of microsponges forms continuous arrangement open towards the exterior surface of microsponges which allows the outward diffusion of the entrapped drug with a controlled rate depending upon the size of the pores.[2, 3]

Celecoxib is a highly selective COX-2 inhibitor and primarily inhibits this isoform of cyclooxygenase (and thus causes inhibition of prostaglandin production) whereas traditional NSAIDs inhibit both COX-1 and COX-2. Celecoxib is approximately 7.6 times more selective for COX-2 inhibition over COX-1. In theory, this selectivity allows celecoxib and other COX-2

inhibitors to reduce inflammation (and pain) while minimizing gastrointestinal adverse drug reactions (e.g. stomach ulcers) that are common with non-selective NSAIDs.[4]

MATERIALS AND METHODS:

Various materials and equipment's used to carry out the experimental work are given in the following list:

Table 1: List of Materials for Formulation

Material	Procured from
Celecoxib	Prudence pharma
Eudragit S100	Evonik
Polyvinyl alcohol	SD fines
Triethyl Citrate	SD fines
Ethanol	Merck
Sodium lauryl sulphate	SD fines
Purified Water	-Inhouse

Table 2: List of Reagent

Sr. No.	Reagents	Suppliers of Materials
1	Hydrochloric acid	SD fines
2	Phosphate buffer 6.8	SD fines
3	Phosphate buffer 7.2	SD fines

Formulation of Microsponges:

Drug loading in microsponges can be effected in two ways, one-step process or by two-step process; based on physico-chemical properties of drug to be loaded. If the drug is typically an inert non-polar material, it will create porous structure. Such drug is called porogen. Porogen drug, which neither hinders the polymerization nor become activated by it and stable to free radicals is entrapped with one-step process.

Quasi-emulsion solvent diffusion method:

The microsponges can also be prepared by quasi-emulsion solvent diffusion method using the different polymer amounts. To prepare the inner phase, polymer is dissolved in ethyl alcohol. Then, drug can be then added to solution and dissolved under ultrasonication at 35˚C. The inner phase is poured into the PVA solution in water (outer phase). After 3 hour of stirring the microsponges were formed. The microsponges were filtered and dried at 40°C for 8 hours.[5]
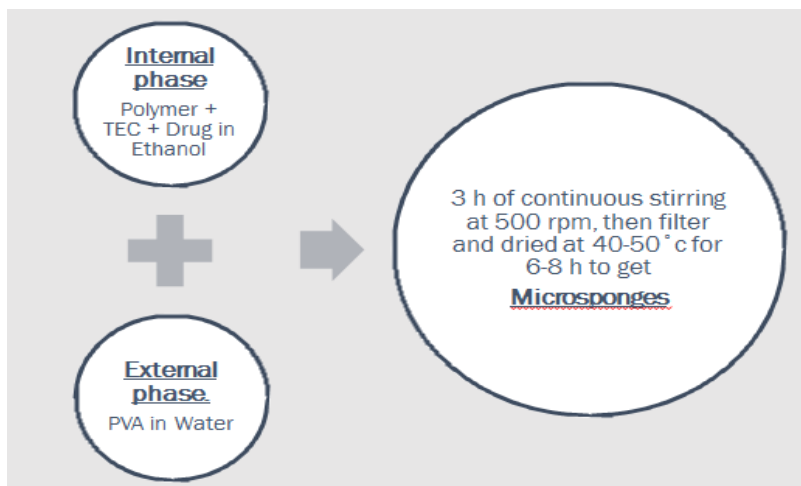

Fig 1: Quasi emulsion solvent diffusion method.

Table 3: Composition of Various Microsponge Formulations:

Batch	Dug: Polymer ratio (w/w)	Drug(mg)	Polymer(mg)	TEC (%, w/v)	Ethanol (ml)	PVA solution (% w/v)
M1	1:1	300	300	1	20	2
M2	2:1	400	200	1	20	2
M3	3:1	600	200	1	20	2
M4	4:1	800	200	1	20	2
M5	5:1	1000	200	1	20	2
M6	1:2	200	400	1	20	2
M7	1:3	200	600	1	20	2

Optimisation of formulation parameters and process factors:[6]

1. Effect of drug:polymer ratio.

Different drug: polymer (CEL: Eudragit S 100) ratios (1:1, 2:1, 3:1, 4:1, 5:1, 1:2 and 1:3) were investigated to prepare the microsponge formulations. In each formulation, ethyl alcohol (20 mL), PVA (400 mg), distilled water (200 mL) and inner phase temperature were kept constant. The microsponge formulations were prepared using centrifugal stirrer at a stirring rate of 500 rpm for 3 hr.

2. Effect of inner phase solvent amount.

The effect of inner phase solvent amount was investigated by using the formulation parameters defined for M1 except the amount of ethyl alcohol. Three different solvent amounts were chosen as 15, 20 and 25 mL.

Effect of stirring speed:
The effect of stirring rate on the microsponge's properties was studied using stirring speeds of300, 400, 500 and 600 rpm for the formulation M1.

Characterisation of Microsponges:
- **Fourier transform infrared analysis:**
To ascertain compatibility Fourier transform infrared analysis (FTIR) spectra of the drug, physical mixture of drug and Eudragit S-100, and formulations M4 and M5

were recorded in potassium bromide disc using a Shimadzu Model 8400 FTIR.

- **Differential scanning calorimetry analysis:**
Analysis using differential scanning calorimetry (DSC) was carried out for the drug, physical mixture of the drug and Eudragit S-100, and formulations M4 (Shimadzu DSC-60 Thermal Analyzer). Accurately weighed samples were transferred to aluminium pans and sealed. All samples were run at a heating rate of 20◦C/min over a temperature range 40◦C–430◦C.

Table 4-Dissolution parameters for Celecoxib microsponges:

Drug name	Dosage form	USP apparatus	Speed (rpm)	Medium	Volume (ml)	Recommended sampling time
Celecoxib	Microsponge	USP – I (Basket)	100	HCL buffer pH 1.2	900	2hr
				Phosphate buffer pH 6.8	900	6hr
				Phosphate buffer pH 7.2	900	2hr

- **Morphology and Particle Size Studies:**
The morphology and surface characteristics of the microsponges were studied using scanning electron microscope (SEM). All the samples were coated with gold–palladium alloy under vacuum. Coated samples were then examined using LEO 430 SEM analyzer.

- **Drug Content and Encapsulation Efficiency:**
Microsponges (100mg) were crushed and extracted using 10mL methanol by vortexing and centrifuging at 2000 rpm for 10min.Then insoluble residue was separated and the supernatant was analysed in HPLC at 248nm after appropriate dilution. Then, the encapsulation efficiency, percentage yield, and drug loading were calculated by the following equation.

Encapsulation efficiency (EE):
$$= \left(\frac{\text{Mass of drug in microsponges}}{\text{Initial mass of drug}} \right) \times 100$$

Percentage yield (PY):
$$= \left(\frac{\text{Mass of obtained microsponges}}{\text{Initial mass of drug + Initial mass of polymer}} \right) \times 100$$

Drug loading (DL):
$$= \left(\frac{\text{Mass of drug in microsponges}}{\text{Mass of microsponges}} \right) \times 100$$

In Vitro Drug Release: [7]
Following procedure was employed throughout the study to determine the in vitro dissolution rate for all the formulations.

Dissolution study of microsponges was carried out in USP dissolution test apparatus I (Electro lab TDT O8L) stirred at 100 rpm and temperature of 37 ± 0.5˚. Drug release was monitored for 10 hr and samples were withdrawn periodically and sink conditions were maintained by replacing with equal amount of fresh dissolution medium. The dissolution was carried out at

different pH condition using HCl buffer (pH 1.2) for 2 hr, phosphate buffer (pH 6.8) for next 6 hr, and phosphate buffer (pH 7.2) for subsequent hours to simulate the GIT condition. After 10 hr study, the samples were analyzed by HPLC at 248 nm. (Table-4).

As the drug is from BCS class 2, 2% SLS solution was used in the dissolution media.

Stability Study:
The stability of microsponges was carried out as per ICH guidelines in accelerated conditions. The microsponge formulation was kept at 40˚C ± 2˚C and 75% ± 5% RH for three months. After 3 months microsponges were analyzed for physical appearance, in vitro drug release, and FTIR spectroscopy.

RESULTS:
Effect of drug polymer ratio on drug content and % yield:

Table 5: Effect of drug polymer ratio on % Yield and drug content.

Batch	Drug: Polymer ratio (w/w)	% Yield	% Drug content
M1	1:1	58.66±1.87	87.09±0.25
M2	2:1	59.72±4.39	78.61±2.25
M3	3:1	65.50±2.77	95.19±1.42
M4	4:1	77.80±2.11	88.58±1.56
M5	5:1	58.50±3.70	91.85±2.68
M6	1:2	51.20±2.85	76.12±1.52
M7	1:3	36.52±1.25	65.18±0.85

Effect of inner phase solvent amount:
It was observed that when the volume of internal phase (ethanol) was increased from 20 to 25 ml, microsponge % yield were decreased. Good microsponges were produced only when 20 ml of internal phase was used.

Table 6: Effect of inner phase solvent amount

Volume of inner Phase (ml)	% Yield
25	56.22
20	77.85
15	Not found

Table 7: Effect of stirring speed on particle size

Batch	Stirring speed(rpm)	Particle size(µm)
M4	300	92±8.21
M4	400	85±12.52
M4	500	60±4.53
M4	600	27±6.32

Effect of stirring speed:

The effect of stirring rate on the size of microsponges was studied. As the stirring speed was increased, microsponges of smaller size were obtained, as shown in Table. When the rate of stirring was increased from 300 to 500 rpm, the mean particle size decreased from 92±4.45 to 60.25±5.67 µm

Characterisation of Microsponges:
Fourier transform infrared analysis:

Prepared microsponges were analyzed by FT-IR to study any drug interaction, there was no any drug interaction as the results shows the peaks of drug and polymer both. Results are shown in following figure.
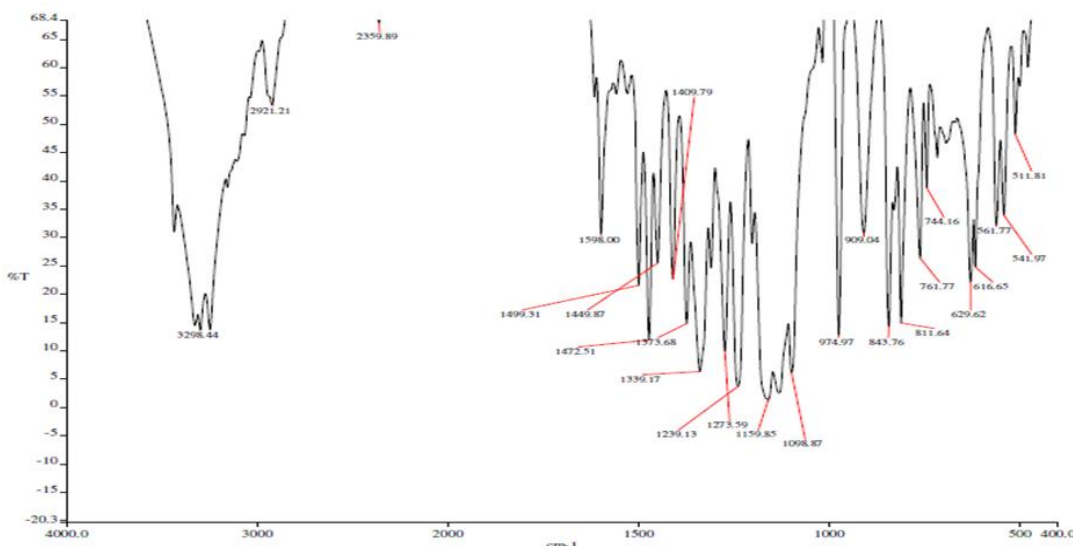

Fig 2: FT-IR result of microsponge

Differential scanning calorimetry analysis:

DSC studies of microsponges was carried out to study any change in melting point of drug due to encapsulation, there was no change in melting point as shown in figure

of microsponges was within the range of 61.12 µm to 67.59µm. The particle size of microsponges was affected by volume of solvent and concentration of Eudragit, as increase in volume of ethanol produces less viscous solution, which resulted in smaller particle size.
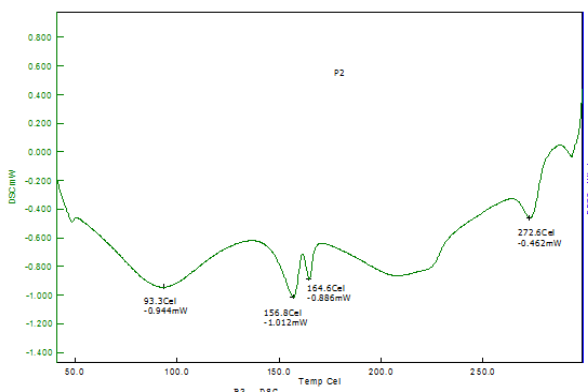
The microsponges' formulation M5 was visualized by scanning electron microscope to assess the morphology of microsponges. SEM image revealed porous surface as shown in Figure and no drug particles were observed on the surface of the microsponges.
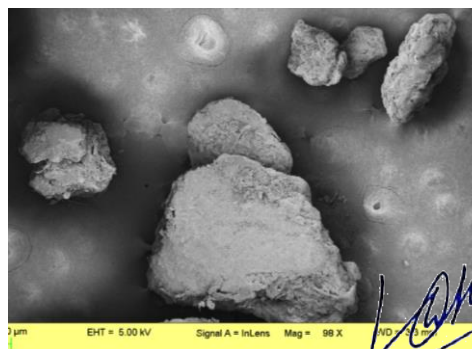

Fig 3: DSC result of microsponge

Morphology and Particle Size Studies:

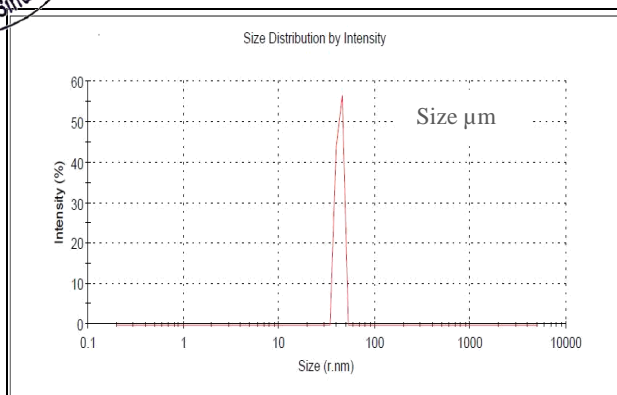The particle size of developed microsponges was analyzed by Zeta Sizer, which showed the average size

Fig 4: SEM image of microsponges

Fig 5: Particle size distribution

In Vitro Drug Release:

The in vitro release of drug from microsponges is shown in Figure. Results of in vitro drug release revealed that 15 to 20% of celecoxib was released from the microsponges in initial 4 h and 71.52% to 85.26 % of drug was released after 10h. The drug release suggested that Eudragit S100 prevented the premature release of curcumin in the upper GIT, since it is a pH sensitive polymer having threshold pH value above 6, which bypasses the GIT and showed drug release above pH 6. Release rate of Celecoxib from microsponges increased after 4 h, due to the exposure of formulations to pH 6 which is above the solubilizing pH of Eudragit S100 polymer.

Table 8: Cumulative % drug release

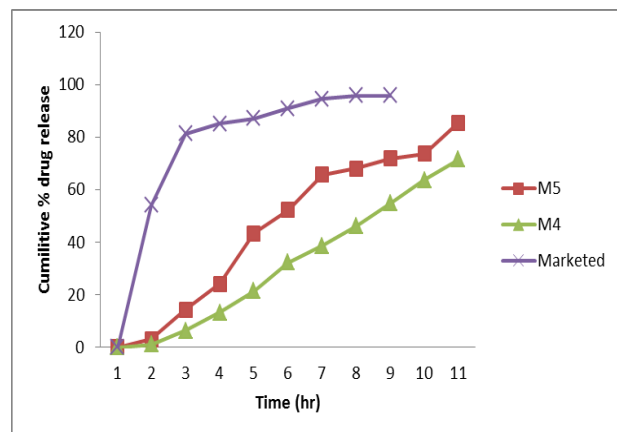| Time (hr)	Cumulative % drug release		
	M5	**M4**	**Marketed**
0	0	0	0
1	3.061±0.25	1.061±0.15	54.00±0.31
2	14.24±0.31	6.248±0.23	81.25±0.85
3	24.18±0.19	13.18±0.56	85.12±1.16
4	43.41±0.28	21.41±0.17	87.13±1.23
5	52.22±1.23	32.22±0.46	90.84±0.45
6	65.61±0.62	38.61±0.86	94.46±0.48
7	68.00±1.12	46.00±1.3	95.75±0.18
8	71.83±0.27	54.83±0.42	95.85±0.24
9	73.63±0.34	63.63±0.31	95.85±0.24
10	85.25±0.29	71.52±0.86	95.85±0.24

Fig 6: Dissolution studies of microsponges

Stability Study:

The stability study for final trial was done for 3 months by packing in air tight container in humidity chamber (40˚C/73% RH)

The results are shown under compatibility results, where all the parameters of formulation including, physical parameters, content uniformity and dissolution profile where within specification limit. So it indicates optimized formulation of celecoxib were stable.

No changes in the FT-IR spectra for each of the formulation was found to check if there were any peak shift and was compared with the FT-IR graph of the formulation taken initially to check stability of the product.

DISCUSSION:

The present study was aimed at developing colon specific drug delivery system using eudragit S100 as a polymer in the formulation of microsponges. It was earlier reported that eudragit S100 can be used as a colon targeting polymer hence exploring his properties in the microsponge formulation. Microsponges are porous in nature and can provide control release of drug that's why microsponge drug delivery was the choice of formulation. Hence optimized formula of celecoxib microsponge provided to be efficient in releasing the drug at specific site for duration of 10 hrs.

The quasi-emulsion solvent diffusion method used for the preparation of the microsponges was simple, reproducible, and rapid. Various drug polymer ratios were tried to get theoptimized formula such as (1:1, 2:1, 3:1, 4:1, 5:1) Furthermore, it was observed that as drug:polymer ratio increased, particle size decreased and production yield increase to the particular limit. This is probably due to the fact that at higher relative drug content, the amount of polymer available per microsponge to encapsulate the drug becomes less, thus reducing the thickness of the polymer wall and hence, smaller microsponges. Out of all the ratios 4:1 was selected as optimized drug polymer ratio.

The effect of stirring rate on the morphology of microsponges was also investigated. The dispersion of the drug and polymer into the aqueous phase was found to be dependent on the agitation speed. As the speed was increased the size of microsponges was reduced and uniform spherical microsponges were formed. It was also noted that at higher stirring rate the production yield was decreased. Possibly at the higher stirring rates the polymer adhered to paddle due to the turbulence created within the external phase, and hence production yield decreased. Different stirring speeds were tried (300 rpm, 400rpm, 500rpm, 600rpm) out of these 500 rpm was selected as optimized stirring speed.

77

Failure to form microsponges on increasing the volume of internal phase from 15 to 20 ml may be due to incomplete removal of internal phase solvent with the result that the droplets could not solidify as most of the internal phase remained in the droplets. This warrants the use of internal phase solvent in an appropriate amount to ensure the formation of quasi emulsion droplets, and solidification of the drug and polymer thereafter.

The microsponge formulations were subjected to in vitro dissolution studies and the data was analysed using various mathematical models. On the basis of highest regression value the best fit was observed for Higuchi matrix model.

This study presents a new approach for the preparation of modified microsponges. The microsponges exhibited characteristics of an ideal delivery system for colon targeting. The unique compressibility of microsponges offers a new alternative for producing different pharmaceutical formulations.

CONFLICT OF INTEREST:
No.

REFERENCES:

1. Rashmi Sareen, Nitin Jain, Ananya Rajkumari, and K. L. Dhar, pH triggered delivery of curcumin from Eudragit-coated chitosan microspheres for inflammatory bowel disease: characterization and pharmacodynamic evaluation. Drug Delivery, Early Online: 1–8
2. Rajendra Jangde, Microsponges for colon targeted drug delivery system: An overview, Asian J. Pharm. Tech. 2011; Vol. 1: Issue 4, Pg 87-93
3. M. S. Charde, P. B. Ghanawat, A. S. Welankiwar, J. Kumar and R. D. Chakole, Microsponge A Novel New Drug Delivery System: A Review, International Journal of Advances in Pharmaceutics 2 (6) 2013
4. William J. Sandborn, et al, Safety of Celecoxib in Patients with Ulcerative Colitis in Remission: A Randomized, Placebo-Controlled, Pilot Study, Clinical Gastroenterology and Hepatology, Volume 4, Issue 2, 2006, 203-211
5. Rashmi Sareen, Kavita Nath, Nitin Jain, and K. L. Dhar, Curcumin Loaded Microsponges for Colon Targeting in Inflammatory Bowel Disease: Fabrication, Optimization, and In Vitro and Pharmacodynamic Evaluation, BioMed Research International. Volume 2014
6. Mine Orlu, Erdal Cevher, Ahmet Araman, Design and evaluation of colon specific drug delivery system containing flurbiprofen microsponges International Journal of Pharmaceutics 318 (2006) 103–117
7. Renuka Khatik, et al, Colon-specific delivery of curcumin by exploiting Eudragit-decorated chitosan nanoparticles in vitro and in vivo, Nanopart Res (2013) 15:1893

Principal
V P College Of Pharmacy, Madkhol
Tal. Sawantwadi, Dist. Sindhudurg

In-vitro Anti-cancer assay and apoptotic cell pathway of newly synthesized benzoxazole-N-heterocyclic hybrids as potent tyrosine kinase inhibitors

Sulaksha Desai[a,b], Vidya Desai[a,b,*], Sunil Shingade[c]

[a] Department of Chemistry, Dnyanprassarak Mandal's College and Research Centre, Assagao, Bardez, Goa 403507, India
[b] Department of Chemistry, Goa-University, Taleigao, Goa, India
[c] Department of Pharmaceutical Chemistry, PES's Rajaram and Tarabai Bandekars College of Pharmacy, Pharmagudi, Ponda, Goa, India

ABSTRACT

A series of benzoxazole-N-heterocyclic hybrids have been synthesized by a one-pot strategy. Molecular docking study revealed that such compounds have the ability to inhibit enzyme protein tyrosine kinase. The findings of this work have been the successful synthesis of benzoxazole scaffolds, featuring hybrids of benzoxazole with quinoline and quinoxaline respectively. The molecular docking studies have showed these compounds to be inhibitors of tyrosine kinase enzyme which triggers growth of cancer cells. The cytotoxicity study of compounds **4a-f** showed better potency against breast cancer cell lines MCF-7 and MDA-MB-231 in contrast to oral and lung cancer cell lines KB and A549. The tyrosine kinase activity was measured using Universal Tyrosine Kinase Assay kit using horseradish peroxide (HRP)-conjugated anti-phosphotyrosine kinase solution as a substrate. The compounds **4c** exhibited maximum inhibition in the activity of enzyme tyrosine kinase with IC$_{50}$ value $0.10 \pm 0.16 \mu M$, than other compounds which were studied and thus proved to be inhibitors of enzyme tyrosine kinase. The selective index of all four compounds was found out to be greater than two, indicating the non-toxic behaviour, i.e. good anti-cancer activity. Further, fluorescence microscopic study helped to characterize the mode of cell death, which was found to be late apoptosis as indicated by the orange fluorescence. The SAR analysis has also been carried out.

1. Introduction

Cancer is affecting millions of lives all around the world [1,2]. With the sophisticated and different changing lifestyle, the growth of cancer disease has erupted rapidly. The most common type of cancers include lung cancer, oral cancer [3] and breast cancer. Nowadays, due to chemotherapeutic treatment most of them lead to metastasis, disease to liver, bone, lungs and bronchitis. Several types of breast cancer carcinoma have been reported that has been responsible for painstaking deaths all round the world. In view of this there is great need to search for newer breast cancer drug targets. Moreover, the scope to develop novel therapy strategies becomes the need and a challenging task. From cancer drug target study basal like subtypes triple negative breast cancer (TNBC) constitutes to about 80% of basal like tumors and is responsible for 10–15% breast carcinoma and also shows lack of expression of both hormone receptor (Progesterone and Estrogen) and HER2-receptor over expression [4–5]. A drug target for such cancer becomes evident as TNBC and basal like cancers are considered to be in the lead as an aggressive disease with greater chances of metastasis. The

therapy for such conditions namely, Trastuzumab (Fig. 1. I) cuts the risk of recurrence to half-compared to chemotherapy alone. Trastuzumab is given through veins in every 3 weeks for 1 year [6–9]. Scaffold containing heterocyclic conjugates such as 3-pyrimidinylazaindole analogue, (Fig. 1. II) a potent inhibitor of triple negative breast cancer which cuts the risk to upto 90% of tumor growth inhibition as compared to the other leads [10].

Human protein kinase forms a large family of enzymes commonly known as human Kinome encoded by about 1.7% of different types of human genes [11]. In this group of enzymes, tyrosine kinase has been the first protein kinase which has been well identified, described with respect to its location in the cell. Keeping in view the structural features, small molecule kinase inhibitors can be of great help to design and develop targeted therapies against breast cancer. The advantage of such inhibitors is high selectivity, better efficacy and specific action on protein kinase receptors.

In the designing of small drug like molecules, molecular hybridisation of heterocyclic compounds could be challenging task to gain potency in acting against tyrosine kinase enzymes. Thus, our focus was
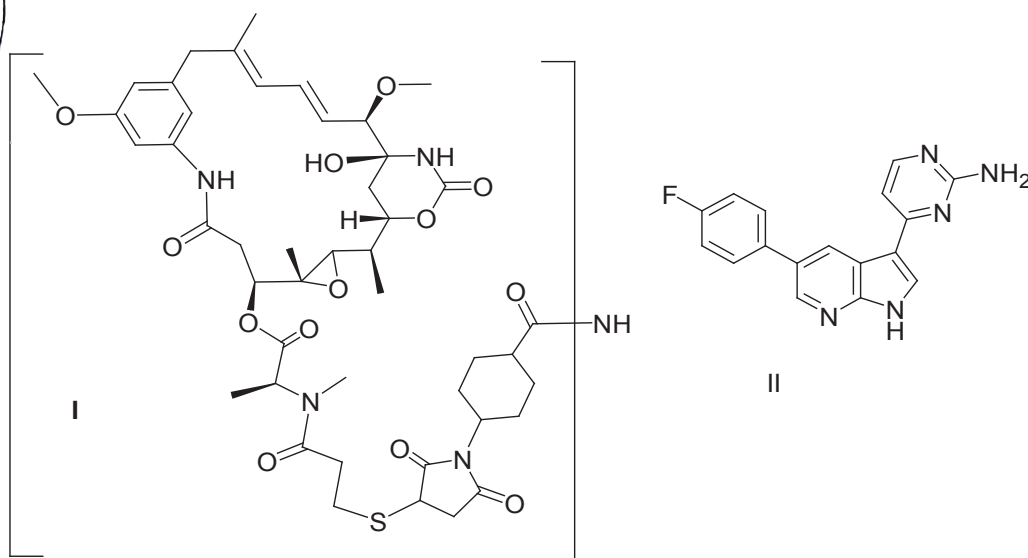
Fig. 1. Representative Structures of breast cancer drugs: I. Trastuzumab, sold under the brand name Herceptin among others, is a monoclinical antibody, used to treat HER2 positive breast cancer; II. 3-Pyrimidinylazaindole, a potent inhibitor of triple negative breast cancer.
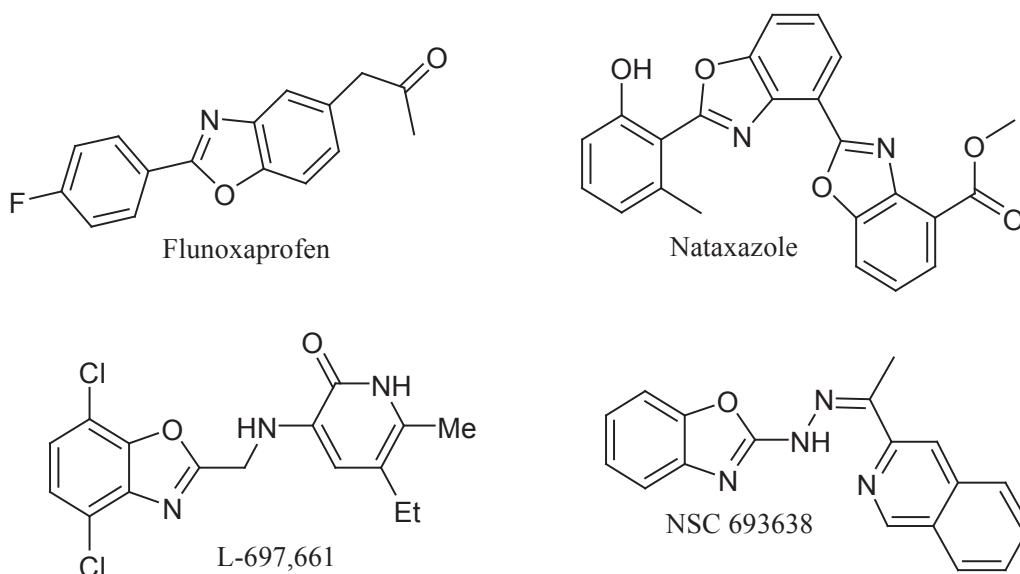

Fig. 2. Bioactive Compounds containing Benzoxazole moiety: flunoxaprofen-NSAIDs, L-697,661 a reverse transcriptase inhibitor, Nataxazole an anti-tumor, NSC693638- an anticancer agent.

on benzoxazole as a core unit as it forms an important class of bicyclic heterocycles having wide spectrum of biological applications [12]. Benzoxazole ring as a core pharmacophoric unit is found in various class of natural and synthetic compounds showing varied biological properties and has been studied for their antibacterial and anti-fungal [13,14], anticancer [15,16] and HIV-1 reverse transcriptase inhibitors [17]. It constitutes subunits of commercially available drug molecules such as; Flunoxaprofen which is a non-steroidal anti-inflammatory drug [18], NSC693638- an anticancer agent [19], L-697,661 a reverse transcriptase inhibitor, [20] Nataxazole, an anti- tumor agent [21] related to anti-tumor drugs like UK-1 and AJ19561 [22]. Fig. 2 The synthesis of benzoxazolyl-carbohydrazide derivatives and their *in-silico* docking and *in-vitro* anti-cancer study has been also reported [23]. Combretastin A-4 and benzoxazole analogues have been reported to exhibit more potent anti-cancer activity then the standard drug against A-549 and MCF-7 cell lines [24].

Nitrogen-based heterocycles are an important class of compounds in pharmaceutical and agrochemical industries. Their structural diversity

has made them attractive targets in the synthesis of alkaloids and important precursors to many biologically important active compounds. They have emerged as integral parts of various drugs known in day to day life. Some of the nitrogen heterocycles of biological importance includes: quinoxaline, indoles, quinolines, pyridines etc. Designing of heterocyclic hybrids [25] has led to newer breakthrough in the need for treatment of cancer and so it was visualized that heterocyclic hybrids of *N*-heterocycles with benzoxazole would have a promising effect on the biological activity. Thus, in continuation to our work on designing heterocyclic molecules of biological importance using ecofriendly strategies [26–29] herein, we present the synthesis of benzoxazoles using silica chloride. This methodology was further extended towards synthesis of six novel heterocyclic scaffolds. The molecular docking studies and biological evaluation has also been discussed, revealing our compounds to have the best anti-cancer activity. Development of solid acid catalyzed [30–33] synthesis of benzoxazoles and their action as inhibitors of protein kinase enzyme has been the focus of the work.
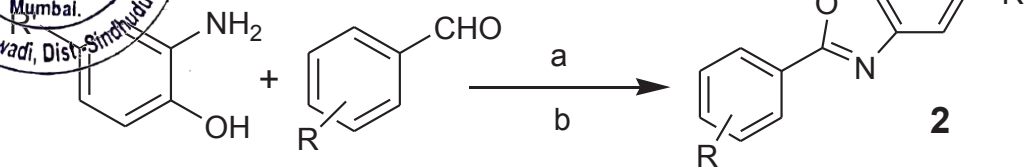
Scheme 1. One-pot synthesis of benzoxazole derivatives (2a-r) Reagents and conditions: (a) 1mmole of the 2-aminophenol and substituted benzaldehyde, 1 eq silica chloride, (b) 120 °C, solvent-free.

2. Results and discussion

2.1. Chemistry

The target benzoxazole was synthesized from condensation of 2-aminophenol derivatives with differently substituted aromatic aldehydes via Schiff base intermediate using previously prepared silica chloride [34] under solvent free conditions. The optimization of the reaction conditions revealed that catalyst not in mole ratio but in 1 equivalent and temperature of about 120 °C gave the cyclised product in short time of about 3–4 h. Consequently, a wide variety of 2-aryl benzoxazole derivatives having different functional groups was obtained successfully in good yields in the range of 70–80%. (Scheme 1, Table 1)

However, our focus was on designing of novel heterocyclic scaffolds with benzoxazole as the core unit. Our previous work on quinoxalinyl chalcones depicted good anti-tubercular and anti-cancer activity [35]. As a continuation to the work on designing of heterocyclic hybrids, an attempt has been made to prepare the new substituted benzoxazole derivatives bearing heterocyclic moiety. Six new benzoxazole conjugates **4a-f** has been prepared by the same strategy under solvent free conditions from commercially available aldehydes, previously synthesised quinoxaline-2-carbaldehyde [36] and 2-chloro-3-formyl quinolone [37]. (Scheme 2) All the six benzoxazole analogues were obtained in good yields. (Table 2)

Their structures were confirmed by ^{1}H NMR, ^{13}C NMR, and Melting points. The IR spectra showed disappearance of OH and C=O peak, C=C peak at 1605 cm^{-1}, C=N peak at 1677 cm^{-1} and peak at 1301 cm^{-1} attributed to C−O peak. The ^{1}H NMR spectra of the compounds **2a-r** showed an average spectrum in which appeared two doublets at δ 8.20 ppm (Ar−H, 3′ & 5′position) and δ 7.51 ppm (Ar−H; 2′ & 6′) . In addition, protons of the fused benzene ring appeared as

three multiplets at δ7.79–7.75 ppm (−CH=C−N−), δ 7.57–7.61 ppm for C5-H, δ7.36–7.39 ppm for C7-H and C6-H; ^{13}C NMR spectra of compounds revealed the presence of C=N at the range of 164.01C-Cl at the range of 150.3. The structures of *N*-heterocyclic hybrids **4a-f** were confirmed by ^{1}H NMR, ^{13}CNMR, and HRMS data. The calculated M + H ion peak matched with that of the observed M + H ion peak, which confirmed the structure.

2.2. Biological evaluation

2.2.1. Virtual screening

The promising approach to cancer therapy has been the targeted therapies which lead to beneficial clinical effects. Tyrosine kinase is an important target due to its role in modulation of growth factor signalling, it causes increase in tumor cell proliferation and growth, induces anti-apoptotic effects and promotes angiogenesis and metastasis. Because of all these effects, receptor tyrosine kinase has been a key target for cancer therapy. Tyrosine kinases are enzymes which catalyses the transfer of γ- phosphate group from adenosine triphosphate to target proteins. They play an important role in diverse normal cellular regulatory processes [38]. It is characterised by immunoglobulin-like sequences in their amino-terminal extracellular domains, a lipophilic transmembrane segment and an intracellular carboxyl-terminal domain which includes its catalytic site. Ligand binding induces dimerisation of these tyrosine kinase receptor and results in autophosphorylation of their cytoplasmic domains and activation in activity of tyrosine kinase. The 2-aminobenzoxazole and benzimidazole derivatives and pyrazolyl-benzoxazole derivatives have been proved to be active tyrosine kinase inhibitors due to strong binding affinity with enzyme [39,40]. Hence, we chose enzyme tyrosine kinase as a target for the molecular docking study of the synthesised benzoxazole-*N*-heterocylic hybrids.

The crystal structure of the epidermal growth factor receptor tyrosine kinase domain with 4-anilinoquinazoline inhibitor erlotinib (PDB ID: 1M17) was used for the docking studies, obtained from Protein Data Bank. The protein file was prepared by the removal of water molecules, addition of polar hydrogens and removal of other bound ligands. The synthesized benzoxazole-*N*-heterocyclic conjugates **2a-r** and **4a-f** were virtually screened for its anti-cancer activity against tyrosine kinase domain with 4-anilinoquinazoline inhibitor erlotinib as target enzyme. (Table 3) The molecular docking study revealed that compounds **4a, 4c and 4d** acts as good inhibitors of tyrosine kinase due to characteristic features. (Fig. 3) However, compounds **2a-r** were also found to be active with the target PDB ID: 1M17. As depicted in Fig. 4, Compound **4a** makes four hydrogen bond interactions at the active site of the enzyme. Three interaction with the nitro group present on phenyl ring; of which one interactions raised from H-bond interaction between nitrogen atom of the NO$_2$ group with Thr766 (1.55 A^o) and two interaction arised from H-bond interaction between oxygen atom of nitro group and CYS751 (1.52 A^o) and Thr830 (1.52 A^o). The remaining one arose from oxazole ring of benzoxazole moiety. The oxygen atom interacts with Met769 (1.55 A^o).

Compound **4c** makes two hydrogen bond interactions at the active site of the enzyme. One interactions arose from nitrogen atom of oxazole ring, where the nitrogen forms H-interaction with Thr766 (1.52 A^o). while the other is raised from H-bond interaction of nitrogen atom of quinoxaline ring with Met769 (1.55 A^o). Compound **4d** makes
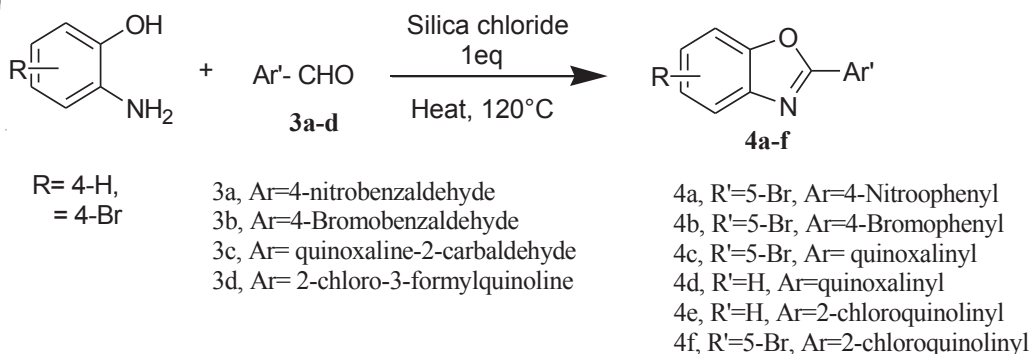
Table 1
Synthesis of benzoxazole derivatives **2a-r**[a].

Comp 2	R	R'	Yield[b]	Melting Point[c] °C
a	2,4- Cl	H	75%	125–127 (1 2 7)
b	4- Cl	H	75%	144–148 (148–150)
c	4- Br	H	71%	150–152(157–158)
d	3-NO$_2$	H	79%	99–102(103–105)
e	2-NO$_2$	H	72%	97–100(98–102)
f	4-OMe	H	77%	114–116 (113–114)
g	4-NO$_2$	H	79%	256–260 (2 6 8)
h	H	H	78%	98–100 (1 0 1)
i	2-Cl	H	70%	68–72(73)
j	4-Me	H	79%	104–106 (101–103)
k	3-Cl	H	72%	120–122 (122–124)
l	4-OH, 5-NO$_2$	H	75%	170–174 (1 7 8)
m	2-OH, 5-NO$_2$	H	71%	188–192 (1 8 8)
n	4-F	H	79%	90–92 (92–95)
o	3-Br	H	72%	133–137 (136–138)
p	4-NMe$_2$	H	70%	179–182(182–183)
q	5-Br, 4-OH, 3-OMe	H	78%	187–190 (190–192)
r	4-OH-3,5- Br	H	70%	166–169 (168–170)

[a] Reaction conditions: Schiff base(1mmole), silica chloride 1equivalent.
[b] Isolated yields.
[c] Determined using thiels tube paraffin method.

R (OH, NH$_2$) + Ar'-CHO **3a-d** → (Silica chloride 1eq, Heat, 120°C) → **4a-f** (R benzoxazole–Ar')

R= 4-H, = 4-Br

3a, Ar=4-nitrobenzaldehyde
3b, Ar=4-Bromobenzaldehyde
3c, Ar= quinoxaline-2-carbaldehyde
3d, Ar= 2-chloro-3-formylquinoline

4a, R'=5-Br, Ar=4-Nitroophenyl
4b, R'=5-Br, Ar=4-Bromophenyl
4c, R'=5-Br, Ar= quinoxalinyl
4d, R'=H, Ar=quinoxalinyl
4e, R'=H, Ar=2-chloroquinolinyl
4f, R'=5-Br, Ar=2-chloroquinolinyl

Scheme 2. Synthesis of novel 2-Arylbenzoxazole scaffolds 4a-f.

Table 2
One-pot Synthesis of benzoxazolyl scaffolds **4.**

Entry	Compound 4	Time	Yield[a]	Melting Point[b] °C
1	a	2.5 h	80%	158–162
2	b	2.5 h	72%	228–232
3	c	3 h	74%	160–164
4	d	3 h	80%	189–192
5	e	3 h	75%	102–108
6	f	3 h	76%	170–175

[a] Isolated yields.
[b] Determined using thiels tube paraffin method.

three hydrogen bond interactions at the active site of the enzyme. The interaction arising from nitrogen atom of the quinoxaline, shows H-bonding which interaction with Met769 (1.55 A°). The remaining two interactions are raised from nitrogen and oxygen atom of oxazole ring with Thr766 (1.52 A°). (Fig. 4)

2.2.2. Anticancer evaluation

On the basis of enzymatic inhibitory potency against 1M17, compounds **4a-f** was selectively used as candidates for exploring the mechanisms of anti-cancer. The anti-proliferative activity has been carried out against MDA MB-231 (ER-negative) & MCF-7 (Breast Cancer), A549 (Lung Cancer), KB (Oral Cancer) and HEK293 (Normal Human Kidney
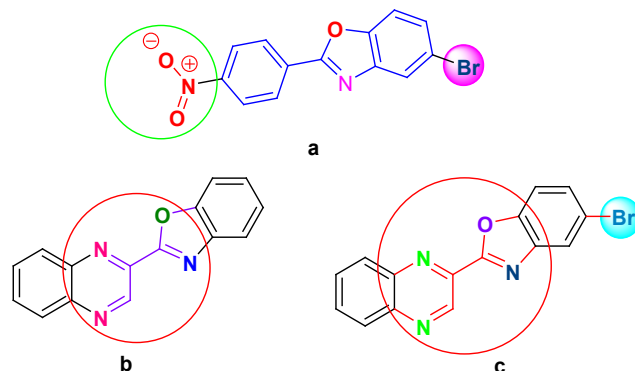

Fig. 3. Structural features of compounds responsible for the cytotoxicity: (a) Compound 4a; (b) Compound 4c; (c) Compound 4d.

Cells) by MTT (3-(4,5-dimethylthiazol-2-yl)-2,5-diphenyltetrazolium bromide) assay method [41]. Using graph Pad Prism Version5.1, the IC$_{50}$ of compounds has been calculated by taking a percentage of Inhibition Tyrosine Kinase Enzyme at six different concentrations of treatment.

All the six benzoxazole-*N*-conjugates **4a-f** exhibited cell proliferation with IC$_{50}$ values in the range of 0.42 to 14.39 μM. As shown in Table 4, the samples showed moderate to good activity comparable to

Table 3
Molegro docking score for benzoxazole derivatives **2a-r** and **4a-f.**

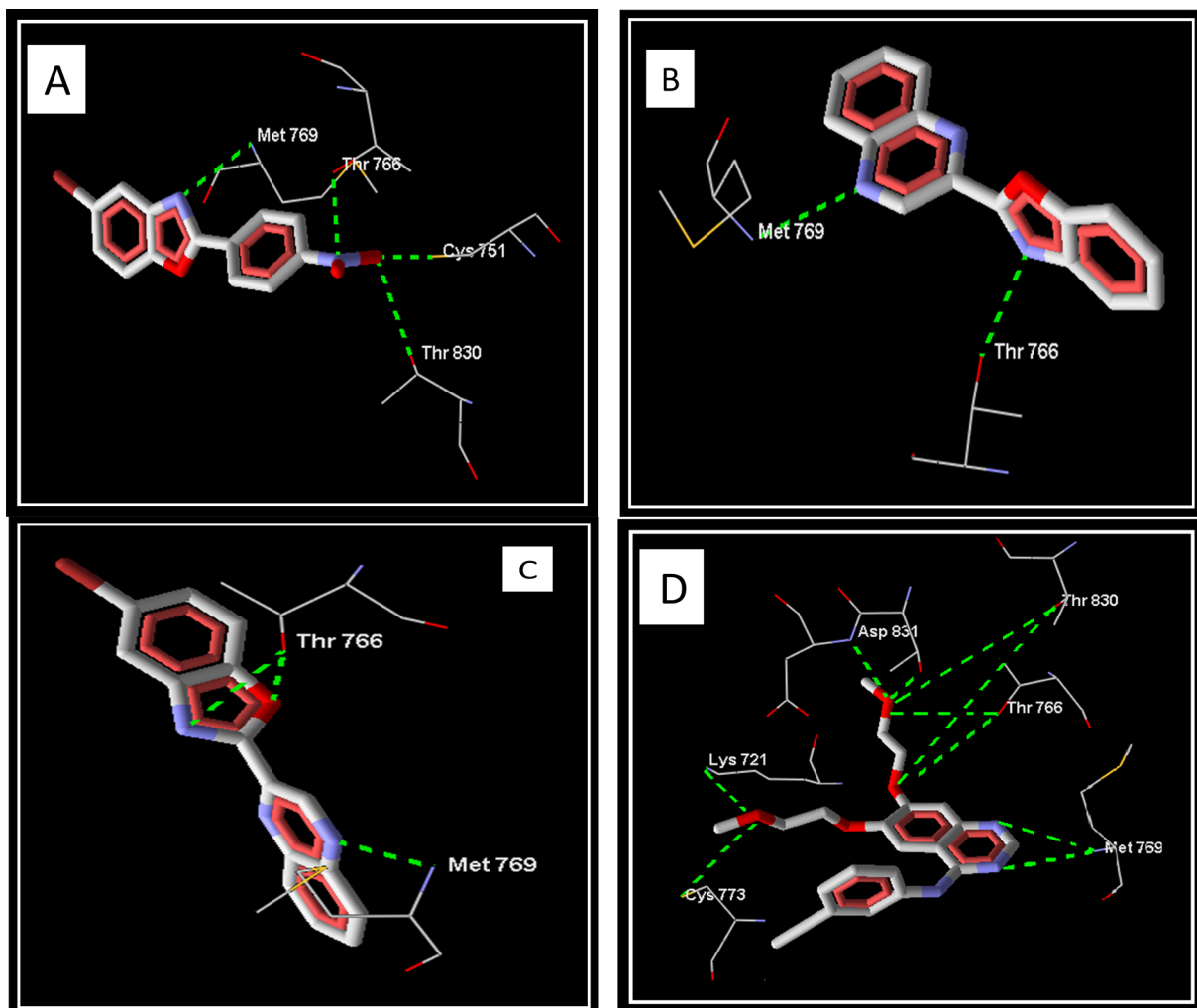| Code	MolDock Score	Rerank Score	Protein	H bond	Heavy atom count	Kcal/mol	Docking Score
B2a	−86.5224	−64.8155	−90.5300	2	19	−5.08955	−86.0269
B2b	−80.5605	−61.4823	−86.9539	1	19	−5.03503	−79.6663
B2c	−80.2853	−62.0941	−86.7351	3	17	−5.01783	−79.4664
B2d	−79.8709	−62.0032	−101.419	3	17	−5.1842	−97.9248
B2e	−96.1274	−66.7314	−99.1471	5	17	−3.7073	−97.9981
B2f	−80.6788	−61.6469	−86.0643	2	17	−4.13724	−83.9878
B2g	−92.6515	−72.1225	−104.053	2	17	−4.8123	−86.6232
B2h	−81.1186	−66.7681	−89.5901	3	16	−4.09693	−76.124
B2i	−80.4031	−54.6825	−89.813	3	16	−3.77365	−71.5362
B2j	−73.0934	−56.8369	−79.4259	0	16	−3.5958	−73.2504
B2k	−79.7784	−61.9172	−85.919	1	16	−4.01128	−79.2865
B2l	−90.1899	−71.7397	−102.058	3	16	−5.0177	−100.482
B2m	−97.8936	−71.8246	−101.476	3	19	−5.1523	−96.9324
B2n	−75.3016	−58.9796	−81.593	0	19	−3.71931	−80.8615
B2o	−78.559	−62.499	−88.8241	0	19	−3.86762	−79.1946
B2p	−83.1269	−60.3583	−87.3281	1	17	−3.11882	−87.9088
B2q	−81.1726	−45.0394	−100.153	3	19	−4.2722	−78.8718
B2r	−79.7915	−58.6621	−88.1242	1	19	−3.59923	−86.9973
B4a	−79.8709	−62.0032	−101.419	4	17	−4.2037	−81.4409
B4b	−80.3296	−63.3705	−87.2282	1	17	−4.9468	−93.4702
B4c	−90.1899	−71.7397	−102.058	2	17	−4.7468	−93.4702
B4d	−92.6515	−72.1225	−104.053	3	17	−4.6325	−91.9065
B4e	−89.4501	−64.1618	−99.8916	1	17	−3.71632	−95.1771
B4f	−89.7198	−70.4287	−97.4172	1	16	−3.24967	−91.2059

Fig. 4. Molecular docking data: the compounds docked in best of its conformation into the binding site of 1M17. (A) Binding mode of compound 4a forming four hydrogen bond interaction. (B) Binding mode of compound 4c forming two hydrogen bond interaction. (C) Binding mode of compound 4d forming three hydrogen bond interaction. (D) Binding interaction of ligand AQ4-1M17 forming 10 hydrogen bond interaction.

that of standard drugs, especially compound **4a, 4c** and **4d** showed higher anti-proliferation activity with $IC_{50} = 0.56 \pm 0.07$, $0.58 \pm 0.05\,\mu M$; $IC_{50} = 0.53 \pm 0.02$, $0.50 \pm 0.08\,\mu M$ and $IC_{50} = 0.73 \pm 0.02$, $0.60 \pm 0.06\,\mu M$ against MDA-MB-231(TNBC-triple negative breast cancer) and MCF-7 (human breast cancer) cell lines. Compound **4b, 4e** and **4f** showed moderate activity with IC_{50}

Table 4
IC_{50} values ($\mu M \pm$ S.E.) of compounds **4a, 4b, 4c, 4d, 4e** and **4f** against four different cell lines and normal human cell lines.

Comp	IC$_{50}$ μM				
	MDA MB-231[a]	MCF-7[b]	A549[c]	KB[d]	HEK293[e]
4a	0.56 ± 0.07	0.58 ± 0.05	0.70 ± 0.11	0.82 ± 0.08	10.11 ± 0.19
4b	1.09 ± 0.05	1.10 ± 0.03	0.97 ± 0.09	0.71 ± 0.12	3.27 ± 0.20
4c	0.53 ± 0.02	0.50 ± 0.08	0.82 ± 0.20	0.90 ± 0.05	14.39 ± 0.28
4d	0.73 ± 0.02	0.60 ± 0.06	0.87 ± 0.08	0.86 ± 0.10	8.39 ± 0.19
4e	0.98 ± 0.04	0.94 ± 0.03	0.89 ± 0.11	0.85 ± 0.04	6.04 ± 0.23
4f	0.85 ± 0.01	0.91 ± 0.02	0.83 ± 0.06	0.98 ± 0.03	7.21 ± 0.05
Paclitaxel[f]	0.3 ± 0.02	–	–	–	–

[a] MDA-MB-231 cell line- is an epithelial, human breast cancer cell line established from pleural effusion of a 51-year old Caucasian female with metastatic memmary adenocarcinoma.

[b] MCF-7 is a human breast cancer cell line with estrogen, progesterone and glucocorticoid receptors. It is derived from pleural effusion of 69-year old Caucasian metastatic breast cancer in 1970.

[c] A549 ia a human cancer cell line, derived from the rezige and culturing of cancerous lung tissues in the explanted tumor of 58-year old Caucasian metastatic male.

[d] KB is derived from an epidermal carcinoma of the mouth, cells contain human papilloma virus18 (HPV-18) sequence.

[e] HEK293 –derived from Human embryonic kidney 293 cells in tissue culture.

[f] Paclitaxel- used as standard drug.

values 1.09 ± 0.05, 0.98 ± 0.04 and 0.85 ± 0.01 μM against MDA-MB-231 and also against MCF-7 cell lines with the IC_{50} values 1.10 ± 0.03, 0.94 ± 0.04 and 0.91 ± 0.02 μM respectively. The higher anti-proliferation against KB (oral cancer) cell line with IC_{50} value of 0.71 ± 0.12 was exhibited by compound **4b**. Compound **4a**, **4d** and **4e** showed comparable anti-proliferation against KB cell line with IC_{50} value 0.82 ± 0.08, 0.86 ± 0.10 and 0.85 ± 0.04 μM respectively. Compound **4c** and **4f** exhibited moderate anti-proliferation effect. Considering the anti-proliferation effect against A549 (lung cancer), compound 4a showed good anti-proliferation with the IC_{50} value 0.70 ± 0.11 μM. Compound **4c**, **4d**, **4e** and **4f** showed moderate anti-proliferation against A549 (Lung cancer) cell line with IC_{50} value 0.8 μM as compared to the other samples. The results were compatible with the docking studies.

Following this, the *in-vitro* cytotoxic activity of all the tested compounds was analyzed against normal HEK-293 cell lines by MTT colorimetric assay [41]. The colorimetric results revealed that none of the six evaluated compounds exhibited any significant toxicity effect on normal HEK-293 cells. Selectivity index (SI) reveals the differential activity of a pure compound. Higher SI value is attributed to less toxicity and more selectivity. Whereas, a compound with SI value < 2 indicates cytotoxicity of the pure compound. As shown in Table 5 all samples were proved to be non-toxic on the normal tumor cells. The effect of benzoxazole-*N*-heterocyclic hybrids **4a-f** on viability of MDA MB-231 (ER-negative), MCF-7 (Breast Cancer), A549 (Lung Cancer), KB (Oral Cancer) and HEK293 (Normal Human Kidney Cells) was investigated and represented graphically as variation in percentage of viability with respect to time and concentration. (Fig. 5)

2.2.3. Enzyme inhibition studies

The effect of benzoxazole-*N*-heterocyclic hybrids **4a-f** on tyrosine kinase activity *in-vitro* was carried out using Fetal Bovine Serum (FBS) cell culture treated with indicated amounts of benzoxazole-*N*-heterocyclic hybrids for indicated time. The whole cell extracts were extracted and incubated with tyrosine kinase substrate for the specified time mentioned in the procedure. The plot of relative rate of inhibition in activity of enzyme tyrosine kinase with respect to different concentration of compounds **4a-f** (Fig. 6) indicates that compounds **4a-f** induced a dose dependent decrease in the enzyme activity. (Table 6) It was summarized from the results of the enzyme inhibition studies that, compound **4c** exhibited higher inhibition in activity of enzyme Tyrosine kinase with the IC_{50} value of 0.10 ± 0.16 μM, compounds **4a**, **4d** and **4e** also exhibited good inhibitory action on the activity with IC_{50} value in the range 0.31–0.43 μM. Compound **4b** was found to be least active in inhibiting the growth of enzyme with IC_{50} value 0.86 ± 0.42 μM. With decrease in the concentration of compounds **4a-f,** the rate at which the enzyme grow was decreased, with compound **4c** exhibiting the highest inhibition in the activity of enzyme. All compounds demonstrated good rate of inhibition of tyrosine kinase enzyme at highest concentration but as the concentration decreased the effect of inhibition was found to decrease.

Table 5
Selective index (SI) [f] of compounds.

Comp	SI^f-MDA MB-231	SI^f-MCF-7	SI^f-A549	SI^f-KB
4a	9.55	9.53	9.41	9.29
4b	2.18	2.17	2.30	2.56
4c	13.86	13.89	13.57	13.49
4d	7.66	7.79	7.52	7.52
4e	5.06	5.30		5.19
4f	6.36	6.30	6.38	6.23

[f] **SI**-Selective index, calculated as IC_{50} HEK/IC_{50} DTE the respective cell lines.

2.2.4. Cell morphology studies by fluorescence microscopy

Fluorescence microscopy study was employed to study the mode of cell death induced by synthesized benzoxazole-*N*-heterocyclic hybrids **4a**, **4c** and **4d** in comparison to the standard *cis*-platin by virtue of acridine orange/ ethidium bromide staining. The mode of cell death, whether early or late apoptosis can be characterized based on the fluorescence properties. Acridine orange was taken up by both viable and apoptotic (dead) cells by emitting green fluorescence. Cells with disrupted membrane integrity were stained by ethidium bromide, i.e. late apoptotic cells and necrotic cells. Late aoptotic cells have orange to red nuclei with condensed and fragmented chromatin, and early apoptotic cells show green fluorescence nuclei. Necrotic cells have uniform orange to red nuclei with organised structure. Thus, from the results (Fig. 7) it was visualised that, viable cells without treating with synthesised compound **4a**, **4c**, **4d** showed green fluorescent nucleus with acridine orange Fig. 7**a**, Whereas, late apoptotic cells when treated with compounds **4a**, **4c** and **4d** exhibited yellow orange fluorescence with nuclear membrane babbling. Fig. 7**b-d**; thus signifies apoptotic mode of cell death.

Further confirmation of the apoptotic mode of cell death was done by using DAPI staining method, wherein; cells treated with compounds and the viable cells were stained with 4′, 6′- diamine-2′-phenylindole dihydrochloride (DAPI). Untreated cells showed intact nucleus Fig. 8**a** whereas, treated cells showed nuclear condensation and nuclear fragmentation. Fig. 8**b–d**.

2.2.5. SAR studies

The following Structure activity relationship (SAR) analysis has been executed based on the results of the cytotoxicity studies of benzoxazole-*N*-heterocyclic hybrids **4a-f** against five different cancer cell lines. All the compounds were found to show good cytotoxicity effect against MDA-MB- 231 and MCF-7 breast cancer cell lines as compared to other cell lines. Compound **4a**, **4c** and **4d** exhibited good anti-cancer activity due to strong interaction with the enzyme active site and their characteristic structural features. Figs. 3 and 9. As in compound **4a**, the presence of electron withdrawing group (i.e. Nitro) onto the phenyl ring and also the presence of bromo substituent on the benzoxazole moiety enhance the cytotoxicity effect. Replacement of the nitro group by halogen (i.e. Br) as in compound **4b,** has moderate effect on cytotoxicity. In case of compound **4c**, replacing the phenyl ring with quinoxaline ring and also the presence of bromo substituent on the benzoxazole ring exhibits higher effect on cytotoxicity, so also compound **4d** with quinoxaline moiety exhibited similar effects. Quinoline moiety was found to lower the cytotoxicity effect as in compound **4e** and **4f.**

3. Conclusion:

In conclusion, a newly designed synthesis of benzoxazole has been achieved in an ecofriendly reaction conditions. Such benzoxazole hybrids **2a-r** and **4a-f** has been evaluated as anti-proliferative agents, having virtually screened as good inhibitors of enzyme protein tyrosine kinase, the key enzyme that triggers triple negative breast cancer. Comparative cell cytotoxicity studies against five different cancer cell lines MCF-7, MDA-MB-231, KB, A549 and HEK-293 revealed that all six benzoxazole hybrids **4a-f** showed good inhibitory potency against all cell lines. It was visualized from the anti-cancer activity results that, compounds **4a**, **4c** and **4d** demonstrated excellent inhibitory potency against MDA-MB-231 and MCF-7 breast cancer cell lines with the IC_{50} value in the range of 0.50–0.73 μM as compared to standard drug Paclitaxel (IC_{50}; 0.030 ± 0.02 μM). Compounds **4a-f** was also found to be potent against A549 (lung cancer) with IC_{50} values in the range of 0.70 to 0.97 μM.

Comparing the anti-cancer potency against all five cancer cell lines, the target compounds **4a**, **4c** and **4d** exhibited better anti-proliferation effect against MDA-MB-231 and MCF-7 cell lines. Cytotoxicity against HEK-293; human embryonic kidney cell line was also evaluated and
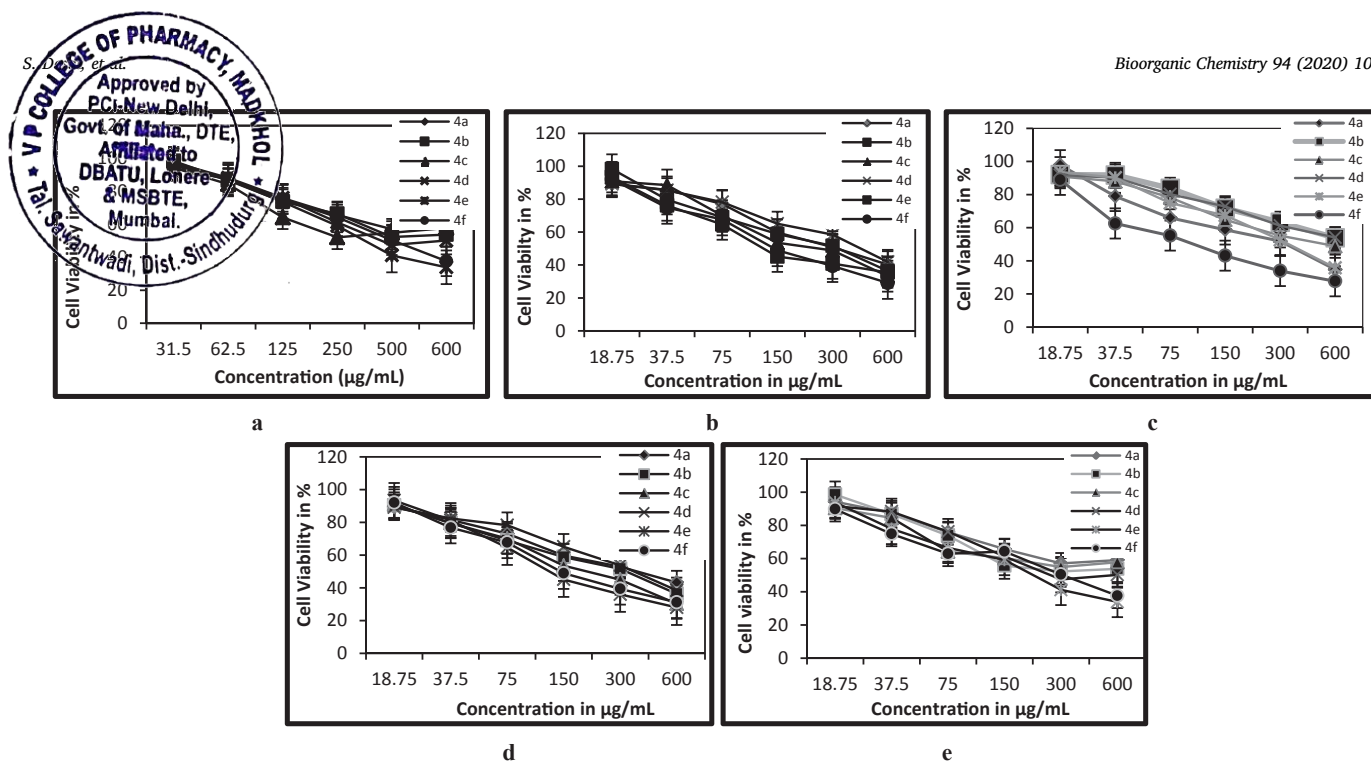
Fig. 5. Graphical representation of cell viability exhibited by 4a, 4b, 4c, 4d, 4e and 4f for five different cell lines: (a)MDA-MB-231, (b) MCF-7, (c) A549, (d)KB, (e) HEK293.
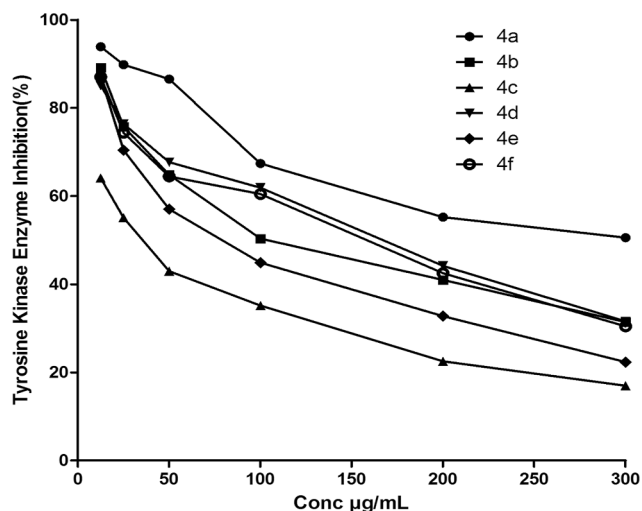

Fig. 6. Graphical representation of enzyme Tyrosine kinase inhibition by compounds 4a-f: Plot of concentration in µg/mL v/s rate of inhibition.

Table 6
Enzyme inhibition of Tyrosine kinase enzyme by compounds **4a-f.**

Compound code	IC$_{50}$ value[a]
4a	0.31 ± 0.11
4b	0.86 ± 0.42
4c	0.10 ± 0.16
4d	0.35 ± 0.17
4e	0.43 ± 0.21
4f	0.56 ± 0.24

[a] IC$_{50}$ values measured in µM.

selectivity was determined. The selective index value in the range of 2.17–13.89 was displayed by the compounds screened. The docking results revealed that compounds **4a**, **4c** and **4d** had good interaction with the active site of enzyme tyrosine kinase. Further, enzyme

inhibition study of compounds **4a-f** proved that, all compounds inhibits the activity of enzyme tyrosine kinase with IC$_{50}$ value in the range of 0.10–0.86 µM, with maximum inhibition being exhibited by compound **4c** with IC$_{50}$ value 0.10 ± 0.16 µM. The results were found to be compatible with the docking studies, thus demonstrating that compound **4a**, **4c** and **4d** act as potent inhibitors of tyrosine kinase. Accordingly, a mode of cell death was studies using double staining and DAPI method thus signified the mode of cell death to be late apoptosis. SAR analysis reveals the influence of benzoxazole *N*-heterocyclic hybrids in defining its cytotoxicity and anticancer activity.

On contrary, the *in-vitro* anti-tubercular screening [42] of the compounds **2a-r** against *Mycobacterium tuberculosis* H$_{37}$RV strain exhibited excellent anti-tubercular activity with the MIC value ranging from 1.6 to 25 µg/mL compatible with the standard drugs Pyrazinamide, Streptomycin and Ciprofloxacin, however, compounds **4a-f** were active only upto MIC value of 50 µg/mL, thus indicating that these compounds are selective inhibitors of tyrosine kinase enzyme. (Fig. 10)

4. Experimental section

4.1. Chemistry

4.1.1. General methods

All the chemicals were purchased from Avra synthesis; Lobachemie, Finar. Apparatus has been purchased from J-Sil and Agarwal. Melting points were determined by using thiels tube method using open capillaries and have been uncorrected. IR was recorded on SHIMADZU FTIR affinity-1. The NMR spectra were measured in CDCl$_3$ or DMSO at RT on a Brucker AV-II 400 spectrometer. δ is given in ppm relative to tetramethylsilane as an internal reference. Thin layer chromatography was performed using DDC-fertigfolien ALUGRAM^{R}Xtra SIL G/UV$_{254}$ (Macherey-Nagel GmbH & Co.KG) Compounds were visualized by illumination under UV light (254 nm) or by use of phosphomolybdic acid stain followed by heating. Melting points were determined using an open capillary tube method and were uncorrected. Chemical shifts are expressed in parts per million relative to tetramethylsilane, which was used as internal standard, coupling constant (J) are in hertz (Hz), and signals are designated as follows: s, singlet; d, doublet; t, triplet; q,
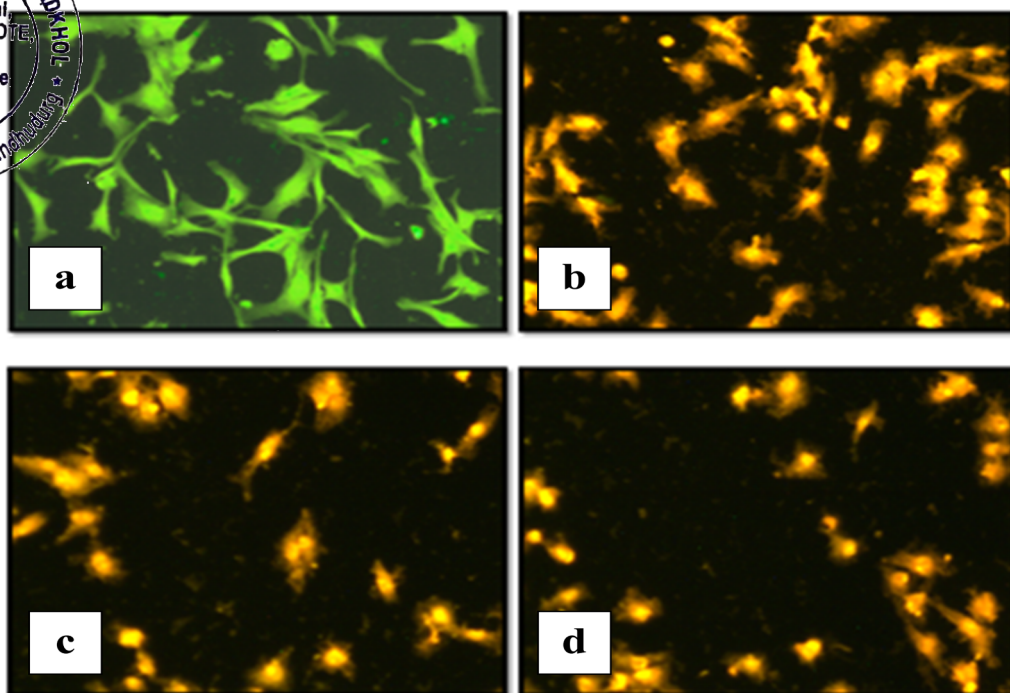
Fig. 7. Fluorescence microscopy images of cells stained with acridine orange/ ethidium bromide, a) viable cells, b) Cells treated with compound 4a, c) cells treated with compound 4c, d) cells treated with compound 4d.

quartet; m, multiplet; dt, doublet of triplet; ddd, double of doublet of doublet, dq, doublet of quartet. All solvents were dried prior to use and stored over 4Aº molecular sieves.

4.1.2. Synthesis of benzoxazole derivatives *2a-r* and *4a-f* (Scheme 1 & 2)

To the flask containing a mixture of substituted benzaldehyde (1mmole) and 2-aminophenol (1mmole) was added silica chloride (1 eq) and was heated on a sand bath at 120 °C, TLC was taken after every 1 h. After 4 h, TLC showed appearance of new spot. The product was isolated by first separating out the catalyst by filtration using organic solvent; the organic layer was dried using anhydrous sodium sulfate and evaporated under vacuum. The solid thus obtained was
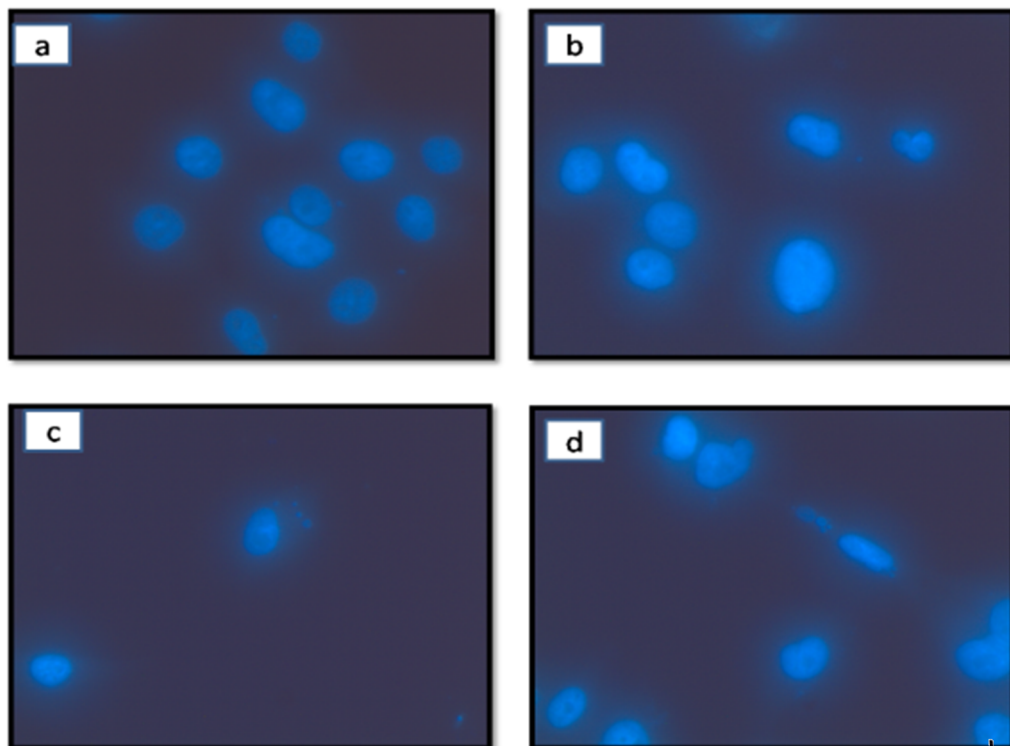

Fig. 8. Fluorescence microscopy images of cells stained with DAPI, showing (a) viable cells, (b) Cells treated with compound 4a, (c) cells treated with compound 4c, (d) cells treated with compound 4d.
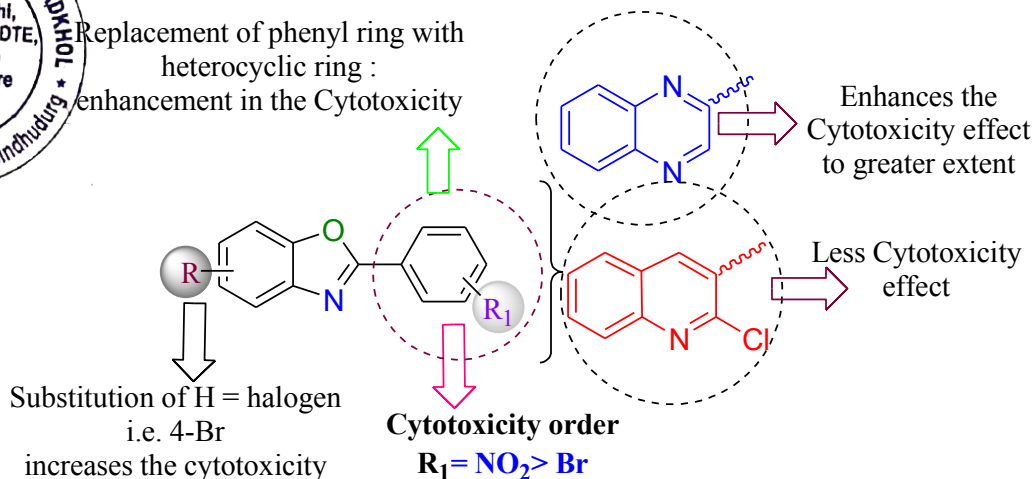
Replacement of phenyl ring with heterocyclic ring : enhancement in the Cytotoxicity

Enhances the Cytotoxicity effect to greater extent

Less Cytotoxicity effect

Substitution of H = halogen i.e. 4-Br increases the cytotoxicity

Cytotoxicity order
$R_1 = NO_2 > Br$

Fig. 9. Structural representation of SAR from cytotoxicity study of benzoxazole hybrids 4a-f.

recrystallized using petroleum ether and its % yield and melting points were determined. The results are tabulated in Table 1 and Table 2.

4.1.2.1. 2-(2′, 4′-dichlorophenyl)-1, 3-benzoxazole (2a). This compound was prepared according to general procedure and it was obtained as buff coloured solid; yield: 75%, m. p.: 125–127 °C; IR (KBr, cm^{-1}): 3010, 1605 (C=C), 1677 (C=N), 1030; ^{1}H NMR (400 MHz, δ, ppm, CDCl$_3$): 7.37–8.15(m, 4H, Ar—H), 8.0 (s, 1H, J = 6.26 Hz, 3′- H), 7.62 (dd, 1H, J = 6.26, 1.8 Hz, 5′-H), 7.24 (dd, 1H, J = 1.8 Hz, 6′-H); ^{13}C NMR (100 MHz, δ, ppm, CDCl$_3$): 161.81, 150.1, 141.125, 135.66, 133.89, 129.54, 128.90, 128.12, 127.88, 124.98, 124.11, 119.859, 110.372.

4.1.2.2. 2-(4′-chlorophenyl)-1, 3-benzoxazole (2b). This compound was prepared according to general procedure and it was obtained as buff coloured solid; yield: 75%, m. p.: 144–148 °C; IR (KBr, cm^{-1}): 3015, 1657 (C=N), 1607 (C=C), 1035 (C—O), 780; ^{1}H NMR (400 MHz, δ, ppm, CDCl$_3$): 7.27–8.07(m, 4H, Ar—H), 7.92 (ddd, 2H, J = 8.2, 1.8 Hz, 3′ & 5′-H), 7.814 (ddd, 1H, J = 1.6, 8.4 Hz, 2′ & 6′-H); ^{13}C NMR (100 MHz, δ, ppm, CDCl$_3$): 164.81, 151.1, 140.125, 135.70, 129.35, 129.35, 128.88, 128.88, 127.57, 124.92, 124.15, 119.859, 110.383.

4.1.2.3. 2-(4′-bromophenyl)-1, 3-benzoxazole (2c). This compound was prepared according to general procedure and it was obtained as buff coloured solid; yield: 71%, m. p.: 150–152 °C; IR (KBr, cm^{-1}): 3011, 1640 (C=N), 1600 (C=C), 1550, 1034 (C—O), 730; ^{1}H NMR (400 MHz, δ, ppm, CDCl$_3$): 7.42–8.02(m, 4H, Ar—H), 7.83 (ddd, 2H, J = 8.5, 1.76 Hz, 3′ & 5′-H), 7.77 (ddd, 1H, J = 1.58, 8.36 Hz, 2′ & 6′-H); ^{13}C NMR (100 MHz, δ, ppm, CDCl$_3$): 162.81, 150.8, 142.125, 136.70, 132.35, 132.35, 129.88, 129.88, 127.67, 124.98, 124.20, 119.859, 112.

4.1.2.4. 2-(3′-Nitrophenyl)-1, 3-benzoxazole (2d). This compound was prepared according to general procedure and it was obtained as buff coloured solid; yield: 79%, m. p.: 99–100 °C; IR (KBr) (ν_{max}, cm^{-1}): 3010, 1639 (C=N), 1599 (C=C), 1450, 1350, 1036; ^{1}H NMR (400 MHz, δ, ppm, CDCl$_3$): 8.88 (ddd, 1H, J = 1.6, 1.0, 1.56 Hz, 2′-H), 8.58 (dt, 1H, J = 1.8, 8.6, 1.56 Hz, 4′-H), 7.58–8.2(m, 4H, Ar—H), 8.18 (dt, 1H, J = 1.6, 1.8, 8.0 Hz, 6′-H), 7.68 (ddd, 1H, J = 7.96, 8.02, 1.02 Hz, 5′-H); ^{13}C NMR (100 MHz, δ, ppm, CDCl$_3$): 163.81, 151.3, 142.125, 140.27, 127.29, 127.15, 125.22, 124.99, 124.11, 119.89, 117.30, 116.65, 110.372.

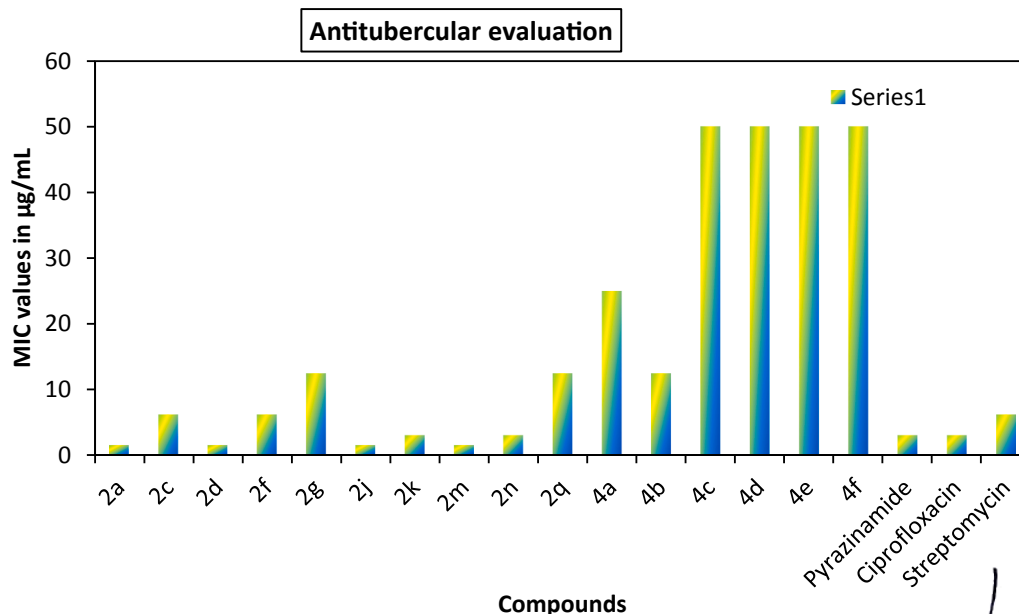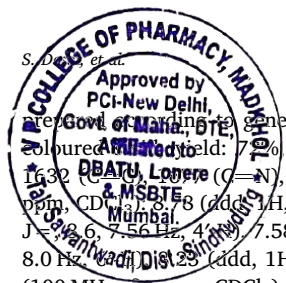*4.1.2.5. 2-(2′-Nitrophenyl)-1, 3-benzoxazole (2e)*. This compound was

Fig. 10. *In-vitro* anti-tubercular evaluation against *Mycobacterium tuberculosis* by Alamar Blue Dye Assay method.

pared according to general procedure and it was obtained as buff coloured solid; yield: 72%, m. p.: 98–103 °C; IR (KBr, cm^{-1}): 3011, 1632 (C=N), 1550, 1380, 1030; ^{1}H NMR (400 MHz, δ, ppm, CDCl$_3$): 7.78 (ddd, 1H, J = 1.0, 1.78, 7.9 Hz, 3′- H), 8.02 (dd, 1H, J = 1.2, 6.7.56 Hz, 4′-H), 7.58–8.2(m, 4H, Ar–H), 8.18 (dt, 1H, J = 1.6, 8.0 Hz, 6′-H), 8.08 (ddd, 1H, J = 7.96, 8.02, 1.02 Hz, 5′-H); ^{13}C NMR (100 MHz, δ, ppm, CDCl$_3$): 162.98, 153.3, 142.125, 140.27, 127.29, 127.15, 125.22, 124.99, 124.11, 119.89, 117.30, 116.65, 110.372.

4.1.2.6. 2-(2′-Chlorophenyl)-1, 3-benzoxazole (2f). This compound was prepared according to general procedure and it was obtained as buff coloured solid; yield: 70%, m. p.: 68–72 °C; IR (KBr, cm^{-1}): 3010, 1657 (C=N), 1607 (C=C), 1035 (C–O), 780; ^{1}H NMR (400 MHz, δ, ppm CDCl$_3$): 7.32–8.17(m, 4H, Ar–H), 7.9 (dt, 2H, J = 8.2, 1.8 Hz, 3′-H), 7.80 (dt, 1H, J = 1.6, 8.4 Hz, 5′-H); ^{13}C NMR (100 MHz, δ, ppm, CDCl$_3$): 163.81, 150.3, 140.25, 135.80, 129.85, 129.15, 128.78, 128.18, 127.77, 125.02, 124.75, 118.89, 113.383.

4.1.2.7. 2-(4′-Nitrophenyl)-1, 3-benzoxazole (2 g). This compound was prepared according to general procedure and it was obtained as buff coloured solid; yield: 79%, m. p.: 256–260 °C; IR (KBr, cm^{-1}): 3010, 1639 (C=N), 1599 (C=C), 1450, 1350, 1036; ^{1}H NMR (400 MHz, δ, ppm CDCl$_3$): 8.98 (dd, 2H, J = 1.6, 8.2 Hz, 3′ & 5′- H), 8.56 (dd, 2H, J = 8.3, 1.7 Hz, 2′ & 6′-H), 7.58–8.2(m, 4H, Ar–H); ^{13}C NMR (100 MHz, δ, ppm, CDCl$_3$):164.81, 152.3, 142.125, 140.27, 131.21, 131.21, 125.99, 125.11, 120.89, 118.30, 117.65, 117.65, 113.372.

4.1.2.8. 2-Phenyl-1, 3-benzoxazole (2 h). This compound was prepared according to general procedure and it was obtained as buff coloured solid; yield: 78%, m. p.: 98–100 °C; IR (KBr, cm^{-1}): 3010, 1605 (C=C), 1550 (C=N), 1030; ^{1}H NMR (400 MHz, δ, ppm CDCl$_3$): 7.37–8.15(m, 4H, Ar-H), 7.17–7.80(m, 4H, Ar'-H); ^{13}C (100 MHz, δ, ppm, CDCl$_3$):162.81, 150.1, 141.125, 128.90, 128.90, 128.88, 127.99, 127.99, 127.1, 124.98, 124.11, 119.859, 110.372.

4.1.2.9. 2-(4′-Methoxyphenyl)-1, 3-benzoxazole (2i). This compound was prepared according to general procedure and it was obtained as buff coloured solid; yield: 77%, m. p.: 114–116 °C; IR (KBr, cm^{-1}): 3010, 1620 (C=N), 1590 (C=C), 1210, 1030; ^{1}H NMR (400 MHz, δ, ppm CDCl$_3$): 7.29–7.90 (m, 4H, Ar-H), 7.89 (dd, 2H, J = 1.75, 8.8 Hz, 2′ & 6′- H), 7.34 (dd, 2H, J = 8.8, 1.75 Hz, 3′ & 5′-H), 3.84 (s, 3H, OMe); ^{13}C NMR (100 MHz, δ, ppm, CDCl$_3$): 164.399, 160.42, 150.11, 128.92, 128.92, 127.43, 124.89, 124.211, 119.85, 114.783, 114.783, 110.347, 55.89.

4.1.2.10. 2-(4′-Methylphenyl)-1, 3-benzoxazole (2j). This compound was prepared according to general procedure and it was obtained as buff coloured solid; yield: 79%, m. p.:104–106 °C; IR (KBr) (ν_{max}, cm^{-1}): 3030, 1605 (C=N), 1580 (C=C), 1030; ^{1}H NMR (400 MHz, δ, ppm, CDCl$_3$): 7.30–8.08(m, 4H, Ar-H), 7.84 (dd, 2H, J = 1.5, 7.8 Hz, 2′ & 6′- H), 7.52 (dd, 2H, J = 7.88, 1.5 Hz, 3′ & 5′-H), 2.34 (s, 3H, Me); ^{13}C NMR (100 MHz, CDCl$_3$) (δ, ppm): 161.81, 150.1, 141.125, 135.66, 133.89, 129.54, 128.90, 128.12, 127.88, 124.98, 124.11, 119.859, 110.372.

4.1.2.11. 2-(3′-Chlorophenyl)-1, 3-benzoxazole (2k). This compound was prepared according to general procedure and it was obtained as buff coloured solid; yield: 72%, m. p.: 120–122 °C; IR (KBr) (ν_{max}, cm^{-1}): 3020, 1635 (C=N), 1600 (C=C), 1030, 760; ^{1}H NMR (400 MHz, δ, ppm, CDCl$_3$): 7.88 (dt, 1H, J = 1.6, 1.0, 1.56 Hz, 2′- H), 7.82 (dd, 1H, J = 8.6, 1.56 Hz, 4′-H), 7.46–8.10 (m, 4H, Ar-H), 7.78 (dt, 1H, J = 1.6, 1.8 Hz, 6′-H), 7.68 (dd, 1H, J = 7.86, 8.2 Hz, 5′-H); ^{13}C NMR (100 MHz, δ, ppm, CDCl$_3$):162.81, 151.1, 140.125, 138.66, 135.89, 127.54, 125.90, 124.88, 124.12, 123.98, 120.11, 119.59, 110.72.

4.1.2.12. 2-(4′-Hydroxy, 5′-nitrophenyl)-1, 3-benzoxazole (2l). This compound was prepared according to general procedure and it was obtained as buff coloured solid; yield: 75%, m. p.:170–174 °C; IR (KBr, cm^{-1}): 3200, 3010, 1630 (C=N), 1600 (C=C), 1550, 1350, 1030; ^{1}H NMR (400 MHz, δ, ppm, CDCl$_3$):8.8 (dd, 1H, J = 1.65, 2.8 Hz, 6′-H), 8.25 (dd, 1H, J = 1.6, 7.9 Hz, 2′-H), 7.52–8.02 (m, 4H, Ar-H), 7.35 (dd, 1H, J = 7.9,2.6 Hz, 3′-H); ^{13}C NMR (100 MHz, δ, ppm, CDCl$_3$): 161.81, 150.1, 141.125, 135.66, 133.89, 129.54, 128.90, 128.12, 127.88, 124.98, 124.11, 119.859, 110.372.

4.1.2.13. 2-(2′-Hydroxy, 5′-nitrophenyl)-1, 3-benzoxazole (2m). This compound was prepared according to general procedure and it was obtained as buff coloured solid; yield: 71%, m. p.: 188–192 °C; IR (KBr, cm^{-1}): 3210, 1635 (C=N), 1600 (C=C), 1580,1359, 1030; ^{1}H NMR (400 MHz, δ, ppm, CDCl$_3$): 8.79 (dd, 1H, J = 3.11, 1.7 Hz, 6′-H), 8.34 (dd, 1H, J = 1.7, 7.6 Hz, 3′-H), 7.52–8.02 (m, 4H, Ar-H), 7.38 (dd, 1H, J = 8.6,1.4 Hz, 4′-H); ^{13}C NMR (100 MHz, δ, ppm, CDCl$_3$): 161.81, 150.1, 141.125, 135.66, 133.89, 129.54, 128.90, 128.12, 127.88, 124.98, 124.11, 119.859, 110.372.

4.1.2.14. 2-(4′-Fluorophenyl)-1, 3-benzoxazole (2n). This compound was prepared according to general procedure and it was obtained as buff coloured solid; yield: 79%, m. p.: 90–92 °C; IR (KBr, cm^{-1}): 3010, 1660 (C=N), 1610 (C=C), 1030 1000; ^{1}H NMR (400 MHz, δ, ppm, CDCl$_3$): 7.30–8.05(m, 4H, Ar-H), 7.83 (dd, 2H, J = 1.2, 8.12 Hz, 2′ & 6′-H), 7.34 (dd, 2H, J = 8.12, 1.02 Hz, 3′ & 5′-H); ^{13}C NMR (100 MHz, δ, ppm, CDCl$_3$): 164.4, 163.35, 150.11, 141.125, 133.4, 133.4, 127.5, 124.98, 124.33, 119.85, 117.8, 117.98, 110.76.

4.1.2.15. 2-(3′-Bromophenyl)-1, 3-benzoxazole (2o). This compound was prepared according to general procedure and it was obtained as buff coloured solid; yield: 72%, m. p.: 133–137 °C; IR (KBr, cm^{-1}): 3010, 1655 (C=N), 1610 (C=C), 1030, 760; ^{1}H NMR (400 MHz, δ, ppm, CDCl$_3$):7.42–8.1 (m, 4H, Ar-H), 7.77 (dt, 1H, J = 1.5 Hz, 2′- H), 7.64 (dd, 1H, J = 1.5, 8.1 Hz, 4′-H), 7.57 (dt, 1H, J = 1.5, 1.4, 7.8 Hz, 6′-H), 7.51 (dd, 1H, J = 8.0, 7.8 Hz, 5′-H) ; ^{13}C NMR (100 MHz, δ, ppm, CDCl$_3$):163.67, 150.11, 141.125, 132.5, 130.89, 130.11, 129.89, 127.99, 125.76, 124.98, 124.311, 119.03, 110.9.

4.1.2.16. 2-(4′-N-dimethylaminophenyl)-1, 3-benzoxazole (2p). This compound was prepared according to general procedure and it was obtained as buff coloured solid; yield: 70%, m. p.: 179–182 °C; IR (KBr, cm^{-1}): 3100, 3010, 1605 (C=N), 1590 (C=C), 1030; ^{1}H NMR (400 MHz, δ, ppm, CDCl$_3$):7.2–7.8 (m, 4H, Ar–H), 7.8 (dd, 2H, J = 1.45, 8.8 Hz, 2′ & 6′- H), 6.75 (dd, 2H, J = 8.8, 1.5 Hz, 3′ & 5′-H), 2.89 (s, 6H, Me); ^{13}C NMR (100 MHz, δ, ppm, CDCl$_3$):: 164.4, 151.22, 150.11, 141.125, 131.3, 131.3, 127.87, 124.90, 124.311, 119.85, 111.3, 111.3,110.2, 40.5.

4.1.2.17. 2-(5′-Bromo-4′-hydroxy-3′-methoxyphenyl)-1,3-benzoxazole (2q). This compound was prepared according to general procedure and it was obtained as buff coloured solid; yield: 78%, m. p.: 187–192 °C; IR (KBr, cm^{-1}): 3250, 3010, 1610 (C=N), 1590 (C=C), 1030, 780; ^{1}H NMR (400 MHz, δ, ppm, CDCl$_3$): 7.16–7.88 (m, 4H, Ar–H), 7.53 (d, 1H, J = 2.0 Hz, 2′- H), 7.32 (d, 1H, J = 2.0 Hz, 6′-H), 4.5 (brs, 1H, OH), 3.7(s, 1H, OMe); ^{13}C NMR (100 MHz, δ, ppm, CDCl$_3$): 163.67, 150.1, 149.8, 148.7, 141.25, 130.87, 125.96, 124.93, 124.112, 119.89, 110.49, 110.3, 110.25, 55.21.

4.1.2.18. 2-(3′,5′-Dibromo-4′-hydroxyphenyl)-1,3-benzoxazole (2r). This compound was prepared according to general procedure and it was obtained as buff coloured solid; yield: 70%, m. p.: 166–169 °C; IR (KBr, cm^{-1}): 3300, 3010, 1630 (C=N), 1600 (C=C), 1030, 780; ^{1}H NMR (400 MHz, δ, ppm, CDCl$_3$): 7.16–7.89 (m, 4H, Ar–H), 7.76 (d, 2H, J = 2.0 Hz, 2′ & 6′-H), 4.5 (brs, 1H, OH); ^{13}C NMR (100 MHz, δ, ppm, CDCl$_3$):163.67, 152.11, 150.4, 141.3, 130.71, 130.71, 111.08, 111.08,

110.07, 124.07, 124.21, 125.52.

4.1.2.19. 5-Bromo-(4'-nitrophenyl)-1, 3-benzoxazole (**4a**). This compound was prepared according to general procedure and it was obtained as buff coloured solid; yield: 80%, m. p.: 228–232 °C; IR (KBr, cm⁻¹): 3050 (C=N), 1600 (C=C), 1550, 1380, 1030; ¹H NMR (400 MHz, δ, ppm, CDCl₃): 8.28 (dd, 2H, *J* = 8.8 Hz, 3′ & 5′-H), 7.99(d, 1H, *J* = 8.6 Hz, 7- H), 7.97 (dd, 1H, *J* = 8.8 Hz, 2′ & 6′-H), 7.82 (d, 1H, 4-H), 7.53 (dd, 1H, *J* = 8.6 Hz, 6-H); ¹³C NMR (100 MHz, δ, ppm, CDCl₃):164.04, 150.03, 142.53, 131.3, 131.3, 129.37, 128.62, 124.27, 119.66, 118.03, 117.3, 117.3, 114.7. HRMS: (M + H) Obs: 317.196; Cal: 317.218.

4.1.2.20. 5-Bromo-2-(4'-bromophenyl)-1, 3-benzoxazole (**4b**). This compound was prepared according to general procedure and it was obtained as buff coloured solid; yield: 72%, m. p.: 158–162 °C; IR (KBr, cm⁻¹): 3010, 1655 (C=N), 1620 (C=C), 1030, 780, 760; ¹H NMR (400 MHz, δ, ppm, CDCl₃):8.06 (s, 1H, *J* = 2.7 Hz, 4-H), 7.87(dd, 1H, *J* = 2.7, 8.3 Hz, 7- H), 7.83 (dd, 1H, *J* = 8.6 Hz, 2′ & 6′-H), 7.80 (dd, 2H, *J* = 8.6 Hz, 3′ & 5′-H), 7.28 (dd, 1H, *J* = 7.9 Hz, 6-H); ¹³C NMR (100 MHz, δ, ppm, CDCl₃):164.04, 149.63, 141.23, 132.6, 132.6, 129.37, 128.62, 128.62, 119.66, 118.03, 117.87, 117.2, 114.7. HRMS: (M + H) Obs: 350.90 (100.0%); Cal: 350.89.

4.1.2.21. 2-(5-Bromophenyl-1, 3-benzoxazol-2yl)quinoxaline (**4c**). This compound was prepared according to general procedure and it was obtained as buff coloured solid; yield: 80%, m. p.: 189–192 °C; IR (KBr, cm⁻¹): 3010, 1665 (C=N), 1617 (C=C), 1030, 780; ¹H NMR (400 MHz, δ, ppm, CDCl₃): 9.3 (s, 1H, 3-H), 8.47 (ddt, 1H, *J* = 8.2, 1.9, 3.5 Hz, 5-H), 8.36 (dt, 1H, *J* = 3.5, 1.9, 8.4 Hz, 8- H), 8.06 (dt, 1H, *J* = 8.4, 7.9, 6-H), 7.87 (dd, 1H, *J* = 8.4, 7.3 Hz, 7′-H), 7.(dd, 1H, *J* = 7.7 Hz, 7-H), 7.89 (dd, 1H, *J* = 8.5 Hz, 6′-H), 7.72 (dt, 1H, *J* = 7.9 Hz, 5′-H); ¹³C NMR (100 MHz, δ, ppm, CDCl₃):161.5, 152.01, 149.7, 145.8, 142.35, 141.9, 141.78, 132.52, 129.28, 128.56, 128.08, 119.43, 117.84. HRMS: (M + H)⁺ Obs: 326.26; Cal: 326.25.

4.1.2.22. 2- (1, 3-benzoxazol-2-yl) quinoxaline (**4d**). This compound was prepared according to general procedure and it was obtained as buff coloured solid; yield: 74%, m. p.: 160–164 °C; IR (KBr, cm⁻¹): 3010, 1650 (C=N), 1607 (C=C), 1030; ¹H NMR (400 MHz, δ, ppm, CDCl₃):9.4 (s, 1H, 3-H), 8.47 (ddt, 1H, *J* = 8.12, 3,48, 1.96 Hz), 8.35 (dd, 1H, *J* = 8.4 Hz, 8- H), 8.1 (dd, 1H, *J* = 8.6 Hz), 8.03 (dd, 1H, *J* = 8.0, 6-H), 7.99 (dd, 1H, *J* = 8.4, 4.5 Hz, 7′-H), 7.96 (dd, 1H, *J* = 7.7 Hz, 7-H), 7.89 (dd, 1H, *J* = 8.5 Hz, 6′-H), 7.72 (dt, 1H, *J* = 7.9 Hz, 5′-H) ; ¹³C NMR (100 MHz, δ, ppm, CDCl₃): 161.4, 152.04, 148.58, 145.64, 142.29, 141.53, 141.01, 131.10, 128.8, 127.97, 125.44, 124.3, 121.14, 115.41, 111.54. HRMS: (M + H)⁺ Obs: 247.08; Cal: 247.07.

4.1.2.23. 3-(1, 3-benzoxazol-2yl) − 3-chloroquinoline (**4e**). This compound was prepared according to general procedure and it was obtained as buff coloured solid; yield: 75%, m. p.: 102–108 °C; IR (KBr, cm⁻¹): 3010, 1665 (C=N), 1637 (C=C), 1030, 830; ¹H NMR (400 MHz, δ, ppm, CDCl₃): 7.37–8.15(m, 4H, Ar−H), 8.0 (s, 1H, *J* = 6.26 Hz, 3′- H), 7.62 (dd, 1H, *J* = 6.26, 1.8 Hz, 5′-H), 7.24 (dd, 1H, *J* = 1.8 Hz, 6′-H); ¹³C NMR (100 MHz, δ, ppm, CDCl₃): 161.81, 150.1, 141.125, 135.66, 133.89, 129.54, 128.90, 128.12, 127.88, 124.98, 124.11, 119.859, 110.372. HRMS: (M + H)⁺ Obs: 280.05; Cal: 280.04.

4.1.2.24. 3-(5-Bromophenyl- 1, 3-benzoxazol-2yl) − 3-chloroquinoline (**4f**). This compound was prepared according to general procedure and it was obtained as buff coloured solid; yield: 76%, m. p.: 170–175 °C; IR (KBr, cm⁻¹): 3010, 1660 (C=N), 1620 (C=C), 1030, 830; ¹H NMR (400 MHz, δ, ppm, CDCl₃): 7.37–8.15 (m, 4H, Ar−H), 8.0 (s, 1H, *J* = 6.26 Hz, 3′- H), 7.62 (dd, 1H, *J* = 6.26, 1.8 Hz, 5′-H), 7.24 (dd, 1H,

J = 1.8 Hz, 6′-H); ¹³C NMR (100 MHz, δ, ppm, CDCl₃):161.81, 150.1, 141.125, 135.66, 133.89, 129.54, 128.90, 128.12, 127.88, 124.98, 124.11, 119.859, 110.372. HRMS: (M + H)⁺ Obs: 294.07; Cal: 294.06

4.2. Biological evaluation

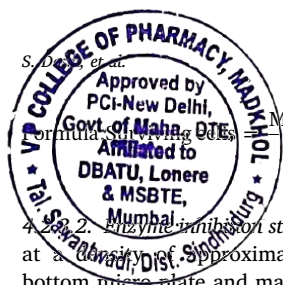### 4.2.1. Virtual screening: Protein structure preparation

The molecular docking study was performed using Molegro Virtual Docker (MVD-2013, 6.0). The crystal structure of the enoyl- ACP reductase (InhA) complexed with an isonicotinic-acyl-NADH inhibitor and epidermal growth factor receptor tyrosine kinase domain with 4-anilinoquinazoline inhibitor erlotinib (PDB ID: 1M17) were downloaded from Protein Data Bank (PDB ID: 1ZID). Molecular docking studies of the synthesized compounds/ligands were performed in order to understand the various interactions between the ligand and enzyme active site in detail. The molecular docking study was performed for the target compounds by using MVD-2013 (Version: 6.0).

4.2.2. Molecular docking study

The synthesized compounds were built using Chemdraw 11.0. The 2D structures were then converted into energy minimized 3D structures and were saved as MDL Molfile (.mol2). The coordinate files and crystal structures of enoyl-acpreductase (InhA, PDB ID: 1ZID) and tyrosine kinase (PDB ID: 1M17) were obtained from the RCSB PDB website. The protein files were prepared by the removal of water molecules, addition of polar hydrogens and removal of other bound ligands. In the present study, the binding sites were selected based on the amino acid residues, which are involved in binding with isonicotinic-acyl-NADH inhibitor of InhA and erlotinib as obtained from protein data bank, which would be considered as the probable best accurate regions as they are solved by experimental crystallographic data. The docking protocol was carried out for the synthesized compounds as listed in Table 3 using MVD-2013 (6.0) software using the standard operating procedures.

4.2.3. Anti-cancer Evaluation:

4.2.3.1. General procedure for evaluation of anti-cancer inhibitory activity. The anti-cancer activity of the compounds has been accessed by MTT assay. Initially, MTT stock solution has been prepared by taking 5 mg in 1 mL of PBS. MCF-7 cell line has been used for the study. The cell line was maintained in 96 wells micro titer plate containing MEM media supplemented with 10% heat inactivated fetal calf serum(FCS), containing 5% mixture of Gentamicin (10 μg), Penicillin (100units/mL) and streptomycin (100 μg/mL) in presence of 5% CO₂ at 37 °C for 48–72 h. In-vitro growth inhibition effect of test compounds was assessed by colorimetric or spectrophotometric determination of conversion of MTT into Formazan blue by living cells. Initially the supernatant from the plate was removed and fresh MEM solution was added and was treated with different concentrations of extract or compound appropriately diluted with DMSO. In our study, 10, 20, 25, 30 and 50 μL (10 mg/mL prepared in DMSO) of stock solutions were added to respective wells containing 100 μL of the medium. Thereby making the final concentrations as 10, 20, 25, 30 and 50 μg/mL. After 48hrs of incubation at 37 °C in a humidified atmosphere of 5% CO₂, stock solution of 3-(4, 5-dimethylthiazol-2-yl)-2, 5- diphenyl tetrazolium bromide was added to each well (20 μL, 5 mg per mL in sterile phosphate buffered saline) for further 4 h incubation. The supernatant carefully aspirated, the precipitated crystals of Formazan blue were solubilised by adding DMSO and optical density was measured at wavelength of 570 nm by using LISA plus. The results were represented as mean of five readings upto the concentration at which the OD of treated cells was reduced by 50% with respect to the untreated control. During this assay, reduction of yellow 3-(4, 5-dimethylthiazol-2-yl)-2, 5-diphenyl tetrazolium bromide was measured by mitochondrial succinate dehydrogenase.

$$\text{Formula Stimulating OD} = \frac{\text{Mean OD of test compound}}{\text{Mean OD at control}} \times 100$$

4.2.2.2. Enzyme inhibition studies. Cell Treatment- The cells were seeded at a density of approximately 1×10^5 cells/well in a 96-well flat-bottom micro plate and maintained at 37 °C in 95% humidity and 5% CO_2 for overnight. Cells were treated with different concentration of test samples. Then cells were incubated for another 24 h. The cells in well were washed twice with phosphate buffer solution, and 1 mL of extraction buffer was added. Using cell scraper cells were recovered carefully and centrifuge the cells at 4 °C for 10 min at 10,000 rpm. Collect the supernatant and store as further analysis.

Tyrosine Kinase Assay- Collected supernatant was diluted 25 times with kinase reacting solution provided along with kit. The diluted control was added and treated to sample in each well in duplicate. Then 10 μL of 40 mM ATP-2Na solution was added into each well and mixed well. Further, incubated for 30 min at 37 °C.Then the samples were removed, the wells were washed 3 times with wash buffer. 100 μL of blocking solution was added into each well and incubated for 30 min at 37 °C. The blocking solution was discarded and then 50 μL of Anti-phosphotyrosine - HRP solution was added into each well and in-cubatedt for 30 min at 37 °C. Now, the antibody solution was discarded and then each well was washed 4 times with washing buffer. Further, 100 μL of HRP substrate solution (TMBZ) was added into each well. Incubated for 30 min at 37 °C. Finally, 100 μL of stop solution was added into each well in the same order as HRP substrate solution. The absorbance is measured at 450 nm with a plate reader.

%Inhibition = 1 − (Abs of sample/Abs of control) × 100

4.3. Cell morphology studies by fluorescence microscopy

4.3.1. Double staining (Acridine orange-Ethidium bromide)

The cells were seeded at a density of approximately $1x10^4$ cells/well in a 24 well flat bottom micro plate containing cover slips and main-tained at 37 °C in CO_2 incubator for overnight. More than the IC_{50} of synthesised compounds was treated at 72 hrs. After the incubation, cells were washed with PBS and fixed with 4% paraformaldehyde for 30 min. 20 μL of dye mixture was incubated for half an hour, examined under fluorescent microscope.

4.3.2. Dapi

The cells were seeded at a density of approximately $1X10^5$ cells/well in a 12 well flat bottom micro plate containing cover slips and main-tained at 37 °C in CO_2 incubator for overnight. More than the IC_{50} of synthesised compounds was treated at 72 hrs. After the incubation, cells were washed with PBS and fixed with 4% paraformaldehyde for 30 min. 20 μL of dye mixture was incubated for 20 min, examined under fluorescent microscope.

Declaration of Competing Interest

The authors declare no conflicts of interest.

Acknowledgements

Appendix A. Supplementary material

Supplementary data to this article can be found online at https://doi.org/10.1016/j.bioorg.2019.103382.

References

[1] P. Anand, A.B. Kunnumakkara, C. Sundaram, K.B. Harikumar, S.T. Tharakan, O.S. Lai, B. Sung, B.B. Aggarwal, Cancer is preventable disease that requires major lifestyle changes, Pharma. Res. 25 (2008) 2097–2116.

[2] H. Lage, E. Aki-Sener, I. Yalcin, High anti-neoplastic activity of new heterocyclic compounds in cancer cells with resistance against classical DNA topoisomerase-II targeting drugs, Inter. J. Cancer 119 (1) (2006) 213–220.

[3] S. Vijayan, D.S. Janardhanam, M. Karthikeyan, J. Sunitha, R.J. Raghunatham, Laison between microorganisms and oral cancer, Pharm. Bioappl. Sci. 7 (2015) 354–360.

[4] D. Foulkes, L.E. William, J.S. Smith, R. Filho, Triple negative breast cancer, New Eng. J. Med. 363 (20) (2010) 1938–1948.

[5] S. Dawood, Triple negative breast cancer: Epidemiology and management options, Drugs 70 (2010) 2247–2258.

[6] D.J. Slamon, B.J. Leyland, S. Shak, Addition of Herceptin (humanized antiHer-2 antibody) to first line chemical for Her-2 overexpressing metastatic breast cancer markedly increased anti-cancer activity: A randomized multinational controlled phase III trial, Proc. Am. Soc. Clin. Oncol. 17 (1998) 377.

[7] D.J. Slamon, G.M. Clark, S.G. Wong, W.J. Levin, A. Ullrich, Guire Mc, Human breast cancer: correlation of relapse & survival with amplification of Her-2/new oncogene, Science 235 (1987) 177–182.

[8] D.J. Slamon, B.J. Leyland, S. Shak, H. Fuchs, V. Paton, A. Bajamonde, Use of che-motherapy plus a monoclonal antibody against Her-2 for metastatic breast cancer that over expresses Her-2, New Eng. J. of Med. 344 (2001) 783–792.

[9] M.M. Goldenberg, Trastuzumaz, a recombinant DNA- derived humanized mono-clonal antibody, a novel agent for the treatment of metastatic breast cancer. Trastuzumaz, a recombinant DNA- derived humanized monoclonal antibody, a novel agent for the treatment of metastatic breast cancer, Clin. Ther. 21 (1999) 309–318.

[10] U. Singh, G. Chashoo, S.U. Khan, P. Mahajan, A. Nargotra, G. Mahajan, A. Singh, A. Sharma, M.J. Mintoo, S.K. Guru, H. Aruri, Design of novel 3-pyr-imidinylazaindole CDK2/9 inhibitors with potent in vitro and in-vivo anti-tumor efficacy in a triple negative breast cancer model, J. Med. Chem. 60 (2017) 9470–9489.

[11] G. Manning, D.B. Whyte, R. Martinez, T. Hunte, S. Sudarsanam, The protein kinase complement of human genome, Science 298 (2002) 1912–1934.

[12] J. Easmon, G. Pinstinger, K.S. Thies, G. Heinisch, J. Hofman, Synthesis, structure activity relationship and antitumor studies of benzoxazolyl hydrazones derived from alfa-N-acyl heteroaromatics, J. Med. Chem. 49 (2006) 6343–6350.

[13] C. Ramalingam, S. Balasubramanyam, S. Kabilan, M.J. Vasudevan, Synthesis study of antibacterial and antifungal activities novel 1-[2-(benzoxazol-2-yl)ethoxy]-2,6-diarylpiperidine-4-ones, Eur. J. Med. Chem. 39 (2004) 527–533.

[14] G. Turan-Zitouni, S. Demirayak, A. Ozdemir, Z.A. Kaplacikli, M.T. Yilidiz, Synthesis and evaluation of bis-thiazole derivatives as new anti-cancer agents, Eur. J. Med. Chem. 39 (2003) 267.

[15] S.M. Rida, F.A. Ashour, S.A. El-Hawash, M.M. ElSemary, M.H. Badr, M.A. Shalaby, Synthesis of some novel benzoxazole derivatives as anti-HIV-1 and anti-microbial agents, Eur. J. Med. Chem. 20 (2005) 949–959.

[16] D. Kumar, M.R. Jacob, M.B. Reynolds, S.M. Kerwin, Synthesis and evaluation of anti-cancer benzoxazole and benzimidazole related to UK-1.Bioorg, Med. Chem. 10 (2002) 3997–4004.

[17] L. Perrin, A. Rakik, S. Yearly, C. Baumberger, Kinloch de Loies S, Pechiere M, Hirschel B. Combined therapy with Zidovudine and L-697-661 in primary HIV in-fection, AIDS. 10 (1996) 1233.

[18] A. Kaur, S. Wakode, D.P. Pathak, Benzoxazole: The molecule of diverse pharma-cological importance, Int. J. Pharm. and Pharm. Sci. 7 (2015) 16–23.

[19] J.A. Grobler, G. Ornadula, M.R. Rice, A.L. Simcoe, D.J. Hazuda, M.D. Miller, HIV-I reverse transcriptase plus-strand initiation exhibits preferential sensitivity to non-nucleoside reverse transcriptase inhibitors in-vitro, J. Biol. Chem. 282 (2007) 8005.

[20] P.S.M. Sommer, R. Almeida, K. Schneider, Nataxazole: a new benzoxazole deriva-tive with antitumor activity produced by Streptomyces sp Tu6176, J. Antibiot. 61 (2008) 683–686.

[21] L.Q. Sun, J. Chen, M. Bruce, J.A. Deskus, J.R. Person, K. Takaki, G. Johnson, L. Iben, R.E. Mahale, C. Xu, Synthesis and structure activity relationship of novel benzox-azole derivatives as melatonin receptor agonists, Bioorg. Med. Chem. Lett. 14 (2004) 3794.

[22] F.M. Maghaddam, G.R. Bardajee, H. Ismaili, S.M.D. Taimoory, Facile and efficient one-pot protocol for the synthesis of benzoxazole and benzothiazole derivatives using molecular iodine as catalyst, Synth. Commun. 36 (2006) 2543.

[23] G. Shitha, V.K. Bhaiamma, G. Babu, C.R. Biju, In-silico docking investigation, synthesis and in-vitro anticancer study of benzoxazole derivatives, J. Drug Deliv. Therapeut. 4 (2014) 122–126.

[24] T. Stefanski, R. Mikstacka, R. Kurczab, Z. Dutkiewicz, M. Kucinska, M. Murias, P.M. Zielinska, A. Teubert, M. Kaczmarek, Design, synthesis and bio-logical evaluation of novel combretastatin A-4 thio derivatives as microtubule targeting agents, Eur. J. Med. Chem. 144 (2018) 797–816.

[25] Singh U, Hashoo G, Khan SU, Mahajan P, Nargotra A, Mahajan S, Singh A, Sharma A, Mintoo MJ, Guru SK, Aruri H, Thatikonda T, Sahu P, Hibber P, Kumar V, Mir SA,

Govta et al. Madishetti S, Nandi U, Singh G, Mondhe M, Bhushan S, Malik F, Migwari G, Vishwakarma A, Singh PP. Design of novel pyridinylazaindole CDK2/a inhibitor with potent invitro and invivo antitumor afficacy in triple negative breast cancer model. J. Med. Chem. 2017; 60(23):9470-9489.

[26] V.G. Desai, P. Satardekar, S. Polo, K. Dhumaskar, Regioselective synthesis of 1, 3, 5-trisubstituted Pyrazoles, Synth. Commun. 42 (2012) 836–842.

[27] S. Naik, V. Desai, Use of solid-supported reagents towards synthesis of 2-arylbenzoxazole, 3, 5-diarylisoxazole and 1, 3, 5-triarylpyrazole, Green Sustain. Chem. 3 (2013) 1–7.

[28] V.G. Desai, S.R. Naik, K.L. Dhumaskar, O-Iodoxybenzoic acid mediated synthesis of 3, 5-diarylisoxazole and isoxazole-3-carboxylic acids, Synth. Commun. 44 (2014) 1453–1460.

[29] V.G. Desai, S.R. Desai, IBX-mediated, efficient, metal-free approach towards synthesis of flavones, Curr. Org. Synth. 14 (2017) 1180–1184.

[30] M.R. Saidi, Y. Pourshojaei, F. Aryanasab, Highly efficient Michael addition reaction of amines catalyzed by silica-supported aluminium chloride, Synth. Commun. 39 (2009) 1109.

[31] R. Gupta, M. Gupta, S. Paul, R. Gupta, Silica-supported ZnCl$_2$-highly active and reusable heterogenous catalyst for the one-pot synthesis of dihydropyrimidinones-thiones, Can. J. Chem. 85 (2007) 197.

[32] T.V. Kamble, R.K. Kadam, S.N. Joshi, B.D. Muley, HClO$_4$-SiO$_2$ as novel and re-cyclable catalyst for the synthesis of bis-indolylmethanes and bis-indolyl glyco-conjugates, Catal. Commun. 8 (2007) 498.

[33] V.T. Kamble, V.S. Jamode, N.S. Joshi, A.V. Biradar, R.Y. Deshmukh, An efficient method for the synthesis of acylals from aldehydes using silica-supported perchloric acid (HClO$_4$), Tetrahedron Lett. 47 (2006) 5573.

[34] H.N. Karade, M. Sathe, M.P. Kaushik, Synthesis of 4-aryl substituted 3.4-dihy-dropyrimidinones using silica chloride under solvent free conditions, Molecules 12 (2007) 1341–1351.

[35] V. Desai, S. Desai, S.N. Gaonkar, U. Palyekar, S.D. Joshi, S.K. Dixit, Novel qui-noxalinyl chalcone hybrids scaffolds as enoyl ACP reductase inhibitors: Synthesis, molecular docking and biological evaluation, Bioorg. Med. Chem. Lett. 27 (2017) 2174–2180.

[36] Mohan K. PhD thesis. Cochin University of Science and Technology: Cochin India, December 1990.

[37] A. Srivastava, R.M. Singh, Vilsmeir Haack reagent: A facile synthesis of 2-chloro-3-formyl quinolines from N-arylacetamides and transformation into different func-tionalities, Ind. J. Chem. 44 (2005) 1868–1875.

[38] A. Arora, E.A. Scholar, Role of tyrosine kinase inhibitors in cancer therapy, J. Pharmacol. Exp. Ther. 315 (2005) 971–979.

[39] M.H. Potashman, J. Bready, A. Coxon, T.M. DeMelfi, L. DiPietro, N. Doerr, D. Elbaum, J. Estrada, P. Gallant, J. Germain, Y. Gu, J.-C. Harmange, S.A. Kaufman, R. Kendall, J.L. Kim, G.N. Kumar, A.M. Long, S. Neervannan, V.F. Patel, A. Polverino, P. Rose, S.V. Plas, D. Whittington, R. Zanon, H. Zhao, Design, synthesis and evaluation of orally active benzimidazoles and benzoxazoles as vas-cular endothelial growth factor-2 receptor tyrosine kinase inhibitors, J. Med. Chem. 50 (2007) 4351–4373.

[40] D. Berta, M. Villa, A. Vulpetti, E.R. Felder, Pyrazole-benzoxazole derivatives as protein kinase inhibitors. Design and validation of a combinatorial library, Tetrahedron 61 (2005) 10801–10810.

[41] A. Doyle, J.B. Griffiths, Cell and tissue culture for medicinal research, Cell Biochem. Function. Willey and Sons, New York, 1999.

[42] The anti mycobacterial activity of compounds were assessed against M. tuberculosis H37 RV strain using microplate Alamar Blue assay (MABA). Briefly, 200μl of sterile deionzed water was added to all outer perimeter wells of sterile 96 wells plate to minimized evaporation of medium in the test wells during incubation. The 96 wells plate received 100 μl of the Middle brook 7H9 broth and serial dilution of com-pounds were made directly on plate.The final drug concentrations tested were 100 to 0.2 μg/ml.Plates were covered and sealed with parafilm and incubated at 37°C for five days.After this time, 25μl of freshly prepared 1:1 mixture of Almar Blue reagent and 10% tween 80 was added to the plate and incubated for 24 hrs. A blue color in the well was interpreted as no bacterial growth, and pink color was scored as growth. The MIC was defined as lowest drug concentration which prevented the color change from blue to pink.

RESEARCH ARTICLE
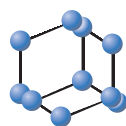
Design, Synthesis, and Characterization of Novel Linomide Analogues and their Evaluation for Anticancer Activity

Rudrax N.S. Priolkar[1], Sunil Shingade[1,*], Mahesh Palkar[2] and Shivalingrao M. Desai[1]

[1]*Department of Pharmaceutical Chemistry, PES's Rajaram and Tarabai Bandekar College of Pharmacy, Farmagudi, Goa 403401, India;* [2]*Department of Pharmaceutical Chemistry, KLEU's College of Pharmacy, Hubli, Karnataka 580031, India*

Abstract: ***Background***: According to WHO, in 2017, about 90.5 million people suffered from cancer and about 8.8 million deaths occurred due to disease. Although the chemotherapeutic agents have decreased the mortality among the cancer patients but high toxicity and non-specific targets are still major drawbacks.

Many researchers have identified linomide, a 4-hydroxy-2-quinolone derivative, as a lead molecule for the development of anticancer agents. With this background, we thought of the following objective.

Objective: The objective of this research work involves the synthesis of a series of *N*-(2-(4-hydroxy-2-oxo-1-phenyl-1,2-dihydroquinolin-3-yl)-2-oxoethyl)-*N*-alkyl substituted benzene sulfonamides IVa-d (1-3) by replacing the anilide moiety at the third position of linomide with sulfamoylacyl and also *N*-methyl by *N*-phenyl functionality. To perform *in silico* anticancer activity by using Molegro Virtual Docker (MVD-2013, 6.0) software and *in vitro* anticancer activity by MTT assay.

Methods: The starting material 4-hydroxy-1-phenylquinolin-2(1*H*)-one was treated with *N*-bromosuccinamide to yield compound II. Condensation of compound II with primary amines resulted in compounds IIIa-d, which, on coupling with substituted aromatic sulfonyl chlorides yield the title compounds IVa-d (1-3).

Results: All the synthesized compounds were satisfactorily characterized by spectral data. The results of docking revealed that the synthesized compounds exhibited well-conserved hydrogen bonds with one or more amino acid residues in the active pocket of EGFRK tyrosine kinase domain (PDB ID: 1m17). The MolDock Score of compound IVd-1 (-115.503) was the highest amongst those tested. The *in vitro* anticancer activity results showed that compound IVc-1 (R= -(CH$_2$)$_2$-CH$_3$; R′= -H) and IV d-1 (R= -CH$_2$-C$_6$H$_5$; R′= -H) were found to be most potent against K562 cell line with an IC$_{50}$ of 0.451 µM/ml and 0.455 µM/ml respectively. Compound IVd-1 also showed better potency against A549 cell line with IC$_{50}$ value of 0.704 µM/ml.

Conclusion: The results of *in silico* and *in vitro* anticancer activity are in agreement with each other. Compound IV d-1 was found to be most active of the series.

Keywords: Linomide, quinolin-2-one, *N*-bromosuccinimide, sulfonamides, anticancer, docking.

1. INTRODUCTION

Cancer is one of the first leading causes of death in economically developed countries and the second leading cause of death in developing countries [1]. The disease has been globally responsible for 8.2 million deaths in the year 2017. World Health Organization has reported that the number of new cancer cases in the world is estimated to rise by about 70% over the next two decades. From the year 2012 to 2030, the number of deaths due to cancer worldwide is estimated to increase by about 60% [2].

There have been numerous advancements and a wide array of research on the drugs, which are used to treat cancer patients. They are designed to either kill the cancer cells or modify their growth. However, the selectivity of these molecules is also a matter of concern as these drugs often bring

*Address correspondence to this author at the Department of Pharmaceutical Chemistry, PES's Rajaram and Tarabai Bandekar College of Pharmacy, Farmagudi, Goa, India; Tel:+91-7972431213;
E-mail: sunil.shingade@gmail.com

exhibit cytotoxicity towards most of the dividing cells and they do not spare DYES of non-cancerous cells. Also, these drugs tend to exhibit severe side effects and systemic toxicity [3, 4].

A wide spectrum of biological activities possessed by the quinolin-2-one nucleus has been the crucial factor in the exploration and development of compounds based on this moiety by synthetic scientists [5-8]. The biological importance and clinical significance of a number of naturally occurring alkaloids and also synthetic molecules having quinolone nucleus such as waltherione A, waltherione C and waltherione D as anti-HIV agents; flindersine as an antibacterial and antifungal agent; dictamine for smooth muscle contraction, *etc*, and synthetic analogues like aripiprazole as an antipsychotic agent, carteolol in the ophthalmic preparations as β-blocker are widely used [9-12]. Compounds containing quinolone moiety are seen to have promising pharmacological potential and good selectivity towards some specific targets.

Many researchers have identified linomide Fig. (**1**), a 4-hydroxy-2-quinolone derivative, as a lead molecule for the development of anticancer agents [13-15]. Hence, an effort was made to design and synthesize novel linomide analogues by modifying the substituent on ring nitrogen and by replacing the anilide moiety at the 3rd position of linomide with a sulfamoylacyl- side chain. Thus, there is a need to develop novel bioactive molecules, which would overcome the side effects and toxicity caused by the existing antineoplastic agents; without compromising for any therapeutic efficacy. In view of these findings, it was contemplated to design and synthesize novel linomide derivatives and to evaluate their *in silico* and *in vitro* biopotential.
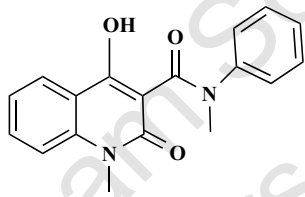

Fig. (1). Linomide structure.

2. MATERIALS AND METHODS

2.1. General Information

Chemicals used for the synthesis were purchased from Molychem (Mumbai) and SD-Fine Chem Ltd. (Mumbai). All the reagents and solvents were of laboratory grade. The reactions were monitored by Thin Layer Chromatography (TLC) using precoated plates. Melting Points of the synthesized compounds were determined by Thiele's melting point apparatus and are uncorrected. Fourier Transform Infrared (FTIR) spectra were recorded on shimadzu IR affinity-1 spectrophotometer by KBr disc method. The ^{1}H NMR and ^{13}C NMR were recorded on Bruker Avance II 400 NMR spectrometer using deuterated dimethylsulfoxide (DMSO-d_6) as the solvent and tetramethylsilane (TMS) as an internal standard. Chemical shifts are expressed as delta (δ) values in parts per million (ppm). Mass spectra were recorded on Waters, Q-TOF Micromass (LC-MS). *In silico* molecular docking study was carried out on the synthesized derivatives using Molegro Virtual Docker 2007 (version 6.0).

2.2. Synthesis

2.2.1. Synthesis of 3-(2-bromoacetyl)-4-hydroxy-1-phenyl-quinolin-2(1H)-one (II)

Compound 3-acetyl-4-hydroxy-1-phenylquinolin-2(1*H*)-one (I) was synthesized as per the literature [5]. A solution of compound I (10 mmol) and *p*-toluenesulfonic acid (*p*-TsOH) (20 mmol) in acetonitrile (50 ml) was taken in a round bottom flask. To this solution, *N*-Bromosuccinimide (NBS) (10 mmol) was slowly added and stirred. The reaction mixture was refluxed for 2 hours and then cooled to room temperature. The solvent was evaporated in vacuum and the residue was dissolved in chloroform (50 ml), washed with three portions (20 ml each) of distilled water and the chloroform layer was evaporated to obtain the solid product (II), recrystallized from benzene and dried.

2.2.2. Synthesis of 4-hydroxy-3-(2-(alkylamino)acetyl)-1-phenylquinolin-2(1H)-one (IIIa-d)
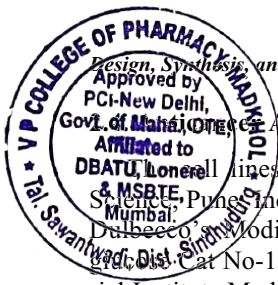
Compound **II** (1 mmol) and a primary amine (1 mmol) were refluxed at 85 ºC in ethanol with 0.2 g of sodium bicarbonate for a period of 22-24 hours. The solution obtained was evaporated using IKA rota-evaporator to obtain the crystalline product. The product was recrystallized using methanol.

2.2.3. Synthesis of N-(2-(4-hydroxy-2-oxo-1-phenyl-1,2-dihydroquinolin-3-yl)-2-oxoethyl)-N-alkyl substituted benzenesulfonamide {IVa-d (1-3)}

A mixture of compound III (0.05 mol) and a substituted aromatic sulfonylchloride (0.05 mol) was refluxed with pyridine (15 ml) for a period of 6 hours. The reaction was monitored by TLC (n-hexane:ethyl acetate; 2:8). After completion of the reaction, the reaction mixture was poured in 50 ml of ice water and refrigerated overnight. The solid product was precipitated, filtered, washed with three portions (10ml each) of distilled water and dried. Recrystallization was performed with methanol as the solvent.

2.3. Molecular Docking Study

In silico molecular docking study of the title compounds was carried out using Molegro Virtual Docker (MVD) 2007 (version 6.0). The selected molecules were built using Chemdraw 12.0.2. The 2D structures were then converted into energy minimized 3D structures, which were saved as MDL MolFile (.mol2). The coordinate file and crystal structure of epidermal growth factor receptor (EGFR) tyrosine kinase domain complexed with a 4-anilinoquinazoline inhibitor (PDB ID: 1m17) were obtained from the RCSB-PDB website. The protein file was prepared by the removal of water molecules, addition of polar hydrogens, and removal of other bound ligands. The site at which binding of the complexed inhibitor occurs was selected as the active site for docking of the molecules. The docking protocol was carried out for synthesized compounds using MVD-2007 (version 6.0) software using the standard operating procedure. The MolDock scores and the hydrogen bonding of the test compounds were compared with those of linomide and imatinib; taken as reference standards for the study [16].

2. Anticancer Activity

All cell lines (procured from National Centre for Cell Science, Pune, India) were cultured in suitable media [A549: Dulbecco's Modified Eagle's Medium (DMEM) with low glucose Cat No-11965-092; and K564: Roswell Park Memorial Institute Medium (RPMI) Cat No-AL180A] supplemented with 10% heat inactivated fetal calf serum (FBS) and 1% Antibiotic – Antimycotic 100X solution. The cells were seeded at a density of approximately 5×10^3 cells/well in a 96-well flat-bottom micro plate and maintained at 37 ºC in 95% humidity and 5% CO_2 overnight. The cell lines were treated with 400, 300, 200, 100, 50 and 25 µg/ml concentrations of the samples. The cells were incubated for another 48 hours. The cells in well were washed twice with phosphate buffer solution, and 20 µl of the 3-(4,5-dimethythiazol-2-yl)-2,5-diphenyl tetrazolium bromide (MTT) staining solution (5 mg/ml in phosphate buffer) was added to each well and plate was incubated at 37 ºC. After 4 hours, 100 µl of DMSO was added to each well to dissolve the formazan crystals, and given formula. Using Graph Pad Prism Version 5.1, the IC_{50} of the compounds were determined. Paclitaxel ($IC_{50}= 0.3$ µM/ml; determined using the same procedure) was used as a standard for comparison.

Cell viability (%) =, *Mean optical density of the test compound-Mean optical density of negative control.* x 100

3. RESULTS

3.1. Characterization

The synthesized compounds were characterized by spectral analysis. Spectral data of representative compounds is presented herewith.

3.1.1. Spectral data of 3-(2-bromoacetyl)-4-hydroxl-1-phenylquinolin-2(1H)-one (II)

IR (KBr, cm^{-1}): 3244.27 (–OH); 3072.60 (aromatic C-H); 1643.35 (-C=O acetyl); 1598.99 (-C=O cyclic amide); 850.31 (C-Br).

3.1.2. Spectral data of 4-hydroxy-3-(2-(methylamino)-acetyl)-1-phenylquinolin-2(1H)-one (IIIa)

IR (KBr, cm^{-1}): 3421.72 (–OH); 3250 (-NH); 3103.46 (aromatic C-H); 2883.58 (aliphatic C-H); 1612.49 (-C=O cyclic amide).

3.1.3. Spectral data of 4-hydroxy-3-(2-(ethylamino)acetyl)-1-phenylquinolin-2(1H)-one (IIIb)

IR (KBr, cm^{-1}): 3429.23 (-OH); 3345.89 (-NH); 3061.03 (aromatic C-H); 2987.74 (aliphatic C-H); 1658.78 (-C=O acetyl); 1610.56 (-C=O cyclic amide).

3.1.4. Spectral data of 4-hydroxy-3-(2-(benzylamino)-acetyl)-1-phenylquinolin-2(1H)-one (IIId)

IR (KBr, cm^{-1}): 3448.72 (-OH); 3385.25 (–NH); 3012.81 (aromatic C-H); 2889.37 (aliphatic C-H); 1610.56 (-C=O acetyl); 1591.27 (-C=O cyclic amide). ^{1}H NMR (DMSO-d_6, δ ppm): 11.15 (s, 1H, -OH); 8.22-6.47 (m, 14H, Ar-H); 4.78 (s, 1H, -NH); 3.35 (s, 2H, -CH$_2$); 2.56 (s, 2H, -CH$_2$).

3.1.5. Spectral data of N-(2-(4-hydroxy-2-oxo-1-phenyl-1,2-dihydroquinolin-3-yl)-2-oxoethyl)-N-methylbenzenesulfonamide (IVa-1)

IR (KBr, cm^{-1}): 3062.96 (aromatic C-H); 2922.16 (aliphatic C-H); 1631.78 (-C=O acetyl); 1612.49 (-C=O amide); 1367.53 (S=O of sulfonamide).

3.1.6. Spectral data of N-(2-(4-hydroxy-2-oxo-1-phenyl-1,2-dihydroquinolin-3-yl)-2-oxoethyl)-N,4'-dimethylbenzenesul-fonamide (IVa-2)

IR (KBr, cm^{-1}): 3064.89 (aromatic C-H); 2881.86 (aliphatic C-H); 1631.78 (-C=O acetyl); 1612.49 (-C=O amide); 1366.45 (S=O of sulfonamide). ^{1}H NMR (DMSO-d_6, δ ppm): 12.43 (s, 1H, -OH); 8.23-6.57 (m, 13H, Ar-H); 3.94 (s, 2H, -CH$_2$); 2.95 (s, 3H, -CH$_3$); 2.52 (s, 3H, -CH$_3$). ^{13}C NMR (DMSO-d_6, δ ppm): 182.18 (1C, -C=O); 166.13 (1C, -C=O); 161.09 (1C, -C-OH); 139.37-108.98 (18C, Ar-C); 58.88 (1C, -CH$_2$); 34.67 (1C, -CH$_3$); 21.20 (1C, -CH$_3$). Mass (m/z): 462 [M$^+$].

3.1.7. Spectral data of N-(2-(4-hydroxy-2-oxo-1-phenyl-1,2-dihydroquinolin-3-yl)-2-oxoethyl)-N-methyl-4'-nitrobenzenesul-fonamide (IVa-3)

IR (KBr, cm^{-1}): 3082.92 (aromatic C-H); 2924.09, 2852.72 (aliphatic C-H); 1630.68 (-C=O acetyl); 1604.82 (-C=O amide); 1554.26 (-NO$_2$); 1358.47 (S=O of sulfonamide). ^{1}H NMR (DMSO-d_6, δ ppm): 12.46 (s, 1H, -OH); 8.04-6.61 (m, 13H, Ar-H); 3.93 (s, 2H, -CH$_2$); 2.51 (s, 3H, -CH$_3$). ^{13}C NMR (DMSO-d_6, δ ppm): 179.25 (1C, -C=O); 165.47 (1C, -C=O); 160.52 (1C, -C-OH); 138.79-115.72 (19C, Ar-C); 54.153 (1C, -CH$_2$); 31.93 (1C, -CH$_3$). Mass (m/z): 493 [M$^+$].

3.1.8. Spectral data of N-(2-(4-hydroxy-2-oxo-1-phenyl-1,2-dihydroquinolin-3-yl)-2-oxoethyl)-N-ethylbenzenesulfonamide (IVb-1)

IR (KBr, cm^{-1}): 3062.96 (aromatic C-H); 2974.09, 2922.16 (aliphatic C-H); 1658.78 (-C=O acetyl); 1612.49 (-C=O amide); 1325.10 (S=O of sulfonamide). ^{1}H NMR (DMSO-d_6, δ ppm): 17.16 (s, 1H, -OH); 8.21-6.31 (m, 14H, Ar-H); 2.73-2.69 (m, 4H, -CH$_2$); 1.33-1.19 (t, 3H, -CH$_3$). Mass (m/z) = 463 (M$^+$).

3.1.9. Spectral data of N-(2-(4-hydroxy-2-oxo-1-phenyl-1,2-dihydroquinolin-3-yl)-2-oxoethyl)-N-ethyl-4'-methylbenzenesul-fonamide (IVb-2)

IR (KBr, cm^{-1}): 3025.54 (aromatic C-H); 2976.16, 2918.30 (aliphatic C-H); 1666.50 (-C=O acetyl); 1620.21 (-C=O amide); 1330.41(S=O of sulfonamide). ^{1}H NMR (DMSO-d_6, δ ppm): 16.82 (s, 1H, -OH); 8.16-6.39 (m, 13H, Ar-H); 3.14 (s, 3H, -CH$_3$); 2.76-2.71 (m, 4H, -CH$_2$); 1.32-1.20 (t, 3H, -CH$_3$). Mass (m/z) = 477 (M$^+$).

3.1.10. Spectral data of N-(2-(4-hydroxy-2-oxo-1-phenyl-1,2-dihydroquinolin-3-yl)-2-oxoethyl)-N-propylbenzenesulfona-mide (IVc-1)

IR (KBr, cm^{-1}): 3419.79 (-OH); 3064.89 (aromatic C-H); 2958.80, 2926.01, 2872.01, 2582.72 (aliphatic C-H); 1624.06 (-C=O acetyl); 1610.56 (-C=O amide); 1325.10 (S=O of sulfonamide). ^{1}H NMR (DMSO-d_6, δ ppm): 17.05 (s, 1H, -OH); 8.10-6.42 (m, 14H, Ar-H); 2.82-2.69 (m, 6H, -CH$_2$); 1.29-1.18 (t, 3H, -CH$_3$). Mass (m/z) = 477 (M$^+$).

Spectral data of N-(2-(4-hydroxy-2-oxo-1-phenyl-1,2-dihydroquinolin-3-yl)-2-oxoethyl)-N-benzenesulfona-mide (IVd-1)

IR (KBr, cm^{-1}): 3051.62, 3032.10 (aromatic C-H); 2922.18, 2850.79 (aliphatic C-H); 1631.26 (-C=O acetyl); 1610.56 (-C=O amide); 1360.97 (S=O of sulfonamide). ^{1}H NMR (DMSO-d_6, δ ppm): 10.63 (s, 1H, -OH); 8.15-6.31 (m, 19H, Ar-H), 3.97 (s, 4H, -CH$_2$). Mass (m/z) = 525 (M$^+$).

3.1.12. Spectral data of N-(2-(4-hydroxy-2-oxo-1-phenyl-1,2-dihydroquinolin-3-yl)-2-oxoethyl)-N-benzyl-4'-nitrobenzenesul-fonamide (IVd-3)

IR (KBr, cm^{-1}): 3048.37 (aromatic C-H); 2924.09, 2852.72 (aliphatic C-H); 1631.78 (-C=O acetyl); 1612.49 (-C=O amide); 1548.98 (-NO$_2$); 1367.53 (S=O of sulfonamide). ^{1}H NMR (DMSO-d_6, δ ppm): 11.34 (s, 1H, -OH); 8.09-6.28 (m, 18H, Ar-H), 4.08 (s, 4H, -CH$_2$). Mass (m/z) = 570 (M$^+$).

3.2. Molecular Docking Study

In silico molecular docking study was performed on the synthesized molecules using EGFR tyrosine kinase complexed with a 4-anilinoquinazoline inhibitor (PDB ID: 1m17). MolDock scores and hydrogen bonding of the test compounds were compared with that of linomide and imatinib as standards. Results of the study are reported in Table **2**. Crystal structure of the target protein is presented in Fig. (**2**). Hydrogen bonding interactions of best poses of representative compounds are presented in Fig. (**3**).

3.3. Anticancer Activity

Selected molecules were tested for their *in vitro* anticancer activity against K562 (chronic myelogenous leukemia) and A549 (lung cancer) cell lines by MTT assay method. The percentage cell viability of the cell lines upon treatment with the test compounds is reported in Tables (**3, 4**). The percentage cell viability was plotted versus concentrations of the test compounds used in the study as shown in Fig. (**4, 5**). The IC$_{50}$ values were thus determined and compared to establish the relative potency of the compounds (Table **5**).

4. DISCUSSION

4.1. Synthesis

The synthetic route of the compounds is outlined in Scheme (**1**). The compounds were satisfactorily characterized by IR, NMR and mass spectral data. Bromination of compound I was confirmed by Beilstein test giving a green flame and Lassaigne's test giving a pale yellow precipitate indicative of bromine in compound II. IR spectrum of compound II exhibited C-Br stretch at 850.31 cm^{-1} further confirming the reaction. Presence of –NH stretch at 3450-3300 cm^{-1} and absence of C-Br stretch in the IR spectra; as well as characteristic singlet for one proton of -NH at δ 5.0-4.5 in ^{1}H NMR spectra of compounds IIIa-d confirms the condensation of brominated compound II with primary amines. Compounds from series IV did not show the –NH stretch in their IR spectra and singlet for –NH in ^{1}H NMR spectra. However-

er, the presence of –S=O stretch for sulfonamide at 1375-1355 cm^{-1} and structural verification of the derivatives with ^{1}H NMR spectra is indicative of complete synthesis of the desired compounds IVa-d (1-3). The physicochemical parameters of the synthesized compounds are presented in Table **1**.

4.2. Molecular Docking Study

In silico molecular docking study was performed on the compounds with Molegro Virtual Docker (MVD-2007, 6.0). Fig. (**2**) shows the structure of EGFR-tyrosine kinase complexed with a 4-anilinoquinazoline inhibitor obtained from Protein Data Bank with the PDB ID: 1m17.
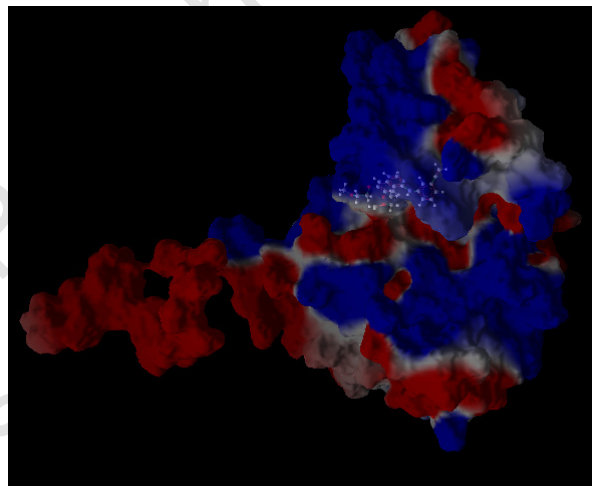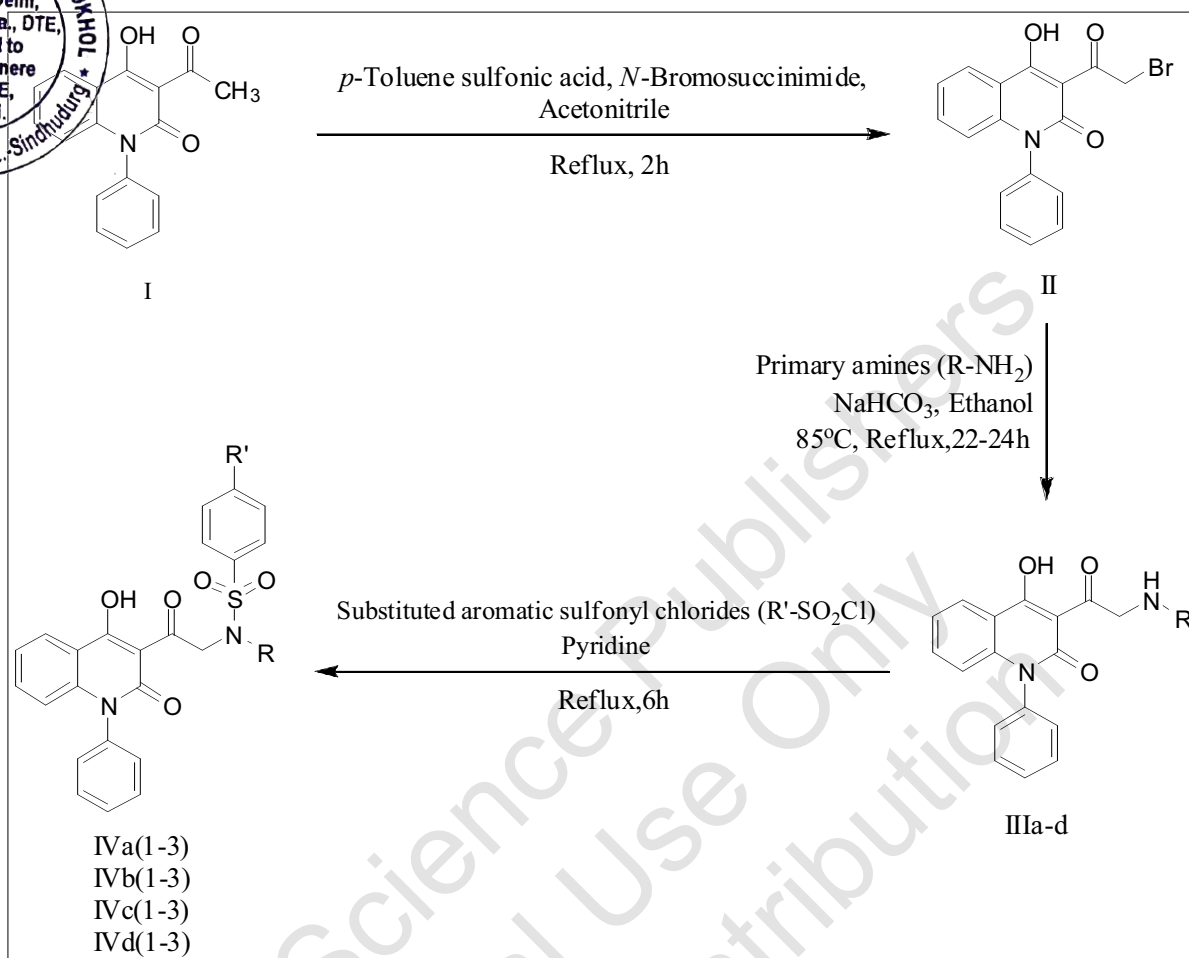

Fig. (2). Structure of EGFR-tyrosine kinase domain complexed with 4-anilinoquinazoline inhibitor (PDB ID: 1m17).

The crystal structure of the target enzyme including forty amino acids from the carboxyl-terminal tail has been determined to 2.6-A resolution. Unlike any other kinase enzymes, the EGFR family members possess constitutive kinase activity without a phosphorylation event within their kinase domains. Despite its lack of phosphorylation, the EGFRK activation loop adopts a conformation similar to that of the phosphorylated active form of the kinase domain from the insulin receptor. It is observed that the key residues of a dimerized structure lying between the EGFRK domain and carboxyl-terminal substrate docking sites are found in close contact with the kinase domain.

The site at which the known 4-anilinoquinazoline inhibitor binds with the target protein was selected as the active site. It is lined with amino acid residues such as Leu694, Met769, Thr830, Asp831, Glu738, Lys721, Cys773; *etc*. Hence to identify other residual interactions of the tested compounds, a grid box (include residues within a 15.0 A radius) large enough to accommodate the active site was constructed. Since 4-anilinoquinazoline is a known inhibitor, the centre of this site was considered as the centre of search space for docking.

Docking of the synthesized compounds with EGFR-tyrosine kinase domain exhibited well conserved hydrogen bonding with the amino acid residues at the active site. The

Scheme 1. Synthesis of novel linomide derivatives IVa-d (1-3).

Table 1.   List of the synthesized derivatives and their physical data.

Compounds	R	R'	Molecular Formula	M.W.	M.P. ºC	%Yield	R_f Value
IVa-1	-CH$_3$	-H	C$_{24}$H$_{20}$N$_2$O$_5$S	448.49	158	65.22	0.67
IVa-2	-CH$_3$	-CH$_3$	C$_{25}$H$_{22}$N$_2$O$_5$S	462.21	166	68.25	0.67
IVa-3	-CH$_3$	-NO$_2$	C$_{24}$H$_{19}$N$_3$O$_7$S	493.49	174	60.16	0.73
IVb-1	-CH$_2$CH$_3$	-H	C$_{25}$H$_{22}$N$_2$O$_5$S	462.52	177	58.84	0.72
IVb-2	-CH$_2$CH$_3$	-CH$_3$	C$_{26}$H$_{24}$N$_2$O$_5$S	476.54	160	62.01	0.75
IVb-3	-CH$_2$CH$_3$	-NO$_2$	C$_{25}$H$_{21}$N$_3$O$_7$S	507.52	163	54.46	0.82
IVc-1	-(CH$_2$)$_2$CH$_3$	-H	C$_{26}$H$_{24}$N$_2$O$_5$S	476.54	172	51.75	0.76
IVc-2	-(CH$_2$)$_2$CH$_3$	-CH$_3$	C$_{27}$H$_{26}$N$_2$O$_5$S	490.57	175	53.54	0.77
IVc-3	-(CH$_2$)$_2$CH$_3$	-NO$_2$	C$_{26}$H$_{23}$N$_3$O$_7$S	521.54	162	45.21	0.88
IVd-1	-CH$_2$-C$_6$H$_5$	-H	C$_{30}$H$_{24}$N$_2$O$_5$S	524.59	168	61.65	0.89
IVd-2	-CH$_2$-C$_6$H$_5$	-CH$_3$	C$_{31}$H$_{26}$N$_2$O$_5$S	538.61	180	66.04	0.93
IVd-3	-CH$_2$-C$_6$H$_5$	-NO$_2$	C$_{30}$H$_{23}$N$_3$O$_7$S	569.59	188	52.89	0.95

Table 2. Results of the molecular docking study showing MolDock scores and interactions of the target molecules with EGFR tyrosine kinase.

|	MolDock Score (Kcal/mol)	Rerank Score	Interaction	HBond[a] (Kcal/mol)	Heavy Atoms	LE1[b]	LE3[c]	Docking Score
IVa-1	-99.1168	-53.4301	-110.512	-8.09774	32	-3.0974	-1.6697	-96.0171
IVa-2	-95.1738	-49.0972	-136.534	-5.66377	33	-2.8841	-1.4878	-94.7389
IVa-3	-86.3277	-17.5217	-93.2907	-6.72265	35	-2.4665	-0.5006	-88.6735
IVb-1	-104.103	-53.7108	-118.244	-5.30767	33	-3.1546	-1.6276	-106.333
IVb-2	-96.7439	-36.4017	-101.846	-6.03921	34	-2.8454	-1.0706	-95.5169
IVb-3	-97.8457	-48.0898	-120.28	-6.53589	36	-2.7179	-1.3358	-101.033
IVc-1	-102.648	-49.4832	-114.897	-2.62174	34	-3.0191	-1.4554	-106.185
IVc-2	-87.1543	-41.0782	-112.497	-4.41565	35	-2.4901	-1.1737	-92.497
IVc-3	-90.1598	-41.5801	-107.291	-4.63897	37	-2.4368	-1.1238	-95.2045
IVd-1	-115.503	-59.3219	-122.184	-7.5	38	-3.0395	-1.5611	-110.688
IVd-2	-78.1731	81.9007	-98.8108	-2.85252	39	-2.0044	-2.1000	-77.2872
IVd-3	-98.3655	-42.3117	-117.843	-4.99407	41	-2.3992	-1.032	-97.2518
Linomide	-75.9616	-52.7986	-112.394	-4.86899	23	-3.3027	-2.2956	-74.5307
Imatinib	-136.699	-92.2362	-160.347	-5.28667	37	-3.6946	-2.4929	-134.421

[a]Hydrogen bonding energy between the protein and ligand
[b]MolDock score divided by heavy atoms count
[c]Rerank score divided by heavy atoms count

Table 3. Cell viability of K562 (chronic myelogenous leukemia) cell lines.

Concentration (µg/ml)	% Cell Viability (K562)			
	IVa-2	IVb-1	IVc-1	IVd-1
400	51.68831	62.13485	41.81818	46.23376
300	64.93507	70.69823	51.94805	52.33766
200	73.63636	76.22078	58.83117	56.88312
100	81.68831	81.2987	68.05195	75.84416
50	84.54545	87.19481	77.53247	83.24675
25	90.38961	94.02597	82.72727	90.38961
Control	100	100	100	100
DMSO	96.7210	96.7210	96.7210	96.7210

Principal
V P College Of Pharmacy, Madkhol
Tal. Sawantwadi, Dist. Sindhudurg
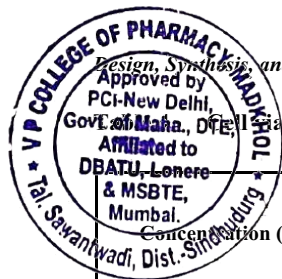
Table 4.   Cell viability of A549 (lung cancer) cell lines.

Concentration (µg/ml)	%Cell Viability (A549)			
	Iva-2	Ivb-1	Ivc-1	Ivd-1
400	55.24319	51.89647	56.93887	52.92280
300	61.57965	55.55556	61.80276	60.01785
200	68.09460	61.89201	68.18385	63.72155
100	70.74967	70.72735	71.79027	75.41276
50	74.83266	72.60152	75.50201	80.45515
25	82.68630	85.72066	83.04328	81.97233
Control	100	100	100	100
DMSO	97.6560	97.6560	97.6560	97.6560

Table 5. IC_{50} values (µM/ml) of the test compounds determined from the plots (Figure 4 and Figure 5) using Graph Pad Prism Version 5.1.

Compounds	K562	A549
IVa-2	1.056	1.605
IVb-1	1.277	1.034
IVc-1	0.451	1.665
IVd-1	0.455	0.704
Paclitaxel	0.30	
Imatinib	0.28	

MolDock scores of the test compounds ranged from -78.1731 to -115.503 while that of linomide was -75.9616. Imatinib was used as the reference standard for comparison of efficiency and exhibited MolDock score of -136.699. All of the designed molecules exhibited MolDock score higher than that exhibited by linomide; with compound IVd-1 having a highest MolDock score of -115.503. The best poses of compounds exhibiting the most promising hydrogen bonding are shown in Fig. (**3**). Hydrogen bonding was observed between –NH of imatinib and carbonyl oxygen of Leu694, heterocyclic nitrogen of pyridine and –NH of Met769; and heterocyclic nitrogen of piperazine and hydroxyl group of Thr766. 4-hydroxy group of linomide exhibited hydrogen bonding with –OH of Thr830 and heterocyclic nitrogen of the quinolone moiety with –OH of Thr766. Compound IVa-2 (MolDock score -95.1738) showed a similar pattern of hydrogen bonding as that of imatinib with 4-hydroxy group and ring nitrogen forming bonds with –NH of Met769 and hydroxyl group of Thr766 respectively. Compounds IVb-1 (MolDock score -104.103) and IVc-2 (MolDock score -87.1543) also exhibited hydrogen bonding with carbonyl oxygen of Leu694. These results show that the novel linomide derivatives possess higher affinity than linomide towards the active site of the target protein EGFRK.

4.3. Anticancer Activity

Based upon the data obtained from the molecular docking study, selected molecules were tested for their *in vitro* anticancer activity against K562 and A549 cell lines by MTT assay method. It was observed that the IC_{50} values of the test compounds ranged from 0.451 µM/ml to 1.477 µM/ml against K562 cell line and from 0.704 µM/ml to 1.665 µM/ml against A549 cell line. The compound IVc-1 (R= -$(CH_2)_2$-CH_3 ; R'= -H) was found to be most potent against K562 cell line with an IC_{50} of 0.451 µM/ml, which is comparable to that of paclitaxel (IC_{50} of 0.3 µM/ml) and imatinib (IC_{50} of 0.28 µM/ml). The compound IVd-1 (R= -CH_2-C_6H_5; R'= -H) showed good potency against K562 cell line with an IC_{50} of 0.455 µM/ml. When tested against A549 cell line, the compound IVd-1 was found to be most active with the least IC_{50} value of 0.704 µM/ml. From the IC_{50} values of the derivatives tested for anticancer activity, it was seen that the derivatives IVa-2, IVc-1 and IVd-1 were more active versus K562 cell line than against A549 cell line.
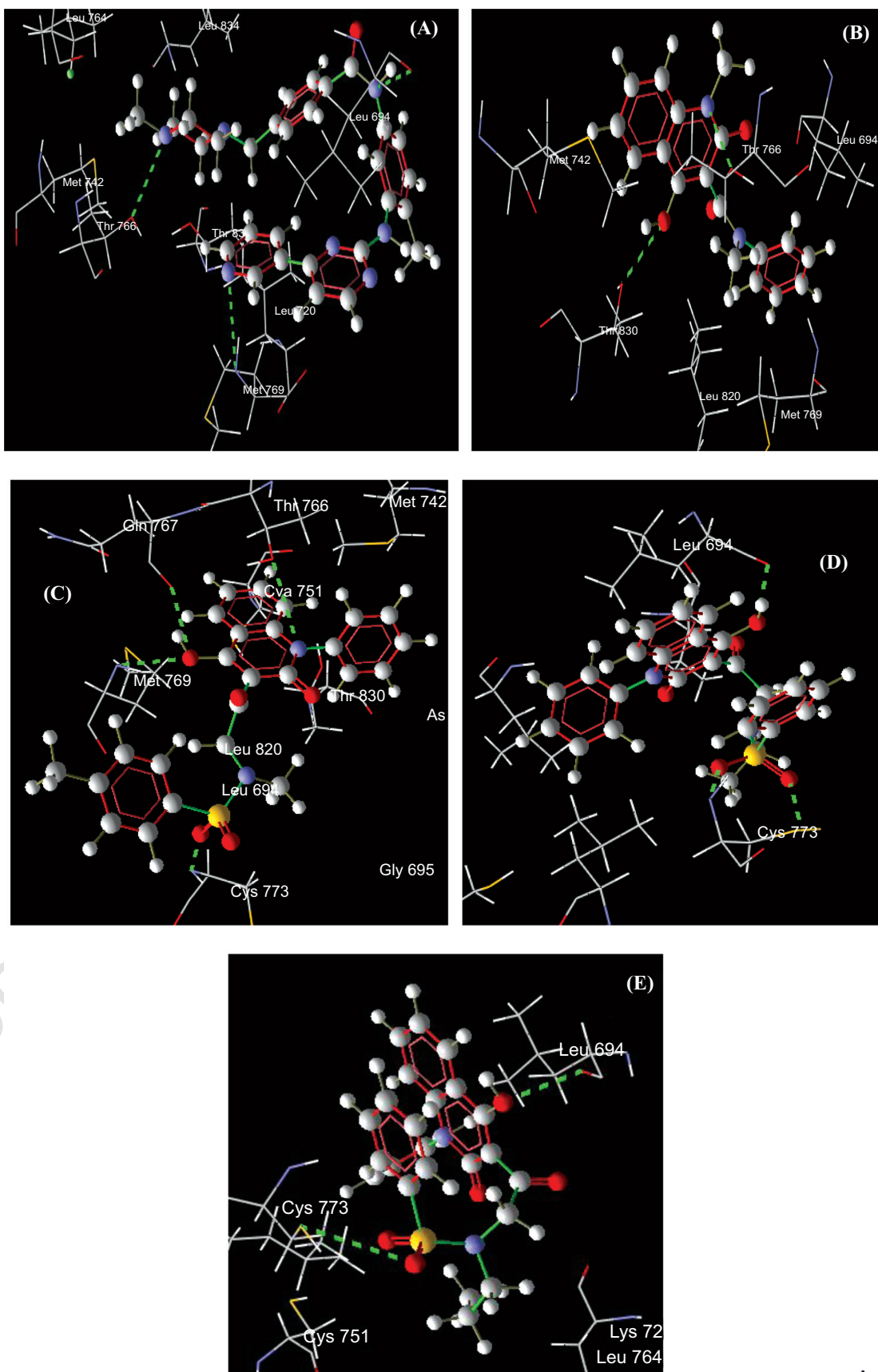
Fig. (3). Hydrogen bonding interactions of best poses of representative compounds with amino acid residues at the active site of protein EGFR tyrosine kinase. (**A**) Imatinib; (**B**) Linomide; (**C**) IVa-2; (**D**) IVb-1; (**E**) IVc-1.
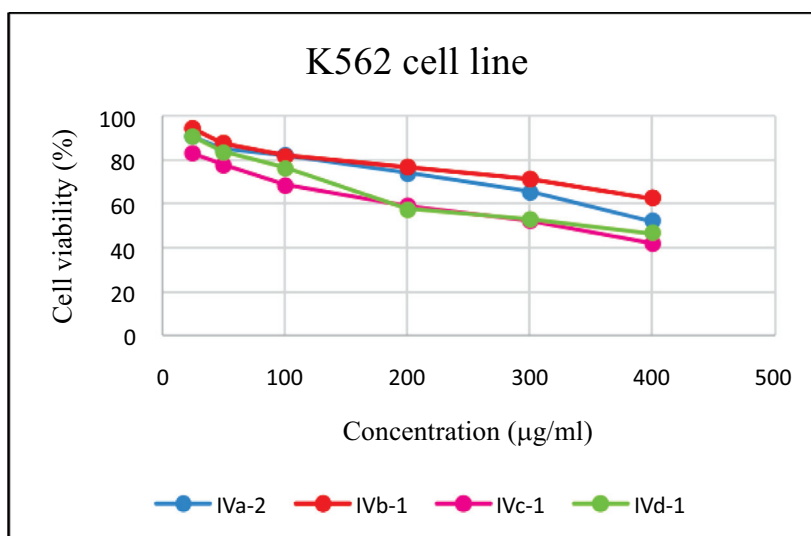
Fig. (4). Plot of cell viability (%) versus concentration (µg/ml) of K562 cell line.
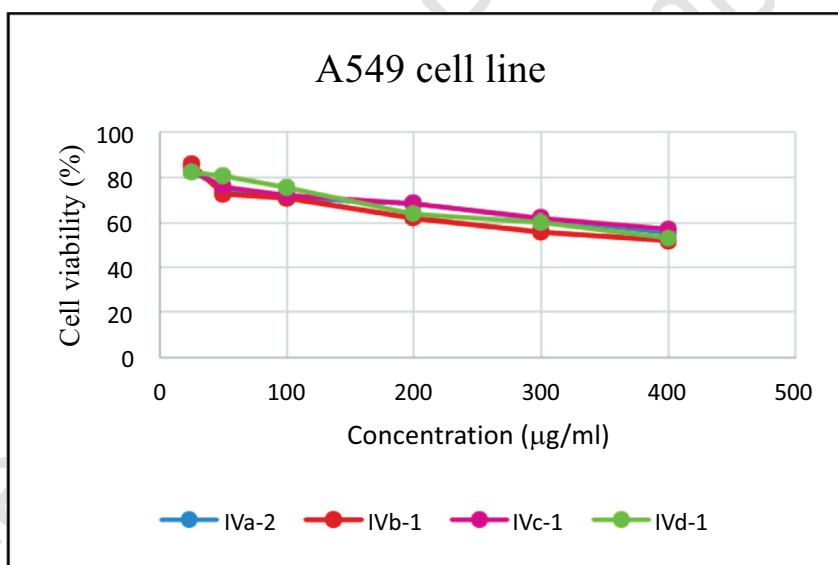

Fig. (5). Plot of cell viability (%) versus concentration (µg/ml) of A549 cell line.

CONCLUSION

The proposed method for the synthesis of novel quinolin-2-one derivatives is convenient and gives good yield. Some of the synthesised compounds showed significant *in vitro* anticancer activity against K562 and A549 cell lines and were comparatively more active against K562 cell line. The compound **IVc-1** (R= -(CH$_2$)$_2$-CH$_3$; R'= -H) exhibited the most potent activity against K562 cell lines. Compound **IVd-1** (R= -CH$_2$-C$_6$H$_5$; R'= -CH$_3$) was proved to be the most cytotoxic compound among the other derivatives against A549 cell lines. Results of the molecular docking study reveal that the synthesized novel analogues of linomide exhibit better affinity towards the EGFRK protein than linomide. Some of the synthesized molecules exhibit conservative hydrogen bonding with the amino acid residues of the active site of the target protein and thus can be studied for further activity.

CONTRIBUTIONS OF AUTHORS

Mr. Rudrax Priolkar (Department of Pharmaceutical Chemistry, PES's Rajaram and Tarabai Bandekar College of Pharmacy, Farmagudi, Ponda-Goa) carried out the synthetic bench work. Dr Sunil Shingade (Department of Pharmaceutical Chemistry, PES's Rajaram and Tarabai Bandekar College of Pharmacy, Farmagudi, Ponda-Goa) assisted in the spectral characterization of the synthesized molecules. Dr Mahesh Palkar (Department of Pharmaceutical Chemistry, KLEU's College of Pharmacy, Hubli-Karnataka) provided his valuable guidance in the molecular docking study. Dr Shivlingrao Mamle Desai (Department of Pharmaceutical Chemistry, PES's Rajaram and Tarabai Bandekar College of Pharmacy, Farmagudi, Ponda-Goa) is the research guide and supervised the overall research work.

ETHICS APPROVAL AND CONSENT TO PARTICIPATE

Not applicable.

HUMAN AND ANIMAL RIGHTS

No Animals/Humans were used for studies that are the basis of this research.

CONSENT FOR PUBLICATION

Not applicable.

AVAILABILITY OF DATA AND MATERIALS

Not applicable.

FUNDING

None.

CONFLICT OF INTEREST

The authors declare no conflict of interest, financial or otherwise.

REFERENCES

[1] Jemal A, Bray F, Center MM, Ferlay J, Ward E, Forman D. Global cancer statistics. CA Cancer J Clin 2011; 61(2): 69-90.
http://dx.doi.org/10.3322/caac.20107 PMID: 21296855

[2] Facts and Figures https://www.cancer.org/content/dam/cancer-org/research/cancerfacts- and-statistics/annual-cancer-facts-and-figures2017 [(Accessed on 09/06/2017).];

[3] Tripathi KD. Essentials of Medical Pharmacology. sixth ed. New Delhi.: Jaypee Brothers Medical Publishers (P) Ltd 2006; pp. ((re-print 2010)): 819-29.

[4] Block JH, Beale JM. Wilson and Gisvold's Medicinal and Pharma-ceutical Chemistry. 12th ed. United States of America: Lippincott Williams and Wilkins 2011.

[5] Thomas K. The pyrano route to 4-hydroxy-2-quinolones and 4-hydroxy-2-pyridones. IL Farmaco 1999; 54: 309-15.
http://dx.doi.org/10.1016/S0014-827X(99)00030-0

[6] Zhang Q, Chen Y, Zheng YQ, et al. Synthesis and bioactivity of 4,10-dimethyl-pyridino[2,3-*h*]quinolin-2(1*H*)-one-9-carboxylic ac-id and its esters. Bioorg Med Chem 2003; 11(6): 1031-4.
http://dx.doi.org/10.1016/S0968-0896(02)00526-6 PMID: 12614889

[7] Ohashi T, Oguro Y, Tanaka T, et al. Discovery of pyrrolo[3,2-c]quinoline-4-one derivatives as novel hedgehog signaling inhibi-tors. Bioorg Med Chem 2012; 20(18): 5496-506.
http://dx.doi.org/10.1016/j.bmc.2012.07.039 PMID: 22910224

[8] Afzal O, Kumar S, Haider MR, et al. A review on anticancer poten-tial of bioactive heterocycle quinoline. Eur J Med Chem 2015; 97: 871-910.
http://dx.doi.org/10.1016/j.ejmech.2014.07.044 PMID: 25073919

[9] Ogino K, Hobara T, Ishiyama H, et al. Antiulcer mechanism of action of rebamipide, a novel antiulcer compound, on diethyldithi-ocarbamate-induced antral gastric ulcers in rats. Eur J Pharmacol 1992; 212(1): 9-13.
http://dx.doi.org/10.1016/0014-2999(92)90065-C PMID: 1313372

[10] Trinquand C, Romanet JP, Nordmann JP, Allaire C. [Efficacy and safety of long-acting carteolol 1% once daily. A double-masked, randomized study]. J Fr Ophtalmol 2003; 26(2): 131-6.
PMID: 12660585

[11] De Fruyt J, Deschepper E, Audenaert K, et al. Second generation antipsychotics in the treatment of bipolar depression: A systematic review and meta-analysis. J Psychopharmacol (Oxford) 2012; 26(5): 603-17.
http://dx.doi.org/10.1177/0269881111408461 PMID: 21940761

[12] Maria GR, Shivlingrao MD, Soniya N, et al. Synthesis and evalua-tion of 2-(4-methoxy-2-oxo-1-phenyl/methyl-1,2-dihydroquinolin-3-yl)-2-methyl-3-(phenyl/substitutedphenylamino)thiazolidin-4-one as antibacterial and anticancer agents. Indian J Chem 2016; 55B: 1254-8.

[13] Shi J, Xiao Z, Ihnat MA, et al. Structure-activity relationships studies of the anti-angiogenic activities of linomide. Bioorg Med Chem Lett 2003; 13(6): 1187-9.
http://dx.doi.org/10.1016/S0960-894X(03)00047-7 PMID: 12643940

[14] Li Q, Woods KW, Wang W, et al. Design, synthesis, and activity of achiral analogs of 2-quinolones and indoles as non-thiol farne-syltransferase inhibitors. Bioorg Med Chem Lett 2005; 15(8): 2033-9.
http://dx.doi.org/10.1016/j.bmcl.2005.02.062 PMID: 15808463

[15] Jochmans D. Novel HIV-1 reverse transcriptase inhibitors. Virus Res 2008; 134(1-2): 171-85.
http://dx.doi.org/10.1016/j.virusres.2008.01.003 PMID: 18308412

[16] Palkar MB, Singhai AS, Ronad PM, et al. Synthesis, pharmacolog-ical screening and in silico studies of new class of Diclofenac ana-logues as a promising anti-inflammatory agents. Bioorg Med Chem 2014; 22(10): 2855-66.
http://dx.doi.org/10.1016/j.bmc.2014.03.043 PMID: 24751552

ORIGINAL RESEARCH ARTICLES

DESIGN, SYNTHESIS AND EVALUATION OF 6-SUBSTITUTED-4-HYDROXY-1-(2-SUBSTITUEDACETYL)-3-NITROQUINOLIN-2(1H)-ONE FOR ANTICANCER ACTIVITY

Bhat S. S.[a], Mamle Desai S. N.[a]*, Narvekar V.[a],

Shingade S. G.[a], Dighe P. K.[b] and Biradar B. S.[c]

ABSTRACT

The present work deals with the synthesis of a series of 6-substituted-4-hydroxy-1-(2- substitued alicyclicaminoacetyl)-3-nitroquinolin-2(1H)-one {IVa-d (1-3)} derivatives and evaluation of their *in vitro* anticancer activity. Docking study was carried out using EGFR-tyrosine kinase binding site (PDB ID: 1m17) revealed encouraging results. The sequence of reactions consists of the initial synthesis of 6-substituted 4-hydroxyquinolin-2(1H)-ones (Ia-d) which were further subjected to nitration reaction to give 6- substituted-4-hydroxy-3-nitroquinolin-2(1H)-one (IIa-d). Condensation of compounds (IIa-d) with chloroacetyl chloride resulted in 6- substituted-1-(2-chloroacetyl)-4-hydroxy-3-nitroquinolin-2(1H)-one (IIIa-d) which was subjected to substitution reaction using various secondary amines yielded the title compounds {IVa-d (1-3)}. All the synthesized compounds were characterized by IR, NMR and Mass spectral data.All the derivatives were tested for their *in vitro* anticancer activity using KB (Oral cancer) cell lines. Among all the synthesized compounds, compound (IVc-2) was found to be the most cytotoxic as compared to the other synthesized derivatives, with IC_{50} values of 0.2406μM/mL against KB cell line.

INTRODUCTION

The alarming rise of cancer has put strains on individuals, families and the society in which they live. Cancer is a generic term for a large group of diseases characterized by the growth of abnormal cells beyond their usual boundaries that can then invade adjoining parts of the body and/or spread to other organs [1]. Cancer is the leading cause of death in developed countries and is reported second leading cause in developing countries. In 2012, there were 14.1 million new cases and 8.2 million cancer-related deaths worldwide. In 2018, 1,735,350 new cases of cancer have been diagnosed in the United States and 609,640 people will die from the disease [2].

Oral cancers are parts of a group of cancers commonly referred to head and neck excluding brain cancer. As per the oral cancer foundation in the year 2018, 53000 Americans have been diagnosed with oral and oropharyngeal cancer and killing around 9750 people. With increase in the consumption of tobacco, alcohol and persistent viral infection(HPV) are the major causes of oral cancer[3].

There have been numerous advances in the research on the drugs which are used to treat cancer patients, but the selectivity of these molecules is also a matter of concern as these drugs often bring about the lysis of

Fig. 1: Linomide [7]

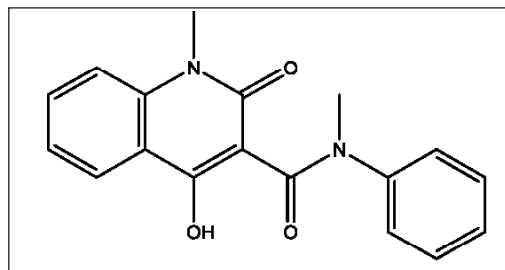a Department of Pharmaceutical Chemistry, PES's Rajaram and Tarabai Bandekar College of Pharmacy, Ponda - 403 401, Goa, India
b Department of Pharmaceutics, PES's Rajaram and Tarabai Bandekar College of Pharmacy, Ponda - 403 401, Goa, India
c Department of Pharmacology, PES's Rajaram and Tarabai Bandekar College of Pharmacy, Ponda - 403 401, Goa, India
*For Correspondence: Email id: smamledesai@rediffmail.com

cancerous cells. Also, these drugs tend to exhibit severe side effects and systemic toxicity.

Some of the important alkaloids present in many shrubs of the Rutaceae family contain quinolin-2-one ring system and found to have wide spectrum of biological activity viz. flindersine for profound anti-bacterial activity, dictamine for smooth muscle contraction, waltherione A, waltherione C and waltherione D as anti-HIV agents etc. The clinical significance of quinolin-2-one derivatives is well documented with rebamipide as antacid, carteolol as β-blocker in ophthalmic preparation, aripiperazole as a antipsychotic drug and also vesnarinone as a cardiotonic, phoshodiestrase- III inhibitor[4,5,6].

Many researchers identified linomide (Fig. 1) as a lead molecule, intended for the discovery of potent cytotoxic effect. Linomide, a 4-hydroxy-2-quinolone derivative, a potent immunostimulant and found to be useful in treating Acute Myeloid leukemia and was withdrawn from the clinical trials due to cardiac side effects[7,8,9]. In the present investigation the phenyl acetyl group present at third position of linomide was replaced by strong electron withdrawing group, i.e. NO_2 and substitution on the ring nitrogen by heterosubstituted acetyl group. Further in silico molecular docking studies of title compounds was carried out using Molegro Virtual Docker (MVD – 2013, version 6.0). In view of these findings, it was taught to design and synthesize novel linomide derivatives and to evaluate their in silico and in vitro biopotential.

MATERIALS AND METHODS

Chemistry

All the chemicals and solvents were procured from S. D. Fine –Chem Limited (Mumbai, India). All the solvents were distilled before use and chemicals were purified by either distillation or recrystallisation before use. Melting Points of the synthesized compounds were determined by Thiele's melting point apparatus and are uncorrected. FT-IR spectra were recorded on SHIMADZU IR AFFINITY-1 spectrophotometer by KBr disc method. The ^{1}H NMR and ^{13}C NMR was recorded on Bruker Avance II 400 NMR Spectrometer using DMSO-d_6 as the solvent and TMS as internal standard. Chemical shifts are expressed as δ value (ppm). Mass Spectra were recorded on Waters, Q-TOF Micromass (LC-MS). In silico study was carried out on synthesized derivatives using Molegro Virtual Docker (version6.0). The starting material for the synthesis of title compounds was synthesized following the literature [10] and the scheme for the synthesis of title compounds is shown in Scheme-1.
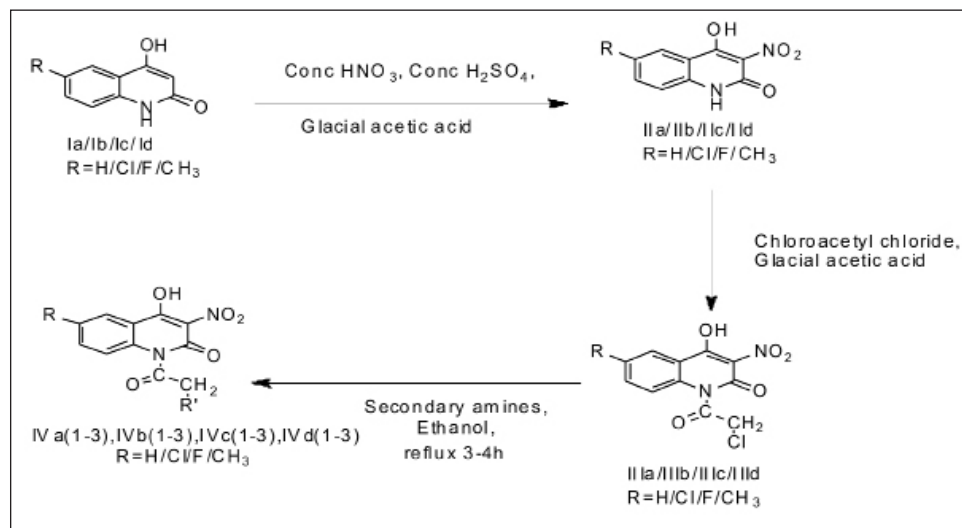
Synthesis of 6-substituted 4-hydroxy-3-nitroquinolin-2(1H)-one (IIa/IIb/IIc/IId)

Compound Ia/Ib/Ic/Id (0.185 mole) was added to 25 ml of glacial acetic acid contained in 250 ml beaker, and introduced into the well stirred mixture of concentrated sulphuric acid. This resulted into warm and clear solution. The solution was placed in freezing mixture with occasional stirring to attain the temperature 0-2 ℃. A cold mixture of 15.5 g (11 mL) of concentrated nitric acid and 12.5 g (7 mL) of concentrated sulphuric acid was added drop wise maintaining the temperature of the solution below 10 ℃. After all the mixed acid was added, beaker was removed from the freezing mixture and allowed to stand it at room temperature for 1 hour. The product obtained was recrystallized using ethanol as solvent.

6-chloro-4-hydroxy-3-nitroquinolin-2(1H)-one (IIb):

IR data (KBr, cm⁻¹): 2993.59, 2864.35 (-CH stretch); 1681.93 (-C=O stretch); 1608.65, 1342.35 (-C-N stretch of NO_2); 771.16 (-C-Cl stretch); ^{1}H NMR data (δ ppm, DMSO-d_6): 12.96 (s, 1H, OH); 8.16-7.17 (m, 4H, Ar-H); 5.82 (s, 1H, NH)

Scheme 1: Synthesis of the 6-substituted-4-hydroxy-1-(2-substituedacetyl)-3-nitroquinolin-2(1H)-ones

21

Synthesis of 6-substituted-1-(2-chloroacetyl)-4-hydroxy-3-nitroquinolin-2(1H)-one (IIIa/IIIb/ IIIc/ IIId)

In a conical flask, 50 mmol of compound IIa/IIb/IIc/IId, 30 ml of glacial acetic acid and 50 mmol of chloroacetyl chloride was mixed. The mixture was then warmed on hot plate with swirling for 5-10 minutes. The product obtained was filtered, washed with water and resulting precipitate was recrystallized using ethanol as solvent.

1-(2-Chloroacetyl)-4-hydroxy-3-nitroquinolin-2(1H)-one (IIIa):

IR data (KBr, cm^{-1}): 3093.82 (Aromatic –CH stretch); 2951.09 (-CH stretch); 1664.57 (-C=O stretch); 1593.20, 1379.10 (-C-N stretch of NO$_2$); ^{1}H NMR data (δ ppm, DMSO-d_6) 11.298(s, 1H, OH); 7.785-7.115 (m, 4H, Ar-H); 5.7307 (s, 2H, -CH2).

Synthesis of 6-substituted-4-hydroxy -1-(2-substituedacetyl)-3-nitroquinolin-2(1H)-one [IVa(1-3)/IVb(1-3)/IVc(1-3)/IVd(1-3)]

To a solution of compound (IIIa/ IIIb/ IIIc/ IIId) (0.004 M) in ethanol (30 ml), the appropriate secondary amine was added (0.004 M). The mixture was heated under reflux for 3-4 hours. The solvent was removed using IKA rotaevaporator to obtain the crystalline product. The product was recrystallized using methanol. The physical data of the compounds synthesised in this manner are shown in Table I.

6-Chloro-4-hydroxy -1-(2-morpholin -4-yl)acetyl)-3-nitroquinolin-2(1H)-one (IVb-1):

IR data (KBr, cm^{-1}): 3045.82 (Aromatic –CH stretch), 2996.21, 2942.10 (-CH stretch), 1645.18 (-C=O stretch), 1558.64, 1372.31 (-C-N stretch of NO$_2$), 1248.42 (-C-O of morpholine), 762.69 (-C-Cl stretch). ^{1}H NMR data (δ ppm, DMSO-d_6): 10.35 (s, 1H, OH), 7.09-7.63 (m, 3H, Ar-H), 5.79 (s, 2H, -CH$_2$), 3.78-3.76 (t, 4H, 2,6-CH$_2$ of morpholine), 3.13-3.12 (t, 4H, 3,5 -CH$_2$ of morpholine). Mass Spectral Data m/z: 369(M+2)

6-Chloro-4-hydroxy -1-(2-piperidin -1-yl)acetyl)-3-nitroquinolin-2(1H)-one (IVb-2):

IR data (KBr, cm^{-1}): 3093.82 (Aromatic –CH stretch), 2958.12, 2915.51, 2854.29 (-CH stretch), 1654.88 (-C=O stretch), 1593.20, 1330.78 (-C-N stretch of NO$_2$), 762.69 (-C-Cl stretch).

6-Chloro-4-hydroxy -1-(2-N-methylpiperazine-1-yl)acetyl)-3-nitroquinolin-2(1H)-one (IVb-3):

IR data (KBr, cm^{-1}): 3052.63 (Aromatic –CH stretch), 2934.84 (-CH stretch), 1648.79 (-C=O stretch), 1551.02, 1321.25 (-C-N stretch of NO$_2$), 784.98 (-C-Cl stretch).
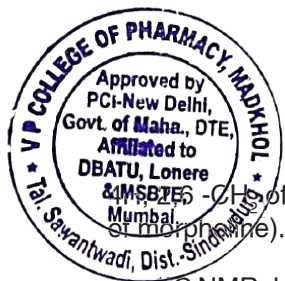
6-Fluoro-4-hydroxy-1-(2-morpholin-1-yl)acetyl)-3-nitroquinolin-2(1H)-one (IVc-1):

IR data (KBr, cm^{-1}): 3083.83 (Aromatic –CH stretch), 2867.42 (-CH stretch), 1657.93 (-C=O stretch), 1558.20, 1332.65 (-C-N stretch of NO$_2$), 1248.42 (-C-O of morpholine).

^{1}H NMR data (δ ppm, DMSO-d_6): 10.35 (s, 1H, OH), 7.57-7.10 (m, 3H, Ar-H), 4.62 (s, 2H, -CH$_2$), 3.78-3.75 (t,

Table I: The physical data of the 6-substituted-4-hydroxy-1-(2-substituedacetyl)-3-nitroquinolin-2(1H)-one compounds

Compound	R	R'	Molecular Formula	Mol. Wt.	m. p. °C	% Yield	R$_f$ Value(n-Hexane :CH3OH;7:3)
IVa-1	H	Morpholine	C$_{15}$H$_{15}$N$_3$O$_6$	333	>300	62.56	0.73
IVa-2	Cl	Piperidine	C$_{16}$H$_{17}$N$_3$O$_5$	331	>300	61.26	0.73
IVa-3	F	N-Methylpiperazine	C$_{16}$H$_{18}$N$_4$O$_5$	346	>300	66.45	0.77
IVb-1	CH$_3$	Morpholine	C$_{15}$H$_{14}$ClN$_3$O$_6$	367	>300	65.32	0.78
IVb-2	H	Piperidine	C$_{16}$H$_{16}$ClN$_3$O$_5$	365	>300	62.56	0.76
IVb-3	Cl	N-Methylpiperazine	C$_{16}$H$_{17}$ClN$_4$O$_5$	380	>300	58.65	0.77
IVc-1	F	Morpholine	C$_{16}$H$_{17}$ FN$_3$O$_6$	351	>300	69.32	0.71
IVc-2	CH$_3$	Piperidine	C$_{16}$H$_{16}$FN$_3$O$_5$	349	>300	58.25	0.73
IVc-3	H	N-Methylpiperazine	C$_{16}$H$_{17}$FN$_4$O$_5$	364	>300	65.29	0.74
IVd-1	Cl	Morpholine	C$_{16}$H$_{17}$N$_3$O$_6$	347	>300	67.59	0.75
IVd-2	F	Piperidine	C$_{16}$H$_{17}$N$_3$O$_5$	331	>300	61.26	0.73
IVd-3	CH$_3$	N-Methylpiperazine	C$_{17}$H$_{20}$N$_4$O$_5$	360	>300	66.34	

-CH$_2$ of morpholine), 3.13-3.10 (t, 4H, 3,5 -CH$_2$ of morpholine).

^{13}C NMR data (δ ppm, DMSO-d_6): 166.03 (1C, -C-F), 158.27 (1C, -C=O), 157.78 (1C, -C=O), 155.43 (-C-N), 135.10 (1C, -C-OH), 122.83 (-C-Ar), 118.54 (-C-Ar), 118.30 (2 Ar-C), 116.63 (-C- Ar), 116.56 (-C- Ar), 99.07 (1C, -CH$_2$), 63.26 (2C, morpholine), 42.91 (2C, morpholine). Mass Spectral Data m/z: 353(M+2)

6-Fluoro-4-hydroxy-1-(2-piperidin-1-yl)acetyl)-3-nitroquinolin-2(1H)-one (IVc-2):

IR data (KBr, cm^{-1}): 3091.89 (Aromatic –CH stretch), 2954.95 (-CH stretch), 1658.72 (-C=O stretch), 1598.99, 1315.45 (-C-N stretch of NO$_2$), 1195.87 (-C-F stretch).

6-Fluoro-4-hydroxy-1-(2-N-methylpiperazin-1-yl) acetyl)-3-nitroquinolin-2(1H)-one (IVc-3):

IR data (KBr, cm^{-1}): 3088.82 (Aromatic –CH stretch), 2958.09, 2853.51 (-CH stretch), 1662.72 (-C=O stretch), 1593.30, 1332.91 (-C-N stretch of NO$_2$).

6-Methyl-4-hydroxy-1-(2-morpholin-1-yl)acetyl)-3-nitroquinolin-2(1H)-one (IVd-1):

IR data (KBr, cm^{-1}): 3098.30 (Aromatic –CH stretch), 2864.83 (-CH stretch), 1653.74 (-C=O stretch), 1590.28, 1338.80 (-C-N stretch of NO$_2$), 1231.41 (-C-O of morpholine).

^{1}H NMR data (δ ppm, DMSO-d_6): 11.95 (s, 1H, OH), 8.39-7.87 (m, 3H, Ar-H), 4.35 (s, 2H, -CH$_2$), 2.51 (s, 6H, -CH$_2$ of morpholine), 1.65-1.55 (d, 2H, -CH$_2$ of morpholine), 1.35 (s, 3H, -CH$_3$). ^{13}C NMR data (δ ppm, DMSO-d_6): 158.74 (1C, -C=O), 156.28 (1C, -C=O), 151.06 (1C, -C-OH), 137.09 (1C, -C-N), 135.50 (1C, -C-Ar), 131.36 (1C, -C-Ar), 130.82 (1C, -C-Ar), 125.81 (1C, -C-Ar), 125.06 (1C, -C-Ar), 124.13 (1C, -C-Ar), 43.73 (1C, -CH$_2$), 22.16 (4C, morpholine), 21.59 (1C, -CH$_3$). Mass Spectral Data m/z: 349 (M+2)

6-Methyl-4-hydroxy-1-(2-piperidin-1-yl)acetyl)-3-nitroquinolin-2(1H)-one (IVd-2):

IR data (KBr, cm^{-1}): 3091.85 (Aromatic –CH stretch), 2953.02, 2912.53, 2852.6 (-CH stretch), 1654.88 (-C=O stretch), 1593.20, 1331.88 (-C-N stretch of NO$_2$).

6-Methyl-4-hydroxy-1-(2-N-methylpiparazin-1-yl) acetyl)-3-nitroquinolin2(1H)-one (IVd-3):

IR data (KBr, cm^{-1}): 3012.65 (Aromatic –CH stretch), 2964.67, 2841.23 (-CH stretch), 1652.18, 1638.74 (-C=O stretch), 1566.47, 1358.35 (-C-N stretch of NO$_2$).

Molecular Docking study [11]

Molecular docking studies of the title compounds {IVa-d (1-3)} were carried out using Molegro Virtual Docker (MVD-2013, 6.0) software.

In order to further validate the experimental results, molecular docking studies of the title compounds (IVa-d) were carried out using Molegro Virtual Docker (MVD-2013, 6.0).

1. All the title compounds were built using Chemdraw12.0.2.

2. The 2D structures were then converted into energy minimized 3D structures which were saved as MDL MolFile (.mol2).

3. The coordinate file and crystal structure of Epidermal Growth Factor Receptor tyrosine kinase domain complexed with a 4-anilinoquinazoline inhibitor (PDB ID: 1m17) were obtained from the RCSB-PDB website.

4. The protein file was prepared by the removal of water molecules, addition of polar hydrogen, and removal of other bound ligands.

5. The site at which binding of the complexed inhibitor occurs, was selected as the active site for docking of the molecules.

6. The docking protocol was carried out for synthesized compounds/ligands using MVD- 2013(6.0) software using the standard operating procedure.

7. The MolDock scores and the hydrogen bonding of the test compounds were compared with those of the 4-anilinoquinazoline ligand. The result of docking study is represented in Table II.

The crystal structure of the target enzyme including forty amino acids from the carboxyl terminal tail has been determined to 2.6 $^\circ$A resolution. Unlike any other kinase enzymes, the epidermal growth factor receptor tyrosine (EGFR) kinase family members possess constitutive kinase activity without a phosphorylation event within their kinase domains. Despite its lack of phosphorylation, the EGFRK activation loop adopts a conformation similar to that of the phosphorylated active form of the kinase domain from the insulin receptor. It is observed that the key residues of a dimerized structure lying between the EGFRK domain and carboxyl-terminal substrate docking sites are found in close contact with the kinase domain .

site at which the known 4-anilinoquinazoline inhibitor binds with the target protein was selected as the active site is shown in Fig. 2. It is lined with amino acid residues such as Leu694, Met769, Thr830, Asp831, Glu738, Lys721, Cys773; etc. Hence to identify other residual interactions of the tested compounds, a grid box (include residues within a 15 °A radius) large enough to accommodate the active site was constructed. Since 4-anilinoquinazoline is a known inhibitor, the centre of this site was considered as the centre of search space for docking.
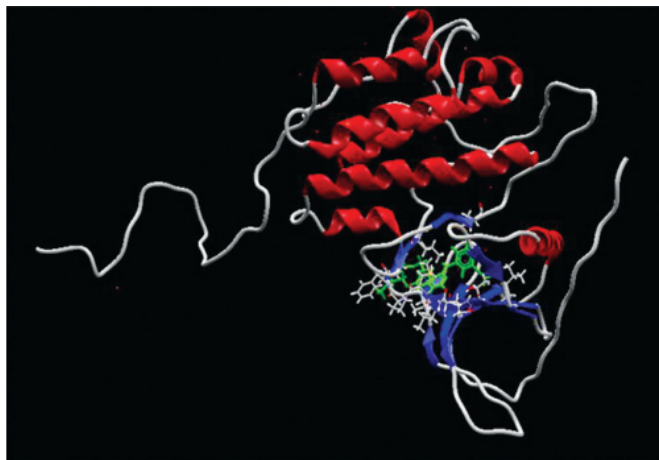

Fig. 2: Structure of EGFR-tyrosine kinase domain complexed with 4-anilinoquinazoline inhibitor (PDB ID: 1m17)
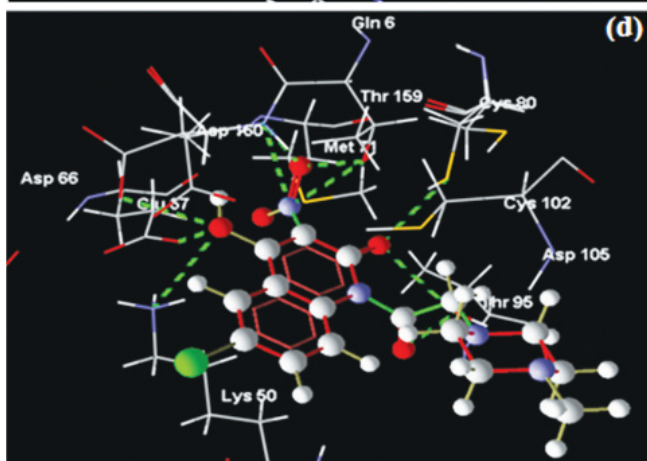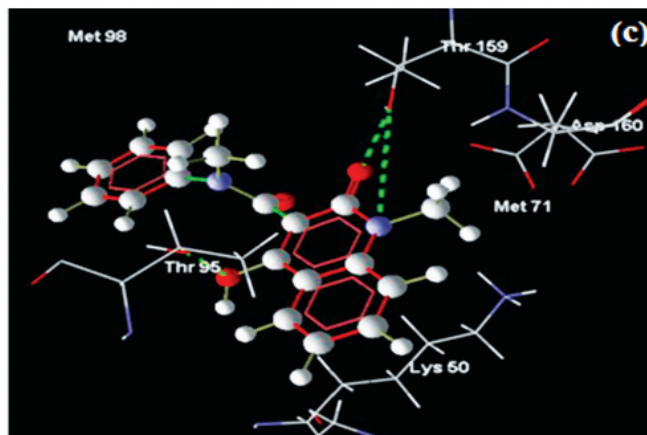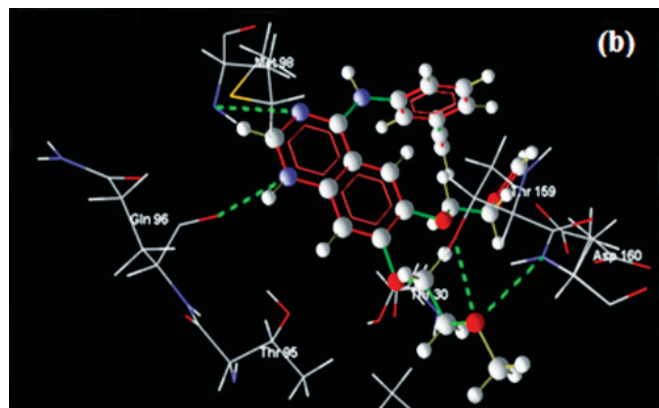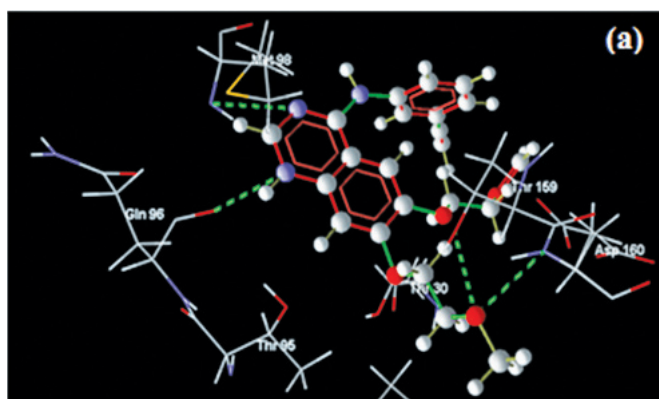

Fig. 3: (a) Ligand 4-anilinoquinazoline docked in best of its conformation (pose) into the binding site of 1m17. The –N at 1st position of the quinazoline moiety forms hydrogen bonds with –NH of Met 98. The –N at 3rd position of quinazoline moiety forms hydrogen bonds with –OH of Gln 96. Etherial oxygen of side chain forms hydrogen bond with -OH of Thr 159 and –NH of Asp 160.

(b): Imatinib docked in best of its conformation (pose) into the binding site of 1m17. The –N from pyridine ring forms hydrogen bonds with –OH of Thr 159 and –NH of Asp 160. The –N from N-methyl piprazine forms hydrogen bond with –NH of Lys 50.

(c): Linomide docked in best of its conformation (pose) into the binding site of 1m17. The –N at 1st position and –C=O at 2nd position of the quinolin-2-one nucleus forms hydrogen bonds with –OH of Thr 159. The –OH at 4th position of quinolin-2-one nucleus the forms hydrogen bonds –OH of Thr 95.

(d): Compound IVb-3 docked in best of its conformation (pose) into the binding site of 1m17. The –C=O at 2nd position of the quinolin-2-one nucleus and –C=O of acetyl part form hydrogen bonds with –OH of Thr 95. The –C=O at 2nd position of the quinolin-2-one nucleus forms hydrogen bonds with 5H of Cys 80. The –N from –NO$_2$ at 3rd position of the quinolin-2-one moiety forms hydrogen bond with –NH and Asp 160 and –OH of Thr 159. The –O from –NO$_2$ at 3rd position of the quinolin-2-one moiety forms hydrogen bonds with –NH and Asp 160 and –OH of Thr 159. The –O from –OH at 4th position of the quinolin-2-one moiety forms hydrogen bond with –OH of Asp 160, –NH of Lys 50 and –OH of Glu 67.

24

Table II: Results of Molecular docking studies of the the 6-substituted-4-hydroxy-1-(2-substituedacetyl)-3-nitroquinolin-2(1H)-one

Compound	MolDock Score	Rerank Score	H-Bond
IVa-1	-99.2707	67.2153	14.6909
IVa-2	-90.7794	48.4538	13.4396
IVa-3	-98.8002	65.0522	13.5822
IVb-1	-78.4697	59.2204	16.0422
IVb-2	-96.7038	64.7984	8.06138
IVb-3	-105.151	80.9078	19.932
IVc-1	-86.4366	71.3299	12.9034
IVc-2	-83.7237	64.6895	2.2442
IVc-3	-81.3611	74.3401	15.629
IVd-1	-78.2474	55.2962	20.2751
IVd-2	-94.4335	14.1275	21.7336
IVd-3	-92.1288	77.6543	19.7467
Imatinib	-111.689	17.5133	8.79356
Linomide	-81.1717	27.4793	3.64.23
1m17	-127.915	78.7372	8.31485

Docking of the synthesized compounds with EGFR-tyrosine kinase domain exhibited well conserved hydrogen bonding with the amino acid residues at the active site. The MolDock scores of the test compounds ranged from -78.2474 to -105.151 while that of linomide was -81.1717. Imatinib was used as the reference standard for comparison of efficiency and exhibited MolDock score of -111.689. Ten out of the twelve designed molecules exhibited MolDock score higher than that exhibited by linomide; with compound IVb-3 having a highest MolDock score of -105.151. These results showed that the novel linomide derivatives possess higher affinity than linomide towards the active site of the target protein EGFRK. The best poses of compounds exhibiting the most promising hydrogen bonding are shown in Fig. (3a-d).

Fig. 3a-d: Molecular docking studies of the title compounds (IVa-d) were carried out using Molegro Virtual Docker (MVD-2013, 6.0) and the results are tabulated in Table II.

Anticancer Activity [12]

3-(4,5-Dimethythiazol-2-yl)-2,5-diphenyl tetrazolium bromide (MTT) Solution was prepared by dissolving 5 mg in 1 ml of Phosphate Buffer Saline (PBS – pH 7.4).

Cytotoxicity Assay

In vitro growth inhibition effect of test compound was assessed by colorimetric spectrophotometric determination of conversion of MTT into "Formazan blue" by living cells. 50 µl of 1×105 cells/ml cell suspension was seeded into each well in a 96 well micro titer plate and final volume was made upto 150 µl by adding Dulbecco's Modified Eagle Media (DMEM media). Dilutions of the test compounds were prepared in DMEM media. 100 µl of the test compounds of different concentrations was added to the wells and incubated for 24 hours, in presence of 5 % CO_2, at 37℃ into CO_2 incubator. After 24 hours, 20 µl of 5 mg/ml MTT reagent was added to the wells. The plate was kept for 4 hours incubation in dark place at room temperature. The plate was covered with aluminum foil, since MTT reagent is photosensitive. The supernatant was carefully removed without disturbing the precipitated Formazan crystals and 100 µl of DMSO was added to dissolve the crystals formed. The optical density (OD) was measured at wavelength of 492 nm. The study was performed in triplicates. The result represents the mean of three readings. The result of cytotoxicity assay is represented in Table IIIa and III b Formula:

Table III b: Cell viability of KB (Oral cancer) cell lines of 6-substituted-4-hydroxy-1-(2-substituedacetyl)-3-nitroquinolin-2(1H)-one

Concentration (µg/mL)	% Cell Viability (KB)											
	IVa-1	IV a-2	IVa-3	IVb-1	IV b-2	IVb-3	IVc-1	IVc-2	IVc-3	IVd-1	IVd-2	IVd-3
100	57.70	70.20	64.10	71.20	64.52	62.10	56.10	43.20	52.70	48.30	44.60	61.10
50	59.20	82.53	79.60	81.00	70.56	71.40	76.10	64.70	68.00	66.10	59.00	63.60
25	69.20	85.13	81.30	84.40	79.82	78.80	89.80	89.00	75.30	75.50	67.00	78.40
12.5	93.70	87.63	82.70	85.50	84.16	86.70	93.80	92.20	76.60	79.30	87.20	83.20
6.25	96.70	91.08	89.90	94.90	90.36	89.50	98.10	98.00	95.20	89.30	97.80	94.10
Control	100	100	100	100	100	100	100	100	100	100	100	100

Principal
V P College Of Pharmacy, Madkhol
Tal. Sawantwadi, Dist. Sindhudurg

$$\text{Survival index in } \% = \frac{\text{Mean OD of test compond}}{\text{Mean OD of control}} \times 100$$

Table III a: IC_{50} value of the compounds in µM/mL against KB cell

Compound	IC_{50}
IVc-2	0.2406
IVd-1	0.2737
IVd-2	0.2447
Imatinib	0.054

RESULTS AND DISCUSSION

The synthetic routes of the compounds are outlined in Scheme 1. The compounds were satisfactorily characterised by IR, NMR and Mass spectral data. The compound (IVc1) was characterized by IR, ^{1}H NMR and ^{13}C NMR. In the IR spectrum, weak band at 3083.83 cm^{-1} were seen due to aromatic C-H stretch; absorption band at 2867.42 cm^{-1} indicated the presence of an aliphatic –CH stretching; a sharp band at 1657.93 cm^{-1} was indicative of the presence of amide carbonyl system; absorption band at 1558.20 and 1332.65 cm^{-1} are characteristic to nitro group; absorption band at 1248.42 cm^{-1} was due to C-O of morpholine ring. This indicated the initial success of the reaction. In the ^{1}H NMR spectrum the siglet at δ 10.35 indicates presence of an -OH group; multiplet at δ 7.57-7.10 indicates presence of 3 protons of aromatic ring; a singlet at δ 4.62 for 2 protons indicates the presence of a –CH$_2$ of acetyl group and triplets at δ 3.78-3.75 and 3.44-3.10 indicates presence of 8H of morpholine and m/z value of 353 [M^{+2}] confirms the success of the reaction.

In the decoupled ^{13}C NMR spectrum; a downfield signal at δ 166.03 was due to C-F; signals for–C-NO$_2$ functional group appeared at δ 158.27 and acyl carbonyl at δ 157.78. C=O of cyclic amide appeared at 155.43. A signal at δ 135.10 was obtained due to C-4 attached to OH of quinolone. The six aromatic carbons of the ring showed the signals at δ 122.83, 118.54, 118.30(2C), 116.63 and 116.56. The 2,6- equivalent carbons of morpholine appeared at δ 63.26 and 3,5-carbons at δ 42.91.

From the series of synthesized 6-substituted-1-(2-chloroacetyl)-4-hydroxy-3-nitroquinolin-2(1H)-one derivatives,were tested for their *in vitro* anticancer activity against KB (Oral cancer) cell lines by MTT assay. Among all, compound IVc-2 showed 50% lysis at 0.2406 µM/mL, compound IVd-1 showed 50 % lysis at 0.2447 µM/mL and compound IVd-2 showed 50 % lysis at 0.2737 µM/mL.

Biological evaluation

From the series of synthesized 6- substituted-4-hydroxy -1-(2-substitued alicyclicamino-1yl)acetyl)-3-nitroquinolin-2(1H)-one {IVa-d (1-3)}, all the compounds were tested for their *in vitro* anticancer activity against KB (oral cancer) by MTT assay method.

CONCLUSION

Twelve derivatives of 6-substituted-4-hydroxy -1-(2-substitued alicyclicamino-1-yl)acetyl)-3-nitroquinolin-2(1H)-one {IVa-d (1-3)} were synthesized , characterized by IR, ^{1}H NMR,^{13}C NMR and Mass spectroscopic analysis and conclusively the structures were established. Selected compounds were evaluated for their *in vitro* anticancer activity against KB (Oral cancer) cell lines based upon MTT assay. From the obtained results it was concluded that among all, compound 6-fluoro-4-hydroxy-1-(2-piperidine-1-yl)acetyl)-3-nitroquinolin-2(1H)-one (IVc-2) was the most potent against KB cell line with IC_{50} values of 0.2406µM/mL and therefore found to be active against *in vitro* anticancer activity. The title compounds were subjected to *in silico* docking studies using Molegro Virtual Docker(MVD-2013, 6.0) software. The compound 6-chloro-4-hydroxy-1-(2-*N*-methylpiperazin-1-yl)acetyl)-3-nitroquinolin-2(1H)-one (Vb-3) showed a highest MolDock Score of -105.151; which is comparable to that of the standard ligand (-127.915) and Imatinib (-111.689). and higher than parent compound linomide (-81.1717). The compound (IVb-3) that showed highest docking score did not show highest *in vitro* anticancer activity against KB cell line. However compound 6-fluoro-4-hydroxy-1-(piperidine-1-yl)acetyl)-3-nitroquinolin-2(1H)-one (IVc-2) with docking score of -83.7237 was found to have highest *in vitro* anticancer activity amongst the series probably because of strong electron withdrawing group fluoro at 6th position, also nitro group present at 3rd position, and piperidine ring system at the 1st position.

ACKNOWLEDGEMENT:

REFERENCES

1. http://www.who.int/cancer/en/ [Accessed on 4th May 2018]
2. https://www.cancer.gov/about-cancer/understanding/statistics [Accessed on 19th March 2019]

3. Available to oral cancerfoundation.org. [Accessed on 12.12.2019]

   Ogino K, Hobara T, Ishiyama H, Yamasaki K, Kobayashi H, Izumi Y, et al. Antiulcer mechanism of action of rebamipide, a novel antiulcer compound, on diethyldithiocarbamate-induced antral gastric ulcers in rats. **Eur. J. Pharmacol**. 1992; 219(1): 9-13.

4. Trianquand C, Romanet JP, Nordmann JP, Allaire C. Efficacy and safety of long-acting carteolol 1% once daily: A double-masked, randomised study. **J. Fr. Opthalmol**. 2003; 26:131-6.

5. De Fruyt J, Deschepper E, Audenaert K, Constant E, Floris M, Pitchot W, et al. Second generation antipsychotics in the treatment of bipolar depression: a systematic review and meta-analysis. **J. Psychopharmacol**. 2012; 26: 603-17.

6. Maria GR, Shivalingrao MD, Soniya N, Jairus F, Prasad T, et al. Synthesis and evaluation of 2-(4-methoxy-2-oxo-1-phenyl/methyl-1,2-dihydroquinolin-3-yl)-2-methyl-3-(phenyl/substitutedphenylamino)thiazolidin-4-one as antibacterial and anticancer agents. **Indian J. Chem**. 2016; 55B:1254-8.

7. Jiangdong S, Zili X, Michael AI, Chandrashekhar K, Bulbul P, Zhigen H , et al. Structure-activity relationships studies of the anti-angiogenic activities of linomide. **Bioorg. Med. Chem. Lett**. 2003; 13:1187-9.

8. Qun L, Keith WW, Weibo W, Nan-Horng L, Akiyo C, Wen-zhen G, et al. Design, synthesis and activity of achiral analogues of 2-quinolones and indoles as non-thiol farnesyltransferase inhibitors. **Bioorg. Med. Chem. Lett**. 2005; 15:2033-9.

9. Jochmans D. Novel HIV-1 reverse transcriptase inhibitors. **Virus Res**. 2008; 134:71-85

10. Thomas K. The pyrano route to 4-hydroxy-2-quinolones and 4-hydroxy-2-pyridones. **IL Farmaco**. 1999; 54:309-415.

11. Palkar MB, Singhai, AS, Ronad PM, Vishwanathswamy A, Boreddy TS, Veerapur VP. Synthesis, pharmacological screening and in silico studies of new class of diclofenac analogues as a promising anti-inflammatory agents. **Bioorg. Med. Chem** .2014;22: 2855-66.

12. Rashad FM, Abd El-Naseer NH, Dawoud IF, Matawe FH. Isolation and Characterization of Antibiotic/Antitumor producing Sterptomyces. **Res. J. Pharm. Biological Chem. Sci.**, 2015; 6(2):1917-29.

Design, synthesis of 6-substituted-4-hydroxy-1-(2-substitutedalicyclicamino) acetyl)quinolin-2(1*H*)-one derivatives and evaluation of their *in vitro* anticancer activity

Alisha Dream Soares[a], Shivalingrao N Mamle Desai*[a], Priyanka Tiwari[a], Mahesh B Palkar[a,b], Sunil G Shingade[a] & Bheemanagouda Biradar[a,c]

[a] Department of Pharmaceutical Chemistry, P.E.S's Rajaram and Tarabai Bandekar College of Pharmacy, Ponda, Goa 403 401, India
[b] Department of Pharmaceutical Chemistry, KLE College of Pharmacy, Vidyanagar, Hubballi 580 031, India
[c] Department of Pharmacology, P.E.S's Rajaram and Tarabai Bandekar College of Pharmacy, Ponda, Goa 403 401, India
E-mail: smamledesai@rediffmail.com

The current research work deals with the design, synthesis of 6-substituted-4-hydroxy-1-(2-substitutedalicyclicamino)acetyl)quinolin-2(1*H*)-one derivatives and evaluation of their *in vitro* anticancer activity. Molecular docking studies of the title compounds have been carried out using Molegro Virtual Docker (MVD-2013, 6.0) software. The compounds exhibited well conserved hydrogen bonds with one or more amino acid residues in the active pocket of EGFRK tyrosine kinase domain (PDB ID: 1m17). The MolDock Score of compound (IIIc-3) is (−96.01) which is comparable to that of the standard ligand (−123.35) and Imatinib (−111.68). Most of the novel analogues of quinolin-2-one exhibit better affinity towards EGFRK protein than linomide (−81.17). These results show that the novel quinoline-2-one derivatives possess higher affinity than linomide towards the active site of the target protein EGFRK. The compounds have been synthesized using appropriate synthetic route. Some of the synthesized compounds have been characterized by UV, IR, ^{1}H and ^{13}C NMR and mass spectral data. Ten derivatives that have better MolDock score have been tested for their *in vitro* anticancer activity using KB (Oral cancer) cell line. Compound (IIIc-3) is found to be the most cytotoxic as compared to the other synthesized derivatives, with IC$_{50}$ values of 1.07 µM/mL against KB(Oral cancer)cell line.

Keywords: Quinolin-2-one, anticancer, KB cell line, Molegro Virtual Docker, EGFRK protein

'Cancer' refers to a large group of diseases characterized by the abnormal growth and proliferation of cells which can further invade adjoining parts of the body and/or spread to other organs. Cancer is the second leading cause of death globally, and was responsible for 8.8 million deaths in 2015, this number is expected to increase to 24 million by 2035 [1]. Globally nearly one in six deaths is due to cancer. It is one of the first leading cause of death in economically developed countries and the second leading cause of death in developing countries[2]. Although current use of chemotherapeutic agents has resulted in reduction of mortality and morbidity among the cancer patients. The major drawback of these anticancer drugs is its high toxicity and nonspecific targeting[3]. Since resistance to this chemotherapeutic drug is a major challenge in the treatment of the disease, discovery of anticancer agents with promising activity and high therapeutic index is the urgent need.

A wide spectrum of biological activities possessed by the quinolin-2-one nucleus has been the crucial factor in exploration and development of compounds based on this moiety by synthetic scientists[4-7]. The biological importance and clinical significance of a number of naturally occurring alkaloids and also synthetic molecules having quinolone nucleus have been documented such as waltherione A, waltherione C and waltherione D as anti-HIV agents; flindersine as an antibacterial and antifungal agent; dictamine for smooth muscle contraction, *etc*. and synthetic analogues like aripiprazole as an antipsychotic drug, carteolol in the ophthalmic preparations as β-blocker are widely used[8-11]. Many researchers identified linomide(1), a quinolin-2-one derivative, as lead molecule for the search of newer anticancer agents[11]. In the present investigation, the methyl group present at first position of linomidewas replaced by hetero-substituted acetyl group and third position was un-substituted and have shown better Mol Dock score.
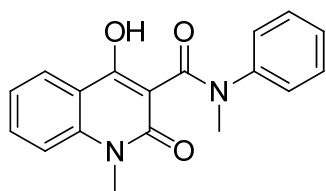
Linomide (1)

Results and Discussion

The starting material for the synthesis of title compounds was synthesized following the literature[12]. The 6-substituted-4-hydroxyquinolin-2(1H)-oneswere subjected to condensation with chloroacetyl chloride gave 6-substituted-1-(2-chloroacetyl)-4-hydroxyquinolin-2(1H)-ones II(a-d) and finally nucleophilic substitution reaction with heterocyclic secondary amines yielded twelve derivatives of 6-substituted-4-hydroxy-1-(2-substituted alicyclicamino-1/4-yl)acetyl)quinolin-2(1H)-ones[IIIa-d(1-3)] (Scheme I). Physical data of all synthesized compounds are given in Table I. Some of the synthesized compounds were characterized by UV, IR, ^{1}H NMR ^{13}C NMR and Mass spectral data. The *in vitro* anticancer activity of ten derivatives that have shown better Mol Dock score were performed by [3-(4,5-dimethylthiazol-2-yl)-2,5-diphenyltetrazolium bromide] MTT assay on KB (Oral Cancer) cell line. Compound (IIIc-3) was found to be the most cytotoxic as compared to the other synthesized derivatives with IC_{50} values of 1.07 µM/mL against KB (Oral cancer)cell line is given in Table II and Table III. The synthesized compounds (IIIa-2), (III-c2),(III c-3) showed IC_{50} values of 1.56, 2.79,1.07 µM/mL respectively and given in Table III. Hence it was concluded that compound 4-hydroxy-6-methyl-1-(2-(4-methylpiperazin-1-yl)acetyl)quinolin-2(1H)-one (III c-3) was the most potent compound against KB cell line with IC_{50} value of 1.07 µM/mL.
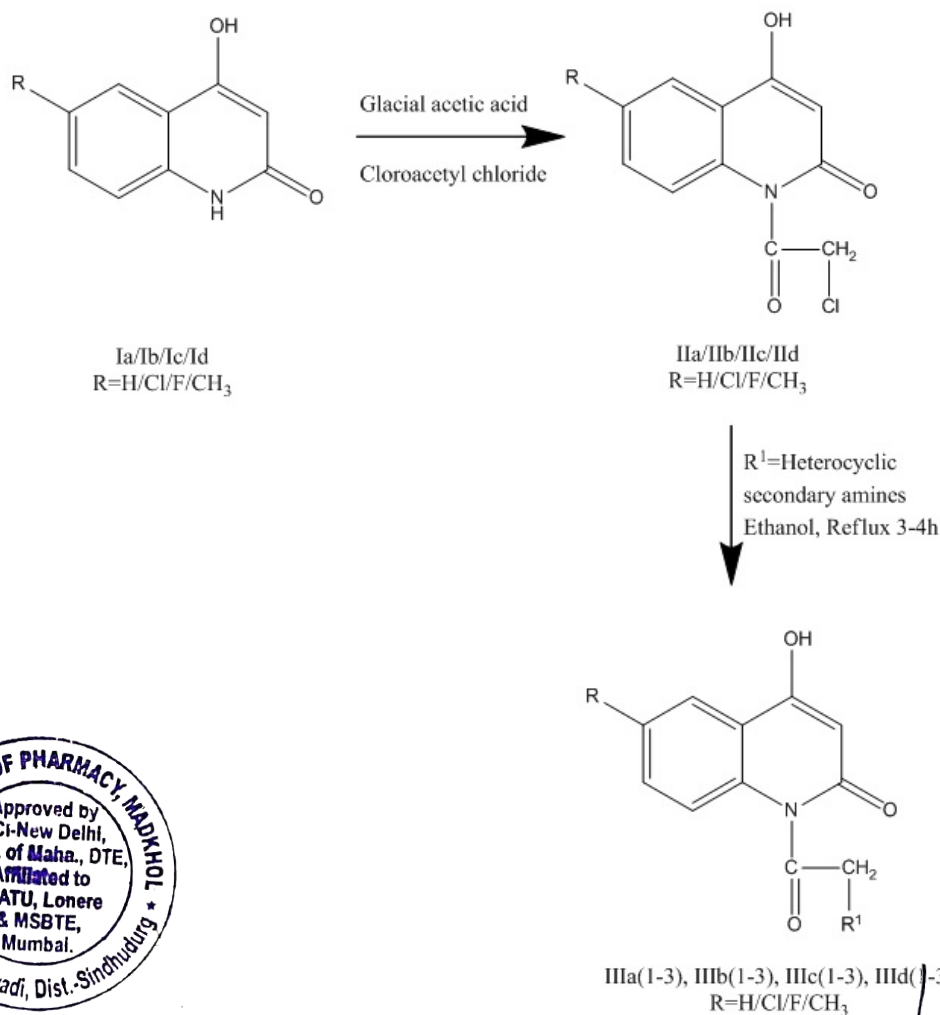
Scheme I — Scheme for synthesis of series of 6-substituted-4hydroxy-1-(2-substitutedalicyclicamino)acetyl)quinolin-2(1H)-one derivatives

Table I — Physical data of the title compounds

Compd	R	R^1	Mol. Formula	Mol. Wt.	m.p. (°C)	Yield (%)	R_f value
III a-1	H	Morpholine	$C_{15}H_{16}N_2O_4$	288	>300	44	0.70
III a-2	H	Piperidine	$C_{16}H_{18}N_2O_3$	286	>300	46	0.69
III a-3	H	N-Methylpiperazine	$C_{16}H_{19}N_3O_3$	301	>300	43	0.72
III b-1	Cl	Morpholine	$C_{15}H_{15}ClN_2O_4$	322	>300	47	0.74
III b-2	Cl	Piperidine	$C_{16}H_{17}ClN_2O_3$	320	>300	43	0.75
III b-3	Cl	N-Methylpiperazine	$C_{16}H_{18}ClN_3O_3$	335	>300	45	0.76
III c-1	CH_3	Morpholine	$C_{16}H_{18}N_3O_3$	302	>300	42	0.77
III c-2	CH_3	Piperidine	$C_{17}H_{20}N_2O_3$	300	>300	40	0.76
III c-3	CH_3	N-Methylpiperazine	$C_{17}H_{21}N_3O_3$	315	>300	46	0.77
III d-1	F	Morpholine	$C_{15}H_{15}FN_2O_4$	306	>300	44	0.74
III d-2	F	Piperidine	$C_{16}H_{17}FN_2O_3$	304	>300	41	0.73
III d-3	F	N-Methylpiperazine	$C_{16}H_{18}FN_3O_3$	319	>300	40	0.76

Table II — Cell viability of synthesized compounds on KB (Oral cancer) cell line

Concentration (µg/mL)	% Cell Viability (KB cell line)									
	IIIa-2	IIIa-3	IIIb-1	IIIb-2	IIIb-3	IIIc-1	IIIc-2	IIIc-3	IIId-1	IIId-2
100	37.2	47.5	63	50.1	70.1	54.1	38.9	37.6	43.7	42.9
50	70.1	74.2	65	65.8	74.4	68.1	48.9	46	48.9	50.4
25	66.3	74.3	74.7	68.4	79	85.9	56.6	52.5	58	65.8
12.5	69.5	79.9	78.6	72.2	80.6	89.2	61.7	58.5	68.9	78.6
6.25	71.1	84	89.4	77.5	85.8	95.7	73.3	65	84.5	84
Control	100	100	100	100	100	100	100	100	100	100
DMSO	96.73	96.73	96.73	96.73	96.73	96.73	96.73	96.73	96.73	96.73

Table III — IC$_{50}$ values of synthesized compound on KB cell line

Compd	IC$_{50}$ µM/mL
IIIa-2	1.56
IIIc-2	2.79
IIIc-3	1.07
Paclitaxel	0.28

Molecular Docking Studies[14]

Molecular docking studies of the title compounds were carried out using Molegro Virtual Docker (MVD-2013, 6.0) software. The compounds exhibited well conserved hydrogen bonds with one or more amino acid residues in the active pocket of epidermal growth factor receptor tyrosine kinase (EGFRK) domain (PDB ID: 1m17). The Mol Dock Score of compound (IIIc-3) was (-96.01) which is comparable to that of the standard ligand (-123.35) and Imatinib (-111.68). Most of the synthesized novel analogues of quinolin-2-one exhibited better affinity towards epidermal growth factor receptor(EGFRK) protein than linomide (-81.17).These results show that the novel quinolin-2-onederivatives possess higher affinity than linomide towards the active site of the target protein EGFRK. Thus the synthesized derivatives possessed a potential to bind with some of the residues of the active site.

The crystal structure of the target enzyme including forty amino acids from the carboxyl-terminal tail has been determined to 2.6-A resolution. Unlike any other kinase enzymes, the EGFR family members possess constitutive kinase activity without a phosphorylation event within their kinase domains. Despite its lack of phosphorylation, the EGFRK activation loop adopts a conformation similar to that of the phosphorylated active form of the kinase domain from the insulin receptor. It is observed that the key residues of a dimerized structure lying between the EGFRK domain and carboxyl-terminal substrate docking sites are found in close contact with the kinase domain[14]. The site at which the known 4-anilinoquinazoline inhibitor binds with the target protein was selected as the active site (Figure 1). It is lined with amino acid residues such as Leu694, Met769, Thr830, Asp831, Glu738, Lys721, Cys773, *etc*. Hence to identify other residual interactions of the tested compounds, a grid box (include residues within a 15.0 A radius) large enough to accommodate the active site was constructed. Since 4-anilinoquinazoline is a known inhibitor, the center of this site was considered as the center of search space for docking. Docking of the synthesized compounds with EGFR-tyrosine kinase domain exhibited well conserved hydrogen bonding with the amino acid residues at the active site. The MolDock scores of the test compounds ranged from-82.90 to-96.01 while that of linomide was-81.15. Imatinib was used as the reference standard for comparison of efficiency and exhibited MolDock score of-111.68. The twelve designed molecules exhibited MolDock score higher than that exhibited

ligand; linomide; with compound III c-3 having a highest MolDock score of-96.01. The MolDock scores of synthesized compounds are summarized in Table IV. These results show that the novel quinoline-2-one derivatives possess higher affinity than linomide towards the active site of the target protein EGFRK.

Experimental Section

All chemicals and reagents were purchased from SD Fine-Chem Limited, Mumbai. Melting points of synthesized compounds were determined by Thiele's melting point apparatus and are uncorrected. UV-Vis λ_{max} were recorded on Shimadzu UV-1800 spectrophotometer using dimethyl formamide as solvent, FT-IR spectra of the synthesized compounds were recorded on Shimadzu IR Affinity-1 spectrophotometer by using KBr pellets. The ^{1}H and ^{13}C NMR spectral data of the derivatives were recorded on Bruker Avance II 400 NMR Spectrometer using DMSO-d_6 as the solvent and TMS

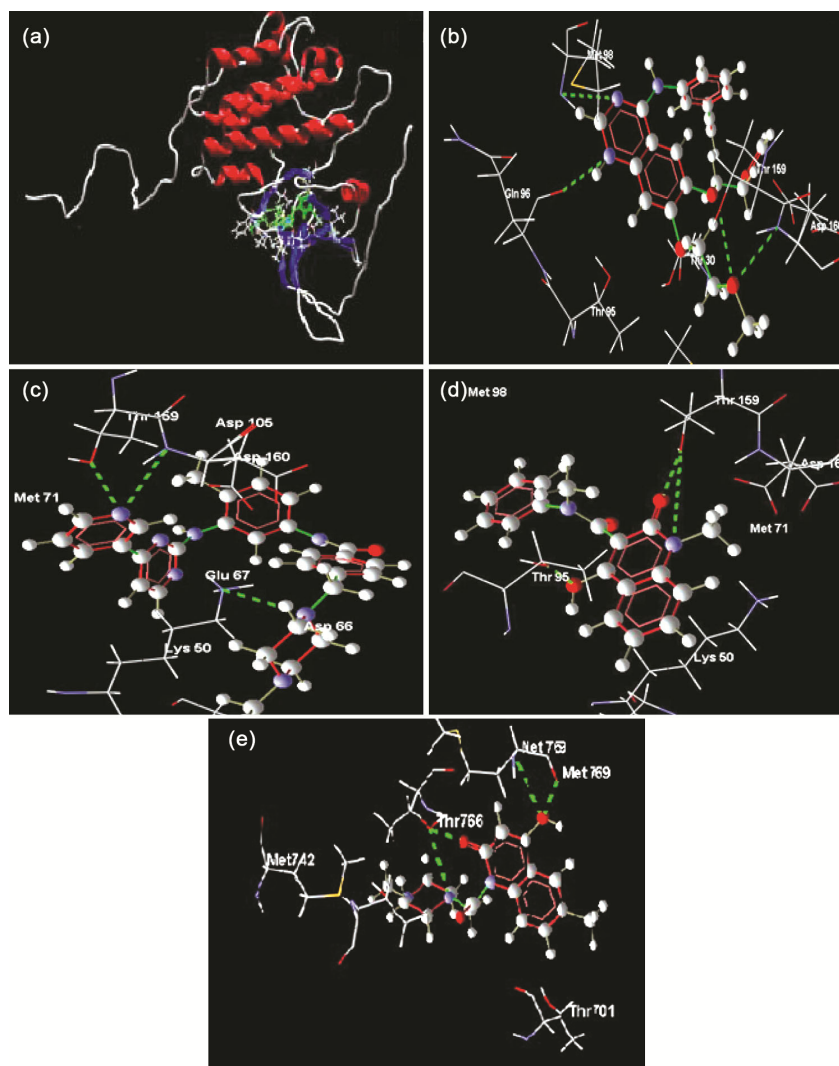Figure 1 — **a**. Structure of EGFR-tyrosine kinase domain complexed with 4-anilinoquinazoline inhibitor (PDB ID: 1m17); **b**. Ligand 4-anilinoquinazoline docked in best of its conformation into the binding site of 1m17. The –N at 1st position of the quinazoline moiety forms H bonds with –NH of Met 98. The –N at 3rd position of quinazoline moiety forms H bonds with –OH of Gln 96. Etherial oxygen of side chain forms hydrogen bond with-OH of Thr 159 and –NH of Asp 160; **c**. Imatinib docked in best of its conformation into the binding site of 1m17. The –N from pyridine ring forms H bonds with –OH of Thr 159 and –NH of Asp 160. The –N from N-methyl piprazine forms H bond with – NH of Lys 50; **d**. Linomide docked in best of its conformation into the binding site of 1m17. The –N at 1st position and –C=O at 2nd position of the quinazoline moiety forms H bonds with –OH of Thr 159. The –OH at 4th position of the quinazoline moiety forms H bonds –OH of Thr 95; **e**. Compound IIIc-3 docked in best of its conformation nto the binding site of 1m17. The –N from N-methyl piperazine ring at 1st position forms H bonds with –OH of Thr 766. The –C=O at 2nd position of the quinolin-2-one moiety forms H bonds with –OH of Thr 766.The –O from –OH at 4th position of the quinolin-2-one moiety forms H bonds with – OH of Met 769 and –NH of Met 769.

Table IV — MolDock Scores of synthesized compounds [IIIa (1-3)/IIIb (1-3)/ IIIc (1-3)/ IIId (1-3)]

Compd	MolDock Score	Rerank Score	H-Bond
III a-1	−85.8853	−50.7614	−7.54332
III a-2	−87.9653	−55.4939	−8.03559
III a-3	−90.7501	−69.3873	−6.59938
III b-1	−87.9591	−59.4054	−7.36858
III b-2	−92.8342	−73.5494	−6.47589
III b-3	−95.9881	−71.7676	−6.67698
III c-1	−84.6997	−67.5085	−6.1219
III c-2	−93.1139	−74.4865	−6.48493
III c-3	−96.0159	−70.3167	−6.59116
III d-1	−82.9092	−68.4856	−9.90704
III d-2	−93.103	−73.5793	−6.41599
III d-3	−88.2352	−13.1662	−3.34145
Imatinib	−111.689	−17.5133	−8.79356
Linomide	−81.1717	−27.4793	−3.6423

as internal standard, chemical shifts are expressed as delta (δ) values (ppm). The Mass spectra (MS) were recorded on Waters, Q-TOF Micromass.

General procedure for the synthesis of 6-substituted-1-(2-chloroacetyl)-4-hydroxyquinolin-2(1*H*)-ones. (IIa/IIb/IIc/IId)

In a clean, dry round bottom flask, 50 mmol of compound Ia/Ib/Ic/Id, 30 mL of glacial acetic acid and 50 mmol of chloroacetyl chloride was mixed in an order under the fume hood. Then the mixture was warmed on a hot plate with swirling for 5-10 min, the precipitate was filtered washed thoroughly with water. The product obtained was recrystallized using ethanol as a solvent.

Spectral data of synthesized compounds

1-(2-Chloroacetyl)-4-hydroxyquinolin-2(1*H*)-one (IIa): UV-Vis λ$_{max}$: 294.32 nm; IR (KBr): 3091.89 (Aromatic –CH stretch), 2951.09, 2860.43(-Aliphatic –CH stretch), 1668.43 cm^{-1} (-C=O stretch); ^{1}H NMR (DMSO-d_6): δ 11.19 (s, 1H, OH), 7.78-7.11 (m, 4H, Ar-H), 5.75 (s, 1H, 3-CH of quinolin-2-one), 5.25 (s, 2H, CH$_2$).

6-Chloro-1-(2-chloroacetyl)-4-hydroxyquinolin-2(1*H*)-one (IIb): UV-Vis λ$_{max}$: 296.48nm; IR (KBr): 3078.39 (Aromatic –CH stretch), 2931.80, 2883.58 (Aliphatic –CH stretch), 1662.64 (-C=O stretch), 864.11 cm^{-1} (C-Cl stretch); ^{1}H NMR (DMSO-d_6): δ 10.29 (s, 1H, OH),7.98-7.49 (m, 3H, Ar-H), 5.71 (s, 1H, 3-CH of quinolin-2-one), 5.38 (s, 2H, CH$_2$).

6-Fluoro-1-(2-chloroacetyl)-4-hydroxyquinolin-2(1*H*)-one (IIc): UV-Vis λ$_{max}$: 296.56nm; IR (KBr): 3088.03(Aromatic –CH stretch), 2945.30, 2900.94 (Aliphatic-CH stretch), 1658.78 (-C=O stretch),

1197.79 cm^{-1} (-C-F stretch); ^{1}H NMR (DMSO-d_6): δ 11.14 (s, 1H, OH), 8.48-7.62 (m, 3H, Ar-H), 5.78 (s, 1H, 3-CH of quinolin-2-one), 5.47 (s, 2H, CH$_2$).

General procedure for the synthesis of 6-substituted-4-hydroxy-1-(2-substitutedalicyclicamino)acetyl)quinolin-2(1*H*)-ones [IIIa (1-3), IIIb(1-3), IIIc(1-3), IIId(1-3)]: To a solution of compound IIa/IIb/IIc/IId 0.004M in ethanol, the appropriate secondary amine (0.004M) was added. The mixture was heated under reflux for 3-4 h at 85°C. The solution obtained was evaporated using IKA rota-evaporator to obtain the crude product. The product was recrystallized using ethanol. The physical characterization data of the title compounds are given in Table I.

Spectral data of synthesized compounds

6-Chloro-4-hydroxy-1-(2-morpholin-4-yl)acetyl)quinolin-2(1*H*)-one (III b-1): UV-Vis λ$_{max}$: 325.56nm; IR (KBr): 3093.82 (Aromatic –CH stretch), 2862.36 (Aliphatic –CH stretch), 1670.35 (-C=O stretch), 754.17 cm^{-1} (-C-Cl stretch); ^{1}H NMR (DMSO-d_6): δ 10.98 (s, 1H, OH), 7.58-7.04 (m, 3H, Ar), 5.53 (s, 1H, 3-quinolin-2-one), 5.29 (s, 2H, acetyl-CH$_2$), 3.69-3.57 (t, 4H, 2,6-CH$_2$ of morpholine), 2.88-2.87 (t, 4H, 3,5-CH$_2$ of morpholine); ^{13}C NMR data (DMSO-d_6): δ 163.23 (1C,-C-Cl), 161.27 (1C,-C=O), 157.88 (1C,-C=O), 137.88 (1C,-C-OH), 130.74 (1C, 3rd C of Quinolin-2-one), 125.08 (1C,-C-Ar), 121.72 (1C,-C-Ar), 119.08 (1C,-C-Ar) 117.07 (2C,-C-Ar), 116.22 (1C,-C-Ar), 71.04,71.02 (2C, 2,6-CH$_2$,Morpholine), 62.98,62.96 (2C, 3,5-CH$_2$, Morpholine), 55.91 (1C,-CH$_2$of acetyl). MS: *m/z* =323 (m+1 peak).

6-Fluoro-4-hydroxy-1-(2-morpholin-4-yl)acetyl)quinolin-2(1*H*)-one (III d-1): UV-Vis λ$_{max}$: 330.56nm; IR (KBr): 3089.96 (Aromatic –CH stretch), 2902.87,2823.79 (Aliphatic –CH stretch), 1669.14 (-C=O stretch), 1400.32 cm^{-1} (-C-F stretch); ^{1}H NMR (DMSO-d_6): δ 11.28 (s, 1H, OH), 7.48-7.27 (m, 3H, Ar) 5.79 (s, 1H,, 3-CH of quinolin-2-one) 5.69 (s, 2H, acetyl-CH$_2$) 3.78-3.75 (t, 4H, 2,6-CH$_2$ of morpholine) 3.10-3.08 (t, 4H, 3,5-CH$_2$ of morpholine). ^{13}C NMR data (DMSO-d_6): δ 163.21 (1C,-C-F) 161.59 (1C,-C=O) 157.88 (1C,-C=O) 135.85 (1C,C-OH) 128.08 (3rd C of quinolin-2-one) 118.98 (1C,-C-Ar) 118.74 (1C,-C-Ar) 117.04 (1C,-C-Ar) 116.96 (1C, -C-Ar) 115.70 (1C, -C-Ar) 115.69 (1C, -C-Ar) 52.07 (1C, -CH2) 63.26 (2C, 2, 6-

morpholine) 45.91 (2C,3, 5-morpholine). MS: m/z = 307(m+1peak).

Biological Activity[15]

The selected 6-substituted-4-hydroxy-1-(2-substitutedalicyclicamino-1/4-yl)acetyl)quinolin-2(1H)-one derivatives were tested for their *in vitro* anticancer activity against KB (Oral cancer) cell line by the following method.

(i) [3-(4,5-Dimethylthiazol-2-yl)-2,5-diphenyltetrazolium bromide] (MTT) Assay: MTT solution preparation (stock solution): 5mg in 1mL of Phosphate buffered saline (PBS). (PBS – pH 7.4).

(ii) Cytotoxicity Assay: *In vitro* growth inhibition effect of test compound was assessed by colorimetric or spectrophotometric determination of conversion of MTT into "Formazan blue" by living cells. 50µl of 1×10^5 cells/mL cell suspension was seeded into each well in a 96 well micro titer plate and final volume was made upto 150 µl by adding Dolbecco's Modified Eagle's Medium (DMEM) media. Dilutions of the test compounds were prepared in DMEM media.

100µl of the test compounds of different concentrations was added to the wells and incubated for 24 h, in presence of 5 % CO_2, at 37°C into CO_2 incubator. After 24 h, 20µl of 5 mg/ mL MTT reagent was added to the wells. The plate was kept for 4 h incubation in dark place at room temperature. The plate was covered with aluminum foil, since MTT reagent is photosensitive. The supernatant was carefully removed without disturbing the precipitated Formazan crystals and 100 µl of DMSO was added to dissolve the crystals formed. The optical density (OD) was measured at wavelength of 492 nm. The study was performed in triplicates and the result represents the mean of three readings using the following formula:

Surviving cells (%) = (Mean OD of test compound/Mean OD of negative control) ×100

Inhibiting cells (%) =100-Surviving cells

The cell viability of the title compounds on KB (Oral cancer) cell line are given in Table II.

Conclusion

From the obtained results of the research work, it can be concluded that compound 4-hydroxy-6-methyl-1-(2-(4-methylpiperazin-1-yl)acetyl)quinolin-2(1H)-one (III c-3) exhibited the highest MolDock score of (-96.01) which is comparable to that of the standard ligand (-123.35) and Imatinib (-111.68). This compound (III c-3) was also found to be the most potent against KB (Oral cancer) cell line with IC_{50} value of 1.07µM/mL. This was observed probably because of the presence of methyl group at 6th position and N-methyl piperazinyl substitution present at the 1st position.

Reference

1   Jemal A, Bray F, Center M, Ferlay J, Ward E & Forman D, *C A Cancer J Clin*, 61 (2011).
2   Kim S K, *Handbook of Anticancer Drugs from Marine Origin* (Springer International Publishing) p.25 (2015).
3   Grant S K, *Cell Mol Life Sci*, 66 (2009) 1163.
4   Thomas K, *Il Farmaco*, 54 (1999) 309.
5   Zhang Q, Chen Y, Zheng Y Q, Xia P, Xia Y & Yang Z Y, *Bioorg Med Chem*, 11 (2003) 1031.
6   Ohashi T, Oguro Y, Tanaka T, Shiokawa Z, Shibata S & Sato Y, *Bioorg Med Chem*, 20 (2012) 5496.
7   Afzal O, Kumar S, Haidar R, Ali R, Kumar R & Jaggi M, *Eur J Med Chem*, 97 (2015) 871.
8   Ogino K, Hobara T, Ishiyama H, Yamasaki K, Kobayashi H & Izumi Y, *Eur J Pharmacol*, 212 (1992) 9.
9   Trianquand C, Romanet J P, Nordmann J P & Allaire C, *J Fr Opthalmol*, 26 (2003) 131.
10   De Fruyt J, Deschepper E, Audenaert K, Constant E, Flori M & Pitchot W, *J Psychopharmacol*, 26 (2012) 603.
11   Maria G R, Shivlingrao M D, Soniya N, Jairus F & Prasad T, *Indian J Chem*, 55B (2016) 1254.
12   Matias F D, Neto A T, Morel A F, Kaufman T S & Larghi E L, *Eur J Med Chem*, 81 (2014) 253.
13   Peter R, Werner F & Wolfgang S, *J Heterocycl Chem*, 29 (1992) 225.
14   Palkar M B, Singhai A S, Ronad P M, Vishwanathswamy A, Boreddy T S & Veerapur V P, *Bioorg Med Chem*, 22 (2014) 2855.
15   Rashad F M, AbdEi-Nasser N H, Dawoud I F & Motawe F H, *Res J Pharm Biol Chem Sci*, 6(2) (2015) 1919.

MEDICINAL
CHEMISTRY
RESEARCH

CrossMark

Design, synthesis, and biological evaluation of 1,3,5-trisubstituted pyrazoles as tyrosine kinase inhibitors

Sinthiya J. Gawandi[1,2] · Vidya G. Desai[1,2] · Sunil G. Shingade[3]

Abstract

We report herein, silica supported molybdic acid mediated oxidative C–N bond formation for the regioselective synthesis of new 1,3,5-trisubstituted pyrazole derivatives. This transformation furnishes a novel synthetic approach with solvent-free neat heat conditions, which was found to be flexible with wide substrate scope and better efficiency towards rapid synthesis of new 1,3,5-trisubstituted pyrazoles. Selected series of the synthesized derivatives were screened for their liability against carcinogenesis. A molecular docking study of the synthesized derivatives was performed in the active site of the tyrosine kinase enzymes. Based on the molecular docking study specific compounds were screened in vitro for their anticancer activity, which showed potent micro molar activity against human MDA-MB-231 breast cancer line and human leukemia cell line K-562 using 3-(4,5-dimethylthiazol-2-yl)–2, 5-diphenyltetrazolium bromide (MTT) assay. Compound **3l** possesses higher inhibitory activity with IC_{50} $0.58 \pm 0.02 \mu M$ against the MDA-MB-231 cell line. Whereas compound **3k** showed higher inhibitory activity with IC_{50} value $0.78 \pm 0.03 \mu M$ against the K-562 cell line. Fluorescence microscopic studies revealed that the compounds showed late apoptotic mode of cell death. These results can lead to further exploitation of tested pyrazole compounds to the highly active drug molecule.

Graphical Abstract
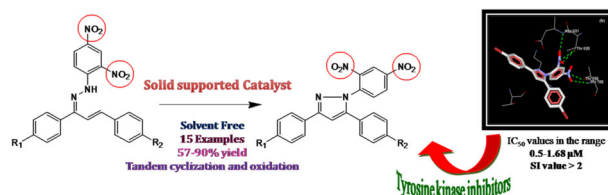
Supplementary information The online version of this article (https://doi.org/10.1007/s00044-018-2282-x) contains supplementary material, which is available to authorized users.

✉ Vidya G. Desai
desai_vidya@gmail.com

1   Department of Chemistry, Dnyanprassarak Mandal's College & Research Centre, Assagao, Bardez 403507, India

2   Goa University, Taleigao, Panaji 403206, India

3   Department of Pharmaceutical Chemistry, PES's Rajaram and Tarabai Bandekar College of Pharmacy, Farmagudi, Ponda, Goa 403401, India

Introduction

Cancer is one of the major chronic degenerative diseases and a prominent cause of deaths world over. Cancers with high prevalence includes lung, prostate, breast, uterine, and stomach (Ayati et al. 2018). In normal cells, protein kinases play a significant role in regulating the cellular functions of cell metabolism, proliferation, motility, and apoptosis. Inversely, in cancer cells, the expression of different kinases is enhanced thereby, deregulating the functions leading to cell growth and proliferation (Trejo-soto et al. 2018). For instance, breast cancer is a complex and heterogeneous

Springer

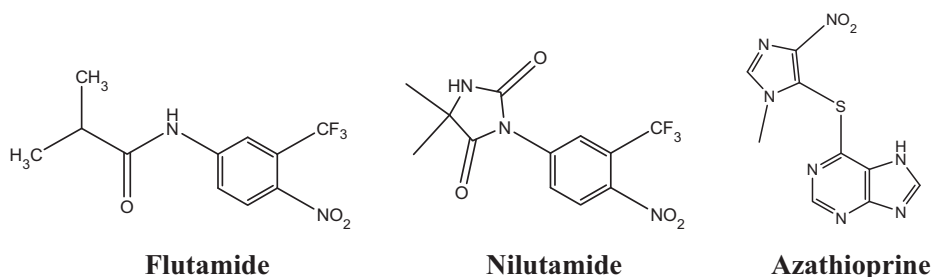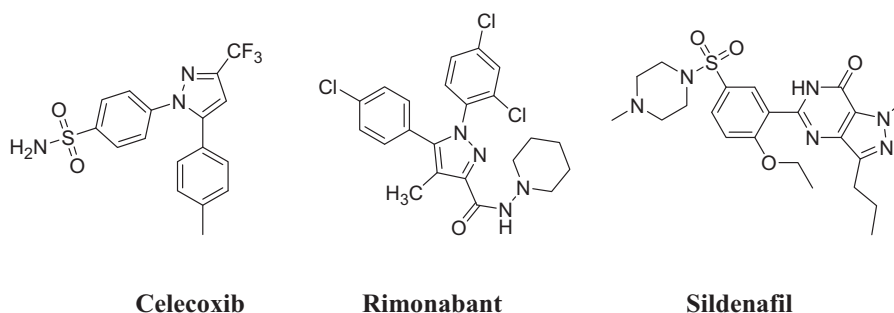**Fig. 1** Structures of anticancer drugs containing nitro group

Flutamide　　　**Nilutamide**　　　**Azathioprine**

Fig. 2 Representative structures of clinically important compounds with pyrazole core structures

Celecoxib　　　**Rimonabant**　　　**Sildenafil**

disease, prevalent in women with around 1.7 million cases diagnosed worldwide every year and the leading cause of death by cancer in women. Existing therapies show detrimental side effects due to their lack of tumor targeting specificity and the emergence of tumor multi-drug resistance (Soudy et al. 2017; Holliday and Speirs 2011).

Enzyme inhibition represents an important phenomenon that defines the drug potency and its efficacy. Potency of a drug is measured in the way it can inhibit the activity of enzymes that trigger the cause of disease. Tyrosine kinase, proteasome (Piwowar et al. 2006), DNA topoisomerases (Topcu 2001), histone deacetylases (Mottamal et al. 2015) and so on enzymes have been widely used as a potential target for anticancer agents. Boom of knowledge in molecular sciences, bioinformatics, and proteomics have been an influential factor in the designing of novel enzyme inhibitors. In this aspect, variation in disubstitution pattern plays an important role in the field of drug discovery. Besides the presence of heterocyclic moiety, aryl substitution on a molecule has an influence on the biological activity. Interestingly, nitro group containing aromatic compounds have proved to possess potent activity against different types of cancer diseases. (Fig. 1) (Olender et al. 2018). Thus, with the growing threat of cancer disease, there is an immense need to synthesize a new drug like molecule that can be developed as a better anticancer agent. Tracking on to achieve this goal, we have synthesized a series of new N-aryl hydrazones and converted them into its pyrazole derivatives and evaluated its anticancer activity.

Pyrazoles represent a key structure in heterocyclic chemistry (Abd El-Karim et al. 2015; Kheder et al. 2014; Kumar et al. 2013) and occupies an important place in

medicinal chemistry as it also constitutes the core structure of clinically interesting compounds, such as Celecoxib (Penning et al. 1997; Ahlstrom et al. 2007), Rimonabant, Sildenafil (Mojzych et al. 2015) etc. (Fig. 2). They are also known to possess enzyme inhibiting properties along with diverse biological activities such as, COX inhibitors (Alam et al. 2016), anticancer (Kumar et al. 2013), anti-microbial (Hafez and El-Gazzar 2016), anti-inflammatory (Keche et al. 2012), anti-oxidant (Renuka and Kumar 2013), anti-convulsant, anti-depressant (Abdel-Aziz et al. 2009), anti-pyretic (Malvar et al. 2014), urease inhibitors (Bole et al. 2011), and anti-viral (Tantawy et al. 2012) activity. They also act as cytotoxic agents (Xia et al. 2007), inhibitors of receptors for advanced glycation end products (Han et al. 2014), as dual inhibitors of acetylcholinesterase as well as monoamine oxidase (Kumar et al. 2013).

We previously reported on the synthesis, screening, and preliminary structure activity relationship studies of quinoxalinyl chalcone hybrid scaffolds as tyrosine kinase inhibitors (Desai et al. 2017). In our present work, Virtual screening of the pyrazole compounds was carried out targeting tyrosine kinase enzyme for anticancer activity. Very few pyrazole derivatives containing N-2, 4-DNP group have been reported (Deng and Mani 2008; Desai and Naik 2013). Our focus was to achieve synthesis of differently substituted 1-(2, 4-dinitrophenyl)-3,5-diaryl-1H-pyrazoles via oxidative cyclization of stable N-(2,4-dinitrophenyl) hydrazones of chalcones.

The presence of 2,4-dinitrophenyl groups in hydrazones retards the formation of pyrazole. As a result, there are no generalized method for the synthesis of such compounds so a new ecofriendly protocol for the regioselective synthesis of 1,3,5-trisubstituted pyrazole has been devised (Scheme 1).

Scheme 1 Design for target compounds
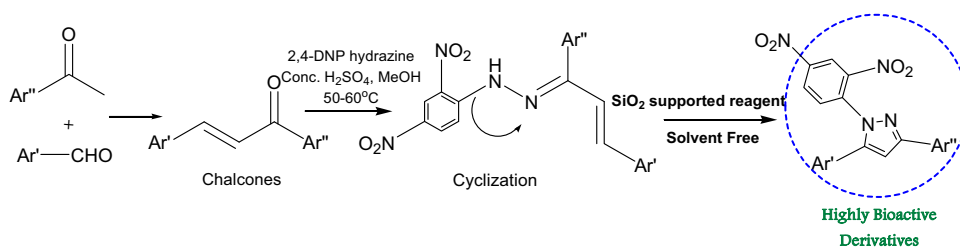
Material and methods

Experimental procedure

Molecular modeling

Protein structure preparation The molecular docking study was performed using Molegro Virtual Docker (MVD-2013, 6.0). The crystal structure of the epidermal growth factor receptor tyrosine kinase domain with 4-anilinoquinazoline inhibitor erlotinib was downloaded from Protein Data Bank PDB ID: 1M17. Molecular docking studies of the synthesized compounds/ligands were performed in order to understand various interactions between the ligand and enzyme active site in detail.

Molecular docking The synthesized compounds were built using Chemdraw 11.0. The two-dimensional structures were then converted into energy minimized three-dimensional structures and were saved as MDL Molfile (.mol2). The coordinate files and crystal structures of tyrosine kinase (PDB ID: 1M17) were obtained from the RCSB PDB website. The protein files were prepared by the removal of water molecules, addition of polar hydrogens and removal of other bound ligands. In the present study, the binding sites were selected based on the amino acid residues, which are involved in binding with tyrosine kinase inhibitors as obtained from protein data bank, which would be considered as the probable best accurate regions as they are solved by experimental crystallographic data. The docking protocol was carried out for the synthesized compounds using MVD-2013 (6.0) software using the standard operating procedures (Palkar et al. 2014).

Cell culture

Breast cancer cell line MCF-7, leukemia cell line K-562, and human embryonic kidney cell line HEK-293 were purchased from the National Center for Cell sciences (NCCS) Pune. The cell lines were cultured in DMEM medium, i.e., Dulbecco's modified Eagle medium, which were supplemented with 10% heat inactivated fetal calf serum (FBS) and 1% Antibiotic–Antimycotic 100X solution and incubated in CO_2 incubator (Eppendorf, New Brunswick, Galaxy 170R, Germany) maintained at 37 °C, 5% CO_2 with 95% humidity until the completion of experiments. The absorption spectrum was measured on a JASCO V670 spectrophotometer.

Cytotoxicity assay

The breast cancer cell line MDA-MB-231, leukemia cell line K-562, and human non-cancerous cell line HEK-293 were cultured in DMEM medium, which was supplemented with 10% heat inactivated fetal calf serum (FBS) and 1% Antibiotic–Antimycotic 100X solution. The cells were seeded at a density of approximately 5×10^3 cells/well in a 96-well flat-bottom micro plate and maintained at 37 °C in 95% humidity and 5% CO_2 for overnight. Different concentration (600, 300, 150, 75, 37.5, 18.75 µg/mL) of test compounds were treated. The cells were incubated for another 72 h. The cells in well were washed twice with phosphate buffer solution, and 20 µL of the MTT staining solution (5 mg/mL in phosphate buffer solution) was added to each well and plate was incubated at 37 °C. After 4 h, 100 µL of dimethyl sulfoxide (DMSO) was added to each well to dissolve the formazan crystals, and absorbance was recorded with a 570 nm using micro plate reader. The IC_{50} values were calculated using graph Pad Prism Version5.1.

Double staining (acridine orange-ethidium bromide)

The cells were seeded at a density of approximately 1×10^4 cells/well in a 24-well flat-bottom micro plate containing cover slips and maintained at 37 °C in CO_2 incubator for overnight. IC50 concentration of synthesized compounds was treated at 72 h. After the incubation, cells were washed with PBS and fixed with 4% paraformaldehyde for 30 min. Twenty microliters of dye mixture was incubated for half an hour, examined under fluorescent microscope.

DAPI (4′,6′-diamine-2′-phenylindole dihydrochloride)

The cells were seeded at a density of approximately 1×10^5 cells/well in a 12-well flat-bottom micro plate containing cover slips and maintained at 37 °C in CO_2 incubator for overnight. More than the IC50 of synthesized compounds was treated at 72 h. After the incubation, cells were washed

with PBS and fixed with 4% paraformaldehyde for 30 min. Twenty microliters of DAPI was incubated for 20 min, examined under fluorescent microscope.

Chemistry

All commercially available reagents were purchased from SD Fine, LobaChemie, and Avra synthesis and used without further purification. Melting points were determined by open capillary tube method and are uncorrected. ^1H (^{13}C) nuclear magnetic resonance (NMR) spectra were recorded at Bruker model 400 MHz instrument using CDCl$_3$. The chemical shifts (δ) are expressed in parts per million relative to the residual deuterated solvent signal and coupling constants (J) are given in hertz. Proton coupling patterns were illustrated as singlet (s), doublet (d), triplet (t), quartet (q), multiplet (m), and broad (br). IR spectra were recorded on a Schimadzu Fourier transform infrared spectrometer using KBr pellets. High resolution mass spectroscopy data were obtained in electron impact (EI) mode. Intensities are reported as percentages relative to the base peak ($I =$ 100%). Synthesis of new 2, 4-dinitrophenyl hydrazones has been reported by our group (Desai and Gawandi 2016).

Synthesis of silica chloride

A mixture of silica–gel (5 g) and thionyl chloride (20 mL) was refluxed for 48 h in a round bottomed flask (100 mL) fitted with a condenser and a guard tube containing CaCl$_2$. The resulting white-greyish powder was filtered and dried.

Synthesis of silica molybdic acid (SMA)

A mixture of silica chloride and sodium molybdate was stirred under refluxing conditions for 3.5 h in n-hexane (5 mL). The reaction mixture was then filtered and washed with distilled water followed by drying at 120 °C in an oven for 6 h. The resulting mixture was then further stirred in 0.1 N HCl solution (40 mL) for 1 h, filtered, washed with distilled water, and dried in an oven at 120 °C for 6 h to obtain the catalyst. Catalyst formation was characterized by XRD analysis. (Ahmed and Siddiqui 2015)

General procedure for the synthesis of pyrazole derivatives (3a–3o)

Substituted hydrazones (1 mmole) and silica supported molybdic acid (1 mmole) were placed in a conical flask and heated at 120 °C. The progress of the reaction was monitored by TLC. After the completion of the reaction, the product was dissolved in ethyl acetate and filtered to recover the catalyst. The solvent was then evaporated under vacuum and the crude mixture was recrystallized from n-hexane to afford the pure

product. The synthesized compounds were characterized on the basis of IR, NMR and Mass spectroscopic data.

1-(2,4-dinitrophenyl)-3,5-diphenyl-1H-pyrazole (3a) Yellow solid, mp: 142–144 °C; IR (KBr) (ν_{max}, cm^{-1}): 3072, 1605, 1538, 1498, 1348 (Desai et al. 2012).

^{1}HNMR (400 MHz, CDCl$_3$) (δ, ppm): 8.72 (d, 1H, $J =$ 2.44, Ar–H), 8.33–8.35 (dd, 1H, $J = 2.52$, $J = 8.4$, Ar–H), 7.84 (d, 1H, $J = 8.4$, Ar–H), 7.25–7.48 (m, 10H, Ar–H), 6.90 (s, 1H, CH); ^{13}C NMR (75 MHz, CDCl$_3$) (δ, ppm): 154.6, 146, 145.4, 140.9, 139.6, 136.5, 130.3, 129, 128.5, 127, 120.6, 119.3, 105.3; HRMS (Electrospray ionisation time-of-flight, [M]$^+$): calcd for C$_{21}$H$_{14}$N$_4$O$_4$, 386.361; found 386.354.

5-(4-chlorophenyl)-1-(2,4-dinitrophenyl)-3-(4-methoxyphenyl)-1H-pyrazole (3b) Yellow solid, mp: 166-170 °C; IR (KBr) (ν_{max},cm^{-1}): 3093, 1608, 1537, 1498, 1348, 1215 (Desai et al. 2012).

^{1}HNMR (400 MHz, CDCl$_3$) (δ, ppm): 8.73 (d, 1H, $J =$ 2.4, Ar–H), 8.33–8.35 (dd, 1H, $J = 2.44$, $J = 8.8$, Ar–H), 7.75 (d, 2H, $J = 8.4$, Ar–H), 7.44 (d, 1H, $J = 8.8$, Ar–H) 6.97–7.36 (m, 6H, Ar–H), 6.82 (s, 1H, CH), 3.85 (s, 3H, OCH$_3$); ^{13}C NMR (75 MHz, CDCl$_3$) (δ, ppm): 162, 153.9, 146.2, 144.4, 140.3, 139.6, 134.6, 133.8, 130.3, 129.4, 128.8, 128.4, 128, 120.6, 119.3, 114.6, 106.3, 55.6; HRMS (ESI-TOF, [M]$^+$): calcd for C$_{22}$H$_{15}$N$_4$O$_5$Cl, 450.832; found 450.823.

3-(4-bromophenyl)-1-(2,4-dinitrophenyl)-5-(4-methoxyphenyl)-1H-pyrazole (3c) Yellow solid, mp: 174–176 °C; IR (KBr) (ν_{max}, cm^{-1}): 3087, 1605, 1538, 1498, 1343, 1215, 594.

^{1}HNMR (400 MHz, CDCl$_3$) (δ, ppm): 8.72 (d, 1H, $J =$ 2.4, Ar–H), 8.36–8.38 (dd, 1H, $J = 0.4$, $J = 8.8$, Ar–H), 7.77 (d, 2H, $J = 8.4$, Ar–H), 7.53 (d, 1H, $J = 8.8$, Ar–H) 6.97–7.48 (m, 6H, Ar–H), 6.85 (s, 1H, CH), 3.83 (s, 3H); ^{13}C NMR (75 MHz, CDCl$_3$) (δ, ppm): 160.8, 154.9, 146.2, 145.3, 144.3, 138.3, 133.6, 133, 130.1, 129.6, 129, 127.4, 124.2, 121.3, 114.2, 111.5, 106.5, 55.6; HRMS (ESI-TOF, [M]$^+$): calcd for C$_{22}$H$_{15}$N$_4$O$_5$Br, 494.022; found 494.023.

1-(2,4-dinitrophenyl)-3,5-bis(4-fluorophenyl)-1H-pyrazole (3d) Yellow solid, mp. 172–174 °C; IR (KBr) (ν_{max}, cm^{-1}): 3090, 1603, 1535, 1496, 1347, 982.

^{1}HNMR (400 MHz, CDCl$_3$) (δ, ppm): 8.75 (d, 1H, $J =$ 2.4, Ar–H), 8.31–8.33 (dd, 1H, $J = 2.8$, $J = 8.8$, Ar–H), 7.87 (d, 2H, $J = 8.0$, Ar–H), 7.56 (d, 1H, $J = 8.8$, Ar–H), 7.02–7.42 (m, 6H, Ar–H), 6.82 (s, 1H, CH); ^{13}C NMR (75 MHz, CDCl$_3$) (δ, ppm): 162.1, 158.6, 146.4, 144.6, 139.6, 132.1, 130.1, 128.4, 128., 120.2, 119.3, 116, 106.2; HRMS (ESI-TOF, [M]$^+$): calcd for C$_{21}$H$_{12}$F$_2$N$_4$O$_4$, 422.082; found 422.084

3,5-bis(4-chlorophenyl)-1-(2,4-dinitrophenyl)-1H-pyrazole (3e) Yellow solid, mp. 200–206 °C; IR (KBr) (ν_{max}, cm^{-1}): 3073, 1602, 1532, 1499, 1344, 620

^{1}HNMR (400 MHz, CDCl$_3$) (δ, ppm): 8.78 (d, 1H, $J = 2.4$, Ar–H), 8.39–8.41 (dd, 1H, $J = 2.8$, $J = 8.8$, Ar–H), 7.69 (d, 2H, $J = 8.4$, Ar–H), 7.55 (d, 1H, $J = 8.8$, Ar–H), 7.10–7.47 (m, 6H, Ar–H), 6.89 (s, 1H, CH); ^{13}C NMR (75 MHz, CDCl$_3$) (δ, ppm): 153.6, 146.4, 145.3, 144.6, 137.4, 135.2, 132.4, 129.6., 128.2, 123.1, 121.1, 106.5; HRMS (ESI-TOF, [M]$^+$): calcd for C$_{21}$H$_{12}$Cl$_2$N$_4$O$_4$, 454.023; found 454.021

5-(4-chlorophenyl)-1-(2,4-dinitrophenyl)-3-(4-fluorophenyl)-1H-pyrazole (3f) Yellow solid, mp. 178–182 °C; IR (KBr) (ν_{max}, cm^{-1}): 3085, 1608, 1536, 1497, 1348, 989, 614.

^{1}HNMR (400 MHz, CDCl$_3$) (δ, ppm): 8.79 (d, 1H, $J = 2.4$, Ar–H), 8.36–8.38 (dd, 1H, $J = 2.42$, $J = 8.8$, Ar–H), 7.77 (d, 2H, $J = 8.72$, Ar–H), 7.57 (d, 1H, $J = 8.8$, Ar–H), 6.98–7.42 (m, 6H, Ar–H), 6.83 (s, 1H, CH); ^{13}C NMR (75 MHz, CDCl$_3$) (δ, ppm): 162.4, 153.6, 146.6, 145.3, 144.5, 139.6, 135.3, 133.1, 132, 130.4, 129.4, 128.6, 128.4, 126.7, 120.6, 114.3, 106.5; HRMS (ESI-TOF, [M]$^+$) : calcd for C$_{21}$H$_{12}$N$_4$O$_4$ClF, 438.053; found 438.054.

1-(2,4-dinitrophenyl)-5-(4-methylphenyl)-3-phenyl-1H-pyrazole (3g) Yellow solid, mp. 154–158 °C; IR (KBr) (ν_{max}, cm^{-1}): 3087, 1603, 1536, 1496, 1350.

^{1}HNMR (400 MHz, CDCl$_3$) (δ, ppm): 8.73 (d, 1H, $J = 2.4$, Ar–H), 8.35-8.37 (dd, 1H, $J = 2.4$, $J = 8.8$, Ar–H), 7.84 (d, 2H, $J = 8.4$, Ar–H), 7.49 (d, 1H, $J = 8.8$, Ar–H), 7.05–7.43 (m, 7H, Ar–H), 6.83 (s, 1H, CH), 2.38 (s, 3H, CH$_3$); ^{13}C NMR (75 MHz, CDCl$_3$) (δ, ppm): 154.6, 146, 145.8, 145.2, 139.6, 138.2, 131.8, 129.8, 129.6, 128.9, 128.8, 128.5, 127, 126, 125.7, 120.9, 106.3, 21.37; HRMS (ESI-TOF, [M]$^+$): calcd for C$_{22}$H$_{16}$N$_4$O$_4$, 400.117; found 400.119.

3-(4-bromophenyl)-5-(4-chlorophenyl)-1-(2,4-dinitrophenyl)-1H-pyrazole (3h) Yellow solid, mp. 138–142 °C; IR (KBr) (ν_{max}, cm^{-1}): 3085, 1608, 1539, 1495, 1348, 742, 552 (Desai et al. 2012).

^{1}HNMR (400 MHz, CDCl$_3$) (δ, ppm): 8.79 (d, 1H, $J = 2.4$, Ar–H), 8.36–8.38 (dd, 1H, $J = 2.44$, $J = 8.8$, Ar–H), 7.69 (d, 2H, $J = 8.4$, Ar–H), 7.45 (d, 1H, $J = 8.8$, Ar–H), 7.10–7.58 (m, 6H, Ar–H), 6.89 (s, 1H, CH); ^{13}C NMR (75 MHz, CDCl$_3$) (δ, ppm): 153.6, 146.2, 145.3, 144.9, 137.7, 134.9, 132.5, 130.1, 129.6, 129.4, 129, 128.6, 127.3, 127.2, 124.1, 121.1, 106.6; HRMS (ESI-TOF, [M]$^+$): calcd for C$_{21}$H$_{12}$N$_4$O$_4$ClBr, 497.972; found 497.98.

1-(2,4-dinitrophenyl)-3-(4-fluorophenyl)-5-(4-methoxyphenyl)-1H-pyrazole (3i) Yellow solid, mp. 142–144 °C; IR (KBr) (ν_{max}, cm^{-1}): 3093, 1608, 1537, 1498, 1348, 1215.

^{1}HNMR (400 MHz, CDCl$_3$) (δ, ppm): 8.75 (d, 1H, $J = 2.4$, Ar–H), 8.35-8.38 (dd, 1H, $J = 2.4$, $J = 8.8$, Ar–H), 7.81 (d, 2H, $J = 7.2$, Ar–H), 7.48 (d, 1H, $J = 8.8$, Ar–H), 6.88–7.26 (m, 6H, Ar–H), 6.79 (s, 1H, CH), 3.83 (s, 3H, OCH$_3$); ^{13}C NMR (75 MHz, CDCl$_3$) (δ, ppm): 164.2, 160.2, 154.3, 145.9, 145.2, 144.6, 138.1, 130.1, 129.5, 127.8, 127.1, 120.9, 120.6, 115.9, 115.6, 114.6, 105.9, 55.8; HRMS (ESI-TOF, [M]$^+$): calcd for C$_{22}$H$_{15}$N$_4$O$_5$F, 434.103; found 434.101.

1-(2,4-dinitrophenyl)-3,5-bis(4-methoxyphenyl)-1H-pyrazole (3j) Yellow solid, mp. 168–170 °C; IR (KBr) (ν_{max}, cm^{-1}): 3105, 1605, 1538, 1505, 1215 (Desai et al. 2012).

^{1}HNMR (400 MHz, CDCl$_3$) (δ, ppm): 8.73 (d, 1H, $J = 2.4$, Ar–H), 8.32–8.34 (dd, 1H, $J = 2.44$, $J = 8.8$, Ar–H), 7.78 (d, 2H, $J = 8.6$, Ar–H), 7.50 (d, 1H, $J = 8.8$, Ar–H), 6.91–7.28 (m, 6H, Ar–H), 6.79 (s, 1H, CH), 3.87 (s, 3H, OCH$_3$), 3.85 (s, 3H, OCH$_3$); ^{13}C NMR (75 MHz, CDCl$_3$) (δ, ppm): 160.2, 154.5, 146, 145.2, 144.6, 137.8, 132.4, 130.1, 129.5, 127.4, 120.4, 114.2, 56.4; HRMS (ESI-TOF, [M]$^+$): calcd for C$_{23}$H$_{18}$N$_4$O$_6$, 446.122; found 446.126.

3,5-bis(4-bromophenyl)-1-(2,4-dinitrophenyl)-1H-pyrazole (3k) Yellow solid, mp. 192–196 °C; IR (KBr) (ν_{max}, cm^{-1}): 3098, 1602, 1532, 1496, 1348, 572; ^{1}HNMR(400 MHz, CDCl$_3$) (δ, ppm): 8.75 (d, 1H, $J = 2.4$, Ar–H), 8.31-8.33 (dd, 1H, $J = 2.8$, $J = 8.8$, Ar–H), 7.87 (d, 2H, $J = 8.4$, Ar–H), 7.53 (d, 1H, $J = 8.8$, Ar–H), 7.03–7.45 (m, 6H, Ar–H), 6.85 (s, 1H, CH); ^{13}C NMR (75 MHz, CDCl$_3$) (δ, ppm): 154.6, 146.4, 145.3, 137.6, 132.4, 130.3, 128.6, 128.2, 123.1, 120.2, 119.3, 116.1, 106.2; HRMS (ESI-TOF, [M]$^+$): calcd for C$_{21}$H$_{12}$Br$_2$N$_4$O$_4$, 541.922; found 541.920.

3-(4-bromophenyl)-1-(2,4-dinitrophenyl)-5-(4-methylphenyl)-1H-pyrazole (3l) Yellow solid, mp. 182–185 °C; IR (KBr) (ν_{max}, cm^{-1}): 3087, 1605, 1538, 1498, 1343, 594.

^{1}HNMR (400 MHz, CDCl$_3$) (δ, ppm): 8.72 (d, 1H, $J = 2.4$, Ar–H), 8.34-8.37 (dd, 1H, $J = 2.4$, $J = 8.4$, Ar–H), 7.81 (d, 2H, $J = 8.0$, Ar–H), 7.55 (d,1H, $J = 8.4$, Ar–H) 7.17–7.50 (m, 6H, Ar–H), 6.85 (s, 1H, CH), 2.38 (s, 3H); ^{13}C NMR (75 MHz, CDCl$_3$) (δ, ppm): 154.6, 146.2, 145.8, 145.18, 139.7, 138.3, 131.8, 129.8, 129.6, 128.9, 128.4, 127., 125.7, 123.5, 120.9, 106.4, 21.4; HRMS (ESI-TOF, [M]$^+$): calcd for C$_{22}$H$_{15}$N$_4$O$_5$Br, 494.022; found 494.023.

1-(2,4-dinitrophenyl)-3-(4-methoxyphenyl)-5-(4-methylphenyl)-1H-pyrazole (3m) Yellow solid, mp. 142–148 °C; IR (KBr) (ν_{max}, cm^{-1}): 3097, 1603, 1542, 1445, 1349, 1217. ^{1}HNMR (400 MHz, CDCl$_3$) (δ, ppm): 8.72 (d, 1H, $J = 2.4$, Ar–H), 8.33-8.36 (dd, 1H, $J = 2.8$, $J = 8.8$, Ar–H), 7.77 (d, 2H, $J = 8.4$, Ar–H), 7.46 (d, 1H, $J = 8.8$, Ar–H) 6.94–7.26. (m, 6H, Ar–H), 6.80 (s, 1H, CH), 3.85 (s, 3H, OCH$_3$), 2.38 (s, 3H, CH$_3$); ^{13}C NMR (75 MHz, CDCl$_3$) (δ,
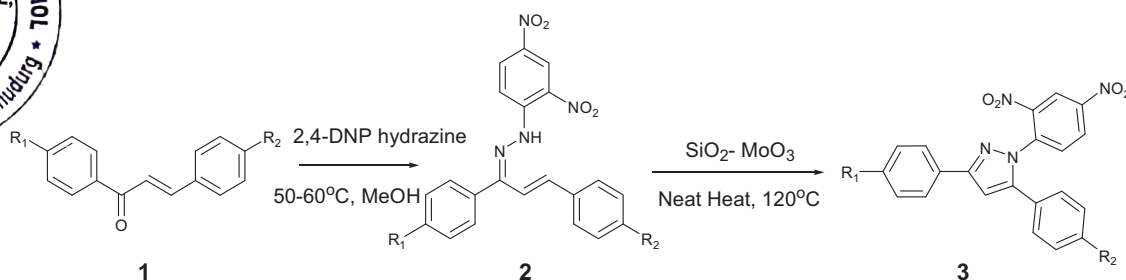
Scheme 2 Synthesis of 1,3,5-trisubstituted pyrazoles

ppm): 160.8, 154.9, 146.2, 145.3, 144.3, 138.3, 133.6, 133, 130.1, 129.6, 129, 127.4, 124.2, 121.3, 114.2, 111.5, 106.5, 55.6, 21.3; HRMS (ESI-TOF, [M]$^+$): calcd for $C_{23}H_{18}N_4O_5$, 430.128; found 430.129.

1-(2,4-dinitrophenyl)-5-(4-fluorophenyl)-3-(4-hydroxyphenyl)-1H-pyrazole (3n)

Yellow solid, mp. 206–208 °C; IR (KBr) (ν_{max}, cm^{-1}): 3596, 3076, 1601, 1532, 1489, 1342, 980.

^{1}HNMR (400 MHz, CDCl$_3$) (δ, ppm): 8.73 (d, 1H, $J = 2.4$, Ar–H), 8.36-8.39 (dd, 1H, $J = 2.4$, $J = 8.8$, Ar–H), 7.75 (d, 2H, $J = 6.4$, Ar–H), 7.46 (d, 1H, $J = 8.8$, Ar–H) 6.88–7.26 (m, 6H, Ar–H), 6.80 (s, 1H, CH); ^{13}C NMR (75 MHz, CDCl$_3$) (δ, ppm): 160.8, 154.9, 152.4, 146.2, 145.3, 144.3, 138.3, 133.6, 132.2, 130.1, 129.6, 128.4, 127.2, 120.9, 116.2, 116.5, 106.5; HRMS (ESI-TOF, [M]$^+$): calcd for $C_{21}H_{13}N_4O_5F$, 420.087; found 420.080.

1-(2,4-dinitrophenyl)-5-(4-nitrophenyl)-3-phenyl-1H-pyrazole (3o)

Yellow solid, mp. 224–226 °C. IR (KBr) (ν_{max}, cm^{-1}): 3089, 1603, 1540, 1484, 1350.

^{1}HNMR (400 MHz, CDCl$_3$) (δ, ppm): 8.79 (d, 1H, $J = 2.4$, Ar–H), 8.41-8.44 (dd, 1H, $J = 2.4$, $J = 8.6$, Ar–H), 8.25 (d, 2H, $J = 7.2$, Ar–H), 7.84 (d, 1H, $J = 8.6$, Ar–H), 7.26–7.51 (m, 7H, Ar–H), 7.03 (s, 1H, CH); ^{13}C NMR (75 MHz, CDCl$_3$) (δ, ppm): 154.6, 148.3, 146.4, 145.8, 144.4, 139.6, 138.4, 131.8, 129.8, 129.4, 128.9, 128.8, 128.5, 127.5, 124.3, 120.9, 106.3; HRMS (ESI-TOF, [M]$^+$): calcd for $C_{21}H_{13}N_5O_6$, 431.086; found 431.102.

Results and discussion

Our preliminary investigations were focused on the development of an ecofriendly reaction conditions for effecting oxidative cyclization. To achieve this, screening of various catalysts and solvents has been carried out. The results revealed that the most suitable reagent for this transformation was SiO_2-molybdic acid, which was then followed by further optimization of reaction conditions. We investigated the effect of the catalyst loading and effect of temperature

Table 1 List of 1,3,5-trisubstituted pyrazole derivatives

Compounds	R_1	R_2	Time in hours	% Yield
3a	H	H	4	66
3b	OMe	Cl	3	77
3c	Br	OMe	4	73
3d	F	F	2.5	78
3e	Cl	Cl	3	88
3f	F	Cl	3.5	84
3g	H	CH$_3$	4	81
3h	Br	Cl	1.5	66
3i	F	OMe	1.5	60
3j	OMe	OMe	3.5	57
3k	Br	Br	2.5	79
3l	Br	CH$_3$	1.5	60
3m	OMe	CH$_3$	2	86
3n	OH	F	2.5	79
3o	NO$_2$	H	3	76

on the model reaction. It was observed that, catalyst not in mol%, but in equimolar amount gave good yield of the cyclized product at 120 °C.

Once the optimized conditions had been developed, we examined the substrate scope and generality of the desired oxidative cyclization reaction. A wide range of newly synthesized substituted 2,4-dinitrophenyl hydrazone derivatives were used for the synthesis of 1,3,5–trisubstiuted pyrazoles (**3a–3o**) (Scheme 2) (Desai and Gawandi 2016). As shown in Table 1, respective hydrazones and equivalent amount of catalyst were heated at 120 °C. After completion, the reaction mixture was washed with ethyl acetate and catalyst was filtered off. Solvent was removed on vacuum and the crude product was recrystallized using n-hexane. It is also worth noting that the purification procedure for the synthesized compounds required only recrystallization instead of tedious and prolonged column chromatographic technique. In order to check the effectiveness of silica molybdic acid, its recycling was performed and was inferred that it can be used over five cycles of reaction without much loss in activity.

Table 2 Molegro docking score for pyrazole derivatives (3a–3o) for anticancer activity

Code	MolDock score (Kcal/mol)	Rerank score (Kcal/mol)	E-inter (protein-ligand)	HBond		Heavy atoms count	Docking score (Kcal/mol)
				No.	Kcal/mol		
3a	−136.051	−90.2738	−132.572	3	−3.46377	29	−139.951
3b	−144.917	−98.7802	−142.843	3	−4.27694	32	−148.045
3c	−149.881	−101.725	−143.373	4	−6.81212	32	−151.798
3d	−148.618	−96.6649	−141.006	5	−6.88374	31	−150.723
3e	−144.812	−82.0598	−137.168	3	−4.70957	31	−144.842
3f	−145.328	−83.7235	−137.104	3	−4.71109	31	−145.484
3g	−137.869	−31.2169	−135.422	0	0	30	−135.477
3h	−138.83	−78.3858	−140.427	7	−10.4638	31	−146.55
3i	−152.306	−90.566	−144.484	3	−4.57163	32	−152.181
3j	−148.609	−98.5868	−141.134	1	−2.05601	33	−148.955
3k	−161.223	−108.857	−152.841	1	−1.90323	31	−159.651
3l	−144.452	−83.159	−136.202	3	−4.71239	31	−144.564
3m	−128.389	−33.1833	−124.899	6	−9.61717	32	−141.594
3n	−141.867	−47.023	−134.386	6	−9.80866	31	−152.178
3o	−158.518	−105.681	−153.638	7	−9.10727	32	−160.755

Under these experimental conditions, cyclization took place better in the presence of electron withdrawing groups on aromatic ring. Compound 3e with electron withdrawing chloro group at 4 positions of 3 and 5 substituted aromatic ring gave excellent yield in 88% in comparison to compound 3a with no substituents in aromatic ring, obtained in 66% yield. On the other side, compound 3j with electron donating methoxy substituent was obtained in 57% yield. Thus, the nature of substituent alters the reactivity of the substrate towards cyclization.

All the synthesized compounds were characterized by IR, ^{1}H NMR, ^{13}C NMR spectroscopy, and mass spectroscopy. The IR spectra of the title products 3a–3o exhibited characteristic absorption bands at 3095 to 3070 cm^{-1} indicating the C–H bond of the pyrazole ring. Also disappearance of absorption bands in the region of frequency at 3300 cm^{-1} pertaining to N–H bond confirms the conversion of hydrazone derivatives to pyrazole. Absorption bands at 1600 to 1610 cm^{-1} could be attributed to the presence of C=N bond. Characteristic absorption peak at 1540 to 1550 cm^{-1} corresponds to the (–NO$_2$) nitro group attached to the carbon atom. ^{1}H NMR analysis further confirms the pyrazole structure. The main distinctive peak in the spectra of all the target compounds is the appearance of the singlet δH at 6.5 to 7.5 ppm signifying the proton attached to C4 of the five membered pyrazole ring. The most deshielded proton was observed in case of the aromatic hydrogen present between the two nitro groups as a doublet at δH 8.79–8.72 ppm. All the aromatic protons showed multiplets at δH 7.50 to 7.10 ppm, thereby marking the formation of pyrazole derivatives. Along with this, 13C NMR spectroscopic study also signifies the pyrazole

formation. Chemical shifts at 154.3, 146.8, 144.4, and 106.2 ppm corresponds to C5=N, C4-NO$_2$, C3-N, and C4-H carbon atoms. The exact molecular weight was also characterized and confirmed by HRMS studies. The ultraviolet spectroscopic studies showed absorbance values at 246 nm.

Anticancer activity

Virtual screening

The synthesized pyrazole compounds were virtually screened for its anticancer activity using tyrosine kinase as the target enzyme (Table 2). The molecular docking study revealed that the compounds 3i, 3k, and 3l act as a very good inhibitors of tyrosine kinase enzyme. As depicted in Fig. 3 compound 3i makes two hydrogen bonding interactions at the active site of the enzyme, among them one interaction comes from the oxygen atom of methoxy group present at fourth position of aromatic ring with Gly772 (1.55 Å) and the other interaction from the oxygen atom of nitro group present on the fourth position of another aromatic ring with Cys773 (2 Å).

The nitro group present on the second and fourth position of aromatic rings in compound 3k makes five hydrogen bonding interactions out of which two are observed between nitrogen and oxygen of nitro group and Thr766 (1.52 and 1.55 Å). The oxygen atoms of nitro group show two interactions with Asp831 (1.55 Å) and Thr830 (1.52 Å) and the nitrogen of nitro group shows one interaction with Thr830 (1.52 Å).

Compound 3l makes two hydrogen bond interactions, the nitrogen and oxygen atoms of nitro group present on fourth

Fig. 3 Molecular docking data: The compounds docked in best of its conformation into the binding site of 1M17. **a** Binding mode of compound **3i** forming one H bond with Cys773, one H bond with Gly772; **b** binding mode of compound **3k** forming one H bond with Asp831, two H bonds with Thr830, two H bonds with Thr766; **c** binding mode of compound **3l** forming two H bonds with Met76
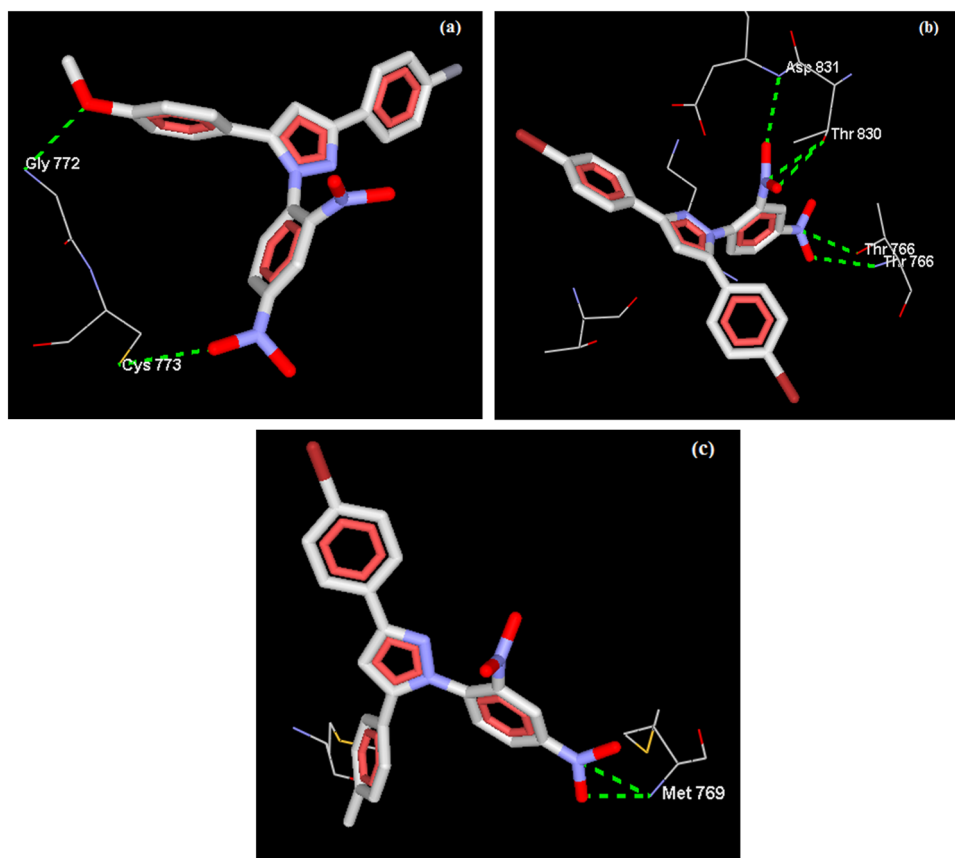

Table 3 IC$_{50}$ values (μM ± S.E.) of compounds **3i**, **3k**, and **3l** against two different cancer cell lines and normal human cell lines

Compounds	MDA-MB-231[a]	K-562[b]	HEK-293[c]	SI[d]-MDA-MB-231	SI K-562
3i	0.93 ± 0.05	1.68 ± 0.08	4.41 ± 0.09	4.70	2.62
3k	0.68 ± 0.04	0.78 ± 0.03	6.02 ± 0.1	8.86	7.72
3l	0.58 ± 0.02	1.22 ± 0.06	39.24 ± 0.12	66.96	32.16
Doxorubicin	0.08 ± 0.01	4.49 ± 1.39	–	–	–
Paclitaxel	0.3 ± 0.02	>100	–	–	–

[a]MDA-MB-231-triple negative breast cancer cell line

[b]K-562- Myelogenous leukemia cell line

[c]HEK-293-human embryonic kidney cells (human non-tumorous cells)

[d]Selective index was calculated as ratio of IC$_{50}$ value of non-tumorous cell line to the IC$_{50}$ value of cancer cell line. IC$_{50}$ values are obtained as the mean ± SD (μM) from three different experiments

position of aromatic ring shows interactions with Met769 (1.55 Å) (Fig 3).

Biological screening

Cancer cell inhibitory activities of the selected compounds On the basis of the enzymatic inhibitory potency against IM17, compounds **3i**, **3k**, and **3l** were selected and evaluated for their anti-proliferative activity against breast cancer cell line MDA-MB-231 (ER-negative) and myelogenous leukemia cell line K-562 using MTT(3-

(4,5-dimethylthiazol-2-yl)-2,5-diphenyltetrazolium bromide) assay method.

All the three selected pyrazole compounds inhibited cell proliferation with IC$_{50}$ values in the range of 0.58 to 1.68 μM. As shown in Table 3, the samples showed moderate to good activity comparable to that of standard drugs, especially compound **3l** showed higher anti-proliferation activity with IC$_{50}$ = 0.58 ± 0.02 μM against TNBC(triple negative breast cancer) MDA-MB-231 cell lines. Also, compound **3l** exhibited moderate activity with IC$_{50}$ value 1.22 ± 0.06 μM against K-562-leukemia cell line.
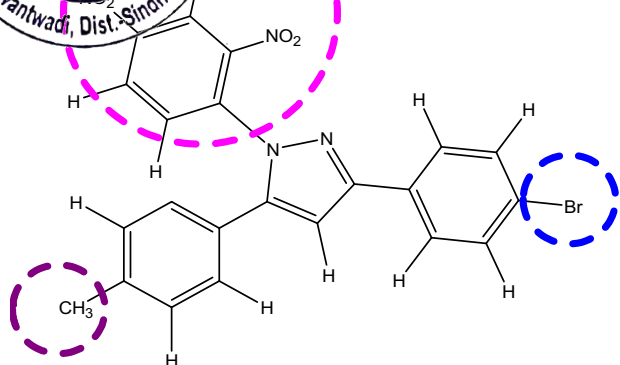
Fig. 4 Structural features of compound **3l** responsible for anticancer activity

Compounds **3i** and **3k** showed moderate activity with IC$_{50}$ values 0.93 ± 0.05 and $0.68 \pm 0.04\,\mu$M against MDA-MB-231 cell lines. In case of K-562 cell line, compound **3k** displayed higher anti-proliferative activity with IC$_{50}$ value $0.78 \pm 0.03\,\mu$M as compared to the other two screened samples, which was compatible with its docking study.

Accompanying this, the in vitro cytotoxic activity of all the tested compounds was assessed against normal HEK-293 cell lines by MTT colorimetric assay. The cytotoxic results revealed that none of the three evaluated compounds exhibited any significant toxicity effect on normal HEK-293 cells. SI, i.e., selectivity index exposes the differential activity of a pure compound. Compound with a higher SI value is said to be more selective and hence less cytotoxic. On the other side, a compound with SI value < 2 indicates cytotoxicity of the pure compound. As seen in Table 3 all
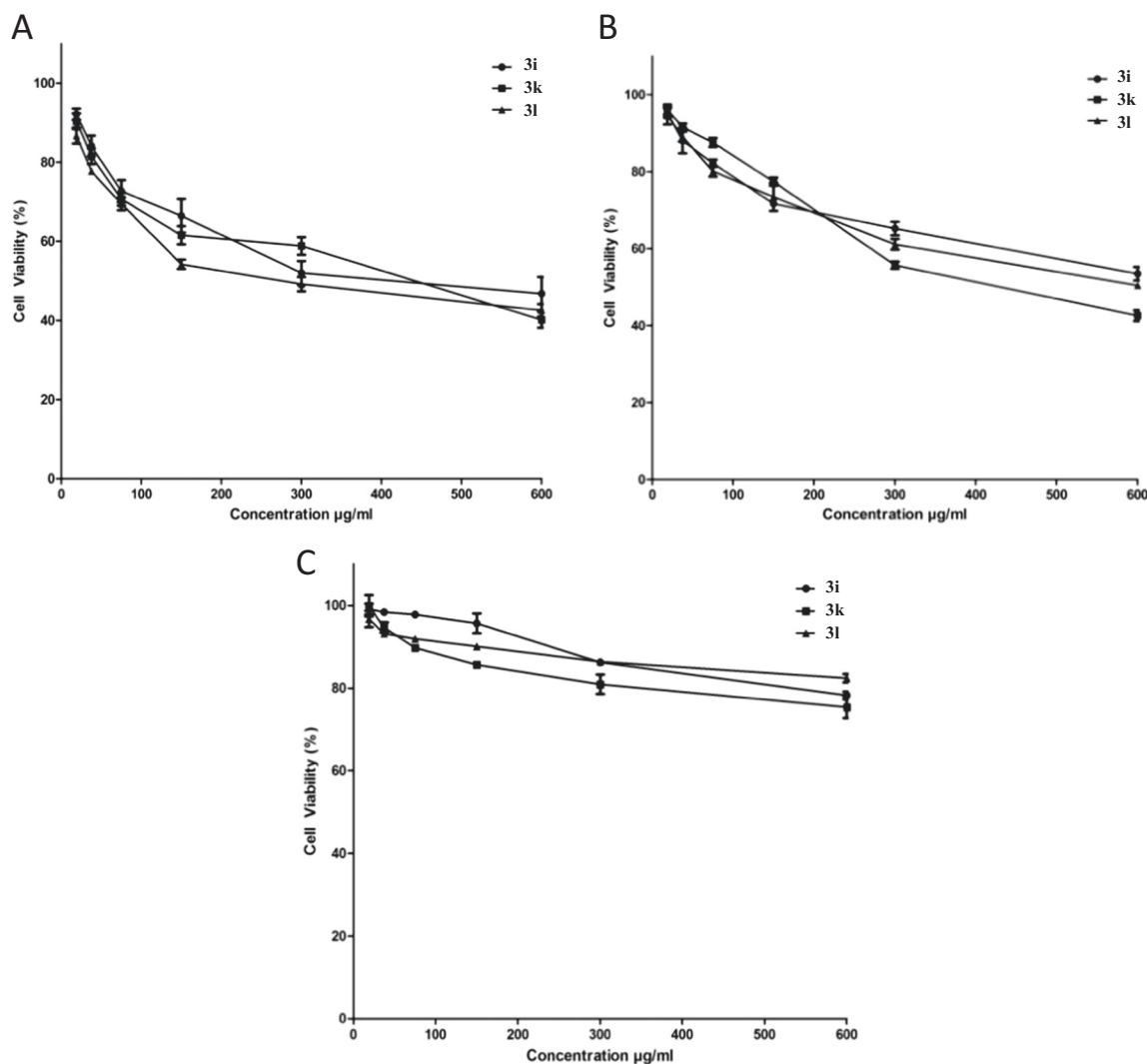

Fig. 5 Graphical representation of cell viability exhibited by **3i**, **3k**, and **3l** for three different cell lines. **a** For MDA-MB-231 cell line, **b** for K-562 cell line, and **c** HEK-293 (non-tumorous) cell line

Fig. 6 Fluorescence microscopy images of cells stained with acridine orange/ethidium bromide. **a** Viable untreated cells, **b** cells treated with compound **3i**, **c** cells treated with compound **3k**, **d** cells treated with compound **3l**

NC

3i

3k

3l
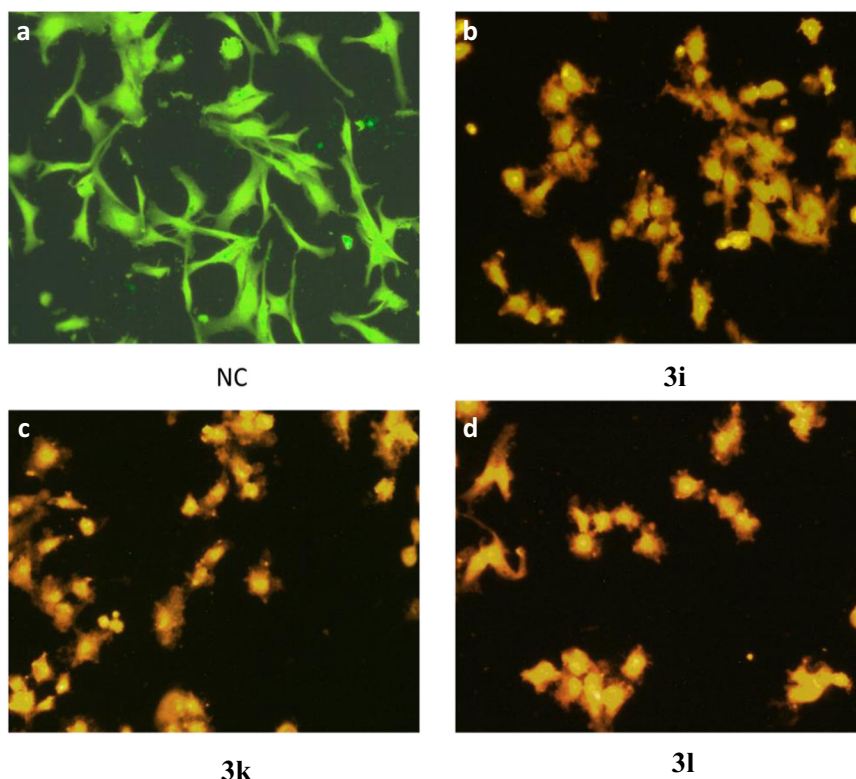
the samples were proved to be non toxic on the normal tumor cells (Fig. 4).

As seen in Fig. 5; the effect of pyrazole derivatives on the viability of MDA-MB-231, K-562 human cancer cell lines and HEK-293 was investigated and represented graphically as variation in percentage of viability with respect to time and concentration.

Cell morphology studies by fluorescence microscopy

Fluorescence microscopy study was used to study how cell death was induced by selected pyrazole compounds **3i**, **3k**, and **3l** in comparison to the standard cis-platin by virtue of acridine orange/ ethidium bromide staining. The fluorescence properties of dyes can help to characterize the mode of cell death, whether early or late apoptosis. Acridine orange is taken up by both viable and apoptotic (dead) cells by emitting green fluorescence. Ethidium bromide will stain only cells with disrupted membrane integrity, i.e., late apoptotic cells and necrotic cells. Staining of acridine orange on live cells showed green fluorescent nuclei, which indicate early apoptosis, while late apoptotic cells have orange to red nuclei with condensed or fragmented chromatin. Necrotic cells have uniform orange to red nuclei with the organized structure. Thus, the results (Fig. 6) demonstrated that the viable cells without treatment of pyrazole compound stained with acridine orange appeared with green fluorescent nucleus Fig. 6a, while late apoptotic cells

showed an orange fluorescence with nuclear membrane bebling Fig. 6b–d thereby signifying the apoptotic mode of cell death.

Further, an apoptotic mode of cell death was confirmed by fluorescence microscopy studies using DAPI staining method wherein, the treated and untreated cells were stained with 4',6-diamidine-2'-phenylindole dihydrochloride (DAPI). As shown in Fig. 7 the cell shrinkage, nuclear fragmentation characterizes the apoptotic mode of cell death by cells treated with compound **3i**, **3k**, and **3l** stained with DAPI.

Conclusion

In conclusion, a novel series of 2,4-dinitrophenyl containing pyrazole derivatives (**3a–3o**) were designed, synthesized, and evaluated as anti-proliferative agents. Keeping in view the significance of presence of electron withdrawing nitro groups, our efforts of achieving oxidative cyclization of N-aryl hydrazones has led to a novel class of bioactive pyrazoles of different substitution patterns in good yields. Recycling of the reagent up to five cycles without any higher loss in catalytic activity and time consumption delivers the efficiency of the green method.

Considering the biological screening results, the pyrazole derivatives showed potent anticancer activity against the MDA-MB-231(ER-negative) human breast cancer cell line

Fig. 7 Fluorescence microscopy images of cells stained with DAPI, showing **a** viable untreated cells, **b** cells treated with compound **3i**, **c** cells treated with compound **3k**, **d** cells treated with compound **3l**
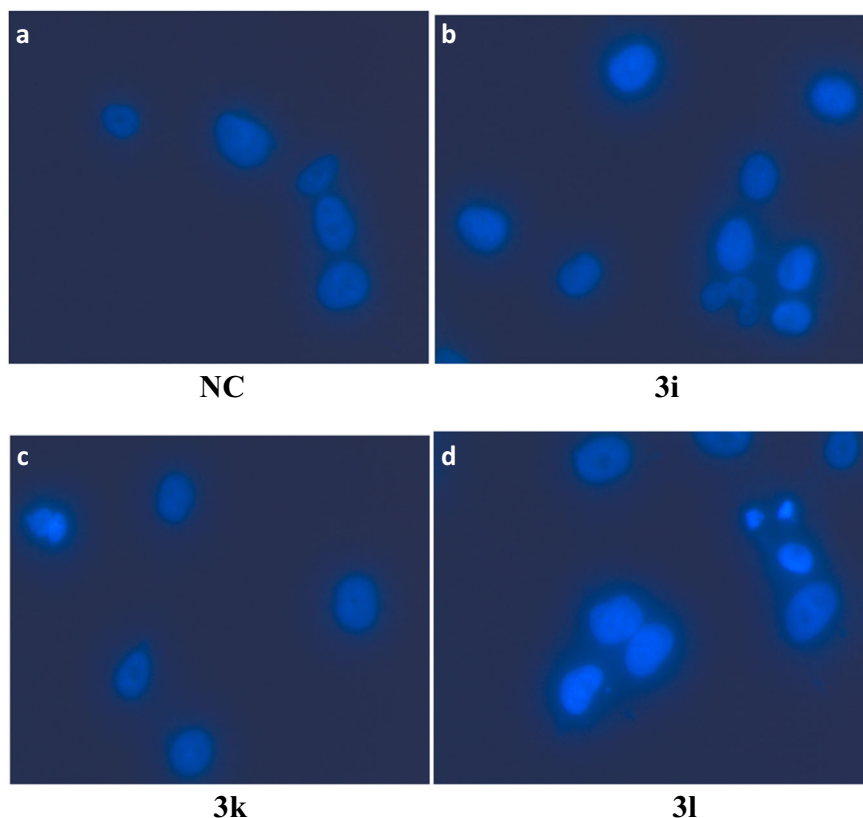
and K-562 leukemia cell line. It was noticed that the selective compounds **3i**, **3k**, and **3l** demonstrated significant minimum inhibitory activity with IC_{50} values in the range 0.5–1.68 µM against cancer cell lines MDA-MB-231 and K-562. Cytotoxicity against the human embryonic kidney cell line HEK-293 was also evaluated and the selectivity was thus assessed. The evaluated compounds displayed moderate SI values ranging from 2.62 to 32.16. The docking studies revealed that compounds **3i**, **3k**, and **3l** had good tyrosine kinase binding interactions. Further, the mode of cell death was characterized by fluorescence microscopy study, to be late apoptosis, which was also supported by DAPI results.

These results were compatible with the docking studies, which revealed that compounds **3i**, **3k**, and **3l** act as potent inhibitor of tyrosine kinase by virtue of hydrogen bonding interactions with nitro group of the aromatic ring at 4 position.

Compliance with ethical standards

References

Abd El-Karim S, Anwar M, Mohamed N, Nasr T, Elseginy S (2015) Design, synthesis, biological evaluation and molecular docking studies of novel benzofuran–pyrazole derivatives as anticancer agents. Bioorg Chem 63:1–12

Abdel-Aziz M, El-Din A, Abuo-Rahma G, Hassan A (2009) Synthesis of novel pyrazole derivatives and evaluation of their anti-depressant and anticonvulsant activities. Eur J Med Chem 44:3480–3487

Ahlstrom M, Ridderstrom M, Zamora I, Luthman K (2007) CYP2C9 structure− metabolism relationships: Optimizing the metabolic stability of COX-2 inhibitors. J Med Chem 50:4444–4452

Ahmed N, Siddiqui Z (2015) Silica molybdic acid catalysed eco-friendly three component synthesis of functionalised tetrazole derivatives under microwave irradiation in water. RSC Adv 5:16707–16717

Alam M, Alam O, Khan S, Naim M, Islamuddin M, Deora G (2016) Synthesis, anti-inflammatory, analgesic, COX1/1-inhibitory

Principal
V P College Of Pharmacy, Madkhol
Tal. Sawantwadi, Dist. Sindhudurg

activity, and molecular docking studies of hybrid pyrazole analogues. Drug Des Dev Ther 10:3529–3543

Ayati A, Esmaeili R, Moghimi S, Bakhshaiesh T, Eslami Z, Majidzadeh K, Safavi M, Emami S, Foroumodi A (2018) Synthesis and biological evaluation of 4-amino-5-cinnamoylthiazoles as chalcone like anticancer agents. Eur J Med Chem 145:404–412

Bole S, Nargund R, Nargund L, Devaraju K, Vedamurthy A, Shruti S (2011) Synthesis and biological evaluation of novel pyrazole derivatives as urease inhibitors. Der Pharma Chem 3:73–80

Desai V, Desai S, Gaonkar SN, Palyekar U, Joshi SD, Dixit SK (2017) Novel quinoxalinyl chalcone hybrid scaffolds as enoyl ACP reductase inhibitors: Synthesis, molecular docking & biological evaluation. Bioorg Med Chem Lett 27:2174–2180

Desai V, Gawandi S (2016) Synthesis of new 2, 4 - dinitro phenyl hydrazone derivatives of chalcones and its biological evaluation. Indo Am J Pharm Res 6:4779–4786

Deng X, Mani N (2008) Regioselective synthesis of 1,3,5-tri-and 1,3,4,5-tetrasubstituted pyrazoles from N-arylhydrazones and nitroolefins. J Org Chem 73:2412–2415

Desai V, Naik S (2013) Use of Solid-Supported Reagents towards Synthesis of 2-Arylbenzoxazole, 3,5-Diarylisoxazole and 1,3,5-Triarylpyrazole. Green & Sustain Chem 3:1–7

Desai V, Satardekar P, Dhumaskar K, Polo S (2012) Regioselective synthesis of 1,3,5-trisubstituted pyrazoles. Syn Comm 42:836–842

Han Y, Kim K, Choi G, An H, Son D, Kim H, Ha H, Son J, Chung S, Park H, Lee J, Suh Y (2014) Pyrazole-5-carboxamides, novel inhibitors of receptor for advanced glycation end products (RAGE). Eur J Med Chem 79:128–142

Hafez H, El-Gazzar A (2016) Synthesis and biological evaluation of N- pyrazolyl derivatives and pyrazolopyrimidine bearing a biologically active sulfonamide moiety as potential antimicrobial agent. Molecules 21:1156–1171

Holliday D, Speirs V (2011) Choosing the right cell line for breast cancer research. Breast Cancer Res 13:215–221

Keche P, Hatnapure G, Tale R, Rodge A, Kamble V (2012) Synthesis, anti-inflammatory and antimicrobial evaluation of novel 1-acetyl-3,5-diaryl-4,5-dihydro (1H) pyrazole derivatives bearing urea, thiourea and sulfonamide moieties. Bioorg Med Chem Lett 22:6611–6615

Kheder N, Mabkhot Y, Zahian F, Mohamed S (2014) Regioselective synthesis of some pyrazole scaffolds attached to benzothiazole and benzimidazole moieties. J Chem 2014:1–5

Kumar V, Kaur K, Gupta G, Sharma A (2013) Pyrazole containing natural products: synthetic preview and biological significance. Eur J Med Chem 69:735–753

Kumar H, Saini D, Jain S, Jain N (2013) Pyrazole scaffold: a remarkable tool in the development of anticancer agents. Eur J Med Chem 70:248–258

Kumar A, Jain S, Parle M, Jain N, Kumar P (2013) 3-Aryl-1-phenyl-1H-pyrazole derivatives as new multitarget directed ligands for the treatment of Alzheimer's disease, with acetylcholinesterase and monoamine oxidase inhibitory properties. EXCLI J 12:1030–1042

Malvar D, Ferreira R, Castro R, Castro L, Freitas A, Costa E, Florentino I, Mafra J, De Souza G, Vanderlinde F (2014) Antinociceptive, anti-inflammatory and antipyretic effects of 1.5-diphenyl-1H-

Pyrazole-3-carbohydrazide, a new heterocyclic pyrazole derivative. Life Sci 95:81–88

Mojzych M, Karczmarzyk Z, Wysocki W, Ceruso M, Supuran C, Krystof V, Lipkowska Z, Kalicki P (2015) New approaches to the synthesis of sildenafil analogues and their enzyme inhibitory activity. Bioorg Med Chem 23:1421–1429

Mottamal M, Zheng S, huang T, Wang G (2015) Histone deacetylase inhibitors in clinical studies as templates for new anticancer agents. Molecules 20:3898–3941

Olender D, Zwawiak J, Zaprutko L (2018) Multidirectional efficacy of biologically active nitro compounds included in medicines. Pharmaceuticals 11:54

Palkar M, Singhai A, Ronad P, Vishwanathswamy P, Boreddy T, Veerapur V, Shaikh M, Rane R, Karpoormath R (2014) Synthesis, pharmacological screening and in silico studies of new class of diclofenac analogues as a promising anti-inflammatory agents. Bioorg Med Chem 22:2855–2866

Penning T, Talley J, Bertenshaw S, Carter J, Collins P, Docter S, Graneto M, Lee L, Malecha J, Miyashiro J, Rogers R, Rogier D, Yu S, Anderson G, Burton E, Cogburn J, Gregory S, Koboldt C, Perkins W, Seibert K, Veenhuizen A, Zhang Y, Isakon P (1997) Synthesis and biological evaluation of the 1,5-diarylpyrazole class of cyclooxygenase-2 inhibitors: Identification of 4-[5-(4-Methylphenyl)-3- (trifluoromethyl)-1H-pyrazol-1-yl]benzenesulfonamide (SC-58635, Celecoxib). J Med Chem 40:1347–1365

Piwowar K, Milacic V, Chen D, Yang H, Zhao Y, Chan T, Yan B, Dou Q (2006) The proteasome as a potential target for novel anticancer drugs and chemosensitizers. Drug Resist Updtaes 9:263–273

Renuka N, Kumar K (2013) Synthesis and biological evaluation of novel formyl-pyrazoles bearing coumarin moiety as potent antimicrobial and antioxidant agents. Bioorg Med Chem Lett 23:6406–6409

Soudy R,H, Etayash H, Bahadorani K, Lavasanifar A, Kaur K (2017) Breast cancer targeting peptide binds Keratin-1 : A new molecular marker for targeted drug delivery to breast cancer. Mol Pharm 14:593–604

Tantawy A, Nasr M, El-Sayed M, Tawfik S (2012) Synthesis and antiviral activity of new 3-methyl-1, 5-diphenyl-1H-pyrazole derivatives. Med Chem Res 21:4139–4149

Topcu Z (2001) DNA topoisomerases as targets for anticancer drugs. J Clin Pharm Ther 26:405–416

Trejo-soto P, Hernandez-campos A, Romo-Mancillar A, Medina-Franco J, Castillo R (2018) In search of AKT Kinase inhibitors as anticancer agents: Structure based design, docking and molecular dynamics studies of 2,4,6-trisubstituted pyridine. J Biomol Struct Dyn 36(2):423–442

Xia Y, Dong Z, Zhao B, Ge X, Meng N, Shin D, Miao J (2007) Synthesis and structure–activity relationships of novel 1-aryl-methyl-3-aryl-1H-pyrazole-5-carbohydrazide derivatives as potential agents against A549 lung cancer cells. Bioorg Med Chem 15:6893–6899

DESIGN, SYNTHESIS, ANTIBACTERIAL AND ANTICANCER ACTIVITY OF 4-HYDROXY-3-(2-SUBSTITUTED-2-THIOXOETHYL)-1-PHENYL/METHYLQUINOLIN-2(1*H*)-ONE DERIVATIVES

Karmali H. A.[a], Mamle Desai Shivalingrao N.[a]*, Shingade S. G.[a], Palkar M. B.[b],
Biradar Bheemanagouda S.[c]

ABSTRACT

A series of title compounds 4-hydroxy-3-(2-substituted-2-thioxoethyl)-1-phenyl/methylquinolin-2(1H)-one were synthesized and purity of the compounds was ascertained by TLC. The structures synthe-sized compounds were characterized by IR, NMR (^{1}HNMR and ^{13}CNMR), Mass spectral data. Molecular docking studies of the compounds were carried out using Molegro Virtual Docker. All the synthesized compounds were evaluated for anticancer activity against two different cell lines: K562 (leukemia) and A549 (lung cancer) and antibacterial evaluation was also carried out against Bacillus subtilis, Staphy-lococcus aureus, Escherichia coli and Pseudomonas aeruginosa. Compound (II-a1) showed MIC of 1 μg/mL against B. subtilis and 4 μg/mL against S. aureus. Compound (II-b1) showed MIC of 4 μg/mL against B. subtilis and 2 μg/mL against S. aureus gram positive bacterial strains. Compound II-a2 showed anticancer activity with IC50 value = 0.765 μM/mL against K562 cell line (leukemia) and II-a3 with IC50 value = 0.774 μM/mL.

INTRODUCTION

The burden of cancer continues to increase throughout the world with increasing adoption to cancer causing behaviors Viz smoking, environmental factors, food style etc[1]. Lung and bronchus cancer is the leading cause in Male comprising of 17% of total new cases and 23% of total cancer deaths, followed by colon and rectus, prostate and pancreas[2]. Leukamia is a cancer of the bone marrow and blood, from 2005 to 2014 the overall leukemia incidence rate is increased by 1.6% per year[3]. Although there have been numerous advancements and a wide array of research on the drugs which are used to treat cancer patients. The selectivity of these molecules is also a matter of concern as these drugs often bring about the lysis of non-cancerous cells. These drugs tend to exhibit severe side effects and systemic toxicity[4].

The quinolin-2-one is an important alkaloid found in many shrubs of Rutaceae family and some alkaloids viz. dictamine known to have smooth muscle contraction and flindesine anti-bacterial property[5]. The therapeutic importance synthetic quinolin-2-one derivatives are well documented with aripiperazole used for schizophrenia, carteolol for glaucoma, rebamipide as an antacid drug[6].

Literature survey reveals linomide, a potent immune stimulatory agent, found to be useful in treating Acute Myeloid leukemia. Fluoroquinolones are the newer generation anti-bacterial antibiotics with wider spectrum of activity[7,8]. Considering the importance of quinolinone derivatives as an anti-cancer and anti-bacterial activity, we taught of synthesizing linomide analogues by modification of phenyl acetyl with hetero substituted thioxoethyl group. Further *in silico* molecular docking studies of the title compounds were carried out using Molegro Virtual Docker (MVD-2013, 6.0)

MATERIALS AND METHODS

Chemicals used for the synthesis were purchased from Molychem, Mumbai and SD-Fine Chem Ltd, Mumbai. All the reagents and solvents were of laboratory grade. The reactions were monitored by thin layer chromatography (TLC) using precoated plates. Melting Points of the synthesized compounds were determined by Thiele's melting point apparatus and are uncorrected. Fourier transform infrared (FTIR) spectra were recorded on SHIMADZU IR AFFINITY-1 spectrophotometer by KBr disc method. The ^{1}H NMR and ^{13}C NMR were recorded

[a] Dept. of Pharm. Chemistry, PES's Rajaram & Tarabai Bandekar College of Pharmacy, Farmagudi, Ponda-Goa - 403 401, India

[b] Dept. of Pharm. Chemistry, KAHER College of Pharmacy, Vidyangar, Hubballi-Karnataka - 580 031, India

[c] Dept. of Pharmacology, PES's Rajaram & Tarabai Bandekar College of Pharmacy, Farmagudi, Ponda-Goa - 403 401, India

* For Correspondence: E-mail - smamledesai@rediffmail.com
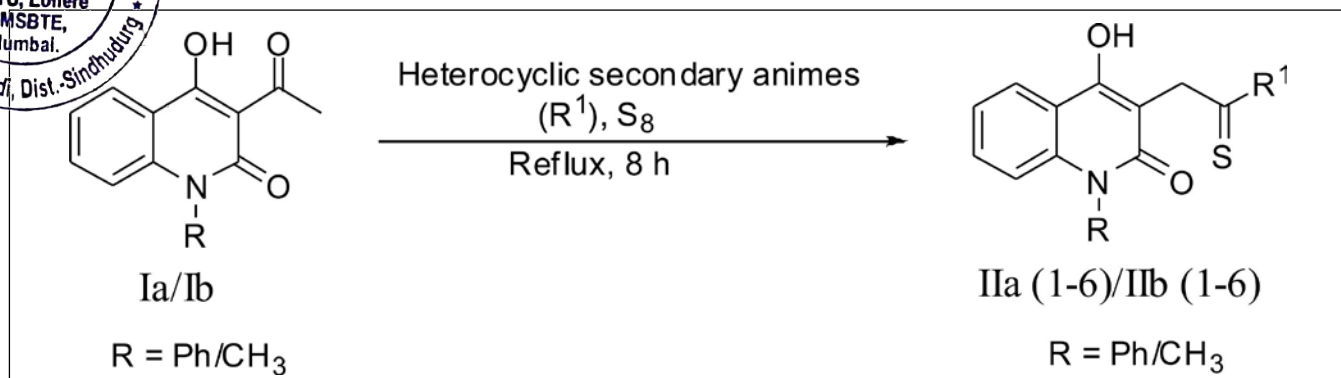
Scheme 1: Synthesis of 4-hydroxy-3-(2-substituted-2-thioxoethyl)-1-phenyl/methylquinolin-2(1*H*)-one derivatives

on Bruker Avance II 400 NMR spectrometer using CDCl$_3$ as the solvent and tetramethylsilane (TMS) as internal standard. Chemical shifts are expressed as delta (δ) values in parts per million (ppm). Mass spectra were recorded on Waters, Q-TOF Micromass (LC-MS). *In silico* molecular docking study was carried out on the title compounds using Molegro Virtual Docker 2007 (version 6.0).

CHEMISTRY

The starting material 1-methyl/phenyl-3-acetyl-4-hydroxyquinoli-2(1*H*)-one was synthesized as per the literature[9]. Further acetyl group at 3rd position was converted to substituted thioamides by Willigerodt-Kindler (WK) reaction as shown in Scheme 1. The three component reaction involves staring material, sulphur and secondary heterocycles, follows nucleophilic addition

reaction of amine to carbonyl carbon center and complex of resulting enamine and sulphur followed through cyclic intermediate yielded the title compounds.

Synthesis of 4-hydroxy-3-(2-substituted-2-thioxoethyl)-1phenyl/methylquinolin-2(1*H*)-one (II-a/II-b)

A solution of amine (1 mmol) with compound (**I-a/I-b,** 3 mmol) and sulfur (2 mmol) were placed in a flask with an air cooled reflux condenser. The obtained mixture was stirred and heated at 80°C for 8 h. Progress of the reaction was monitored by TLC using suitable solvent. The dark brown mixture was cooled to room temperature, washed with water and then extracted with ethyl acetate. The organic layer is separated and dried over anhydrous Na$_2$SO$_4$ and precipitate was filtered and collected. The list of the title compounds are shown in Table I.

Table I: Physicochemical parameters of 4-hydroxy-3-(2-substituted-2-thioxoethyl)-1-phenyl/methylquinolin-2(1*H*)-one derivatives

Compound	R^1	Molecular Formula	M.W.	M. P. ^{0}C	% yield	R$_f$ Value
II-a1	Morpholine	C$_{21}$H$_{20}$N$_2$O$_3$S	380	162-4	89.23	0.73
II-a2	Pyrrolidine	C$_{21}$H$_{20}$N$_2$O$_2$S	364	145-7	88.56	0.61
II-a3	Piperdine	C$_{22}$H$_{22}$N$_2$O$_2$S	378	152-5	87.10	0.73
II-a4	N-Methyl piperazine	C$_{22}$H$_{23}$N$_3$O$_2$S	393	135-7	87.23	0.83
II-a5	1-Ethyl piperazine	C$_{23}$H$_{25}$N$_3$O$_2$S	407	140-3	89.12	0.88
II-a6	2-Methyl pyrrolidine	C$_{22}$H$_{22}$N$_2$O$_2$S	378	148-50	83.33	0.65
II-b1	Morpholine	C$_{16}$H$_{18}$N$_2$O$_3$S	318	130-3	88.23	0.76
II-b2	Pyrrolidine	C$_{16}$H$_{18}$N$_2$O$_2$S	302	121-4	85.56	0.66
II-b3	Piperdine	C$_{17}$H$_{20}$N$_2$O$_2$S	316	126-8	87.50	0.63
II-b4	N-Methyl piperazine	C$_{17}$H$_{21}$N$_3$O$_2$S	331	131-4	82.23	0.86
II-b5	1-Ethyl piperazine	C$_{18}$H$_{23}$N$_3$O$_2$S	345	134-6	80.20	0.88
II-b6	2-Methyl pyrrolidine	C$_{17}$H$_{20}$N$_2$O$_2$S	316	127-5	81.40	0.71

Principal
V P College Of Pharmacy, Madkhol
Tal. Sawantwadi, Dist. Sindhudurg

Molecular docking study[10]

In silico molecular docking study of the title compounds was carried out using Molegro Virtual Docker (MVD-2007, version 6.0). The selected molecules were built using Chemdraw 12.0.2. The 2D structures were then converted into energy minimized 3D structures which were saved as MDL MolFile (.mol2). The coordinate file and crystal structure of epidermal growth factor receptor (EGFR) tyrosine kinase domain complexed with a 4-anilinoquinazoline inhibitor (PDB ID: 1m 17) were obtained from the RCSB-PDB website is shown in Fig. 1. The protein file was prepared by the removal of water molecules, addition of polar hydrogens, and removal of other bound ligands. The site at which binding of the complexed inhibitor occurs, was selected as the active site for docking of the molecules. The docking protocol was carried out for synthesized compounds using MVD-2007 (version 6.0) software using the standard operating
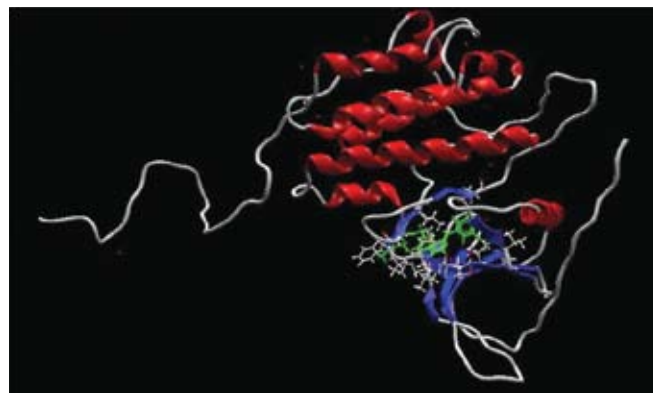

Fig. 1: Structure of EGFR-tyrosine kinase domain complexed with 4-anilinoquinazoline inhibitor (PDB ID: 1m17)

procedure. The MolDock scores and the hydrogen bonding of the test compounds were compared with those of linomide and imatinib; taken as reference standards for the study.

Table II: Antibacterial activity results of 4-hydroxy-3-(2-substituted-2-thioxoethyl)-1-phenyl/methylquinolin-2(1*H*)-one derivatives (Zone of Inhibition in mm)

Compound	Concentration (µg)	Gram positive bacteria		Gram negative bacteria	
		B. s.	**S. a.**	**E. c.**	**P. a.**
II-a1	200	25	18	-	-
	100	21	15	-	-
	50	18	12	-	-
	25	14	10	-	-
II-b1	200	24	20	-	-
	100	22	19	-	-
	50	19	16	-	-
	25	16	12	-	-
II-a2	200	26	22	-	-
	100	24	20	-	-
	50	20	18	-	-
	25	18	15	-	-
II-b2	200	28	25	-	--
	100	25	22	-	-
	50	21	18	-	-
	25	18	16	-	-
II-a3	200	25	26	--	-
	100	21	24	-	-
	50	19	19	-	
	25	15	15	-	

Compound	Concentration (µg)	Gram positive bacteria		Gram negative bacteria	
		B. s.	S. a.	E. c.	P. a.
II-b3	200	23	24	-	-
	100	22	22	-	-
	50	19	20	-	-
	25	16	18	-	-
II-a4	200	24	22	-	-
	100	23	20	-	-
	50	20	19	-	-
	25	18	18	-	-
II-b4	200	25	23	-	-
	100	23	20	-	-
	50	22	19	-	-
	25	20	18	-	-
Norfloxacin	200	31	32	26	27
	100	27	28	23	25
	50	26	27	19	24
	25	20	23	15	19

S. a. - Staphylococcus aureus, *B. s. - Bacillus subtilis*, *E. c. - Escherichia coli*, *P. a. - Pseudomonas aeruginosa*

Table III: Result of Minimum inhibitory concentration (MIC in µg/mL) of 4-hydroxy-3-(2-substituted-2-thioxoethyl)-1phenyl/methylquinolin-2(1*H*)-one derivatives

Compound	Gram positive bacteria		Gram negative bacteria	
	S. a.	B. s.	E. c.	P. a.
II-a1	4	1	-	-
II-b1	2	4	-	-
Norfloxacin	2	2	2	< 4

S. a. - Staphylococcus aureus, *B. s. - Bacillus subtilis*, *E. c. - Escherichia coli*, *P. a. - Pseudomonas aeruginosa*

ANTIBACTERIAL ACTIVITY

Zone of Inhibition[11]

The few colonies of organism (about 3 to 10) required for microbial activity were mixed in a test tube containing 25 mL of Soyabean Casein Digest medium (Trypton Soya broth) maintaining aseptic conditions by a wire loop. The tubes were incubated for 2-5 h to produce a bacterial suspension of moderate cloudiness. The tubes were poured into previously dried petri plates and kept for 2 h to settle. A 5 mm well was bored and solution containing the synthesized compounds were added to the respective plates in concentrations of 200, 100 50 and 25 µg. Each plate was incubated for 24 h at 37°C for bacterial growth. The diameters of zone of inhibition were measured and compared with a reference standard drug norfloxacin. The results of antibacterial activity at different concentrations are given in Table II.

Minimum Inhibitory Concentration[12]

The antibacterial activity was also determined by minimum inhibitory concentration (MIC) method. The synthesized derivatives were tested against the bacterial strains wherein norfloxacin was used as a standard drug. The MIC was determined in the range of concentrations from 128 to 0.25 µg/mL.

Brain heart infusion (BHI) broth was used to carry out MIC. The tubes were incubated for 24 h and observed for turbidity. The dilution tube with lowest concentration of the compound causing apparently complete inhibition of growth of organism was taken as MIC, norfloxacin was used as the reference standard. The compound showing promising MIC is reported in Table III.

Anticancer activity[13]

The cell monolayers of A549-Human Lung Carcinoma and K562 leukemia cell lines were carefully and gently washed with warm phosphate buffered saline using a multichannel pipette after being treated with xenobiotic. A 100 µL of culture medium containing 1-(4,5-
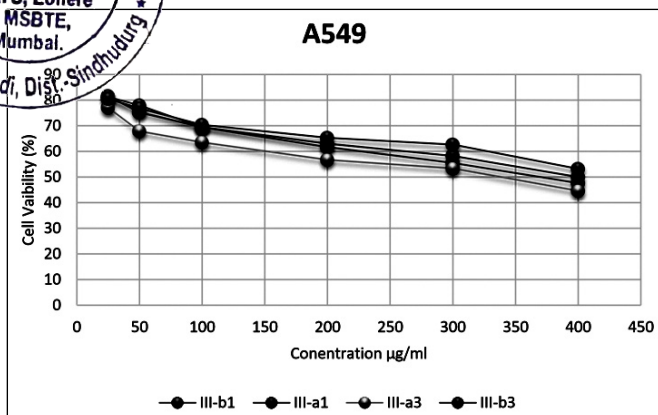
A549

Fig. 2: Graph of cell viability (%) of A549 cells
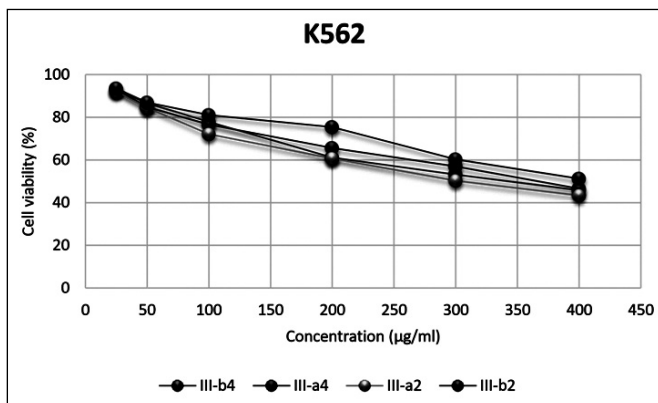

K562

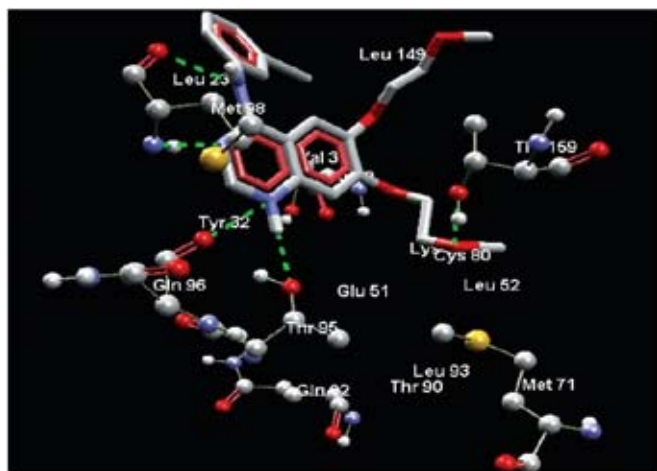**Fig. 3: Graph of cell viability (%) of K562 cells**

Fig. 4: Ligand 4-anilinoquinazoline docked in best of its conformation (pose) into the binding site of 1m17

dimethylthiazol-2-yl)-2,5-diphenyltetrazolium bromide solution (MTT) in the ratio of 10:1 was added to each well. Some wells were kept without cells and incubated with MTT for obtaining blank readings. The cells were kept in a cell incubator for 1-3 h and were carefully removed. 100 µL of dimethyl sulfoxide was added to the plates and gently shaken to resuspend formazan.

Table IV: Results of *in vitro* anticancer activity of 4-hydroxy-3-(2-substituted-2-thioxoethyl)-1-phenyl/methylquinolin-2(1*H*)-one derivatives by MTT Assay

Compound	K562 (IC$_{50}$ value in µM/mL)	A549 (µM/mL)
II-a1	-	1.331
II-a2	0.765	-
II-a3	-	0.774
II-a4	0.954	-
II-b1	-	1.235
II-b2	1.693	-
II-b3	-	2.553
II-b4	0.977	-
Paclitaxel	0.3	0.3

The plates were then kept aside until a homogenised colour was obtained. The results of anticancer activity are given in Table IV and V and % viability is shown in Fig. 2 and 3.

RESULTS

4-Hydroxy-3-(2-morpholino-2-thioxoethyl)-1-phenylquinolin-2(1*H*)-one (II-a1)

IR (KBr, cm^{-1}): 3421.72 (-OH), 3035.96 (Ar. -C-H str.), 2966.52, 2924.09 (aliphatic -C-Hstr.), 1604.75 (-C=O amide), 1107.23 (-C-O). ^{1}H NMR (CDCl$_3$, δ ppm): 15.96 (s, 1H, -OH), 8.23-6.53 (m, 9H, Ar-H), 3.91-3.88 (t, 4H, -CH$_2$ of 2,6-morpholine), 3.43-3.39 (t, 4H, -CH$_2$ of 3,5-morpholine), 1.75 (s, 2H, -CH$_2$ of thioxoethyl). ^{13}C NMR (CDCl$_3$, δ ppm): 200.29 (1C, -C=O amide), 166.17 (1C, -C=S), 158.28 (1C, C-OH), 132.17 - 117.64 (13C, aromatic carbon), 66.02 (2C, -CH$_2$ of morpholine), 54.85 (2C, -CH$_2$ of morpholine), 21.03 (1C, -CH$_2$ of thioxoethyl). MS: [M+1] at m/z 381.

4-Hydroxy-1-phenyl-3-(2-(pyrrolidin-1-yl)-2-thioxoethyl)quinolin-2(1*H*)-one (II-a2)

IR (KBr, cm^{-1}): 3392.79 (-OH); 3035.96 (Ar -C-H str.), 2874.23, 2875.82 (aliphatic -C-H str.), 1600.98 (-C=O amide). ^{1}H NMR (CDCl$_3$, δ ppm): 15.57 (s, 1H, -OH), 7.62 - 6.57 (m, 9H, Ar-H), 3.15-2.95 (m, 4H, -CH$_2$ of 2,5-pyrrolidine), 1.72-1.68 (t, 4H, -CH$_2$ of 3,4-pyrrolidine), 2.00 (s,2H, CH$_2$ of thioxoethyl).

4-Hydroxy-1-phenyl-3-(2-(piperidin-1-yl)-2-thioxoethyl)quinolin-2(1*H*)-one (II-a3)

IR (KBr, cm^{-1}): 3383.14 (-OH), 3003.17 (Ar -C-H str.), 2941.44, 2858.51 (aliphatic -C-H str.), 1604.77

**Table V: Results of *in vitro* anticancer activity of 4-hydroxy-3-(2-substituted-2-thioxoethyl)
-1-phenyl/methylquinolin-2(1*H*)-one derivatives by MTT Assay**

Cell Viability (K562)				
	Compound			
Concentration (µg/mL)	II-b4	II-a4	II-a2	II-b2
400	45.860930	46.523180	43.377480	51.241720
300	53.145690	57.036420	50.248340	60.347680
200	61.175500	65.645690	60.761590	60.761590
100	77.897350	76.572850	72.102650	81.043050
50	86.589400	84.850990	84.437090	86.920530
25	92.798010	93.211920	92.135770	93.543050
Control	100	100	100	100
DMSO	97.8321	98.0218	97.9634	97.9560
Cell Viability (A549)				
	Compound			
Concentration (µg/mL)	II-b1	II-a1	II-a3	II-b3
400	47.67550	50.01348	44.63750	53.24307
300	55.51093	58.25123	53.41365	62.65060
200	61.66890	63.04418	56.76038	65.32798
100	69.43329	69.45962	63.58768	70.41499
50	77.95627	75.21374	67.91611	76.88532
25	81.25837	81.64168	77.15306	80.54440
Control	100	100	100	100
DMSO	97.8725	97.9658	97.8952	97.7854

Table VI: Results of molecular docking studies of compounds (II-a1-6) and (II-b1-6)

Compound	MolDock Score	Rerank Score	H-Bond
II-a1	-117.961	-83.8496	-4.00558
II-a2	-108.566	71.5712	-2.5
II-a3	-102.881	-68.6642	-2.5
II-a4	-104.562	-85.5812	0
II-a5	-119.498	-88.4289	-6.68138
II-a6	-122.771	-91.7104	-6.23296
II-b1	-97.2409	-61.3587	-2.17128
II-b2	-106.978	-85.2503	-6.02057
II-b3	-93.1921	-76.5449	-4.59032
II-b4	-97.9473	-57.5244	-7.58735
II-b5	-96.3541	-75.2687	-4.12885
II-b6	-102.356 -	-31.7143	-5.70129
4-Anilinoquinazoline	-112.04	-75.7482	0

=O amide). [superscript1]H NMR (CDCl$_3$, δ ppm): 15.25 (s, 1H, -OH), 7.61 - 6.40 (m, 9H, Ar-H), 2.39-2.22 (t, 4H, -CH$_2$ of 2,6-pipridine) 2.21-2. (m, 6H, -CH$_2$ of 3,4,5-pipridine), 1.88 (s, 2H, CH$_2$ thioxoethyl). MS: [M+1] at m/z 379.

4-Hydroxy-1-methyl-3-(2-morpholino-2-thioxoethyl)quinolin-2(1*H*)-one (II-b1)

IR (KBr, cm[superscript-1]): 3446.79 (-OH), 3032.79 (Ar -C-H str.), 2920.23, 2854.65 (aliphatic -C-H str.), 1627.92 (-C=O amide), 1111.00 (-C-O). [superscript1]H NMR (CDCl$_3$, δ ppm): 15.68 (s, 1H, -OH), 7.58 – 7.00 (m, 4H, Ar-H), 4.00-3.95 (t, 4H, -CH$_2$ of 2,6-morpholine), 3.77-3.74 (t, 4H, -CH$_2$ of 3,5- morpholine), 2.94 (s, 3H, N-CH$_3$), 1.97 (s, 2H, -CH$_2$ of thioxoethyl). MS: [M+1] at m/z 319.

4-Hydroxy-1-methyl-3-(2-(pyrrolidin-1-yl)-2-thioxoethyl)quinolin-2(1*H*)-one (II-b2)

IR (KBr, cm[superscript-1]): 3446.79 (-OH), 3032.10 (Ar -C-H str.), 2966.52, 2926.01 (aliphatic -C-H str.), 1602.85 (-C=O amide). [superscript13]C NMR (CDCl$_3$, δ ppm): 202.72(1C, -C=O amide), 164.92 (1C, -C=S), 160.95 (1C, C-OH), 138.93 - 120.84 (7C, aromatic carbon); 46.14 (2C, -CH$_2$ of pyrrolidine), 34.28 (1C, -CH$_2$ of thioxoethyl), 32.83 (1C, N-CH$_3$), 26.47 (2C, -CH$_2$ of pyrrolidine). MS: [M+1] at m/z 303.

4-Hydroxy-1-methyl-3-(2-(piperidin-1-yl)-2-thioxoethyl)quinolin-2(1*H*)-one (II-b3)

IR (KBr, cm[superscript-1]): 3396.64 (-OH), 3012.81 (Ar -C-H str.), 2939.52, 2856.58 (aliphatic -C-H str.), 1604.77 (-C=O amide). [superscript1]H NMR (CDCl$_3$, δ ppm): 15.40 (s, 1H, -OH), 7.67 – 7.00 (m, 4H, Ar-H), 2.70-2.62(t, 4H, -CH$_2$ of 2,6-pipridine), 2.59-2.51(m, 6H, -CH$_2$ of 3,4,5-pipridine), 3.10 (s, 3H, N- CH$_3$), 1.70 (s, 2H, -CH2 of thioxoethyl). MS: [M+1] at m/z 317.

Molecular docking study

Molecular docking studies of the title compounds (II-a1-6) and (II-b1-6) were carried out using Molegro Virtual Docker (MVD-2013, 6.0) and the results are tabulated in Table VI.

DISCUSSION

Docking of synthesized compounds with the EGFRK enzyme exhibited well-conserved hydrogen bonds with one or more amino acid residues in the active pocket. Molecular docking study was carried out to compare the binding between the synthesized compounds (II-a{1-6}/II-b{1-6}) and 4-anilinoquinazoline inhibitor; with the EGFRK. The bonding interactions of 4-anilinoquinazolie inhibitor are shown in Fig. 4.

The MolDock Scores of the derivatives (II-a{1-6}/II-b{1-6}) ranged from -122.771 to -93.1921; while the MolDock Score of the standard 4-anilinoquinazoline ligand was found to be -112.04.

The –NH at 1[superscriptst] position of the quinazoline moiety forms hydrogen bond with –C=O of Gln96 and –OH of Thr95. The nitrogen at 3[superscriptrd] position of the quinazoline moiety shows hydrogen bonding interaction with –NH of Met98. The –NH at 4[superscriptth] position of quinazoline moiety forms hydrogen bond with –C=O of Met98. The oxygen from the terminal methoxy group in the side chain interacts with –OH of Thr159.

It was observed that compound II-a2 showed MolDock Score of -108.566; which is comparable to that of the standard ligand (-112.04). Analysis of the docking result of compound II-a2 showed binding of –OH at 4th position of quinolin-2-one nucleus with –C=O of Gln96 and the same –OH group showed interaction with the –OH of Thr95 is shown in Fig. 5.

Since the standard ligand is well positioned in the cavity at the active site, we can observe more significant interactions with the amino acid residues; than those shown by the synthesized derivatives but similarities in the interactions shown by the ligand and the compound II-a2 with the amino acid residues are also seen in the figure 5 and hence from the analysis we can conclude that the derivatives possess a potential to establish interaction with some of the residues at the active site; and the docking study can be used to develop more selective and potent pharmacological agents.

CONCLUSION

From the results it was concluded that compounds had good antibacterial activity against Gram positive bacterial strains which was comparable with reference standard norfloxacin and were ineffective against gram negative bacterial strains. 4-Hydroxy-3-(2-morpholino-2-thioxoethyl)-1-phenylquinolin-2(1*H*)-one (II-a1) exhibited highest zone of inhibition against *B. subtilis* and 4-hydroxy-1-methyl-3-(2-morpholino-2-thioxoethyl)quinolin-2(1*H*)-one (II-b1) exhibited highest zone of inhibition against *S. aureus*. Compound (II-a1) showed MIC of 1 µg/mL against *B. subtilis* and (II-b1) showed MIC of 2 µg/mL against *S. aureus*. The antibacterial inhibition exhibited by the compounds was equivalent to the reference standard norfloxacin.

Compound II-a2 [4-hydroxy-1-phenyl-3-(2-(pyrrolidin-1-yl)-2-thioxoethyl)quinolin-2(1H)one] exhibited most promising anticancer activity with IC_{50} value 0.765 µM/mL against K562 leukemia cell line and against A549 lung cancer cell line compound II-a3 [4-hydroxy-1-phenyl-3-(2-(piperidin-1-yl)-2-thioxoethyl)quinolin-2(1H)-one] was found to be the most potent with IC_{50} value 0.774 µM/mL when compared to the reference standard Paclitaxel with IC_{50} 0.3 µM/mL.

ACKNOWLEDGEMENT

REFERENCE:

1. Charles S., Lynn T. & Richard A., Lung Cancer: Epidemiology, Etiology and Prevention. **Clin. Chest Med**, 2011; 32(4): 212.

2. Jemal A., Bray F., Center M., Ferley J., Ward E. & Forman D. Global Cancer Stastistics. **CA Cancer J. Clin.,** 2011; 61(2):69-90.

3. www.cancer.org/cancer/leukemia. Accessed on 16.07.2018

4. Forest T.S., Randall Clark C. Antineoplastic agents, Wilson and Gisvold's Medicinal and Pharmaceutical Chemistry, Twelfth ed. Lippincott Williams and Wilkins, New Delhi. 2011, 355-57.

5. Rajadhyax A., Mamle Desai S., Naik S., Tari P. Synthesis of 4-methoxy-1-phenyl/methyl-3[5-(phenyl/substitutedphenyl)-4,5-dihydro-(1H)-pyrazole-3-yl] quinolin-2(1H)-one derivatives as antibacterial agents. **Indian. J. Het. Chem.** 2015; 25: 173-6.

6. Maria de Graca R., Mamle Desai S., Soniya N., Jairus F. & Prasad T. **Indian J. Chem.,** 2016; 55(B): 1254-58.

7. Shi J., Xiao Z., Ihnat MA., Li PK. Structure-activity relationship studies of the antiangiogenic activities of linomide. **Bioorg. Med. Chem. Lett.,** 2003; 13(6): 1187-9.

8. Saeed R.K., Annastasiah M, Roberto P, John T.I. Modified synthesis and antiangeiogenic activity of linomide. **Bioorg. Med. Chem. Let.,** 2011;11: 451-56

9. Thomas K. The pyrano route to 4-hydroxy-2-quinolones and 4-hydroxy-2-pyridones. **IL Farmaco**. 1999; 54:309-15.

10. Palkar M.B., Singhai A.S, Ronad P.M., Vishwanathswamy A., Boreddy T. S., Veerapur V.P., et al. Synthesis, pharmacological screening and in silico studies of new class of diclofenac analogues as a promising anti-inflammatory agents. **Bioorg. Med. Chem.,** 2014; 22: 2855-66

11. Kavangh F, Analytical Microbiology. Academic Press, New York; 1963,87-124.

12. Schwalbe R., Steele-Moore L, Goodwin A. Antimicrobial susceptibility testing protocols. CRC Press, Taylor & Francis Group, Boca Raton; 2007:75-80.

13. Rashad F.M., Abd El-Naseer N.H., Dawoud I.F. & Matawe F.H., Isolation and Characterization of Antibiotic/Antitumor producing Sterptomyces. **Res. J. Pharm, Bio. Chem. Sci.,** 2015;6(2):1917-29.

Principal
V P College Of Pharmacy, Madkhol
Tal. Sawantwadi, Dist. Sindhudurg